

Contract No:

This document was prepared in conjunction with work accomplished under Contract No. DE-AC09-08SR22470 with the U.S. Department of Energy (DOE) Office of Environmental Management (EM).

Disclaimer:

This work was prepared under an agreement with and funded by the U.S. Government. Neither the U. S. Government or its employees, nor any of its contractors, subcontractors or their employees, makes any express or implied:

- 1) warranty or assumes any legal liability for the accuracy, completeness, or for the use or results of such use of any information, product, or process disclosed; or
- 2) representation that such use or results of such use would not infringe privately owned rights; or
- 3) endorsement or recommendation of any specifically identified commercial product, process, or service.

Any views and opinions of authors expressed in this work do not necessarily state or reflect those of the United States Government, or its contractors, or subcontractors.



HANFORD DOUBLE SHELL WASTE TANK CORROSION STUDIES – FINAL REPORT FY2017

R. E. Fuentes

April 2018

SRNL-STI-2018-00116, Revision 0



DISCLAIMER

This work was prepared under an agreement with and funded by the U.S. Government. Neither the U.S. Government or its employees, nor any of its contractors, subcontractors or their employees, makes any express or implied:

1. warranty or assumes any legal liability for the accuracy, completeness, or for the use or results of such use of any information, product, or process disclosed; or
2. representation that such use or results of such use would not infringe privately owned rights; or
3. endorsement or recommendation of any specifically identified commercial product, process, or service.

Any views and opinions of authors expressed in this work do not necessarily state or reflect those of the United States Government, or its contractors, or subcontractors.

Printed in the United States of America

**Prepared for
U.S. Department of Energy**

Keywords: *Hanford, double-shell tanks,
vapor space corrosion, pitting protocol*

Retention: *Permanent*

HANFORD DOUBLE SHELL WASTE TANK CORROSION STUDIES – FINAL REPORT FY2017

R. E. Fuentes

April 2018

Prepared for the U.S. Department of Energy under
contract number DE-AC09-08SR22470.



REVIEWS AND APPROVALS

AUTHOR:

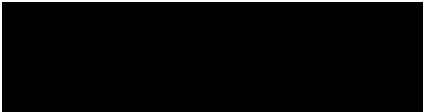


R. E. Fuentes, Materials Science and Technology

4/12/18

Date

TECHNICAL REVIEW:

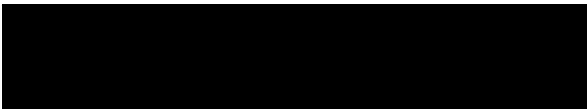


P. Shukla, Materials Science and Technology

4-12-2018

Date

APPROVALS:



B. J. Wiersma, Manager, Savannah River National Laboratory

4-12-18

Date



C. Girardot, Manager, Washington River Protection Solutions

4.12.2018

Date



J. L. Castleberry, Manager, Washington River Protection Solutions

April 11, 2018

Date

ACKNOWLEDGEMENTS

Technical assistance in performing experiments and characterizations were provided by K. J. Kalbaugh, B. Hill and M. Van Swol. QEPAS system for detection and measurements of ammonia in vapor space was performed by D. Hitchcock and B. Peters. The statistical model, design of experiments and analysis efforts of New Limits task was achieved by S. P. Harris. Monte Carlo N-Particle code was performed by C. Verst. In addition, helpful consultations with L. Stock and R. Sindelar and the WRPS Corrosion Sub-group provided direction for these activities. These efforts are greatly appreciated.

EXECUTIVE SUMMARY

Corrosion studies of Hanford Double-Shell Tanks (DSTs) at Savannah River National Laboratory (SRNL) were focused on New Limits testing using statistically design matrices for a high concentration of hydroxide (1.2 M) and testing at various interior points to establish corrosion control guidelines towards pitting corrosion. Ammonia was also added into the statistical design to determine inhibition effects. Additional electrochemical studies of individual organic species and nitrous oxide were tested in a AN-102 based simulant with no organics to compare inhibiting properties of a specific specie and measure any electrochemical improvement towards pitting corrosion. Studies of Vapor Space Corrosion (VSC) were conducted on concentrated and dilute Direct Feed Low Activity Waste (DFLAW) based chemistries and on Leak Detection Pit (LDP) and Ground Water (GW) simulants using Electrical Resistance (ER) measurements for the corrosive Vapor Space (VS) environment with and without Vapor Corrosion Inhibitor (VCI) application. Lastly, SRNL focused on enhanced corrosion studies by air radiolysis using Monte Carlo N-particle (MCNP) code to determine gamma doses near the primary and secondary liner of a DST and utilizing a model to predict the concentration of nitric acid that can be produced by radiolysis and the effect it can have on pH. The changes on pH were studied by a long-term immersion testing using GW simulants at a specific pH to determine the corrosion susceptibility of lower pH on carbon steel. Conclusions and a summary are enumerated below.

1. New Limits

New Limits testing was continued during FY17. Statistically designed matrices for hydroxide concentration up to 1.2 M and interior points of the waste chemistry envelope were utilized. Combining the Plackett-Burman and Box-Behnken statistically design testing performed in FY16 with these tests, a total of 95 tests were analyzed using logistic regression. Statistically significant chemical variables that affect the solution corrosivity towards pitting corrosion were determined. An expression, referred to as the pitting factor, was evaluated as a criterion to determine limits for pitting corrosion. Additionally, it was observed that ammonia concentration did not significantly influence the pitting model, although a mild inhibition effect was observed in a borderline condition.

The corrosion behavior of carbon steel exposed to AN-102 simulant with no organic species was compared to that for simulants with individual organic species or saturated nitrous oxide gas. Inhibition decreased in comparison to no organic species simulant according to the following order: Glycine, Iminodiacetic Acid, Ammonia, Dibutylphosphate and N-butylamine. Saturated nitrous oxide did not change significantly influence the corrosion behavior.

2. Vapor Space Corrosion Tests

DFLAW simulants at concentrated and dilute Na concentrations were used to investigate ammonia inhibition of Vapor Space Corrosion (VSC). Corrosion rates were on average higher for coupons exposed to the dilute than the concentrated Na DFLAW simulant. The solution for dilute Na DFLAW simulant caused more aggressive corrosion in immersed samples and in sample in the vapor phase of the solution compared to concentrated Na DFLAW simulant.

Ammonia detection using Quartz-enhanced Photoacoustic Spectroscopy (QEPAS) system was evaluated by testing different flow rates (50- 200 sccm) and at a range of pressures (200-650 Torr). This resulted, as expected, in a linear response, and it was determined that a constant pressure was required for an accurate concentration measurement. The system was placed at the exhaust of one of the vessels from the VSC setup. Since moisture can condense onto the Quartz Tuning Fork (QTF) of QEPAS; dampening QEPAS and can

result in large variations in detection signal. A new sensor that is specifically designed to measure NH_3 in air was procured and testing will continue during FY18.

LDP and GW simulants treated with VCI were used to study the effectiveness of VpCI®-337 at inhibiting VSC. Corrosion rates for the coupons that were exposed for 4 months were unaffected by the VCI application as they were similar on average to samples that were not treated with VCI. ER probe measurements, used to assess the corrosion environment and its effects with VCI, showed that the GW VS environment was more aggressive than LDP VS. The ER probes exposed to the simulants treated with VCI were protected for approximately 30 days, while the probes exposed to untreated simulants (hereafter defined as unprotected probes) corroded immediately. The unprotected ER probes were dipped in VCI after two months exposure and placed back into test. The corrosion rate decreased for approximately 10 days. However, the ER probe data suggests that the effectiveness of dipping carbon steel into VpCI®-337 as application for inhibitor is short lived and will not significantly reduce carbon steel corrosion in LDP and GW conditions.

3. Enhanced Corrosion due to Air Radiolysis

The MCNP code was used to calculate a position-dependent and time-dependent radiation flux, a resultant detector response and the effective dose rate for the exterior of AY-102 DST tank. A gamma dose rate of approximately 100 rad/hr was calculated for locations around the primary tank. Using a Humid Air Radiolysis Model (HARM) and assuming stagnant air conditions and no interactions with concrete, water droplets may reach pH 5 in approximately 500 hours, or around 3 weeks. Long immersion tests were performed to determine the severity of corrosion for GW simulant at two pH values: 6 and 5. Corrosion rates were obtained at an average of 18.7 mpy and 99.6 mpy for GW simulant at pH 6 and 5, respectively. Compared to results from FY16 in which the initial pH was 7.6, and was monitored during the 4 months but not adjusted, it represents a corrosion rate increase of almost double when the pH is 6 and almost 10 times when the pH is 5. Although the concentration of the acid is minimal in large volumes of ground water (i.e., mL or higher volumes), the pH of droplets of water may decrease significantly and contribute to VSC. Therefore, it is recommended that an inhibition strategy by using a different application of a VCI or maintaining relative humidity lower than 10% on the space between the annulus and secondary liner and around the primary liner may help decrease corrosion rate to maintain the integrity of the carbon steel liner.

TABLE OF CONTENTS

LIST OF TABLES	x
LIST OF FIGURES	x
LIST OF ABBREVIATIONS	xiii
1.0 Introduction	15
2.0 Background	15
2.1 New Limits Corrosion Studies	15
2.2 Vapor Space Corrosion Testing at SRNL	17
2.3 Liquid Air Interface and Total Immersion Corrosion testing of LDP and GW simulants at SRNL ..	17
3.0 Task Description and Activities	18
3.1 Task 1: New Limits Testing	18
3.2 Task 2: Vapor Space Corrosion for DSTs	18
3.2.1 Part A: Ammonia inhibition VSC testing	18
3.2.2 Part B: Ammonia detection with Quartz-Enhanced Photoacoustic Spectroscopy probe	18
3.2.3 Part C: VCI for DST secondary liner	18
3.3 Task 3: Enhanced corrosion due to air radiolysis	19
4.0 Experimental Procedure	19
4.1 Electrochemical Testing of Simulants	19
4.1.1 Material sample	19
4.1.2 Simulants	20
4.1.3 Testing Apparatus	24
4.2 Vapor Space Corrosion Testing	24
4.2.1 Materials	24
4.2.2 Simulants	25
4.2.3 Testing Apparatus	26
4.2.4 VCI for the suppression of corrosion of carbon steel exposed in LDP and GW simulants	28
4.2.5 Gas sensing probe for ammonia detection	30
4.3 Liquid Air Interface and Total Immersion Corrosion Testing	31
4.3.1 Materials	31
4.3.2 Simulants	32
4.3.3 Testing Apparatus	32
5.0 Results and Discussion	34
5.1 New Limits	34
5.1.1 Basis for Pitting Factor as a Criterion for Corrosion Inhibition	38

5.1.1.1 Relationship between Aggressive Anion and Inhibitor Concentrations	38
5.1.1.2 Criterion for Pitting Factor Evaluation.....	40
5.1.1.3 Evaluation of Critical Pitting Factor vs. Previous Corrosion Control Limits	45
5.2 Ammonia effects	46
5.3 Simulated AN-102 with various organic specie and saturated nitrous oxide.....	49
5.4 Vapor Space Corrosion Tests with DFLAW based Simulants at different Sodium (Na) Concentrations	53
5.5 Ammonia detection with QEPAS probe in the exhaust of VSC setup.....	57
5.6 VSC Secondary Wall of Tank AY-102: LDP and GW Corrosion Studies	60
5.7 Enhanced Corrosion due to Air Radiolysis	64
6.0 Conclusions.....	72
6.1 New Limits.....	72
6.2 Vapor Space Corrosion Tests	72
6.3 Enhanced Corrosion due to Air Radiolysis	73
7.0 Quality Assurance.....	73
8.0 References.....	73
9.0 Appendices.....	76

LIST OF TABLES

Table 2-1 Double-Shell Tank Waste Chemistry Limits for Corrosion Control.....	16
Table 2-2 Standardized CPP protocol with the parameters utilized for testing	16
Table 4-1 Chemical Composition of AART128 Rail Car Steel.....	19
Table 4-2 High hydroxide statistically selected simulant chemistries	21
Table 4-3 Statistically selected New Limits interior points.....	22
Table 4-4 Statistically selected simulants to test ammonia effects	23
Table 4-5 AN-102 based simulant with an individual organic specie and nitrous oxide.....	23
Table 4-6 Test conditions for VSC testing.....	26
Table 4-7 Chemical composition of the DFLAW tested simulants	26
Table 4-8 Simulant conditions for each vessel	33
Table 5-1 Electrochemical Testing results of statistically design tests for augmented 1.2 M hydroxide concentration. The tests highlighted in yellow are the statistical “anchor” points.	36
Table 5-2 Electrochemical Testing results of statistically design tests for interior points.....	37
Table 5-3 Electrochemical Testing results of statistically design tests for ammonia inhibition.....	47
Table 5-4 Comparison of similar test with and without ammonia addition.....	48
Table 5-5 Electrochemical results of AN-102 based simulant with individual organic specie and Nitrous Oxide	50
Table 5-6 Weight losses and corrosion rates of coupons at different levels in Vessels 2 to 6.....	56
Table 5-7 Weight losses of coupons at different levels in vessels 7 and 8	63
Table 5-8 Sludge bounds inside DST	65
Table 5-9 Waste description inside DST	65
Table 5-10 Gamma dose rates of sludge towards outer tank	67
Table 5-11 Weight loss and corrosion rate of bullet coupons after two months exposure in GW simulant pH 5	69
Table 5-12 Weight losses and corrosion rates for carbon steel coupons exposed to LDP and GW simulants for 4 months at 45 °C.....	70

LIST OF FIGURES

Figure 4-1 Side picture of the bullet (top) and frontal top picture of the bullet (bottom).....	20
---	----

Figure 4-2 Two coupons mounted individually in epoxy cold mount with wire.....	24
Figure 4-3 Picture of the stainless-steel rod with one coupon hanged at the top and intermediate location and three coupons at the bottom.	25
Figure 4-4 Picture of the Vapor Space Corrosion setup inside the walk-in hood.....	28
Figure 4-5: Picture of a 500 mL glass jar containing the formulation VpCI®-337 from Cortec®	29
Figure 4-6: Mounted carbon steel coupons and ER probe element after being dipped in VCI.	29
Figure 4-7 Data-logger and one of the ER probes used for ER measurements	30
Figure 4-8: Noise Equivalent Concentration QEPAS results with corresponding laser wavelength. The blue, green, and red symbols indicate values in the ppm, ppb, and ppt concentration ranges, respectively [17].	30
Figure 4-9 QEPAS measurements of NH ₃ at varying concentrations.....	31
Figure 4-10 Bullet coupons attached to a modified cap for long-term immersion testing.....	32
Figure 4-11 Long-term corrosion setup showing the two glass water baths on top of individual hotplates.	33
Figure 5-1 Potentiodynamic (a) and G192 test plot (b) for conditions described in Test 22.....	35
Figure 5-2 Example of Log-Log Plot Demonstrating Relationship Between Inhibitor and Aggressive Species [22]	39
Figure 5-3 Pitting Factor as a Function of pH for the experimental “fail” conditions.....	41
Figure 5-4 Pitting Factor as a Function of pH for the experimental “pass” conditions.	41
Figure 5-5 Pitting Factor as a Function of pH for the reference “fail” conditions.....	42
Figure 5-6 Pitting Factor as a Function of pH for the reference “pass” conditions.	43
Figure 5-7 Pitting Factor as a Function of pH for the reference “fail” conditions at low TIC.	44
Figure 5-8 Pitting Factor as a Function of pH for the reference “pass” conditions at low TIC.....	45
Figure 5-9 CPP results of (a) Test 24 from Box-Behnken statistical design and (b) Test 6 (with Ammonia)	49
Figure 5-10 CPP results of Test 0 and after pictures	51
Figure 5-11 CPP curve on right and after pictures of bullet sample on left for (a) Test 2 from FY16 report and (b) Test 7.....	52
Figure 5-12 Post-test pictures of carbon steel discs after two and four months of VS exposure in Vessels 3 and 5; concentrated Na DFLAW simulant at 50 ppm and 0 ppm ammonia in humidified air, respectively	54
Figure 5-13 Post-test photographs of carbon steel discs after four months VS exposure in Vessels 2, 4 and 6; dilute Na DFLAW simulant at 550, 50 ppm and 0 ppm ammonia in humidified air, respectively .	55

Figure 5-14 Variations in measured ammonia concentrations under varying pressures and flow rates.....	58
Figure 5-15 Ammonia calibration curve at a flow rate of 50 sccm and pressure of ~260 torr.	58
Figure 5-16 Picture of QEPAS system attached to an exhaust in VSC setup vessel 2 (first vessel from right to left).	59
Figure 5-17 Pictures of (carbon steel coupons after VS exposure at three different levels and immersed in simulant LDP.....	61
Figure 5-18 Pictures of carbon steel coupons after VS exposure at three different levels and immersed in simulant GW	62
Figure 5-19 ER data as metal loss vs. time for probes placed close to Level 1 of vessels 7 and 8. Two probes were placed on each vessel: one inhibited with VpCI®-337 and one without inhibitor	64
Figure 5-20 AY-102 DST modeled in MCNP6 with resulting gamma doses. Red indicates higher gamma dose rates while blue indicates lower gamma dose rates. Intermediate rates from higher to lower are shown in orange, yellow and green (scale units are in cm).	66
Figure 5-21 Diagram of radiolytic and corrosion reactions that can occur at the surface of carbon steel within a droplet of water.....	68
Figure 5-22 Pictures of bullet coupons from GW simulant pH 5 after two months exposure.....	69
Figure 5-23 Pictures of bullet coupons from GW simulant pH 6 and 5 after four-month exposure.....	70
Figure 5-24 OCP vs. time of carbon steel coupons exposed to GW simulants at pH 6 and 5 for partial and complete immersed coupons.....	71

LIST OF ABBREVIATIONS

μCi/cm	Microcurie per cm
ASTM	American Society for Testing and Materials
CPP	Cyclic Potentiodynamic Polarization
DFLAW	Direct Feed Low Activity Waste
DI	Deionized
DNV-GL	Det Norske Veritas-Germanischer Lloyd
DST	Double-Shell Tank
ER	Electrical Resistance
FY	Fiscal year
GW	Ground Water
HARM	Humid Air Radiolysis Model
LAI	Liquid-Air Interface
LDP	Leak Detection Pit
M/h	Moles per hour
MCNP	Monte Carlo N-Particle Code
mpy	Mils per year
NDE	Non-Destructive Evaluation
OCP	Open Circuit Potential
PNNL	Pacific Northwest National Laboratory
PP	polypropylene
PTFE	Polytetrafluoroethylene
QEPAS	Quartz-enhanced Photoacoustic Spectroscopy
QTF	Quartz Tuning Fork
SCC	Stress Corrosion Cracking
sccm	Standard cubic centimeter
SCE	Saturated Calomel Electrode
SRNL	Savannah River National Laboratory
SRS	Savannah River Site
SST	Single-Shell Tank
TAPI	Tank and Pipeline Integrity
TI	Total Immersion
TIC	Total Inorganic Carbon
TIEP-CSG	Tank Integrity Expert Panel-Corrosion Sub-Group
VCI	Volatile Corrosion Inhibitor

VS	Vapor Space
VSC	Vapor Space Corrosion
WRPS	Washington River Protection Solutions
WTIP	Waste Treatment and Immobilization Plant
Z	Atomic number

1.0 Introduction

Hanford Site radioactive waste is currently stored in underground, carbon steel, single-shell tanks (SSTs) and double-shell tanks (DSTs). A corrosion control program for DSTs is currently in place, which includes a waste chemistry requirements that minimize corrosion. The program is overseen by Tank and Pipeline Integrity (TAPI) group from Washington River Protection Solutions (WRPS).

Corrosion testing that provides the technical bases for the corrosion program is directed by the Tank Integrity Expert Panel-Corrosion Sub-Group (TIEP-CSG). The testing is being performed at three independent laboratories: Det Norske Veritas-Germanischer Lloyd (DNV-GL), Savannah River National Laboratory (SRNL), and the 222-S facility at Hanford operated by WRPS. SRNL has been working in studies related to vapor space corrosion (VSC), development of corrosion chemistry limits to mitigate pitting corrosion, and corrosion protection for the tank secondary liner in DSTs.

During fiscal year (FY) 2017, SRNL focused on three primary activities. Task one focused on electrochemical studies for an augmented statistical design at a high concentration of hydroxide (i.e., 1.2 M) and the inhibition effects of ammonia on the new limits chemistries. Additional electrochemical studies of individual organic species and nitrous oxide were tested in tank AN-102 based simulant with no organics to compare inhibiting properties of a specific organic specie and determine if there is a beneficial or deleterious effect on corrosion. The second task was related to VSC studies. The propensity for VSC was investigated by: (1) laboratory simulation of in-tank vapor space exposure, (2) evaluating the effect of ammonia on VSC for dilute and concentrated DFLAW simulants, (3) the effect of Vapor Corrosion Inhibitor (VCI) of carbon steel exposed in vapor space (VS) of Leak Detection Pit (LDP) and ground water (GW) simulants and the rate and extent of corrosion for the carbon steel/VS environment. Finally, the third task focused on enhanced corrosion studies by air radiolysis. The Monte Carlo N-particle (MCNP) code was utilized to model gamma doses near the primary and secondary liner of a DST. The concentration of nitric acid that can be produced by radiolysis and the effect it can have on pH was determined. The effect of these pH changes on the corrosion of carbon steel were studied by a long-term immersion testing using GW simulants at a specific pH.

2.0 Background

A task plan, developed in FY17, consisted of three main tasks for Hanford DSTs corrosion testing. The priorities for the task plan were New Limits testing to determine chemistry control limits for prevention of localized corrosion, long-term testing for VSC and long-term liquid immersion testing at low pH to simulate acidification of ground water due to radiolytic nitric acid production [1]. The three tasks are enumerated and additional details are provided.

2.1 New Limits Corrosion Studies

The chemistry control program at Hanford relies on sodium hydroxide additions for increasing pH and radiolysis reactions occurring within the waste, leading to production of nitrite from nitrate that acts as an inhibitor of carbon steel. Table 2-1 shows the current control program for Hanford DSTs [2]. It illustrates the nitrate range and temperatures for which inhibitor ranges need to be maintained to control corrosion inside the tanks. Presently, several of the DSTs supernate concentrations are well above 1 M hydroxide and thus inhibited from corrosion.

Table 2-1 Double-Shell Tank Waste Chemistry Limits for Corrosion Control

For [NO ₃ ⁻] Range	Variable	For Waste Temperature (T) Range		
		T < 167 °F (75 °C)	167 °F (75 °C) ≤ T ≤ 212 °F (100 °C)	T > 212 °F (100 °C)
[NO ₃ ⁻] ≤ 1.0 M	[OH ⁻]	0.010 M ≤ [OH ⁻] ≤ 8.0 M	0.010 M ≤ [OH ⁻] ≤ 5.0 M	0.010 M ≤ [OH ⁻] ≤ 4.0 M
	[NO ₂ ⁻]	0.011 M ≤ [NO ₂ ⁻] ≤ 5.5 M	0.011 M ≤ [NO ₂ ⁻] ≤ 5.5 M	0.011 M ≤ [NO ₂ ⁻] ≤ 5.5 M
	[NO ₃ ⁻]/ ([OH ⁻] + [NO ₂ ⁻])	< 2.5	< 2.5	< 2.5
1.0 M < [NO ₃ ⁻] ≤ 3.0 M	[OH ⁻]	0.1 ([NO ₃ ⁻]) ≤ [OH ⁻] < 10 M	0.1 ([NO ₃ ⁻]) ≤ [OH ⁻] < 10 M	0.1 ([NO ₃ ⁻]) ≤ [OH ⁻] < 4.0 M
	[OH ⁻] + [NO ₂ ⁻]	≥ 0.4 ([NO ₃ ⁻])	≥ 0.4 ([NO ₃ ⁻])	≥ 0.4 ([NO ₃ ⁻])
[NO ₃ ⁻] > 3.0 M	[OH ⁻]	0.3 M ≤ [OH ⁻] < 10 M	0.3 M ≤ [OH ⁻] < 10 M	0.3 M ≤ [OH ⁻] < 4.0 M
	[OH ⁻] + [NO ₂ ⁻]	≥ 1.2 M	≥ 1.2 M	≥ 1.2 M
	[NO ₃ ⁻]	≤ 5.5 M	≤ 5.5 M	≤ 5.5 M

The chemistry of the waste may change significantly due to retrieval of waste and return streams from the vitrification facility once the facility is online. It has been projected that the chemistry may shift to a broader range of pH and the waste may become more concentrated with aggressive species (e.g., chloride, sulfate, etc.) than is observed in the current waste chemistry. Therefore, the corrosion control program is being evaluated to adapt to anticipated changes in chemistry.

Pitting corrosion testing is being performed using the standardized Cyclic Potentiodynamic Polarization (CPP) test developed by TIEP-CSG [3] and presented in

Table 2-2.

Table 2-2 Standardized CPP protocol with the parameters utilized for testing

Parameters	Results
Potential Stabilization (hrs.)	2
Start Potential (V vs. OCP)	-0.05
Scan Rate (mV/s)	0.167
Vertex Threshold (mA/cm ²)	1
Finish Potential (V vs. OCP)	0
Sample geometry	bullet
Surface Preparation	600 grit

New Limits testing was initiated in FY16 using a test matrix which was derived by applying Plackett-Burman and Box-Behnken statistical design. The test matrix was used to evaluate pitting corrosion susceptibility at nitrate concentrations from 0.5 to 2 M [4] and to confirm data from Argentina [5]. The data analysis showed that nitrate and chloride were the statistically significant aggressive species while hydroxide and nitrite were the statistically significant inhibitor species.

2.2 Vapor Space Corrosion Testing at SRNL

Vapor space corrosion inside the DSTs at Hanford has occurred in some instances to equipment suspended above the liquid, although no consequential incidents have been reported to date. Testing VSC in a laboratory setting presents a series of challenges since the vapor chemistry is unstable and can change depending on evaporation and condensation of droplets. Previous studies have investigated the mechanism of VSC to obtain the chemical composition of the liquid condensed from vapor space [6] and utilized simulated waste environments to examine corrosion mechanisms [7],[8]. Pacific Northwest National Laboratory (PNNL) found that ammonia and carbon dioxide are the dominant species in the vapor phase that influence carbon steel corrosion. Ammonia has been shown to inhibit VSC [9],[10], whereas carbon dioxide reacts with hydroxide and depletes that inhibitor. Ammonia has been measured inside the tanks and the concentration can vary but it can be as high as 550 ppm (obtained in Tank SY-102). Ammonia in the vapor space is produced through thermal and radiolytically induced reactions between organic waste components and nitrate and nitrite ions.

SRNL studies of VSC were performed during FY14 at different heights above the liquid using 50 and 550 ppm of ammonia in air [11]. Four months of testing with simulants demonstrated that as little as 50 ppm ammonia in the vapor space could inhibit VSC. Testing with LDP and GW simulants at the exterior of tank AY-102 and the possibility of VSC attack for samples close to the liquid level was observed [11]. FY15 testing continued using 0.4 M nitrate simulant at 0.15 nitrite/nitrate ratio using 50 and 550 ppm ammonia at vapor space. Similar conclusions were observed with 50 ppm of ammonia helping to inhibit VSC with coupons located in the vicinity of the liquid level showing more VSC than coupons at elevated levels [12].

During FY16, VSC studies were performed using 50 ppm ammonia and no ammonia in air with a 0.75 nitrite/nitrate ratio simulant at pH 11 and 13. After four months no appreciable corrosion was observed with even less corrosion for the coupons exposed at 50 ppm ammonia. VSC tests with LDP and GW simulants were performed using a VCI to polished and corroded carbon steel coupons. The VCI used was effective in reducing VSC for polished coupons with no appreciable change observed for previously corroded coupons [4].

2.3 Liquid Air Interface and Total Immersion Corrosion testing of LDP and GW simulants at SRNL

Long-term immersion experiments using LDP and GW simulants started in FY14 using partially immersed and completely immersed coupons. The carbon steel corrosion rates were approximately 10 mpy [11],[12] in both partially and completely immersed coupons. pH and Open Circuit Potential (OCP) was recorded daily. The corrosion sub-group inquired as to whether this occurred due to an interaction between the air environment and the solution.

FY16 tests were performed to delineate the effect of air and simulant interface on corrosion. It was determined that at low concentrations of bicarbonate, as in LDP and GW simulants, primarily form am- $\text{Fe}(\text{OH})_3$ with adsorbed bicarbonate or carbonate ions, and lepidocrocite and magnetite [13]. Furthermore, the gradient in concentration that can exist in the solution due to the continuous formation of the mineral phases can contribute in increasing the interfacial pH. Although, the results for FY16 did not conclusively determine that the pH shift was due to corrosion of steel, they seem to corroborate the mechanism of bicarbonate depletion via corrosion of carbon steel [4].

3.0 Task Description and Activities

Several tasks were performed during FY17 and are described in the sections below.

3.1 Task 1: New Limits Testing

Statistical design methods were used to test matrix to include higher hydroxide concentrations (i.e., from 0.6 to 1.2 M) in the pitting model. Interior points, based on previous new limits testing, were also included in the statistical design. Additionally, ammonia effects and the presence of some organics and nitrous oxide in a AN-102 based simulant were evaluated. The standardized CPP protocol was utilized. The results for this task are organized in sections 5.1, 5.2 and 5.3.

3.2 Task 2: Vapor Space Corrosion for DSTs

Legacy carbon steel coupons were exposed to VSC conditions for four months. Solutions were based on dilute and concentrated DFLAW, LDP and GW simulants. Carbon steel coupons were located at three different heights above the simulant to mimic different conditions inside the DST. These conditions were (1) the carbon steel is exposed to a wet/dry cycle with the waste; (2) the carbon steel was wetted at some point and subsequently exposed to humid air only, and (3) carbon steel that was never wetted by the waste and therefore only exposed to humid air. This task was divided in three parts. Part A studied the effects of ammonia inhibition on carbon steel for dilute and concentrated DFLAW simulants. Part B was dedicated to the development of an ammonia sensor for the exhaust of the VSC setup. Part C evaluated the performance of a vapor corrosion inhibitor (VCI) that may be useful in preventing corrosion of the secondary liner. A more detailed description is presented in the next page for each subtask.

3.2.1 *Part A: Ammonia inhibition VSC testing*

The objective of this test was to compare VSC on carbon steel coupons exposed to DFLAW simulants at ppm levels of ammonia in humidified air versus humidified air only. The tests were conducted at 40 °C. The results for this part are shown in section 5.4.

3.2.2 *Part B: Ammonia detection with Quartz-Enhanced Photoacoustic Spectroscopy probe*

The objective for this task was to assess capabilities of the Quartz-Enhanced Photoacoustic Spectroscopy (QEPAS) sensor. Eventually the sensor will be attached to the exhaust of the VSC apparatus to detect the ammonia present. Calibration results for the sensor are presented in section 5.5.

3.2.3 *Part C: VCI for DST secondary liner*

VSC tests, with VpCI®-337 from Cortec® as the VCI, were performed. The test temperature for the vessels was 45 °C. Humidified air was flowing through the vapor space. VCI was applied by dipping the coupons into solution and putting them on a surface for a few hours to partially drying them, and then placing them at different levels inside the vessels. Two ER probes were placed close to Level 1 (i.e., approximately 1" above simulant liquid level) in each of the two vessels. One probe for each vessel was dipped in VpCI®-337, while the second was left without any treatment. After two months, the probe with no treatment was dipped in VpCI®-337 to determine if the corrosion

rate decreases. The objective of this subtask was to measure inhibition effect of the VCI in-situ using a corrosion monitoring technique to determine the efficacy of the VCI for inhibition for solutions near the secondary liner of Hanford DSTs. The results for this part are presented in section 5.6.

3.3 Task 3: Enhanced corrosion due to air radiolysis

Enhanced corrosion due to air radiolysis was investigated using a MCNP code to determine gamma doses near the primary and secondary liner of Hanford DSTs. A Humid Air Radiolysis Model (HARM) was used to calculate the production of nitric acid due to humid air radiolysis. The effect of radiolysis was determined by changing the solution pH to study a worst-case, low pH scenario. A ground water simulant was adjusted at two pH values: 6 and 5 and maintained during the test. Two coupons were placed in each solution: one partially immersed and another fully immersed. The results obtained for this task are presented in section 5.7.

4.0 Experimental Procedure

The carbon steel utilized for this testing was fabricated from AART128 Rail Car Steel. This steel was selected for testing since it approximates the chemistry and microstructure of American Society for Testing and Materials (ASTM) A515, Grade 60 carbon steel, the steel from which the tanks were fabricated [14]. This steel is approximately the same vintage as the tank steel. The chemical composition of the steel is shown in Table 4-1. DNV-GL identified this material as DNV-GL ID# 2232.

Table 4-1 Chemical Composition of AART128 Rail Car Steel

	C	Mn	P	S	Si	Fe
Specification (wt%)	0.24 (max.)	0.9 (max.)	0.035 (max.)	0.04 (max.)	0.13 to 0.33	Balance
Measured (wt%)	0.212	1.029	0.012	0.013	0.061	Balance

In the next pages are the experimental details and conditions in which the carbon steel was used and prepared for electrochemical testing, VSC and Total Immersion (TI)/LAI long immersion testing.

4.1 Electrochemical Testing of Simulants

4.1.1 *Material sample*

The electrochemical testing was performed with “bullet” electrodes that had dimensions: 0.188 in diameter and 1.25 in long (Metal Samples Company part number EL-400). Figure 4-1 shows a picture of the sample after being polished and rinsed. The surface of the shank and nose of the bullet are shown. Before testing, a drill was used to polish the sample to a 600-grit finish. After they were rinsed with deionized (DI) water and acetone, the bullets were examined visually, in some cases with a stereomicroscope, for any defect and to ensure that the sample had a uniform

surface with no initial blemishes. The electrode was attached to a stainless-steel rod protected by a glass holder. A polytetrafluoroethylene (PTFE) fixture was used to prevent liquid contact with the stainless-steel rod and therefore to ensure electrical isolation.

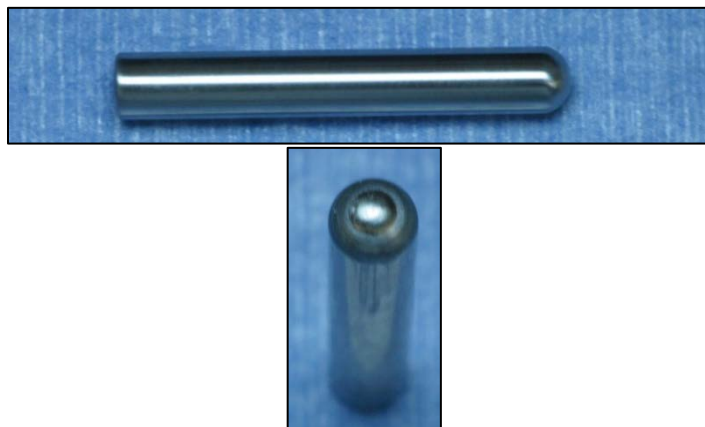


Figure 4-1 Side picture of the bullet (top) and frontal top picture of the bullet (bottom)

4.1.2 *Simulants*

Simulants prepared for the new limits testing at high hydroxide concentration are shown in Table 4-2. The statistical software JMP® v. 11.1.1 from SAS Institute Inc. was used to make the test matrix. The last three tests (highlighted in yellow) were used to provide statistical significance for the augmented statistical design to 1.2 M hydroxide and to tie previous electrochemical testing from FY16 [4]. In addition to these tests, interior points, near boundaries of the corrosion control limit were statistically selected to evaluate the robustness of the model. These points are shown in Table 4-3.

The statistical software package was also utilized to develop a matrix of conditions to evaluate ammonia inhibition effects for pitting corrosion. The simulant compositions to test ammonia effects are presented in Table 4-4.

Solutions were also prepared, based on AN-102 simulant, to evaluate the impact of organic species known to exist in the DST wastes. Since the wastes also contain nitrous oxide, tests were also performed with this compound. The results were compared with the AN-102 based simulant without organics (Table 4-5).

Table 4-2 High hydroxide statistically selected simulant chemistries

Test	Temperature (°C)	Hydroxide (M)	Nitrite (M)	Nitrate (M)	Chloride (M)	Sulfate (M)	Carbonate (M)
1	35	1.2	0	3.75	0	0.13	0.1
2	35	1.2	0	4.75	0	0.07	0.1
3	35	1.2	0	3.1	0.08	0.09	0.1
4	35	1.2	0	2.42	0.16	0.08	0.1
5	35	1.2	0	4.5	0.2	0.03	0.1
6	35	1.2	0	0.94	0.24	0.01	0.1
7	35	1.2	0	0.26	0.32	0.17	0.1
8	35	1.2	0	4.75	0.35	0.07	0.1
9	35	1.2	0	0	0.4	0.02	0.1
10	35	1.2	0.6	4.74	0.08	0.02	0.1
11	35	1.2	0.6	5.32	0.15	0	0.1
12	35	1.2	0.6	3.31	0.16	0.2	0.1
13	35	1.2	0.6	2.68	0.24	0.05	0.1
14	35	1.2	0.6	4.92	0.28	0.06	0.1
15	35	1.2	0.6	1.26	0.32	0.01	0.1
16	35	1.2	0.6	0.63	0.4	0.17	0.1
17	35	1.2	0.6	5.32	0.4	0.01	0.1
18	35	1.2	1.2	4.01	0.16	0.15	0.1
19	35	1.2	1.2	4.17	0.21	0.01	0.1
20	35	1.2	1.2	3.4	0.24	0.1	0.1
21	35	1.2	1.2	1.99	0.32	0.09	0.1
22	35	1.2	1.2	4.57	0.32	0.13	0.1
23	35	1.2	1.2	1.38	0.4	0.01	0.1
24	35	1.2	1.2	4.17	0.4	0.01	0.1
25	35	0.3	0.6	2.75	0.2	0.15	0.1
26	35	0.3	0.6	2.75	0.2	0.07	0.1
27	35	0.3	0.6	2.75	0.2	0.05	0.1

Table 4-3 Statistically selected New Limits interior points

Test	Temperature (°C)	Hydroxide (M)	Nitrite (M)	Nitrate (M)	Chloride (M)	Sulfate (M)	Carbonate (M)	Bicarbonate (M)
1	35	0.3	1.2	0	0	0.2	0.1	0
2	35	0.3	0	0	0	0	0.1	0
3	35	0.3	1.2	0	0.4	0.2	0.1	0
4	35	0.3	1.2	0	0	0	0.1	0
5	35	0.3	1.2	5.5	0.4	0	0.1	0
6	35	1.2	1.2	0	0	0.2	0.1	0
7	35	0.3	0	5.5	0.4	0.2	0.1	0
8	35	0.3	0	5.5	0.4	0.2	0.1	0
9	35	0.3	0	5.5	0.4	0.2	0.1	0
10	35	0.3	0	0	0.4	0	0.1	0
11	35	0.0001	1.2	0.8	0	0.2	0.075	0.025
12	35	0.0001	0.9	0.6	0.025	0.16	0.075	0.025
13	35	0.0001	0.6	0.4	0.05	0.12	0.075	0.025
14	35	0.0001	0.3	0.2	0.075	0.08	0.075	0.025
15	35	0.0001	0	0	0.1	0.04	0.075	0.025

Table 4-4 Statistically selected simulants to test ammonia effects

Test	Temperature (°C)	Hydroxide (M)	Nitrite (M)	Nitrate (M)	Chloride (M)	Sulfate (M)	Ammonium Nitrate (M)	Carbonate (M)
1	35	0.01	0	0	0.4	0.2	0.25	0.1
2	35	0.3	0.6	2.75	0.2	0.1	0	0.1
3	35	1.2	0	5.5	0.4	0	0.25	0.1
4	35	0.01	0	5.5	0.4	0	0	0.1
5	35	1.2	0	0	0.4	0.2	0	0.1
6	35	0.605	0.6	2.75	0.2	0.1	0.125	0.1
7	35	0.01	1.2	5.5	0.4	0.2	0	0.1
8	35	1.2	1.2	5.5	0.4	0.2	0.25	0.1
9	35	0.01	0	5.5	0	0.2	0.25	0.1
10	35	0.01	1.2	0	0	0.2	0	0.1
11	35	0.01	0	0	0	0	0	0.1
12	35	0.3	0.6	2.75	0.2	0.1	0	0.1
13	35	1.2	1.2	0	0.4	0	0	0.1
14	35	0.01	1.2	0	0.4	0	0.25	0.1
15	35	0.01	1.2	5.5	0	0	0.25	0.1
16	35	1.2	1.2	5.5	0	0	0	0.1
17	35	1.2	1.2	0	0	0.2	0.25	0.1
18	35	1.2	0	0	0	0	0.25	0.1
19	35	0.3	0.6	2.75	0.2	0.1	0	0.1
20	35	1.2	0	5.5	0	0.2	0	0.1

Table 4-5 AN-102 based simulant with an individual organic specie and nitrous oxide

Test	Temperature (°C)	Nitrate (M)	Nitrite (M)	Hydroxide (M)	Organic, Concentration (M)
0	40	1.1	0.5	0.01	No organic
1	40	1.1	0.5	0.01	Ammonia, 0.25
2	40	1.1	0.5	0.01	Iminodiacetic Acid, 0.25
3	40	1.1	0.5	0.01	N-Butylamine, 0.25
4	40	1.1	0.5	0.01	Dibutylphosphate, 0.25
5	40	1.1	0.5	0.01	Glycine, 0.25
6	40	1.1	0.5	0.01	Nitrous Oxide, saturated
7	40	1.1	1	0.05	Nitrous Oxide, saturated

4.1.3 Testing Apparatus

Approximately 700 mL of simulant was added to a glass cell that is similar to the cell for corrosion studies designed by Princeton Applied Research (AMETEK). Two carbon graphite rods served as the counter electrode. A saturated calomel electrode (SCE) was used as the reference electrode. Prior to each test, the electrode was checked against a standard before testing (a SCE in 1 M KCl solution not used for testing). The SCE was placed in a bridge containing 0.1 NaNO₃ solution only for solutions with pH 10. For solutions with high pH (i.e. higher than 12), the reference electrode was placed in the simulant. The cell was placed on top of a hotplate with temperature control. REF600 (Gamry) potentiostats were used in this study. Prior to initiating the electrochemical tests, ASTM G5 [15] was performed for quality assurance. ASTM G5 protocols were also run at the conclusion of testing. The standardized CPP protocol was used to gather the data.

4.2 Vapor Space Corrosion Testing

4.2.1 Materials

Circular coupons were cut at the SRNL machine shop from legacy carbon steel. The coupons were 0.625 inch diameter with a thickness of 0.125 inch and polished to a 600 grit finish. The coupons were engraved to identify them. A coated wire was placed in a lateral position to be able to hang the coupons with no electrical connection to the coupon. The coupons were mounted with a two-part clear epoxy solution (EpoKwick® from Buehler) so that one face of the coupon was exposed. Excess epoxy mixture was used with a wood stick to cover around the edges of the discs in cases that the mount did not adhere completely to the sides of coupons. This was done to prevent or minimize crevice corrosion attack.

Prior to using the coupons, they were rinsed with DI water, then acetone and blown dry with air. The coupons are shown in Figure 4-2. Excess epoxy mixture can be seen on the side of the right coupon.

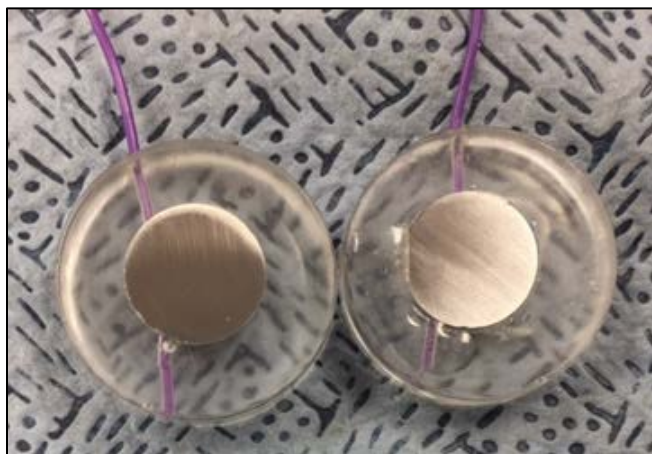


Figure 4-2 Two coupons mounted individually in epoxy cold mount with wire

Coupons were suspended from stainless steel rings that are welded to a stainless-steel rod at three different locations. Two configurations were used depending on the test. For vessels 2, 3, 4, 5 and 6, one coupon was placed at the top and intermediate location of the rod, three at the bottom. This

configuration is shown in Figure 4-3. For vessels 7 and 8, two coupons were placed at the top and intermediate location of the rod and six at the bottom. For all rods, one coupon at the bottom ring was placed lower so it can be continuously immersed in solution.



Figure 4-3 Picture of the stainless-steel rod with one coupon hanged at the top and intermediate location and three coupons at the bottom.

4.2.2 Simulants

VS simulant compositions for each vessel are described in Appendix E. Test conditions for each vessel are shown in Table 4-6.

Table 4-6 Test conditions for VSC testing

Vessel	Solution	Initial pH	Ammonia gas concentration in Air (ppm)	Temperature (°C)
2	Dilute Na DFLAW	10	550	40
3	Concentrate Na DFLAW	10	50	40
4	Dilute Na DFLAW	10	50	40
5	Concentrate Na DFLAW	10	0	40
6	Dilute Na DFLAW	10	0	40
7	Leak Detection Pit	7.6	0	45
8	Ground Water	7.6	0	45

Seven vessels were used. The first five vessels (i.e., 2, 3, 4, 5 and 6) had a composition representing dilute and concentrated DFLAW simulant. The waste chemistry simulant constituents are shown in Table 4-7. Vessels 2, 4 and 6 had the dilute simulants and vessels 3 and 5 had the concentrated simulant chemistry. The composition of the DFLAW simulants were obtained from corrosion studies dedicated to DFLAW corrosion testing, which is still being compiled for a final report. Memos detailing some of the testing are provided in Appendix J. Ammonia in air at was humidified with their respective simulant and flowed through for Vessel 2 at 550 ppm and for Vessels 3 and 4 at 50 ppm.

Table 4-7 Chemical composition of the DFLAW tested simulants

Simulant	Concentration (M)				NO ₂ /NO ₃ ratio
	NaCl	NaNO ₂	Na ₂ SO ₄	NaNO ₃	
Concentrate Na DFLAW (6)*	0.26	2.67	0.18	2.4	1.11
Dilute Na DFLAW (13)*	0.02	0.5	0.1	1.3	0.38

*the number inside the parenthesis indicate the test number from DFLAW memo SRNL-L4400-2017-0018 in Appendix J.

For four vessels (5, 6, 7 and 8), air was humidified with the respective simulant for that vessel. The remaining two vessels, Vessels 7 and 8 had a chemical composition representing the LDP residue and GW found near the secondary liner in the tank AY-102, respectively.

4.2.3 Testing Apparatus

The VSC apparatus is shown in Figure 4-4. Eight glass columns were prepared by the SRNL glass shop for FY14 testing and seven of them were reused this year. These columns are fixed with holding rings that were mounted on an aluminum frame inside a walk-in hood. The columns have dimensions of 1 m by 15 cm and consist of a jacketed glass vessel connected to a glass tube, which is closed at the top with a glass cap. Approximately 1 L of simulant was added to each vessel and the temperature was monitored with a temperature reader (Omega). The gas cylinders provided ammonia gas (550 ppm and 50 ppm) to three of these vessels (Vessel 2, 3 and 4). The cylinders were connected to a mass flow controller and a flowmeter at each gas concentration to maintain a

flow of 5 sccm. Air was used for the remaining vessels and was diverted to four different flowmeters to supply constant air at 5 sccm. Vessel 2, 3, 4, 5 and 6 (from right to left) were connected in parallel to a water circulator that maintained the simulant temperature at 40 °C. The last two vessels from right to left were connected to a water circulator to maintain a simulant temperature of 45°C. Additionally, these vessels were modified to have two additional ports for electrical resistance (ER) probes. The ammonia in air gas and air were bubbled through a bottle filled with the corresponding simulant to humidify the gas before it entered the column. The rods containing the coupons were placed inside the vessels. They simulate different vapor space conditions. These levels are described as follows:

Level 3: Top or high level. This set of coupons was not exposed to the solution prior to testing. The coupons were suspended approximately 36 inches above the simulant. This level is representative of a tank vapor space region that is only exposed to the humidified air, the ammonia (if applicable), and any volatile species from the solution.

Level 2: Intermediate or middle level. The coupons were dipped in simulant for five minutes prior to testing. The coupons were hung at the middle-fixed ring approximately 18 inches above the liquid. This level is representative of a vapor space region of the tank that at one time was exposed to waste, but now has infrequent or no contact with the waste. However, this region is exposed to the humidified air and/or the ammonia gas in air.

Level 1: Bottom or low level. The coupons were dipped in simulant for five minutes prior to testing. The coupons were hung at the bottom fixed ring. These coupons were suspended approximately 1 inch above the liquid level of the simulant. Once every two weeks the coupons were lowered into the simulant for 5 minutes. This level is representative of a vapor space region of the tank that experiences periodic wetting/drying. This sequence could occur due to: a) waste transfers into and out of the tank, b) splashing due to flushing operations, and/or c) solution “creep” above the liquid air interface.

Testing of the coupons in vapor space environment was performed for four months. Specimens at level 1 were removed after two months (i.e., one coupon for vessels 2, 3, 4, 5 and 6 and two coupons for vessels 7 and 8 for a total of 9 coupons). For Level 2, 3, and the immersed coupons, the specimens remained for four months. Coupons were removed from the epoxy cold mount using a special tool and cleaned using ASTM G1 Clarke solution [16] to remove corrosion products and report accurate weight losses.



Figure 4-4 Picture of the Vapor Space Corrosion setup inside the walk-in hood

4.2.4 VCI for the suppression of corrosion of carbon steel exposed in LDP and GW simulants

A VCI strategy is being considered to help minimize VSC of carbon steel for the secondary liner of the tanks. Features that are being considered for selection are handling ease, biodegradability and effectiveness in coating surfaces with protection that can last several years. In discussions with WRPS, several strategies are being considered for deployment of the product under the secondary liner and annulus. It is being considered an atomization technique as well as pumping in and out the inhibitor mixed with water.

The vapor corrosion inhibitor that was used on FY16, VpCI®-337, showed some promise. The sample bottle containing VpCI®-337 is pictured in Figure 4-5. The coupons and an ER probe with a metal shield are displayed in Figure 4-6. The ER probe used and data-logger were obtained from Metal Samples. Carbon steel alloy C1010 was utilized instead of legacy carbon steel due to availability and cost. The data-logger used was model MS4500E. The probe and logger are shown in Figure 4-7. The coupons were mounted in the stainless-steel rod and placed inside the glass vessel for exposure for four months.



Figure 4-5: Picture of a 500 mL glass jar containing the formulation VpCI®-337 from Cortec®

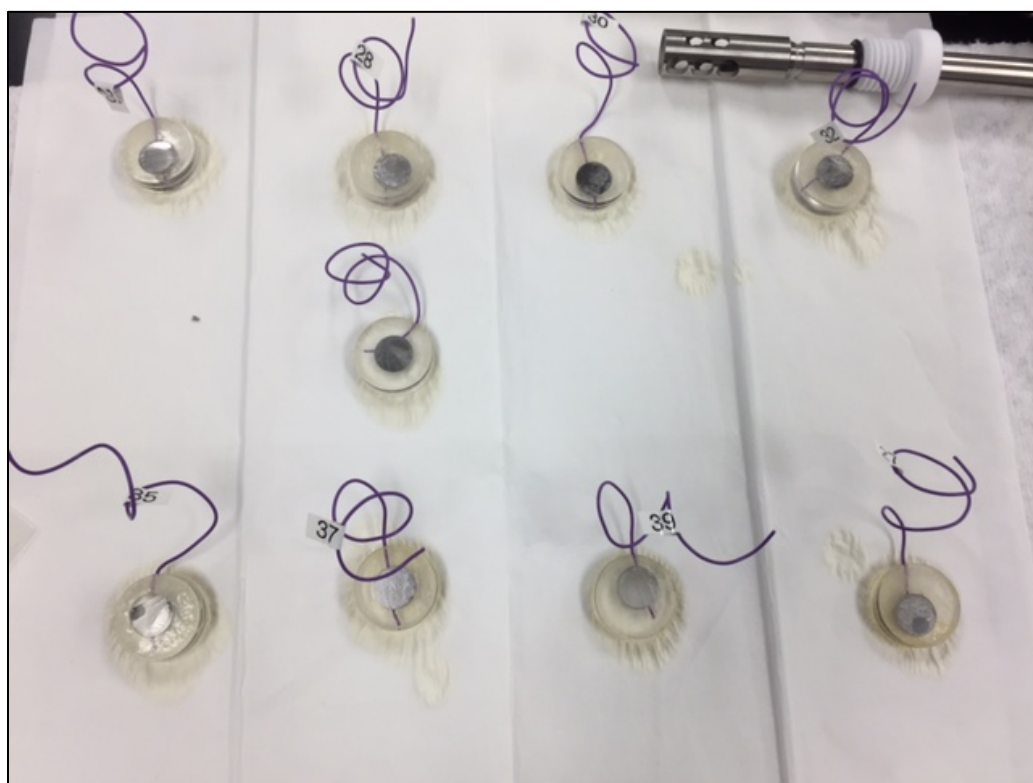


Figure 4-6: Mounted carbon steel coupons and ER probe element after being dipped in VCI.



Figure 4-7 Data-logger and one of the ER probes used for ER measurements

4.2.5 Gas sensing probe for ammonia detection

Quartz-enhanced photoacoustic spectroscopy (QEPAS) is a pass-through type method for measuring trace impurities in gas streams. A previous report provides a more detailed description [4] about QEPAS. The principle behind the sensor is that a gas is excited with a laser and this in turn gives a frequency that can be picked up acoustically using a quartz-turning fork (QTF). Figure 4-8 shows the noise equivalent concentration with corresponding laser wavelength of the QEPAS for investigated gases from Patimisco et al. [17].

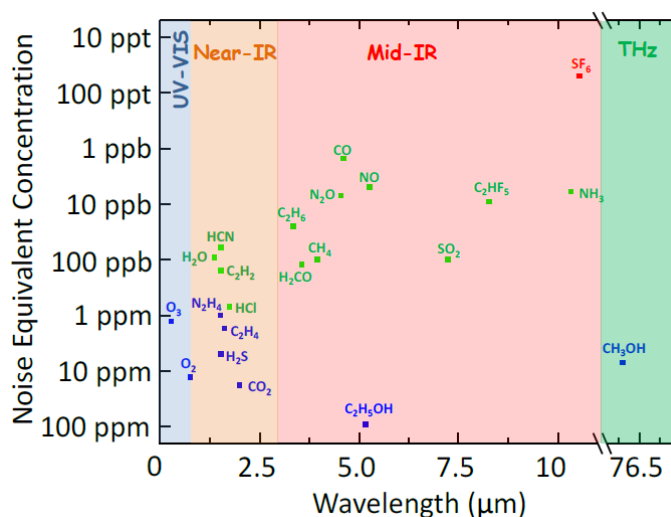


Figure 4-8: Noise Equivalent Concentration QEPAS results with corresponding laser wavelength. The blue, green, and red symbols indicate values in the ppm, ppb, and ppt concentration ranges, respectively [17].

The QEPAS system at SRNL has been tuned to monitor both ammonia (NH_3) and methane (CH_4) in gas streams at varying pressures with detection limits as low as 2 ppm for NH_3 and 10 ppm for CH_4 . It was tested and calibrated during FY16 for ppm levels of ammonia in air concentrations [4]. As shown in Figure 4-9, the QEPAS system could detect all concentrations accurately with an error of approximately 6%. This error/noise is expected to decrease as the system is further tuned for its current operating environment.

QEPAS Measurement of NH_3

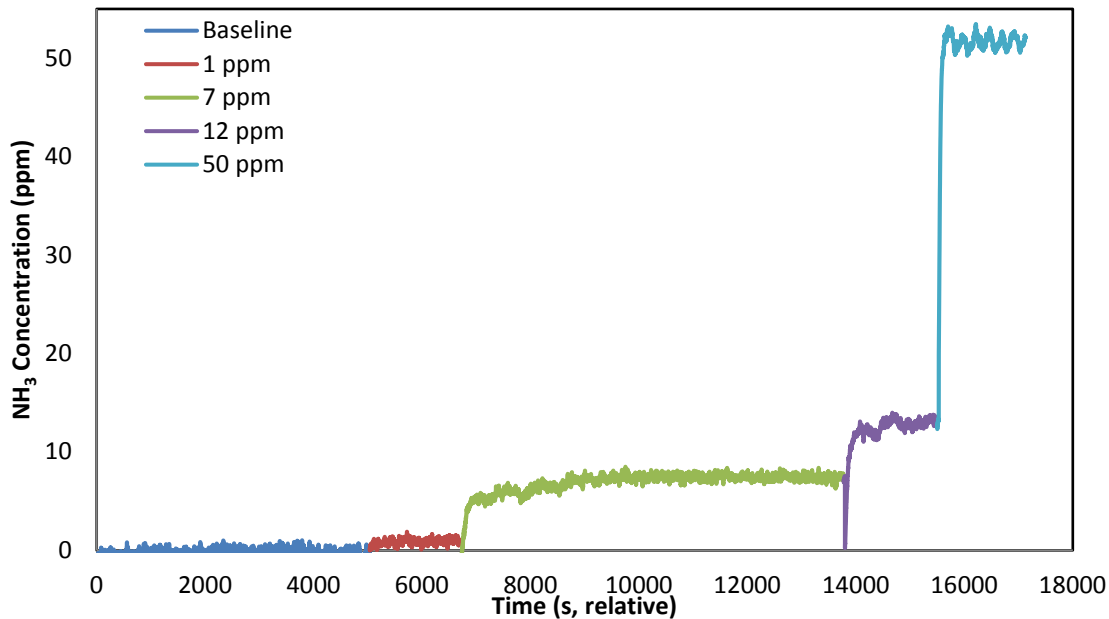


Figure 4-9 QEPAS measurements of NH_3 at varying concentrations

4.3 Liquid Air Interface and Total Immersion Corrosion Testing

4.3.1 *Materials*

The bullet electrodes were also utilized for these tests. Before placing in the test, a drill was used to polish the sample to a 600-grit finish. Then they were rinsed with DI water and acetone. The carbon steel bullet was attached to a stainless-steel rod protected by a glass and placed inside rubber stoppers on a plastic cap to fix it in place for long term testing. A PTFE fixture was used to prevent liquid contact with the stainless-steel rod and ensure electrical isolation. Figure 4-10 shows the two bullet coupons placed in one of the caps. The two different lengths were maintained to ensure one bullet coupon was partially immersed (i.e., LAI) and another was completely immersed (i.e., TI) during the test.



Figure 4-10 Bullet coupons attached to a modified cap for long-term immersion testing

4.3.2 *Simulants*

TI corrosion tests were conducted using GW solutions that simulate the environment on the exterior of AY-102 secondary liner at two different pH: pH 6 and 5. The chemical composition for the simulants can be found in Appendix G. The test temperature was 45 °C.

4.3.3 *Testing Apparatus*

The testing for this task was performed in 1 L polypropylene (PP) containers. The setup is shown in Figure 4-11. As observed, two glass water baths are on top of individual hot plates. A flowmeter supplied air using Tygon® flexible tubing to the humidifier that circulated the humidified air into the two containers. Styrofoam packaging was placed inside the water bath to minimize water evaporation. The temperature of the bath was controlled by placing the hotplate thermocouple into the water surrounding the plastic containers. The flow of air was maintained at 5 to 10 sccm.

The caps of the bottles were modified with holes. Orange stoppers were used to connect the Tygon® tubing and provide an inlet and outlet flow of humidified air and, also, to maintain the glass holders containing the stainless-steel rods in place. The stoppers were sealed with silicone to prevent air leakage. A hole in the middle was used to provide access to a pH probe, a thermocouple, and a reference electrode. The hole was closed off with a rubber stopper when not in use.

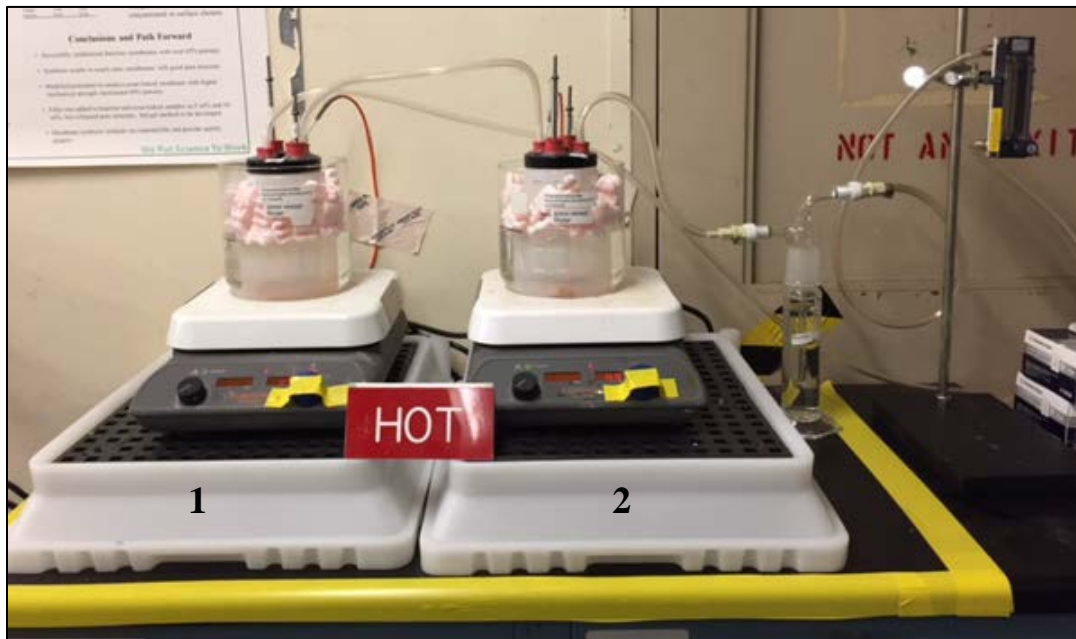


Figure 4-11 Long-term corrosion setup showing the two glass water baths on top of individual hotplates.

Each bottle contained 600 mL of the specified simulant. The bottles were placed inside the glass bath and water was added to reach similar level as the liquid inside the container. The level inside was marked outside the container to account for losses during testing. DI water was added periodically to the glass bath to maintain the same level. Make-up DI water was added in some instances to the containers to also maintain the LAI level, although on a less frequent basis.

pH, temperature and OCP were measured daily during working days. The pH typically trended toward higher values and was adjusted by using acetic acid to decrease pH to reach the desired value. In the instance that the pH was adjusted lower than the desired value (i.e., 0.1 lower), the pH was restored with sodium hydroxide concentration solutions of 0.1 and 0.01 M. The coupons were maintained at this temperature and pH for four months.

At the end of testing the coupons were removed and cleaned using Clarke solution [15] and weight losses were recorded. Table 4-8 shows a summary of the conditions for each container.

Table 4-8 Simulant conditions for each vessel

Container	Temperature (°C)	Simulant	pH
1	45	GW	6
2	45	GW	5

5.0 Results and Discussion

Cyclic potentiodynamic polarization curves and photograph of the samples after testing are shown in Appendices A, B, C and D for the augmented statistical design to 1.2 M Hydroxide, interior points, ammonia effects and AN-102 with an organic specie and nitrous oxide, respectively. Pictures of the coupons after exposure for Tasks 2 and 3 are shown in Appendix F and H, respectively. The results and discussions are enumerated by the various tasks and corresponding subtasks.

5.1 New Limits

Electrochemical testing was continued in FY17 to address pitting corrosion over an entire range of anticipated DST concentrations. The primary objective of this task is to target gaps in the corrosion control program such as pH range between 10 and 13.5, chloride concentrations up to 0.4 M and sulfate concentrations up to 0.2 M to evaluate pitting corrosion. In addition, inhibitor (i.e., managing the total inhibitor concentration added) and sodium concentration optimization will eventually be assessed.

During FY16, the dominant variables affecting pitting corrosion were determined from Plackett-Burman and Box-Behnken statistical design matrices. Details about this testing are compiled in a previous report [4]. The logistic regression approach was adopted for data analysis. The “pass” or “fail” condition was determined from the six categories specified by the pitting test protocol. More information on the categories can be found elsewhere [18]. Categories 1 and 2 were assigned a “0” or pass rating, while categories 4, 5, and 6 were assigned a “1” or fail rating. A category 3, or mixed hysteresis condition that was considered inconclusive, was re-tested using the ASTM G192 test method [19]. The ASTM G192 method is based on the Tsujikawa-Hisamatsu Electrochemical (THE) method derived from the two Japanese researchers that developed the technique [20] and can be used to determine repassivation potentials. In this case, it was used to provide a definite categorization of pass or fail for borderline cases that showed mixed hysteresis. If the results was a pass, “0” was used and if it was a fail “1” was used.

For FY17, the original FY16 test matrix was augmented to include hydroxide concentrations up to 1.2 M [4]. The statistically designed matrix for 1.2 M hydroxide concentration is shown in Table 4-2. The matrix consisted of 24 tests with additional 3 tests that were previously tested in FY16. These latter tests are referred to as statistical “anchor” data. The CPP results with after testing pictures of bullets are presented in Appendix A for original and duplicate experiments. Table 5-1 shows the results of the electrochemical testing based on category, pitting on sample and logistic approach. As observed, there were 4 tests with category 3, 18 tests with category 1, and 3 tests category 5. There was one instance, test 14, in which the categories and the pitting on sample was not consistent between the sample and duplicate.

An example, see Test 22, of the modified ASTM G192 test is shown in Figure 5-1. A potentiodynamic scan was performed after the OCP had been monitored for 2 hours. The scan was continued until the current density reached 1 mA/cm² at 0.5 V vs. SCE. Then, galvanostatic current was maintained at that voltage for 4 hours to allow pits to form and grow. The potential was decreased stepwise, and the current decayed to the passive current density after just three potentiostatic steps. The current density went below the passive current density at 0.10 V vs. SCE. This potential is known as the repassivation potential. Since it is greater than 200 mV higher than

the initial OCP, the test was re-categorized to a “2” and designated as a “pass” or “0” condition for the logistic approach.

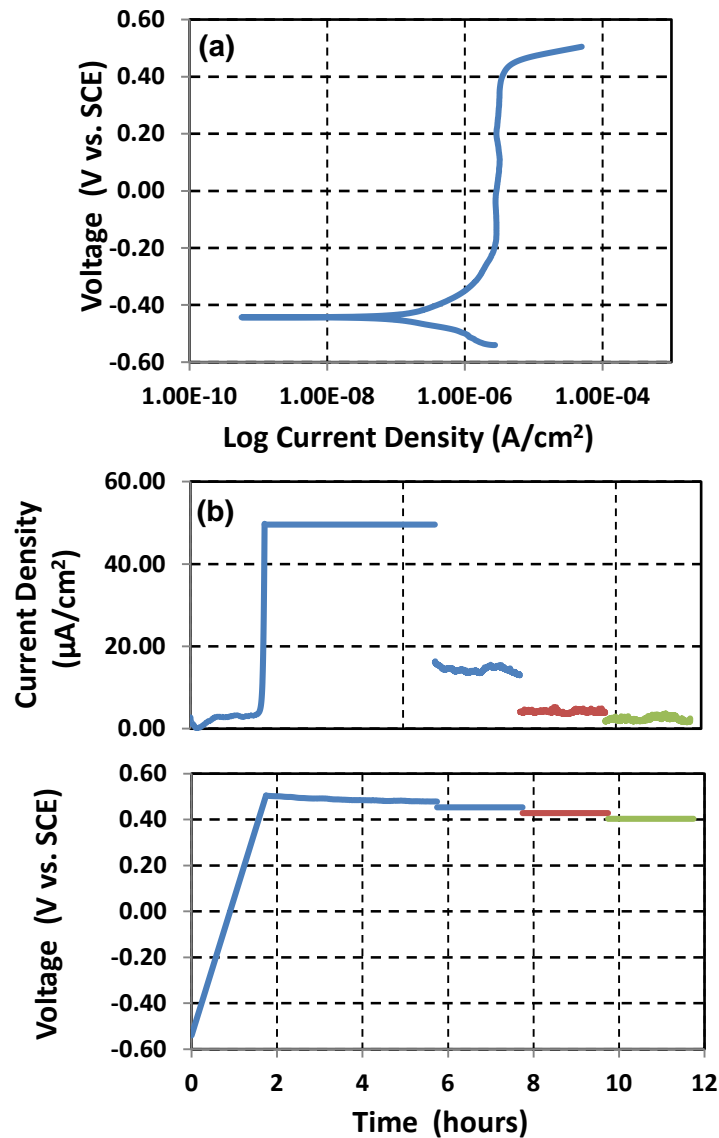


Figure 5-1 Potentiodynamic (a) and G192 test plot (b) for conditions described in Test 22

ASTM G192 tests were conducted in simulants 6, 8, 14, 17, and 22. Tests 6, 8 and 17 still indicated pitting susceptibility, whereas tests 14 and 22 were considered passes. The remainder of the data for the ASTM G192 tests is shown in Appendix A.

Table 5-1 Electrochemical Testing results of statistically design tests for augmented 1.2 M hydroxide concentration. The tests highlighted in yellow are the statistical “anchor” points.

Test	Temperature (°C)	Target pH	Category		Pitting on sample?		Logistic Approach
			run 1	run 2	run 1	run 2	
1	35	13.3	1	1	No	No	0
2	35	13.3	1	1	No	No	0
3	35	13.3	1	1	No	No	0
4	35	13.3	1	1	No	No	0
5	35	13.3	1	1	No	No	0
6	35	13.3	3	3	Yes	Yes	1
7	35	13.3	1	1	No	No	0
8	35	13.3	3	3	Yes	Yes	1
9	35	13.3	1	1	No	No	0
10	35	13.3	1	1	No	No	0
11	35	13.3	1	1	No	No	0
12	35	13.3	1	1	No	No	0
13	35	13.3	1	1	No	No	0
14	35	13.3	1	3	No	Yes	0 ^a
15	35	13.3	1	1	No	No	0
16	35	13.3	1	1	No	No	0
17	35	13.3	3	3	Yes	Yes	1
18	35	13.3	1	1	No	No	0
19	35	13.3	1	1	No	No	0
20	35	13.3	1	1	No	No	0
21	35	13.3	1	1	No	No	0
22	35	13.3	3	3	Yes	Yes	0 ^a
23	35	13.3	1	1	No	No	0
24	35	13.3	1	1	No	No	0
25	35	13.3	5	5	Yes	Yes	1
26	35	13.3	5	5	Yes	Yes	1
27	35	13.3	5	5	Yes	Yes	1

a – This condition passed the ASTM G-192 test and was re-categorized as a “2”.

The JMP® v. 11.1.1 software from SAS Institute Inc. was also used to perform this analysis. These results were combined with the previous results from Plackett-Burman and Box-Behnken statistical design [4] for a total of 80 conditions. Equation 1 and Equation 2 show the model for determining the probability that pitting will occur. Equation 1 calculates the probability that pitting (i.e., a “1” will occur). Equation 2 is the linear relationship between the statistically significant variables. The

statistically significant variables were hydroxide, nitrate, nitrite, and chloride. Inhibitor species are indicated by a positive coefficient, while aggressive species have a negative coefficient.

$$P(1) = \frac{1}{1 + e^{\text{Lin}(0)}} \quad \text{Equation 1}$$

$$\text{Lin}(0) = 2.12 + 8.41 [\text{OH}^-] + 2.12 [\text{NO}_2^-] - 1.20 [\text{NO}_3^-] - 21.76 [\text{Cl}^-] \quad \text{Equation 2}$$

To confirm the robustness of the model equation, 15 conditions consisting of interior points from within the variable space were randomly selected. The simulant compositions are presented in Table 2-1 in the experimental section. The CPP results and bullet pictures are presented in Appendix B for a sample and duplicate run. The results of the electrochemical testing based on category, pitting on sample and logistic approach is presented in Table 5-2. As observed, there were 7 tests with category 5, 6 tests with category 1, and 1 test with category 2. An additional instance with conflicting results was for the test 10 with category 5 for run 1 and 3 for run 2. This test was ultimately classified as a “fail” condition.

Table 5-2 Electrochemical Testing results of statistically design tests for interior points

Test	Temperature (°C)	Target pH	Category		Pitting on sample?		Logistic Approach
			run 1	run 2	run 1	run 2	
1	35	13.3	1	1	No	No	0
2	35	13.3	1	1	No	No	0
3	35	13.3	5	5	Yes	Yes	1
4	35	13.3	1	1	No	No	0
5	35	13.3	5	5	Yes	Yes	1
6	35	13.3	1	1	No	No	0
7	35	13.3	5	5	Yes	Yes	1
8	35	13.3	5	5	Yes	Yes	1
9	35	13.3	5	5	Yes	Yes	1
10	35	13.3	5	3	Yes	Yes	1
11	35	10	1	1	No	No	0
12	35	10	1	1	No	No	0
13	35	10	2	2	Yes	Yes	0
14	35	10	5	5	Yes	Yes	1
15	35	10	5	5	Yes	Yes	1

Combining these conditions with the 80 conditions previously analyzed (95 in total), the logistic regression analysis was repeated. The statistically significant variables continued to be hydroxide, nitrate, and chloride and nitrite. The coefficients for the equations were slightly altered, but were not significantly different compared to the previous equation [4].

$$\text{Lin}(0) = 0.60 + 8.40 [\text{OH}^-] + 2.37[\text{NO}_2^-] - 0.98 [\text{NO}_3^-] - 19.32 [\text{Cl}^-] \quad \text{Equation 3}$$

This equation will be used as a basis to obtain the pitting factor which will be explained in the following subsections.

5.1.1 Basis for Pitting Factor as a Criterion for Corrosion Inhibition

Ideally the pitting factor will be utilized to provide a basis for corrosion control requirements for the waste chemistry. These limits will not have operational gaps and will address other aggressive species such as the halide ions (i.e., Cl, F, etc.). An evaluation was performed to determine practical criterion for the application of this empirical factor for corrosion control.

5.1.1.1 Relationship between Aggressive Anion and Inhibitor Concentrations

Previous corrosion studies have reported that a linear log-log relationship exists between the aggressive anion concentration and the minimum effective inhibitor concentration [21-24]. Matsuda and Uhlig studied the corrosion of iron in the systems $\text{NO}_2^-/\text{Cl}^-$, $\text{NO}_2^-/\text{SO}_4^{2-}$, $\text{CrO}_4^{2-}/\text{Cl}^-$, and $\text{CrO}_4^{2-}/\text{SO}_4^{2-}$ [21]. Mercer et. al. [22] determined the minimum effective nitrite concentration as a function of sulfate, chloride and nitrate concentrations. Congdon et. al. [24] observed a similar relationship for the minimum effective nitrite concentration with these same LAI corrosions in dilute simulated waste solutions. Ondrejcin and Donovan [25] defined a relationship between the hydroxide and nitrite inhibitor species and the nitrate aggressive species that mitigated nitrate stress corrosion cracking of carbon steel.

The linear log-log relationship is given in the following equations:

$$\text{For } [\text{AA}] \leq [\text{AA}]_c, \quad \log [\text{Inh}]_{\min} = \log [\text{Inh}]_c \quad \text{Equation 4}$$

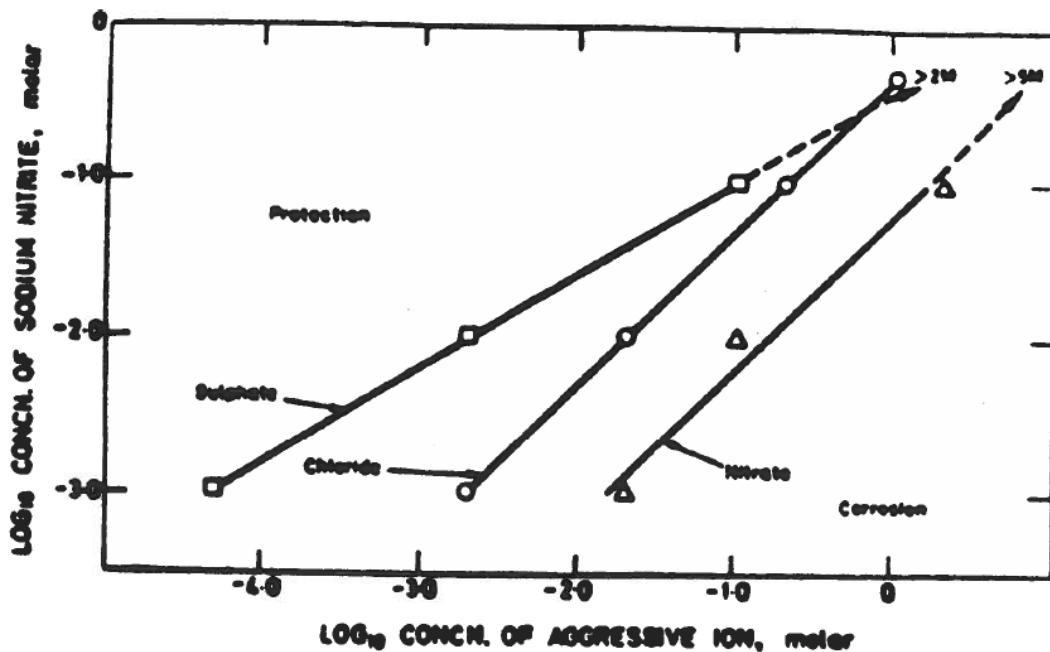
$$\text{For } [\text{AA}] > [\text{AA}]_c, \quad \log [\text{Inh}]_{\min} = a + b \log [\text{AA}] \quad \text{Equation 5}$$

Where [AA] is the concentration of aggressive species, [Inh] is the concentration of inhibitor, c is the critical concentration below which corrosion occurs regardless of the concentration of the aggressive anion, and a and b are empirical parameters. In the work by Congdon [24], the slope of this empirical relationship was dependent on the aggressive anion with $b_{\text{Cl}} > b_{\text{NO}_3} > b_{\text{SO}_4}$ as shown in Figure 5-2. The line with the slope b represented the boundary between pit and not pit conditions. All references reported observing a critical inhibitor concentration that regardless the concentration of the aggressive species was required to mitigate pitting [21-22, 24].

The slope of the log-log plots has been attributed to the ratio of the valencies of the two opposing anions (inhibitor/aggressive anion), although there have been some anomalies noted [26]. The slope has also been attributed to competitive adsorption models based on oxidation [24] and ion exchange [26]. The basis for the critical inhibitor concentration has not been fully explained, however, it seems to be influenced by the presence of other aggressive anions [24].

Many corrosion studies were concerned with relatively simple system having only one aggressive species. Except for Congdon studies, the references cited are limited to single species evaluation. In the case of Congdon studies, the data were analyzed in terms of a controlling aggressive species (e.g., in most cases nitrate). However, in most situations, the other aggressive species were at

relatively low concentrations in comparison to the controlling species. It was acknowledged that the remaining species influenced the critical concentration of inhibitor needed, however, only one aggressive species determined the minimum inhibitor concentration. The controlling aggressive anion changed based on the concentration ratio of the aggressive species to nitrate. For example, at Savannah River Site (SRS) if the $\text{Cl}^-/\text{NO}_3^-$ ratio is greater than 0.03, the chloride species would be the controlling aggressive anion and a different value for b in equation 5 was utilized.



**'Tolerance' of sodium nitrite towards aggressive ions,
sulphate, chloride or nitrate**

Abraded mild steel; 100 day tests at 25°C

Figure 5-2 Example of Log-Log Plot Demonstrating Relationship Between Inhibitor and Aggressive Species [22]

In this situation, the concentrations of the aggressive and inhibitor species have a wider envelope. That is, for example, both chloride and nitrate could be at high concentration levels. Therefore, it was desired to develop an empirical parameter that included all the significant species that could be utilized to assess the likelihood for pitting. As discussed previously, the data were analyzed using a logistic regression approach and a linear expression was obtained (see Equation 3). The result was a probability function that contained linear coefficients in terms of the aggressive and inhibitor species. Assuming the value of the coefficient was representative of the relative contribution to either pitting or inhibition, and that the ratio of inhibitor to aggressive species could be utilized as a criterion for failure (i.e., similar to the empirical value for b in equation 5). The pitting factor, as it is designated, for these tests is shown in equation 6.

$$\text{Pitting Factor} = \frac{\text{Inhibitor Species}}{\text{Aggressive Species}} = \frac{8.52 [\text{OH}^-] + 2.41 [\text{NO}_2^-]}{[\text{NO}_3^-] + 19.6 [\text{Halide}]}$$

Equation 6

where halide concentration is the sum of the chloride and the fluoride concentrations. Note that most of these tests were performed only with the chloride species since the fluoride did not initially appear to be a significant variable within the ranges of all the tested variables. One of the reasons was the low solubility of fluoride in the more concentrated solutions. However, in more dilute solutions, at low chloride levels, the fluoride is present and is a known pitting agent for carbon steel [27]. This reference further states that the pitting potentials are more positive and corrosion rates are lower in the presence of fluorides than those found for similar chloride concentrations. Thus, it is a conservative assumption to assign the same coefficient in the pitting factor relationship as the chloride anion.

5.1.1.2 Criterion for Pitting Factor Evaluation

The experimental data set was examined initially to investigate a pitting factor criterion. The 95 data points from this series of tests were sorted according to whether they were a “pass” (i.e., no pitting) or a “fail” (i.e., pitting). Figure 5-3 shows the pitting factor as a function of pH for the “fail” conditions. Of the 48 tests that failed, all but 2 (~96%) had a pitting factor greater than 1. The two conditions with pitting factors greater than 1 occurred at high hydroxide conditions (1.2 M) and high chloride concentrations (~0.25 M) combined with high nitrate concentrations. Figure 5-4 shows the pitting factor as a function of pH for the “pass” conditions. For the 47 cases that passed, all but 3 (~94%) had pitting factors greater than 1. In these cases, the simulant contained a relatively high chloride concentration (no other aggressive species) and a relatively high hydroxide concentration (no other inhibitor species). These results suggest that pitting factors less than 1 are indicative of pitting susceptibility with high degree of confidence. Pitting factors between 1 and 2 are unlikely to result in pitting, but may pit at high aggressive species concentrations even in well inhibited solutions. Pitting factors greater than 2 are indicative of a condition that is not expected to cause pitting.

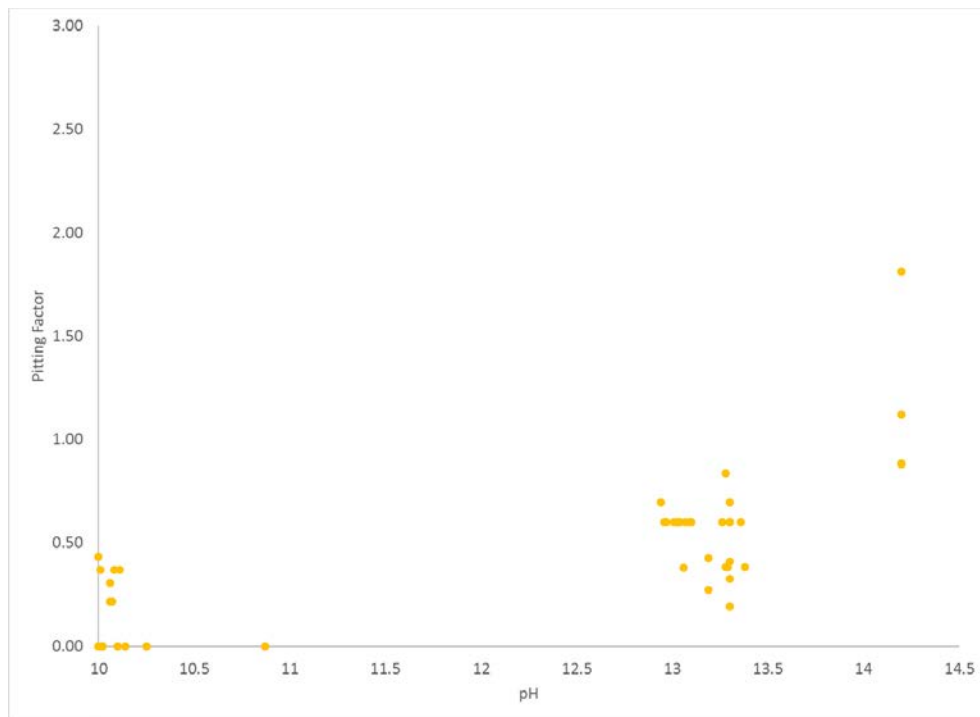
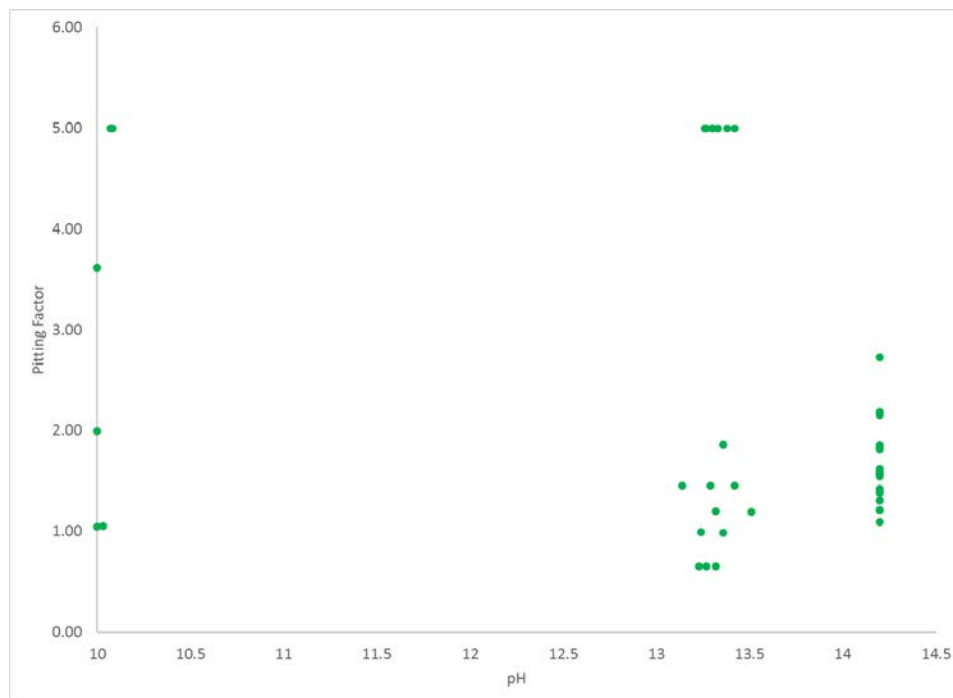


Figure 5-3 Pitting Factor as a Function of pH for the experimental “fail” conditions.



A data set, other than the one reported here was used to determine the pitting factor coefficients, was utilized to further evaluate the critical pitting factor above which no pitting occurs. This data set originated from tests that were performed in Hanford waste simulants between 2005-2017 [28]. The data set included 344 test conditions. Of these, 173 test conditions were within the test ranges for the significant variables that were utilized to develop the pitting factor model. Figure 5-5 shows the pitting factor as a function of pH for the 95 failed tests. Approximately 96% of the failures were at pitting factors less than 1. Of the four failed tests with pitting factors greater than 1, three had values between 1 to 1.5 and the last had a value approaching 2. The nitrate concentration was relatively high and the pH relatively low in all four cases.

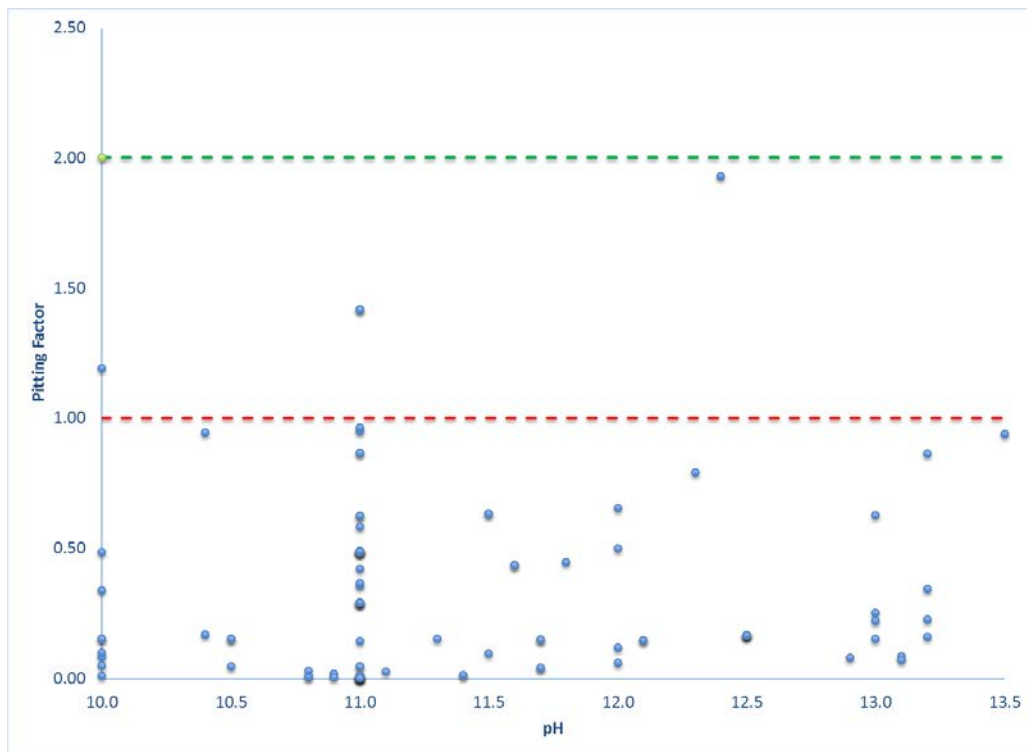


Figure 5-5 Pitting Factor as a Function of pH for the reference “fail” conditions.

The 78 tests that passed were also evaluated to determine if there were instances where the pitting factor suggested that pitting occurs, but no pitting was observed. Figure 5-6 shows the pitting factor as a function of pH for the 78 failed tests. Approximately 45% of the tests had pitting factors greater than 2. Another 26%, or 20 tests, had pitting factors between 1 and 2. Thus, combining the information from the tests that failed, 83% of the time that the pitting factor was between 1 and 2, no pitting was observed. The interesting result was that 29% of the tests had pitting factors less than 1, a region where pitting was anticipated. Again, combining this result with the information from the tests that failed, 20% of the time that the pitting factor was less than 1 no pitting was observed. While this indicates that utilizing a critical pitting factor of 1 (i.e., pitting occurs at all values below this number) it may also indicate that there is another species that is contributing to inhibition.

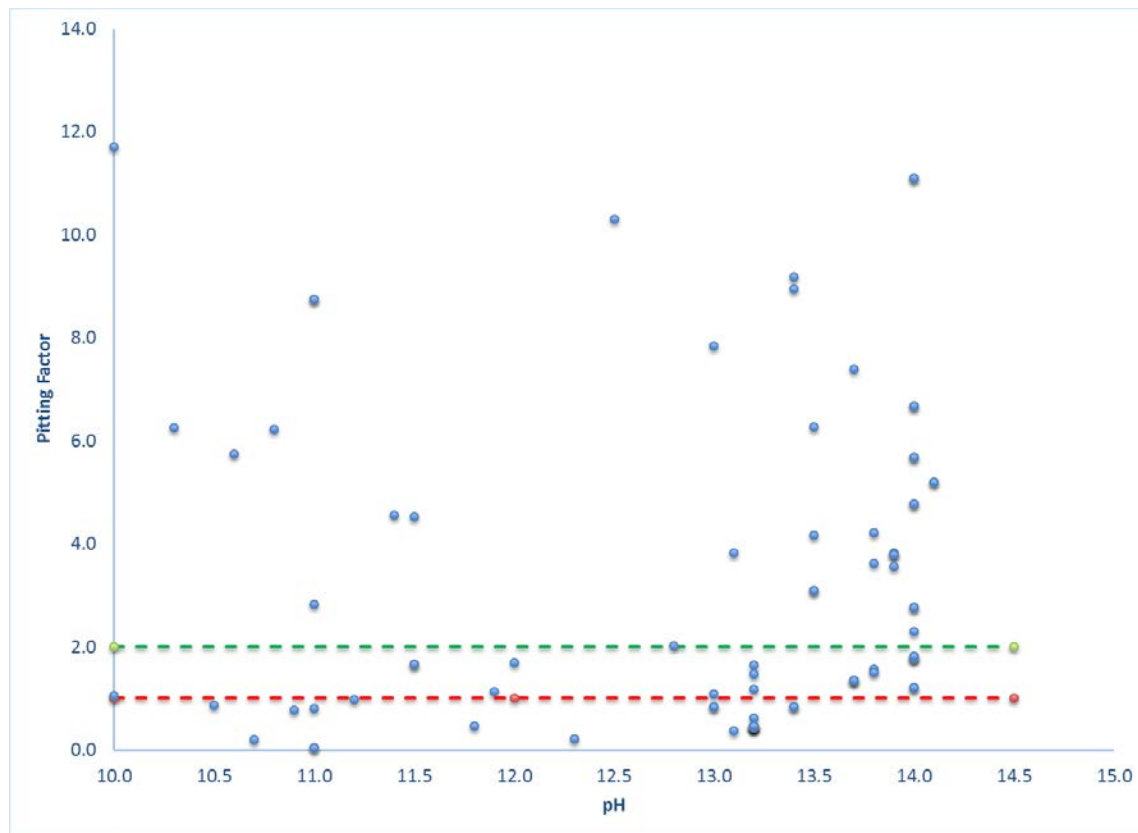


Figure 5-6 Pitting Factor as a Function of pH for the reference “pass” conditions.

The data were re-evaluated to examine the effect of the carbonate species. Due to solubility concerns with the test simulants early in FY16, the test matrices were constrained such that the maximum total inorganic carbon (TIC) was 0.1 M. At this concentration level, TIC was not a significant variable. It is also assumed that at these low TIC values of 0.1 M or less, the chemistry would be less inhibited. The 344 reference data points were sorted again eliminating the higher TIC values, which left a total of 45 cases to evaluate. Figure 5-7 shows the pitting factor as a function of pH for the fail cases. All 22 values were had pitting factors less than 1. Figure 5-8 shows the pitting factor as a function of pH for the pass cases. In 20 of the 23 cases, the pitting factor was greater than 1. For the three exceptions, the total organic carbon concentration was 3.6 M. During the FY16 SRNL test program, the benefit of the organic carbon species was established.

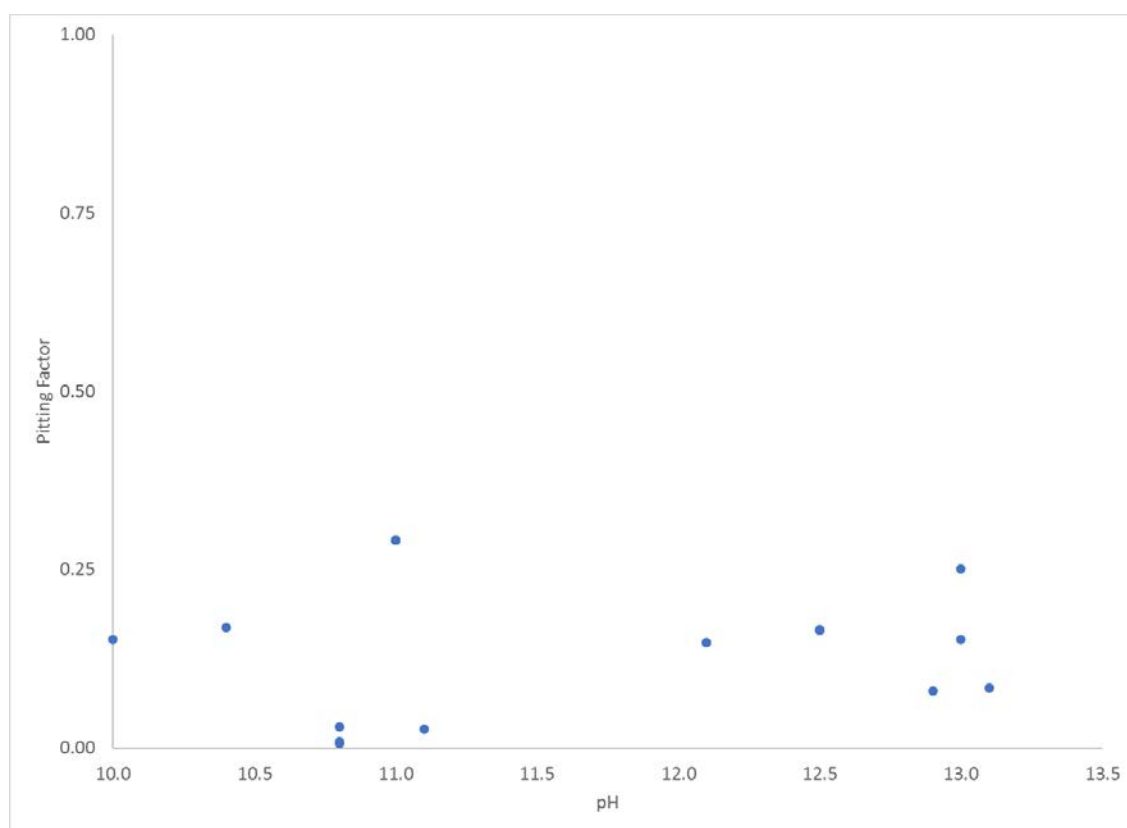


Figure 5-7 Pitting Factor as a Function of pH for the reference “fail” conditions at low TIC.

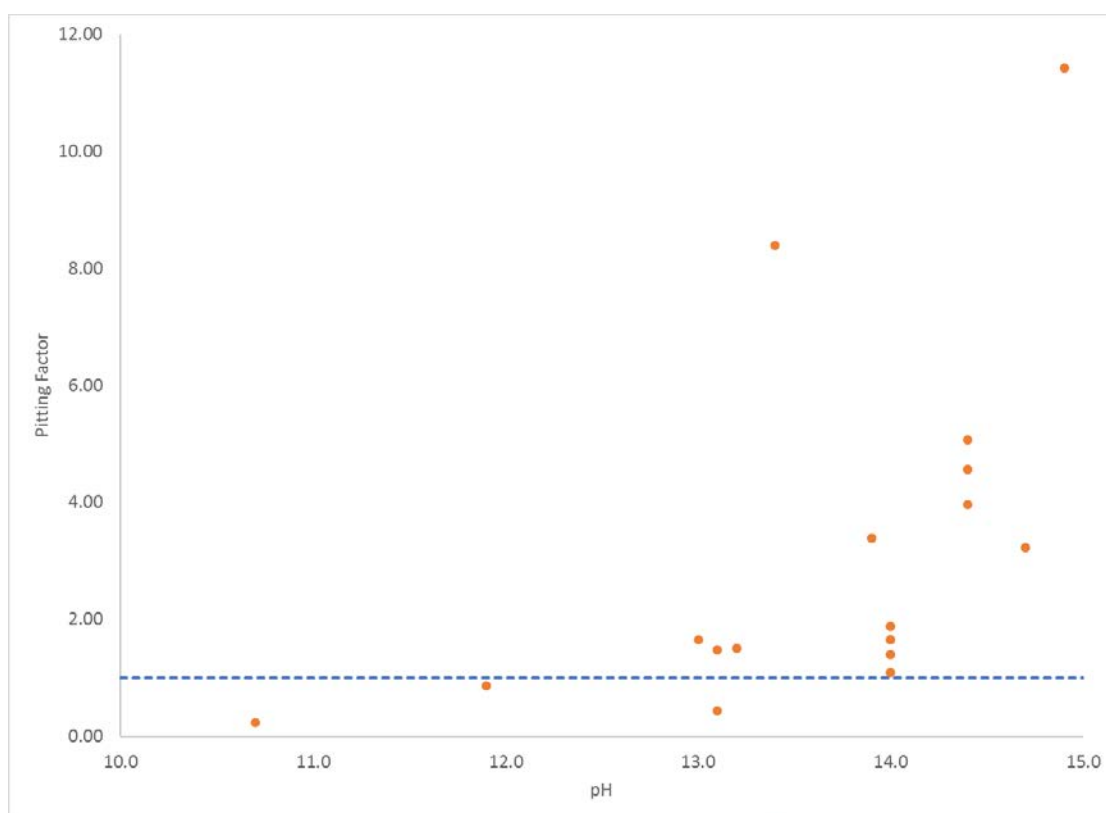


Figure 5-8 Pitting Factor as a Function of pH for the reference “pass” conditions at low TIC.

5.1.1.3 Evaluation of Critical Pitting Factor vs. Previous Corrosion Control Limits

SRS utilizes a $[\text{NO}_2^-]/[\text{NO}_3^-]$ molar ratio to inhibit pitting corrosion in carbon steel waste tanks that contain dilute wastes [29]. In these situations, it is assumed that the pH is approximately 10 and the chloride concentration is negligible. Thus, the pitting factor equation would reduce to:

$$\text{Pitting Factor} = \frac{2.41 [\text{NO}_2^-]}{[\text{NO}_3^-]} \quad \text{Equation 7}$$

If it is assumed that pitting factor transitions from pitting to no pitting between values of 1 and 2, the critical $[\text{NO}_2^-]/[\text{NO}_3^-]$ ratio ranges between 0.41 to 0.83. The minimum ratio for inhibition at SRS is 0.69, which is within the range on the limit established by the pitting factor.

SRS also utilizes an empirical relationship to determine a minimum nitrite concentration that will inhibit pitting due to the chloride ion. At a pH of 10 and temperature of 35 °C (i.e., midpoint temperature for New Limits testing) equation 8 is utilized:

$$\frac{[\text{NO}_2^-]}{[\text{Cl}^-]^{1.34}} = 166 \quad \text{Equation 8}$$

The range of chloride utilized for these tests was 0.01 to 0.4 M. Thus, if the SRS equation was valid, the range of minimum nitrite required to inhibit pitting would be 0.35 M to 48.6 M. While

the lower value seems reasonable, the upper value far exceeds solubility limits for nitrite. The range of chloride concentration utilized to develop the SRS limit was 0.0005 to 0.05 M. Utilization of the SRS equation beyond the bounds of the test range results in impractical results. Therefore, these tests were performed to give a more practical relationship.

SRNL has been recently been involved with developing corrosion control limits for DFLAW return stream [30]. These streams were predicted to have low pH with extremely high levels of chloride. In this case, the pitting factor equation would reduce to:

$$\text{Pitting Factor} = \frac{2.41 [\text{NO}_2^-]}{19.6 [\text{Cl}^-]} \quad \text{Equation 9}$$

Once again, if it is assumed that pitting factor transitions from pitting to no pitting between values of 1 and 2, the critical $[\text{NO}_2^-]/[\text{Cl}^-]$ ranges between 8.1 to 16.2. The minimum ratio for inhibition determined from the DFLAW testing was 10, which is within range on the limit established by the pitting factor. The DF-LAW tests were performed at chloride concentrations between 0.01 M and 1.64 M. These tests were at concentrations within the DF-LAW test range and therefore good agreement is anticipated.

The WRPS corrosion control limits, like the SRS standards, are a combination of minimum concentrations of inhibitors and a minimum ratio of inhibitor to aggressive species. The limits work well except for two situations: 1) Dilute Solutions and 2) Chloride solutions. For a solution with a pH of 12, the minimum ratio is given by Equation 10:

$$\frac{[\text{NO}_2^-] + [\text{OH}^-]}{[\text{NO}_3^-]} > 0.4 \quad \text{Equation 10}$$

This ratio is roughly equivalent to a pitting factor of 1. As shown above this criterion is effective over much of the range, but application in more dilute solutions is more suspect. Finally, the WRPS empirical relationship does not consider the chloride ion, which may make the application of the ratio more suspect at chloride concentrations greater than 0.01 M.

5.2 Ammonia effects

The JMP software package was utilized to design a set of tests to investigate ammonia as an inhibitor in the waste. These tests were not designed so that ammonia would be added to the tank, but rather to assess the benefit of the ammonia already present in the wastes. The addition of ammonia was performed by adding 0.25 M ammonium nitrate and maintaining a pH of solution higher than 12. Maintaining a pH above 12 ensures that the ammonium cation completely dissociates into ammonia [31]. Table 5-3 shows the 20 tests that were statistically designed to test the effect of ammonia and the results for the two runs.

Table 5-3 Electrochemical Testing results of statistically design tests for ammonia inhibition

Test	Temperature (°C)	pH	Category		Pitting on sample?		Logistic Approach
			run 1	run 2	run 1	run 2	
1	35	>12	5	5	Yes	Yes	1
2	35	>12	5	5	Yes	Yes	1
3	35	>12	3	3	Yes	Yes	1
4	35	>12	5	5	Yes	Yes	1
5	35	>12	1	1	No	No	0
6	35	>12	1	1	No	No	0
7	35	>12	5	5	Yes	Yes	1
8	35	>12	1	1	No	No	0
9	35	>12	3	3	Yes	Yes	1
10	35	>12	1	1	No	No	0
11	35	>12	1	1	No	No	0
12	35	>12	5	5	Yes	Yes	1
13	35	>12	1	1	No	No	0
14	35	>12	5	5	Yes	Yes	1
15	35	>12	1	1	No	No	0
16	35	>12	1	1	No	No	0
17	35	>12	1	1	No	No	0
18	35	>12	1	1	No	No	0
19	35	>12	3	3	Yes	Yes	1
20	35	>12	1	3	No	No	0

From the 20 tests, 10 were category 1 “passes”, 6 were category 5 “fails” and 4 were category 3 with inconclusive results. The data was modeled using logistic regression and it was shown that ammonia specie did not have a statistically significant impact on the pitting factor.

To further investigate the effect of ammonia inhibition, a comparison of similar chemistry simulants with and without ammonia was performed using a borderline condition (Category 3). Table 5-4 lists the two experiments used for the comparison. Test 24 was obtained from Box-Behnken statistical design reported in FY16 report [4] and the coupon did not show indication of pitting.

Table 5-4 Comparison of similar test with and without ammonia addition

Test	Hydroxide (M)	Nitrite (M)	Nitrate (M)	Chloride (M)	Ammonium Nitrate (M)	pH	Category		Pitting on sample?	
							run 1	run 2	run 1	run 2
6	0.605	0.6	2.75	0.2	0.125	>12	1	1	No	No
24	0.6	0.6	2.75	0.2	0	13.3	3	3	No	No

The CPP results are displayed in Figure 5-9. The addition of ammonia was beneficial as evidenced by a slightly improved hysteresis response from mixed (Category 3) for the no ammonia case and negative (Category 1) for the ammonia case. Additional studies are needed to assess in more detail the effect of ammonia.

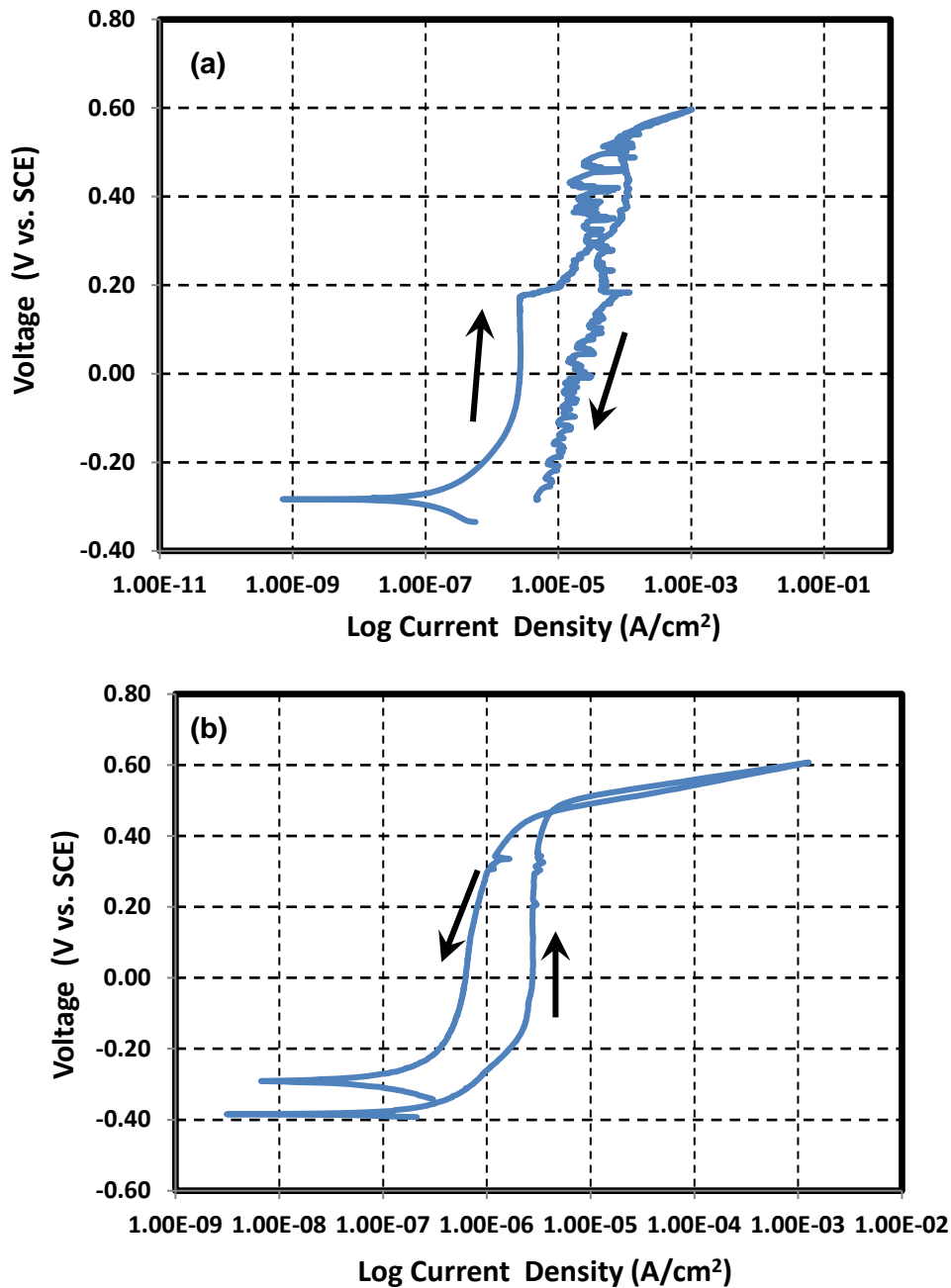


Figure 5-9 CPP results of (a) Test 24 from Box-Behnken statistical design and (b) Test 6 (with Ammonia)

5.3 Simulated AN-102 with various organic specie and saturated nitrous oxide

AN-102 simulant was tested during FY15 with a large concentration variance for nitrate (i.e., 1.1 to 5.5 M), small range and low concentrations for nitrite (i.e., 0.5 to 1.5 M) and very low concentrations of hydroxide (i.e., 0.01 and 0.05 M) at 40 °C. No pitting susceptibility was observed

when the concentration of nitrite was increased to 1.5 M at 0.01 M hydroxide or decreased to 1.0 M at 0.05 M hydroxide independent of the nitrate concentration [12].

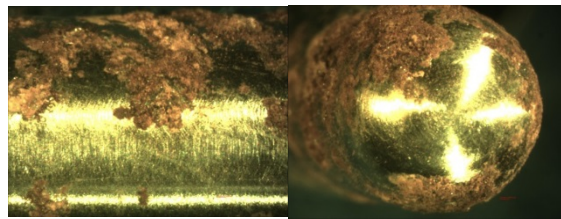
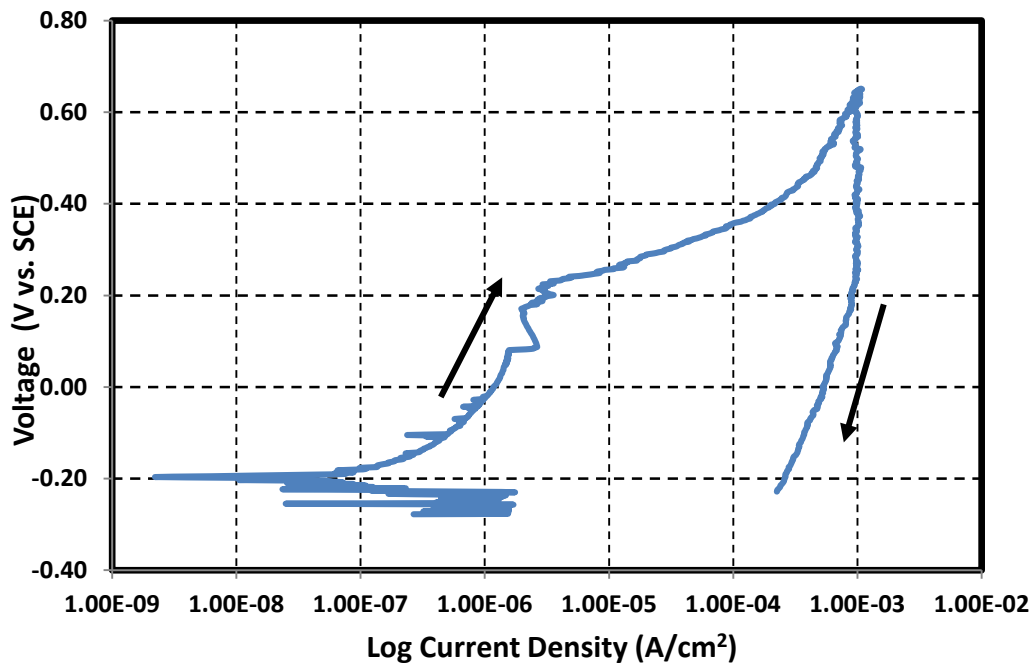
In FY16, all the organic species were removed to study their influence on pitting corrosion. The removal of the organics resulted in heavy metal salts precipitating from solution and forming a residue at the bottom of the cell. Compared to FY15 results, the solutions were found to be more aggressive [4]. No cases of negative hysteresis (i.e., category 1) occurred when testing with solutions that contained no organics. Generally, it was concluded that the presence of organics maintained the homogeneity of the solution and this, in turn, helped prevent pitting corrosion when compared to solutions without organics.

For FY17, several organics, ammonia and saturated nitrous oxide, that are typically observed in Hanford DST wastes, were selected to investigate their inhibition effectiveness compared to a simulant with no organic present. Table 5-5 shows the seven tests and respective organic used with pH and results. Test 0 was the case from FY16 in which no organics were added an AN-102 simulant. For tests 6 and 7, saturated nitrous oxide was bubbled 30 minutes before test and during test albeit with less flow. The CPP results and after pictures of the bullets are presented in Appendix D.

Table 5-5 Electrochemical results of AN-102 based simulant with individual organic specie and Nitrous Oxide

Test	Organic specie	measured pH	Category		Pitting on sample?	
			Run 1	Run 2	Run 1	Run 2
0	No organic	12.12	5	5	Yes	Yes
1	Ammonia	12.05	3	3	Yes	Yes
2	Iminodiacetic Acid	12.31	3	3	Yes	Yes
3	N-Butylamine	13.02	3	5	Yes	Yes
4	Dibutylphosphate	12.16	3	3	Yes	Yes
5	Glycine	12.48	1	3	No	No
6	Nitrous Oxide	12.34	5	5	Yes	Yes
7	Nitrous Oxide	12.97	1	1	Yes	Yes

Figure 5-10 shows the CPP curve and the nose and shank of the bullet sample for test 0. This test was a “fail”. The same simulant with organic additions, on the other hand, resulted in a category 3 CPP curve. Thus, the organics appear to be beneficial to some extent, with some organics more beneficial than others. Most cases in which an organic specie was added resulted in a change in CPP category from a category 5 to a category 3, except for N-butylamine and Glycine. However, for the case of N-butylamine, the reverse scan had a significantly lower current density compared with the test in the simulant without organic. The order of inhibition that was seen with the addition of organics by CPP results and after pictures, from best to worst, were: Glycine, Iminodiacetic Acid, Ammonia, Dibutylphosphate and N-butylamine.



Shank

Nose

Figure 5-10 CPP results of Test 0 and after pictures

Saturated nitrous oxide produced no change in CPP curve compared with Test 0. Both cases experienced severe pitting. A borderline case from the previous test matrix was also tested with nitrous oxide to determine if a “pass” result would become a “fail” result. Test 2 from FY16 was selected [4] because of the higher hydroxide concentration of 0.05 M and higher nitrite concentration (i.e., 1 M). The CPP curve for this test was categorized as a 2 with minor corrosion on the bullet as shown in Figure 5-11 (a). Figure 5-11 (b) shows the saturated solution with nitrous oxide. Photographs of the nose and shank are displayed at the right side of the CPP curves. As observed in the CPP curves, nitrous oxide did not significantly alter the CPP curve as both were considered “pass” conditions.

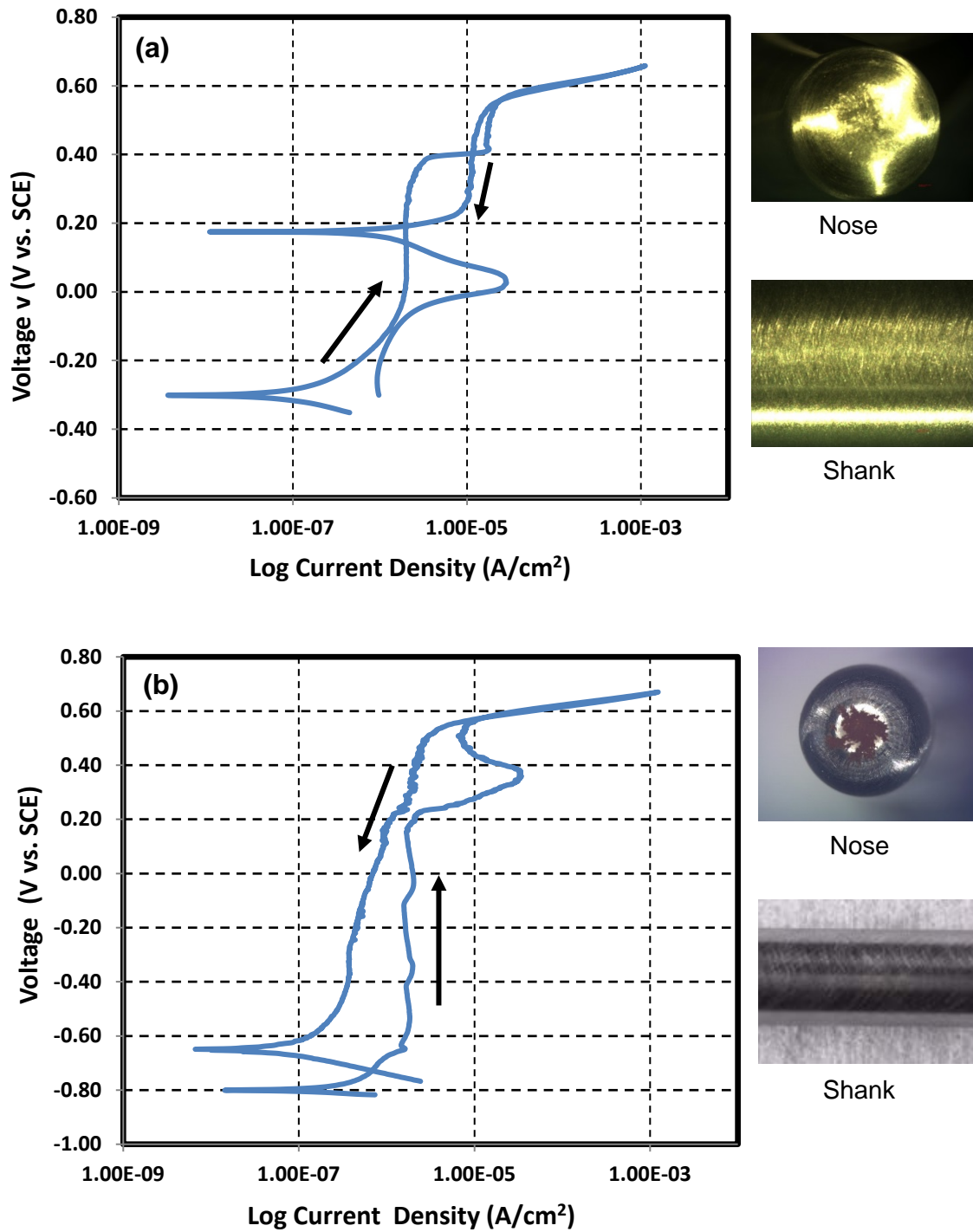


Figure 5-11 CPP curve on right and after pictures of bullet sample on left for (a) Test 2 from FY16 report and (b) Test 7

5.4 Vapor Space Corrosion Tests with DFLAW based Simulants at different Sodium (Na) Concentrations

Ammonia inhibition of VSC was investigated in DFLAW simulants at concentrated and dilute Na concentrations. Pictures of the coupons after a four-month exposure are displayed for vessels 3 and 5 in Figure 5-12 and for vessels 2, 4 and 6 in Figure 5-13.

Figure 5-12 compares a concentrated Na DFLAW simulant with coupons exposed to 50 ppm ammonia and no ammonia. No significant difference was observed with or without ammonia. But, VSC was more aggressive in coupons placed close to the liquid level (Level 1). Weight losses and corrosion rates shown in Table 5-6 displays low corrosion rates (0 - 0.08 mpy) except for coupon 19. The corrosion mechanism for this coupon involved crevice corrosion and can be observed in Appendix F. The samples immersed in concentrated Na DFLAW simulant did not show appreciable corrosion.

The coupons exposed to VS dilute Na DFLAW simulant are compared with pictures in Figure 5-13 at 550 and 50 ppm, and no ammonia. Appreciable VSC was observed especially at Level 1. Additionally, the concentration of ammonia did not appear to influence the degree of VSC observed. Corrosion rates in Table 5-6, showed the average corrosion rates were higher for coupons exposed to dilute Na DFLAW, with samples close to liquid level higher than the coupons farther from liquid level. Ammonia showed some benefit at the level 3 position. The immersed coupons had generally higher corrosion rate that ranged from 0.22 to 1.15 mpy. The solution for dilute Na DFLAW simulant proved to be most aggressive condition.

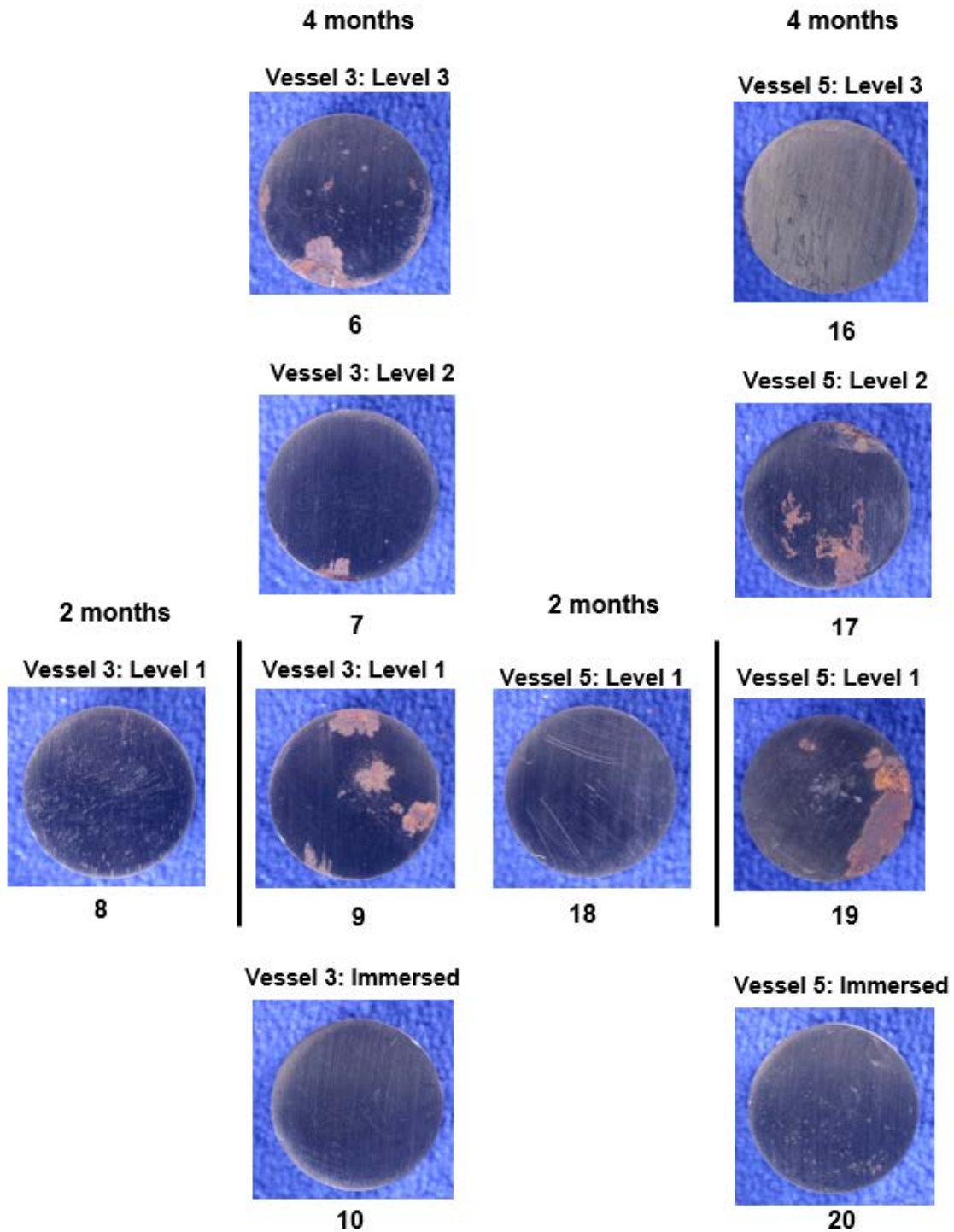


Figure 5-12 Post-test pictures of carbon steel discs after two and four months of VS exposure in Vessels 3 and 5; concentrated Na DFLAW simulant at 50 ppm and 0 ppm ammonia in humidified air, respectively

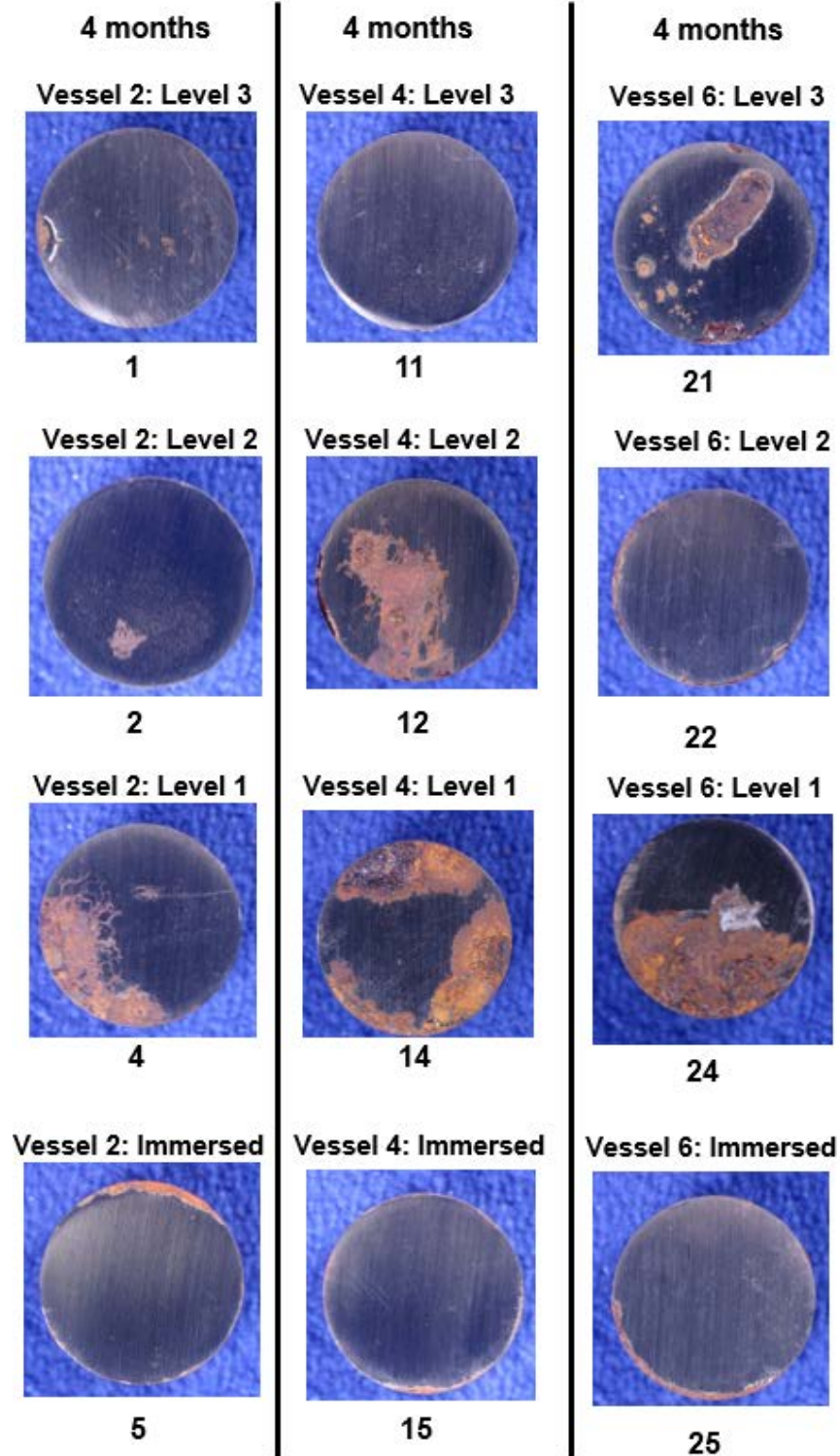


Figure 5-13 Post-test photographs of carbon steel discs after four months VS exposure in Vessels 2, 4 and 6; dilute Na DFLAW simulant at 550, 50 ppm and 0 ppm ammonia in humidified air, respectively

Table 5-6 Weight losses and corrosion rates of coupons at different levels in Vessels 2 to 6

Vessel number (Ammonia concentration)	Coupon number	Level in vessel	Time exposure (month)	mass loss (g)	Corrosion rate (mpy)
2 (550 ppm)	1	High (Level3)	4 months	0.0002	0.02
	2	Middle (Level 2)	4 months	0.0001	0.01
	3	Low (Level 1)	2 months	0.0002	0.03
	4	Low (Level 1)	4 months	0.0009	0.07
	5	Immersed	4 months	0.0027	0.22
3 (50 ppm)	6	High (Level3)	4 months	0.0010	0.08
	7	Middle (Level 2)	4 months	0.0007	0.06
	8	Low (Level 1)	2 months	0.0000	0.00
	9	Low (Level 1)	4 months	0.0011	0.09
	10	Immersed	4 months	0.0001	0.01
4 (50 ppm)	11	High (Level3)	4 months	0.0001	0.01
	12	Middle (Level 2)	4 months	0.0022	0.18
	13	Low (Level 1)	2 months	0.0002	0.03
	14	Low (Level 1)	4 months	0.0106	0.87
	15	Immersed	4 months	0.0089	0.73
5 (no ammonia)	16	High (Level3)	4 months	0.0000	0.00
	17	Middle (Level 2)	4 months	0.0004	0.03
	18	Low (Level 1)	2 months	0.0001	0.02
	19	Low (Level 1)	4 months	0.0042	0.35
	20	Immersed	4 months	0.0004	0.03
6 (no ammonia)	21	High (Level3)	4 months	0.0050	0.41
	22	Middle (Level 2)	4 months	0.0003	0.02
	23	Low (Level 1)	2 months	0.0039	0.64
	24	Low (Level 1)	4 months	0.0106	0.87
	25	Immersed	4 months	0.0140	1.15

5.5 Ammonia detection with QEPAS probe in the exhaust of VSC setup

Work under this task was performed during FY17, and was drafted into a memo [32]. A summary is provided in this report. The QEPAS system was reconfigured and by utilizing a calibrated NH_3 permeation tube, specific dilutions were made at different flow rates and changes in pressure that ranged from 200-650 Torr. Testing the response at varying pressures and flow rates allowed for determination of effects due to changing tank pressures on the system. It was determined during previous experiments that increases in pressure during NH_3 detection resulted in broadening of the absorption lines until two absorption lines merge at pressures above 600 torr. Therefore, pressures above 650 Torr were not tested.

Figure 5-14 shows the effect of changes in pressure and flow rate on the QEPAS output signal. During testing, a constant 50 ppm NH_3 gas concentration was carried into the QEPAS system at a constant flow rate (varied between 50 – 200 sccm) while the total pressure within the cell was varied. As expected, variations in pressure resulted in a linear response of the NH_3 concentration as the number of NH_3 molecules present in the micro-resonator increased. As a result of these variations, it was determined that a constant pressure was required for accurate operation. However, because the variations in concentration were linear for specific flow rates, the pressure could be altered to match field requirements. Changes in flow also resulted in changes in the measured concentration. These changes in concentration, although not linear, were measurable and the sensor can be further calibrated to compensate for these variances. By installing a flow controller upstream and a pressure controller downstream of the QEPAS, more precise control over the flow and pressure within the QEPAS system was achieved.

Based on previous testing as well as considerations for future system connections, a flow rate of 50 sccm was selected for a complete calibration run. Figure 5-15 shows a calibration curve at a flow rate of 50 sccm and pressure of 260 torr for concentrations ranging from 1 to 150 ppm. For concentrations above 150 ppm a secondary calibration curve was required.

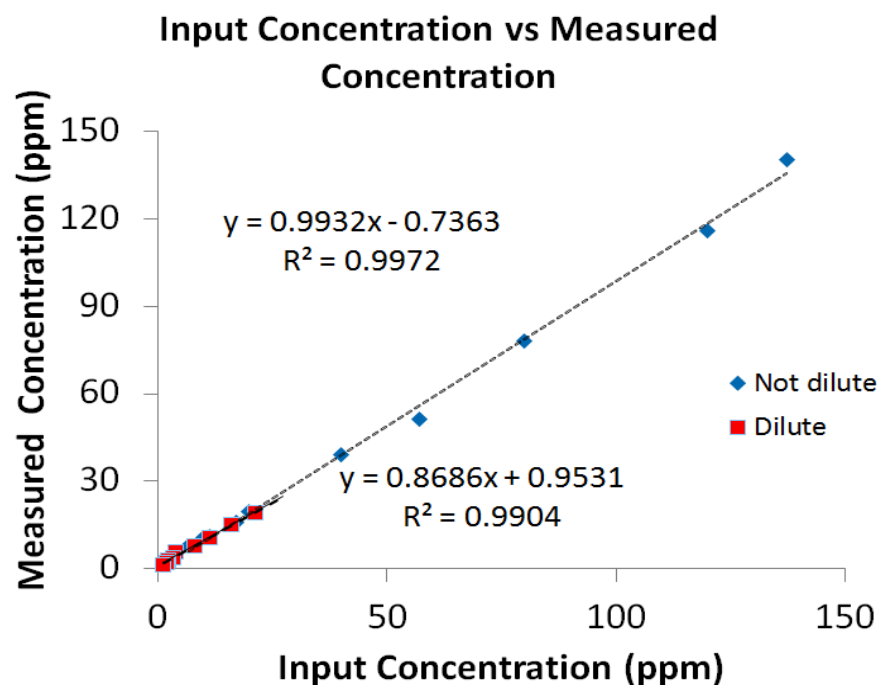


Figure 5-14 Variations in measured ammonia concentrations under varying pressures and flow rates.

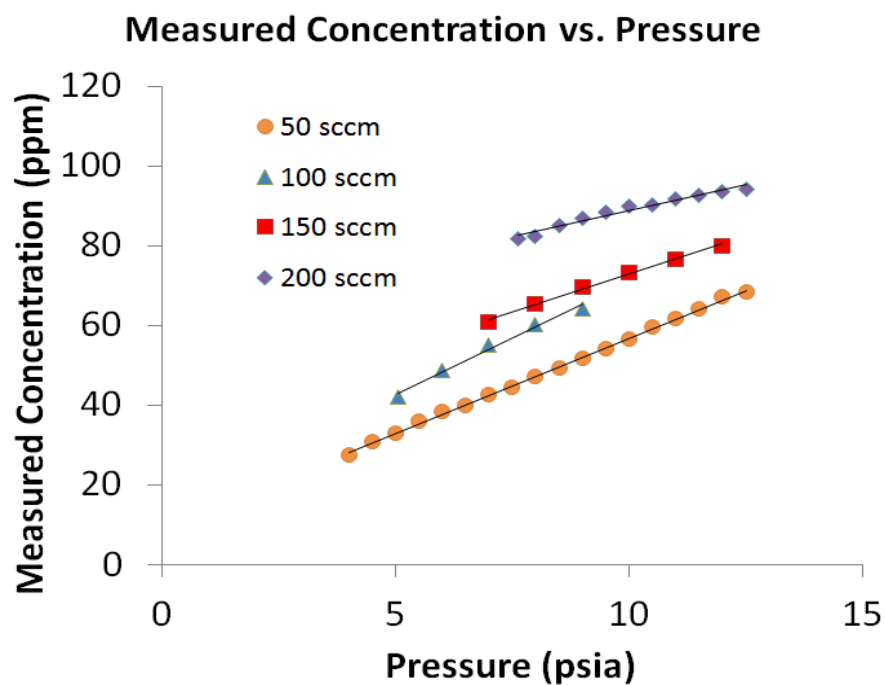


Figure 5-15 Ammonia calibration curve at a flow rate of 50 sccm and pressure of ~260 torr.

The QEPAS system was placed at the exhaust of the VSC for humidified ammonia in air concentration measurements. Figure 5-16 shows a picture of the setup attached to vessel 2 in the system. Initial testing in humid environment indicated that the NH_3 signal was unaffected by moisture. However, if moisture condenses onto the QTF sensor, dampening can be expected and may result in large variations in signal. Therefore, a constant flow should be maintained to limit the possibility of moisture condensation on the QEPAS cell. A new sensor that is specifically designed to measure NH_3 in air was procured and testing will continue during FY18. Throughout FY17 significant progress was made towards proving operational feasibility of a QEPAS sensor. Further progress during FY18 will allow SRNL to determine service life expectancy of the sensor and if any signal fluctuations are expected as a result of corrosive environments. The system is currently awaiting connection to the exhaust of on-going corrosion testing as a first step in determining its efficacy in a head-space monitoring scenario. Once the system is successful in detecting the exhaust gas during live testing, it will undergo further calibration in an attempt to reduce noise and determine its most efficient configuration (including pressure and flow rate).

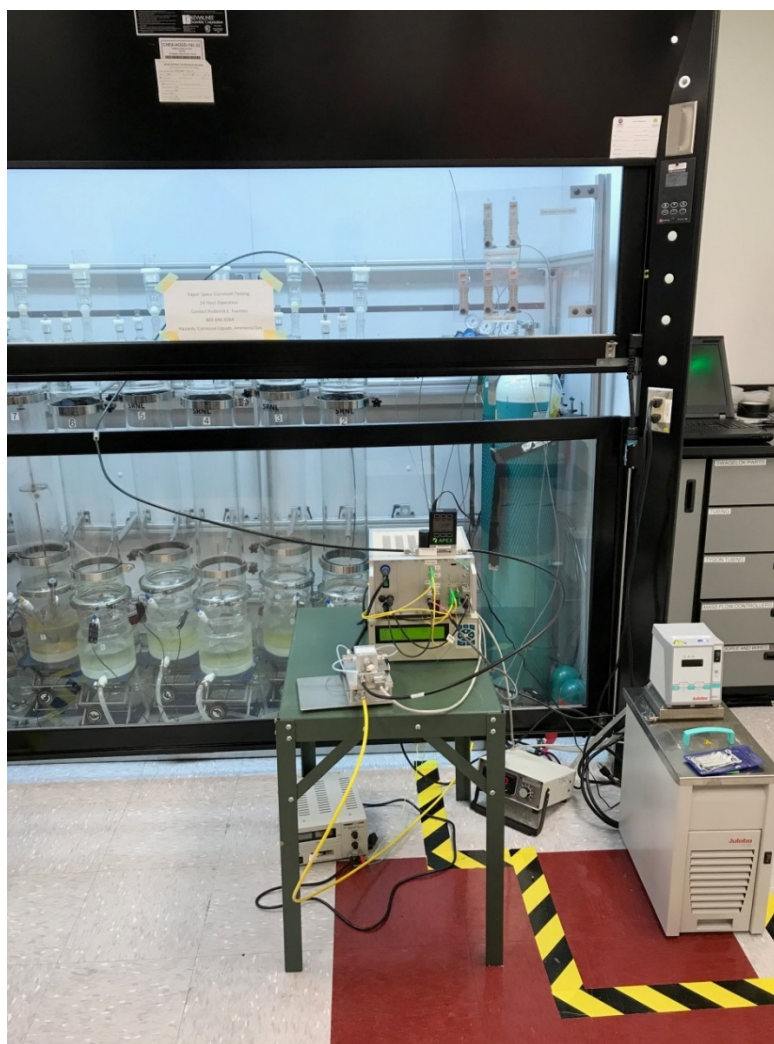


Figure 5-16 Picture of QEPAS system attached to an exhaust in VSC setup vessel 2 (first vessel from right to left).

5.6 VSC Secondary Wall of Tank AY-102: LDP and GW Corrosion Studies

LDP and GW simulants were prepared for corrosion studies to study the effectiveness of VCI to inhibit VSC. The simulants were based on the anticipated solutions adjacent to the exterior of the secondary liner of Tank AY-102. The tests were conducted for four months with coupons located at different levels and one immersed. After two months, two coupons were removed from Level 1 to assess corrosion of a sample that was previously dipped in VCI with a sample with no VCI treatment. GW simulant exposed samples in the VS near the liquid level (Level 1) were the most vulnerable to VSC in previous reports [4],[11],[12]. Figure 5-22 and Figure 5-23 show photographs of the coupons after two and four months of exposure to the LDP and GW simulant, respectively. Coupon weight losses are shown in Table 5-12.

Visually, the photographs displayed a higher corrosion for coupons exposed to GW than LDP simulant. Level 1 coupons demonstrated the highest degree of VSC, as expected. Corrosion rates did not seem to be affected by the presence of the VCI as corrosion rates were on average similar to the non-VCI treated samples. The coupon immersed in the LDP simulant also showed a different corrosion rate than previously reported in FY16, while the coupon immersed in GW showed a similar corrosion rate.

An electrical resistance (ER) probe was used to assess the corrosion environment and its effects with VCI. Generally, corrosion rate measurements are obtained by measuring the resistance of the probe element, which changes over time, as metal loss occurs. The reduction in cross-sectional area of the element, that was fabricated from carbon steel, will increase in electrical resistance as it corrodes. ER data is presented in Figure 5-19 as metal loss versus time. The corrosion rate was measured using the initial and end values for all cases and are observed next to the curve in the same color as the points of the curve. Additional corrosion rates were calculated (in black on Figure 5-19) every two months for the inhibited probes in Vessels 7 and 8. The two corrosion rates were calculated to compare the case after the material corroded to see if the addition of VCI will slow or stop corrosion.

The data in Figure 5-19, it shows that in general, GW VS environment was more aggressive than LDP VS in Level 1, which concurs with the results and appearance of coupons from this level in previous tests. [4],[11],[12]. The results from the inhibited probes indicate that metal loss began to increase after 30 days. The uninhibited probes, on the other hand, began to corrode immediately. Additionally, uninhibited probes, when dipped in the VCI and placed in solution again after two months exposure, had a short period of stability of metal loss that lasted approximately 10 days. The corrosion rates for the second part of the experiment decreased slightly. However, the ER data shows that applying VpCI®-337 as dipping the metal into solution for inhibition has a short-lived effectiveness.

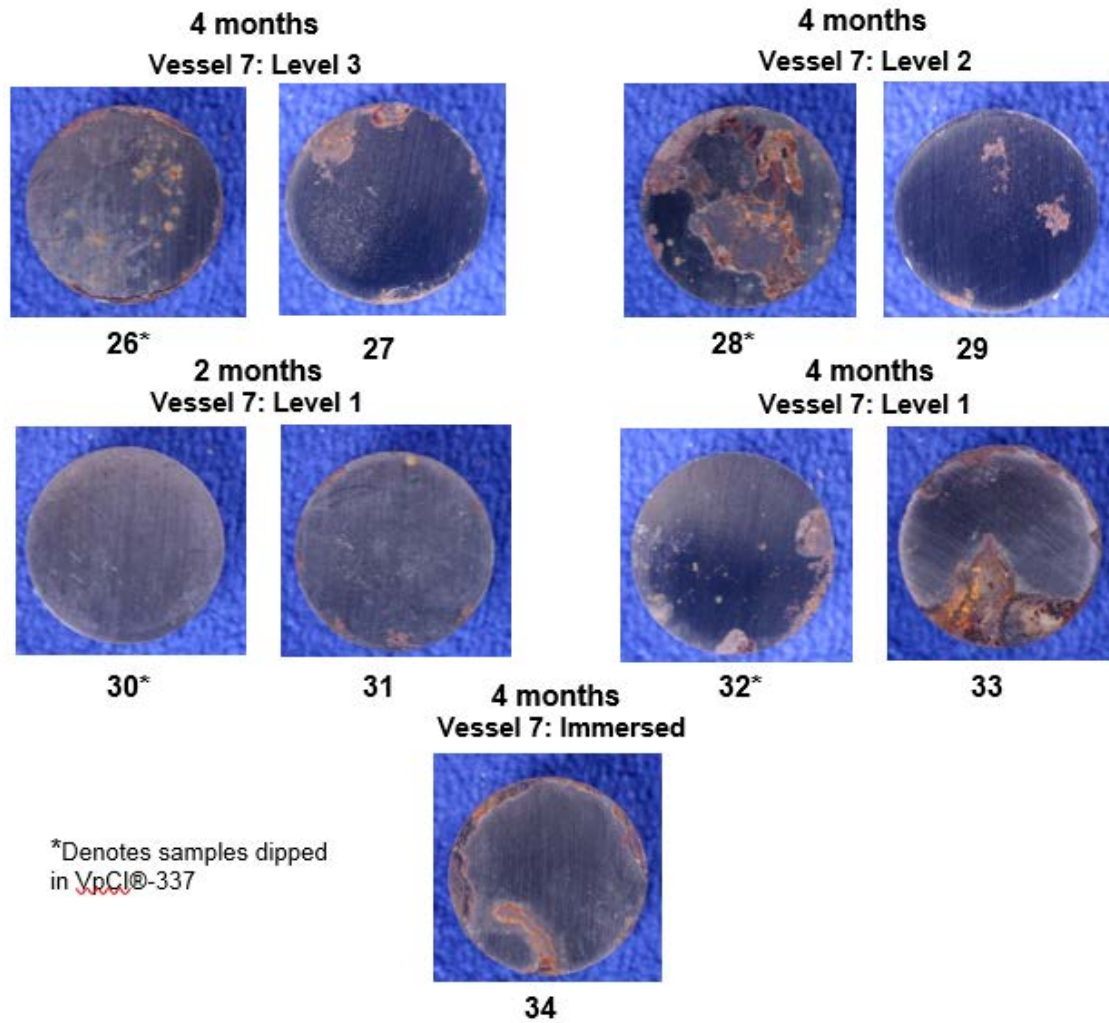


Figure 5-17 Pictures of carbon steel coupons after VS exposure at three different levels and immersed in simulant LDP.

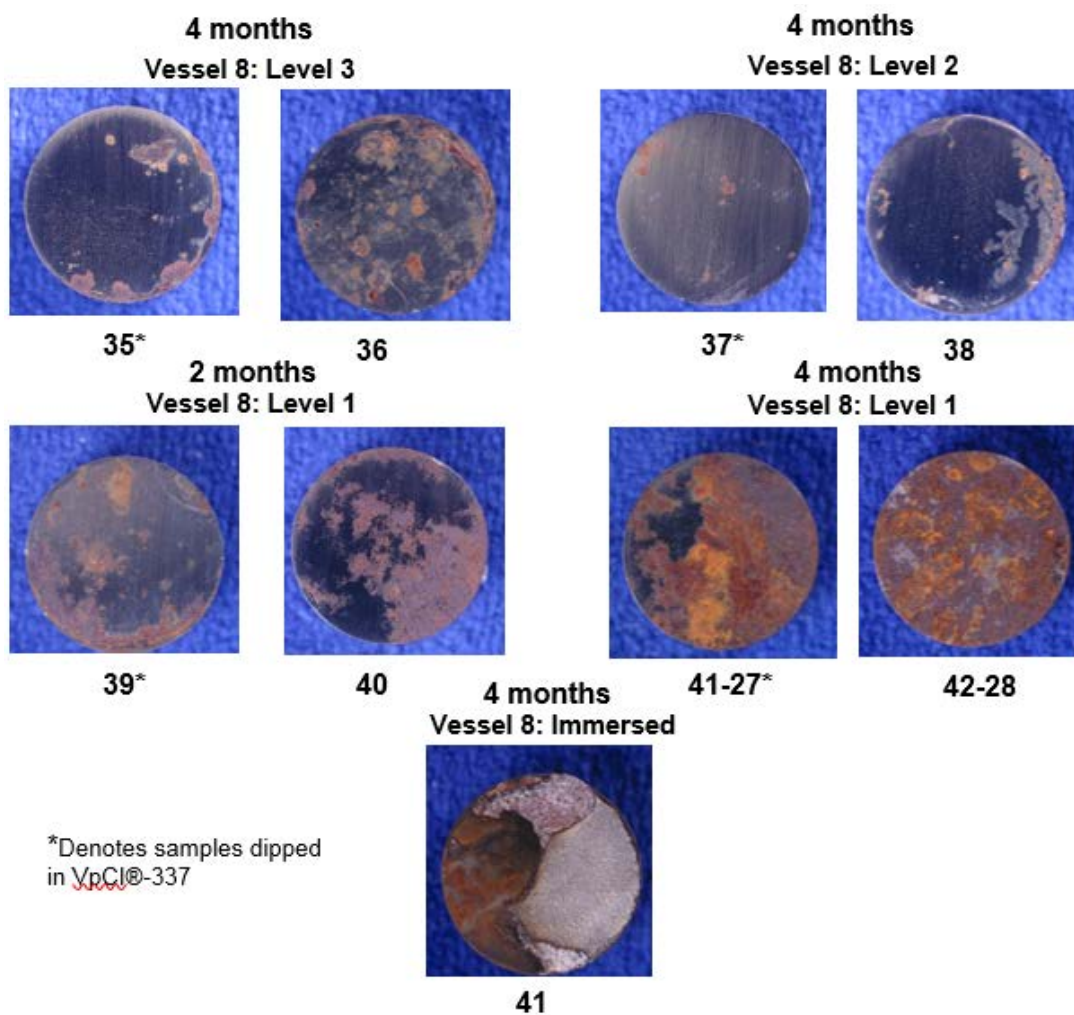


Figure 5-18 Pictures of carbon steel coupons after VS exposure at three different levels and immersed in simulant GW

Table 5-7 Weight losses of coupons at different levels in vessels 7 and 8

Vessel number	Coupon number	Level in vessel	Time exposure (month)	mass loss (g)	Corrosion rate (mpy)
7, 45°C	26*	High (Level3)	4 months	0.0012	0.10
	27	High (Level3)	4 months	0.0016	0.13
	28*	Middle (Level 2)	4 months	0.0029	0.24
	29	Middle (Level 2)	4 months	0.0000	0.00
	30*	Low (Level 1)	2 months	0.0000	0.00
	31	Low (Level 1)	2 months	0.0001	0.02
	32*	Low (Level 1)	4 months	0.0021	0.17
	33	Low (Level 1)	4 months	0.0071	0.59
	34	Immersed	4 months	0.0161	1.33
8, 45°C	35*	High (Level3)	4 months	0.0009	0.07
	36	High (Level3)	4 months	0.0059	0.49
	37*	Middle (Level 2)	4 months	-0.0001	-0.01
	38	Middle (Level 2)	4 months	0.0021	0.17
	39*	Low (Level 1)	2 months	0.0008	0.13
	40	Low (Level 1)	2 months	0.0020	0.33
	41-27*	Low (Level 1)	4 months	0.0053	0.44
	42-28	Low (Level 1)	4 months	0.0090	0.74
	41	Immersed	4 months	0.0917	7.57

* Denotes samples dipped in VpCI®-337

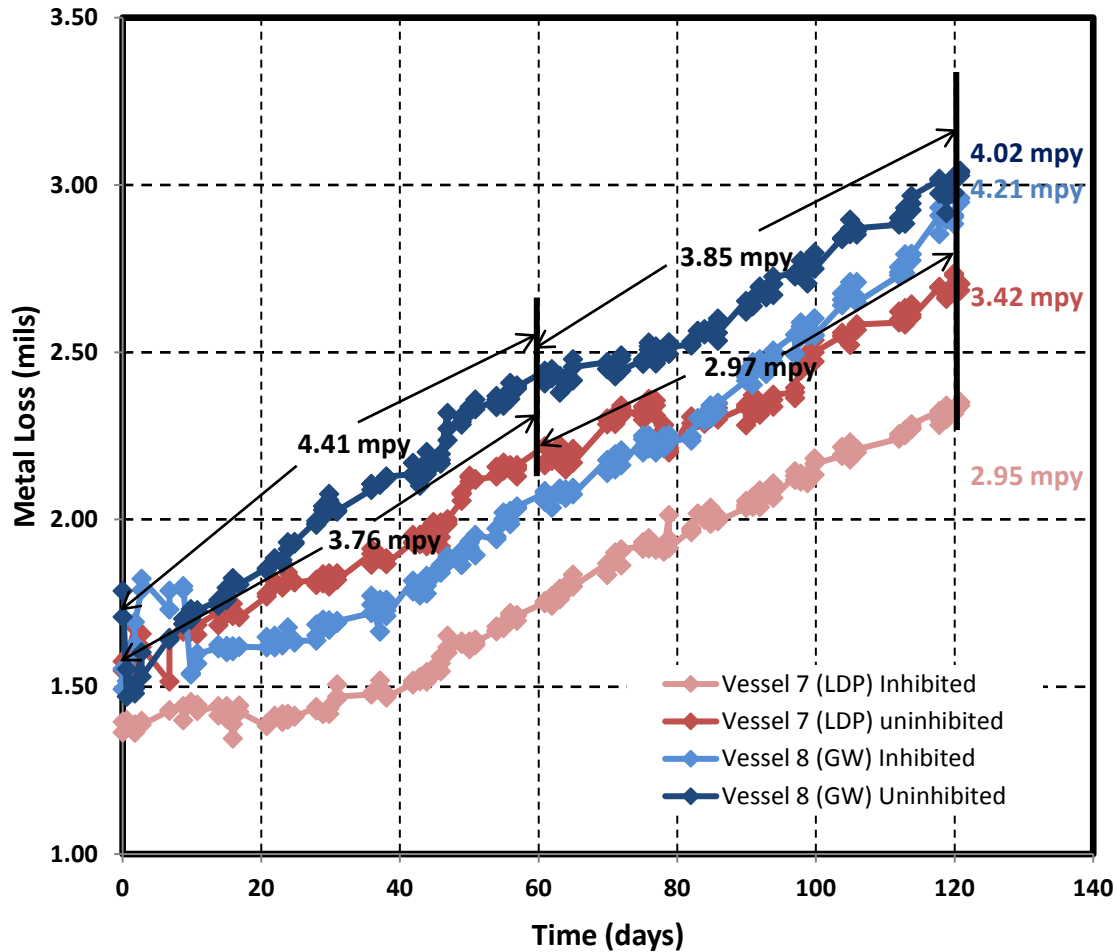


Figure 5-19 ER data as metal loss vs. time for probes placed close to Level 1 of vessels 7 and 8. Two probes were placed on each vessel: one inhibited with VpCI®-337 and one without inhibitor

5.7 Enhanced Corrosion due to Air Radiolysis

The irradiation of air with gamma rays can yield nitrogen dioxide (NO₂) and nitrous oxide (N₂O) by radiolytic reactions. When nitrogen dioxide is in contact with moisture in air, nitric acid (HNO₃) will form in accordance with following equation:



It has been shown that relative humidity in air as low as 10% may form nitric acid by the above equation [32]. Nitric acid condensation on the steel will result in enhanced corrosion of the steel. This mechanism has been observed in a reactor process room at SRS [34]. The plausibility that this

mechanism potentially contributing to failure in AY-102 primary and secondary tank liner is also being investigated.

To obtain the gamma dose rates at points beneath the primary and secondary liner of DSTs, the Monte Carlo n-particle (MCNP) code was used. The MCNP code [35],[36] is a general-purpose Monte Carlo code that can be used for neutron, photon, electron, or coupled transport and can perform shielding modeling and energy deposition calculations. The latest version of the MCNP code, version 6, was used to calculate position-dependent and time-dependent radiation flux, resultant detector response, and effective dose rate for various configurations and scenarios modeled.

The AY-102 DST geometry was modeled based on dimensions gathered from RPP-ASMT-53793 [37] and waste compositions collected from solid layer segments of Core 319 in 2005. A range of waste compositions bounded by these core samples were evaluated in the model to assess the effect of varying Uranium on the resulting dose profile. Cesium-137 concentrations as well as the physical density and volume of AY-102 supernate and sludge layers were taken from RPP-CALC-57237 [38]. Table 5-8 lists the bounding sludge concentrations in weight percent, while Table 5-9 lists the waste description that were used for the modeling.

Table 5-8 Sludge bounds inside DST

Elements	Component Bounds (wt%)
Na	0 - 0.082
Fe	0 - 0.117
Al	0 - 0.0488
Mn	0 - 0.0303
Ni	0 - 0.00423
Cr	0 - 0.00256
U-238	0 - .0144
O	Balance

Table 5-9 Waste description inside DST

	Sludge	Supernate
Cs-137 ($\mu\text{Ci}/\text{cm}^3$)	339.19	185.45
density (g/cm^3)	1.59	1.37
depth (cm)	139.32	243.84

Volumetric F4 mesh tallies were used in MCNP to determine a 3-dimensional gamma flux profile through the sludge, supernate, tanks, refractory and concrete pad. Two distinct radiation source volumes were modeled in the sludge and supernate layers. Each source featured uniform concentrations throughout its volume. Due to the specific interest in dose to the outer tank shells

and pads, only photon sources were considered in this calculation (i.e., the Cs-137 662 keV photon) as Sr-90 and Y-90 beta emission would not penetrate the inner tank wall. Secondary electron contributions through Bremsstrahlung radiation were, however, included in the calculation. Figure 5-20 shows the modeling of the DST and the gamma doses rates. Red indicates higher doses and blue indicates lower doses. Note that the gamma dose rates for the sludge are at the highest, while locations outside the secondary liner for DST are at the lowest. Table 5-10 lists photon dose rates as a function of depth into the base of the DST for the two extrema of Uranium concentrations in the sludge for low and high atomic numbers (Z).

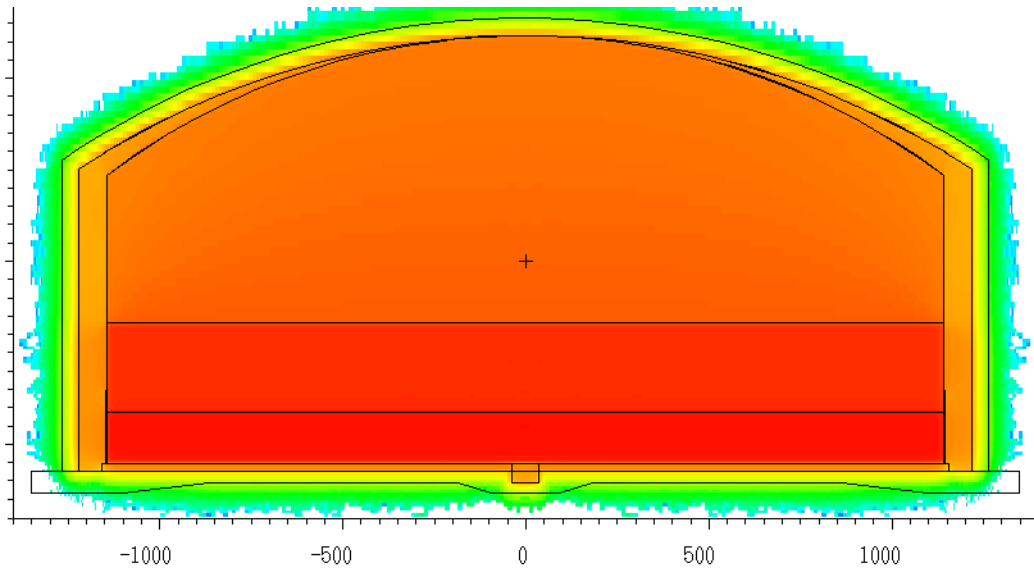


Figure 5-20 AY-102 DST modeled in MCNP6 with resulting gamma doses. Red indicates higher gamma dose rates while blue indicates lower gamma dose rates. Intermediate rates from higher to lower are shown in orange, yellow and green (scale units are in cm).

Table 5-10 Gamma dose rates of sludge towards outer tank

Component	Height (cm)	Dose Rate (Rad/hr)		Normalized Dose Rate	
		Low Z	High Z	Low Z	High Z
Sludge	5	270.5	236.5	0.715	0.746
Inner Tank	-1	75.0	78.9	0.198	0.249
Refractory	-5	52.3	57.2	0.138	0.180
	-10	39.5	42.7	0.104	0.135
	-15	29.3	31.5	0.078	0.099
	-20	21.2	23.2	0.056	0.073
Outer Tank	-22	11.0	12.1	0.029	0.038

Based on these results, the gamma radiation dose is approximately 100 rad/hr in locations around the primary tank. Morco et. al. [32], using HARM, calculated a nitric acid production rate in the gas phase to be 2.0×10^{-8} M/h. This calculation is based on 85% relative humidity, 75 °C in temperature and the volume ratio of air to water of 100 in a droplet. Figure 5-21 shows a diagram of radiolytic reactions that can occur on the gas environment to generate nitric acid gas that can concentrate in a droplet and cause corrosion of steel by iron oxidation.

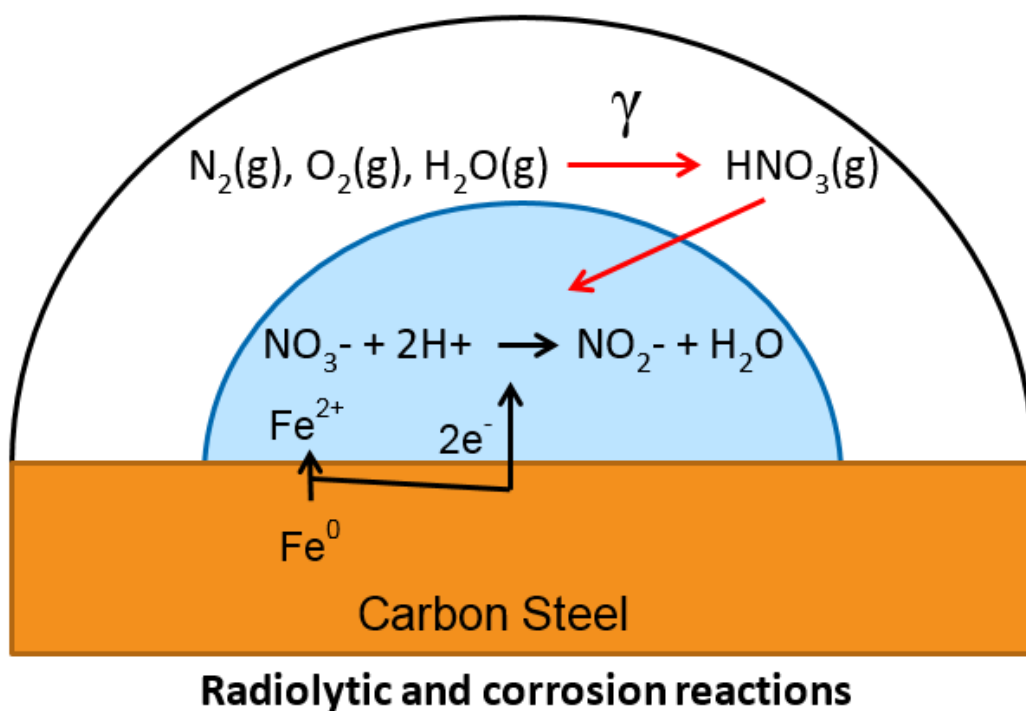


Figure 5-21 Diagram of radiolytic and corrosion reactions that can occur at the surface of carbon steel within a droplet of water

Assuming that between the primary and secondary tank of DSTs there is stagnant air and no interactions with concrete, water droplets condensed on the steel surface can reach pH 5 in approximately 500 hours or around 3 weeks. Based on these results it was decided to test pH of 6 and 5 in a long-term immersion test to see how a change to a pH as low as 5 can affect the corrosion rate of carbon steel. GW simulant was chosen to be used for this test.

Legacy carbon steel in form of bullets were immersed for four months. The pH was monitored daily and adjusted to maintain homogeneity in pH during the long-term testing. After two months at pH 5, the solution was changed out. When changing the solution, the coupons were cleaned to assess a mid-point experiment corrosion rate. Figure 5-22 shows a picture of the coupons exposed to GW simulant at pH 5 after two months. Weight loss and corrosion rates are presented in Table 5-11. Partial immersed correspond to approximately 50% coupon immersion.

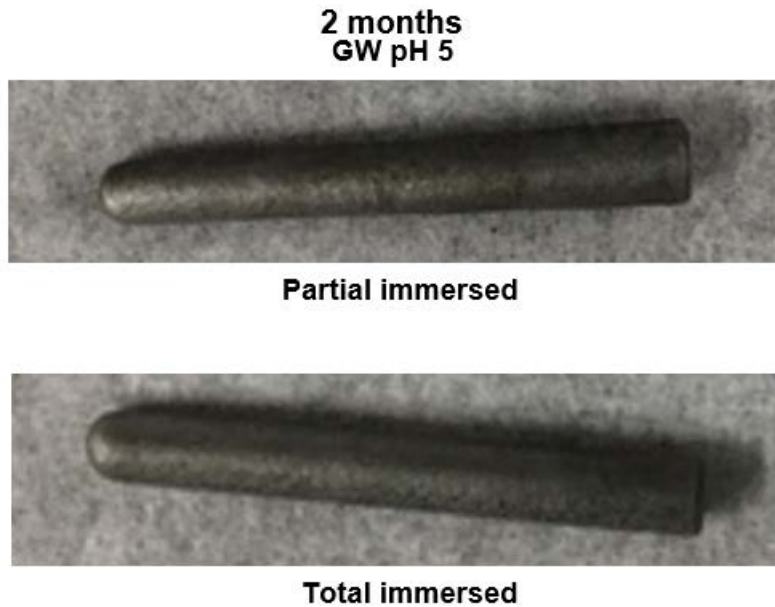


Figure 5-22 Pictures of bullet coupons from GW simulant pH 5 after two months exposure.

Table 5-11 Weight loss and corrosion rate of bullet coupons after two months exposure in GW simulant pH 5

Coupon	Two months exposure GW pH 5	
	weight loss (g)	Corrosion rate (mpy)
Partial immersed	1.4998	96.24
Total immersed	1.6753	107.51

The corrosion rates were calculated using the area of the bullet that was immersed as LAI attack was very active. As shown in the table, very aggressive general attack was observed with corrosion rates of over 95 mpy. The samples were placed back in the test with fresh solution at pH 5, while the coupons at GW pH 6 were not disturbed at this time. After the completion of four months, all the bullet samples were removed and are pictured in Figure 5-23.

The photographs showed a very noticeable difference in the degree of corrosion. The coupons at pH 5 were almost completely corroded with just a small fraction of the coupon left. Weight losses and corrosion rates displayed in Table 5-12 indicate a significantly higher corrosion rate compared to GW at pH 6. Corrosion rates obtained for pH 5 were similar to those at two months and showed a linear continuous rate. The pH change from 6 to 5 increased the corrosion rate by a factor of 5.

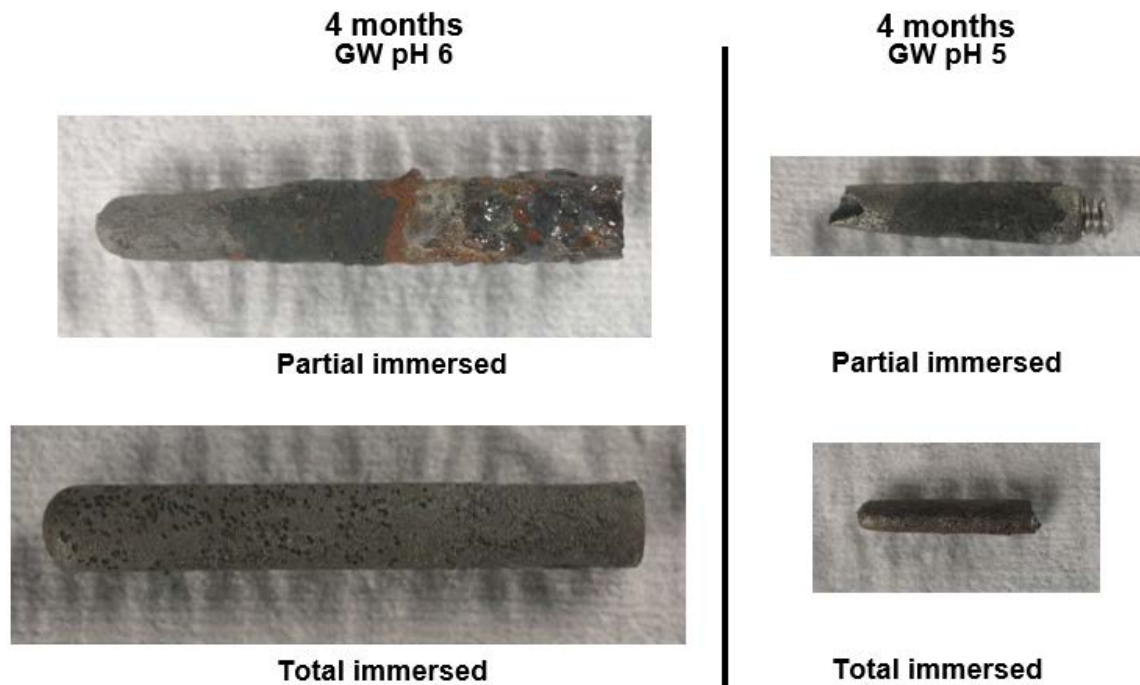


Figure 5-23 Pictures of bullet coupons from GW simulant pH 6 and 5 after four-month exposure.

Table 5-12 Weight losses and corrosion rates for carbon steel coupons exposed to LDP and GW simulants for 4 months at 45 °C.

Solutions	Coupon	Four months exposure	
		weight loss (g)	Corrosion rate (mpy)
GW pH 6	Partial immersion	0.5864	20.2
	Total immersion	0.4973	17.1
GW pH 5	Partial immersion	2.7079	93.1
	Total immersion	3.0870	106.1

Figure 5-24 displays the curve for OCP vs. time for GW simulants at pH 6 and 5 for partial immersed and total immersed coupons. OCPs started at -500 and -650 mV vs. SCE, respectively. During the initial 24 hours, the potential decreased to approximately -660 mV vs. SCE. The potentials are similar to the potential that was observed in previous years [4],[11],[12]. In previous years, a Ag/AgCl reference electrode was utilized, however, since the potential difference between Ag/AgCl and SCE is only 45 mV, a relatively direct comparison can be made between the OCP values. Additionally, as observed in previous years, the potentials from partial immersed coupons were similar to the total immersed coupons during the test. On average, the potentials were stable during the duration of the test, and ranged between -600 to -690 mV vs SCE.

At approximately 2,000 hours or 3 months, the OCPs for GW pH 5 solution increased to less negative values and the OCP for the bullet completely immersed was giving inconsistent results. Upon opening the container to observe the bullet coupons, the completely immersed coupon was disconnected from the stainless-steel rod. However, the partially immersed coupon continued to provide OCP values for the duration of the test. The proximity of potentials, and their stability in an active region, also agree with high activity for corrosion during the long-term exposure.

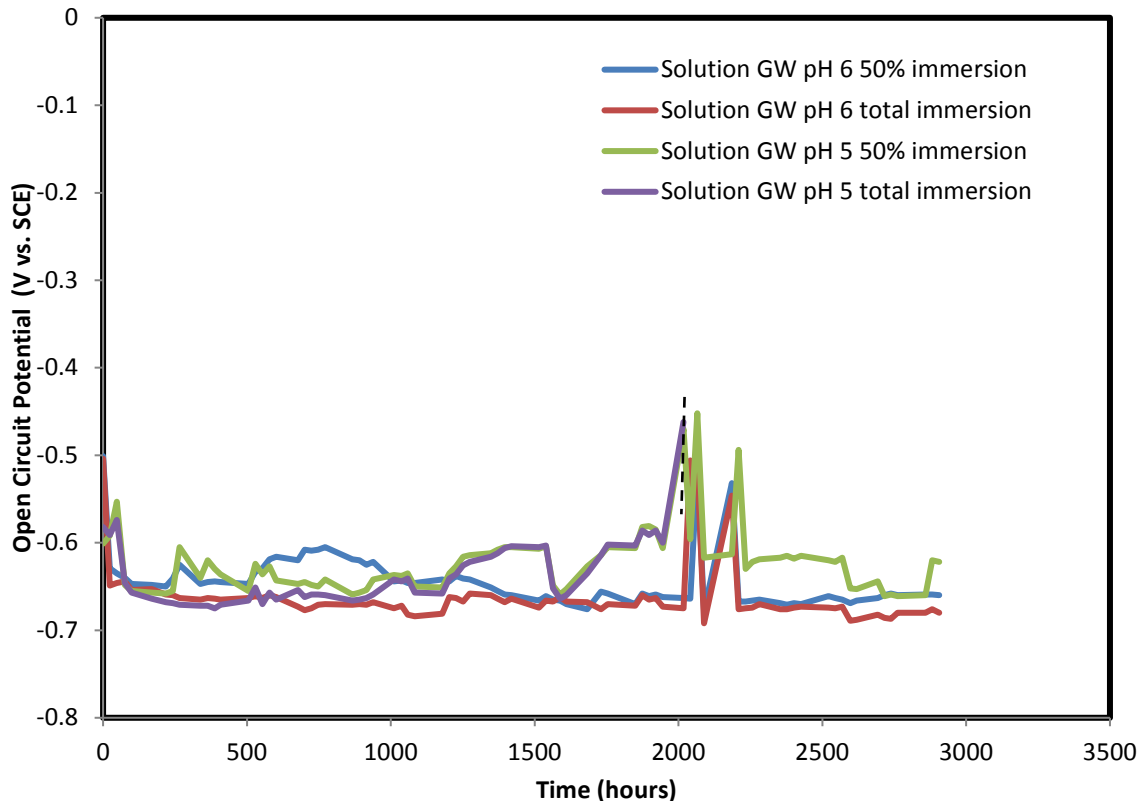


Figure 5-24 OCP vs. time of carbon steel coupons exposed to GW simulants at pH 6 and 5 for partial and complete immersed coupons.

Compared to results from FY16, in which the pH started at 7.6 [4], the corrosion rate nearly doubles when the pH decreases to 6, and increases by a factor of almost 10 times when the pH is 5. The calculated corrosion rates show how aggressive the solution becomes toward carbon steel with a pH decrease. Although the concentration of the acid is minimal in large volumes of ground water (i.e., mL or higher volumes), droplets of water may change to lower pH and help contribute to VSC. Therefore, it is recommended that an inhibition strategy by using a VCI or maintaining relative humidity lower than 10% on the space between the annulus and secondary liner and around the primary liner may help decrease corrosion rate to maintain the integrity of the carbon steel liner.

6.0 Conclusions

In FY17, corrosion studies were performed to support the Hanford DSTs structural integrity. A summary and conclusions of each task is provided.

6.1 New Limits

New Limits testing was continued during FY17. Statistically designed matrices for hydroxide concentration up to 1.2 M and interior points of the waste chemistry envelope were utilized. Combining the Plackett-Burman and Box-Behnken statistically design testing performed in FY16 with these tests, a total of 95 tests were analyzed using logistic regression. Statistically significant chemical variables that affect the solution corrosivity towards pitting corrosion were determined. An expression, referred to as the pitting factor, was evaluated as a criterion to determine limits for pitting corrosion. Additionally, it was observed that ammonia concentration did not significantly influence the pitting model, although a mild inhibition effect was observed in a borderline condition.

The corrosion behavior of carbon steel exposed to AN-102 simulant with no organic species was compared to that for simulants with individual organic species or saturated nitrous oxide gas. Inhibition decreased in comparison to no organic species simulant according to the following order: Glycine, Iminodiacetic Acid, Ammonia, Dibutylphosphate and N-butylamine. Saturated nitrous oxide did not change significantly influence the corrosion behavior.

6.2 Vapor Space Corrosion Tests

DFLAW simulants at concentrated and dilute Na concentrations were used to investigate ammonia inhibition of Vapor Space Corrosion (VSC). Corrosion rates were on average higher for coupons exposed to the dilute than the concentrated Na DFLAW simulant. The solution for dilute Na DFLAW simulant caused more aggressive corrosion in immersed samples and in sample in the vapor phase of the solution compared to concentrated Na DFLAW simulant.

Ammonia detection using QEPAS system was evaluated by testing different flow rates (50- 200 sccm) and at a range of pressures (200-650 Torr). This resulted, as expected, in a linear response, and it was determined that a constant pressure was required for an accurate concentration measurement. The system was placed at the exhaust of one of the vessels from the VSC setup. Since moisture can condense onto the QTF of QEPAS; dampening QEPAS and can result in large variations in detection signal. A new sensor that is specifically designed to measure NH_3 in air was procured and testing will continue during FY18.

LDP and GW simulants treated with VCI were used to study the effectiveness of VpCI®-337 at inhibiting VSC. Corrosion rates for the coupons that were exposed for 4 months were unaffected by the VCI application as they were similar on average to samples that were not treated with VCI. ER probe measurements, used to assess the corrosion environment and its effects with VCI, showed that the GW VS environment was more aggressive than LDP VS. The ER probes exposed to the simulants treated with VCI were protected for approximately 30 days, while the probes exposed to untreated simulants (hereafter defined as unprotected probes) corroded immediately. The unprotected ER probes were dipped in VCI after two months exposure and placed back into test. The corrosion rate decreased for approximately 10 days. However, the ER probe data suggests that the effectiveness of dipping carbon steel into VpCI®-337 as application for inhibitor is short lived and will not significantly reduce carbon steel corrosion in LDP and GW conditions.

6.3 Enhanced Corrosion due to Air Radiolysis

The MCNP code was used to calculate a position-dependent and time-dependent radiation flux, a resultant detector response and the effective dose rate for the exterior of AY-102 DST tank. A gamma dose rate of approximately 100 rad/hr was calculated for locations around the primary tank. Using HARM and assuming stagnant air conditions and no interactions with concrete, water droplets may reach pH 5 in approximately 500 hours, or around 3 weeks. Long immersion tests were performed to determine the severity of corrosion for GW simulant at two pH values: 6 and 5. Corrosion rates were obtained at an average of 18.7 mpy and 99.6 mpy for GW simulant at pH 6 and 5, respectively. Compared to results from FY16 in which the initial pH was 7.6, and was monitored during the 4 months but not adjusted, it represents a corrosion rate increase of almost double when the pH is 6 and almost 10 times when the pH is 5. Although the concentration of the acid is minimal in large volumes of ground water (i.e., mL or higher volumes), the pH of droplets of water may decrease significantly and contribute to VSC. Therefore, it is recommended that an inhibition strategy by using a different application of a VCI or maintaining relative humidity lower than 10% on the space between the annulus and secondary liner and around the primary liner may help decrease corrosion rate to maintain the integrity of the carbon steel liner.

7.0 Quality Assurance

Data for all Tasks were recorded in the electronic laboratory notebook system, notebook number G8519-00126.

Requirements for performing reviews of technical reports and the extent of review are established in manual E7 2.60. SRNL documents the extent and type of review using the SRNL Technical Report Design Checklist contained in WSRC-IM-2002-00011, Rev. 2.

8.0 References

- [1] R. E. Fuentes, "SRNL Task Technical And Quality Assurance Plan for Hanford Double Shell Waste Tank Corrosion Studies-FY17", SRNL-RP-2017-00025, Savannah River National Laboratory, Aiken, SC, February 2017.
- [2] L. M. Stock, J. R. Follett, and E. C. Shallman, "Specifications for the Minimization of the Stress Corrosion Cracking Threat in Double-Shell Tank Wastes," RPP-RPT-47337, Washington River Protection Solutions, Richland, WA, March 2011.
- [3] T. Martin, "Outcomes from the August 2013 Expert Panel Oversight Committee Meeting," RPP-ASMT-56781, Washington River Protection Solutions LLC, Richland, WA, February 2014.
- [4] R. E. Fuentes, "Hanford Double Shell Waste Tank Corrosion Studies-Final Report FY16", SRNL-STI-2016-00721, Savannah River National Laboratory, Aiken, February 2017.
- [5] C. M. Giordano, E. Saenz, D. R. Weier, and R. M. Carranza, "Corrosion of Steel Tanks in Liquid Nuclear Wastes". CORROSION 2006, Paper no. 06635, NACE International, Houston, TX, 2006.
- [6] A.R. Felmy, O. Qafoku, B. Arey, K.D. Boomer, "Chemical Species in the Vapor Phase of Hanford Double-Shell Tanks: Potential Impacts on Waste Tank Corrosion

- Processes” PNNL-19767, Pacific Northwest National Laboratory, Richland, WA, September 2010.
- [7] E. N. Hoffman, “Testing Vapor Space and Liquid-Air Interface Corrosion In Simulated Environments of Hanford Double-Shelled Tanks,” SRNL-STI-2011-00494, Savannah River National Laboratory, Aiken, SC, September 2011.
- [8] J. R. Gray, B. L. Garcia-Diaz, T. H. Murphy and K. R. Hicks, “Vapor Space Corrosion Testing Simulating the Environment of Hanford Double Shell Tanks,” SRNL-STI-2013-00739, Savannah River National Laboratory, Aiken, SC, January 2014.
- [9] R. P. Anantatmula, “DST Pitting Annual Report,” WHC-SD-WM-PRS-016, Rev. 0, Westinghouse Hanford Company, Richland, WA, September 1996.
- [10] J. W. Congdon, “Evaluation of Corrosion Inhibitors for Washed Precipitate – Coupon Test Results,” DPST-86-721, Savannah River Laboratory, Aiken SC, October, 1986.
- [11] R. E. Fuentes, B. J. Wiersma and K. Hicks, “Hanford Double Shell Waste Tank Corrosion Studies-Final Report FY14”, SRNL-STI-2014-00616, Savannah River National Laboratory, Aiken, December 2014.
- [12] R. E. Fuentes, R. B. Wyrwas, “Hanford Double Shell Waste Tank Corrosion Studies-Final Report FY15”, SRNL-STI-2016-00117, Savannah River National Laboratory, Aiken, May 2016.
- [13] S. Savoye, L. Legrand, G. Sagon, S. Lecomte, A. Chausse, R. Messina and P. Toulhoat, “Experimental investigations on iron corrosion products formed in bicarbonate/carbonate-containing solutions at 90 °C”, Corrosion Science, 43, p. 2049, 2001.
- [14] ASTM A515, “Standard Specification for Pressure Vessel Plates, Carbon Steel, for Intermediate- and Higher-Temperature Service”, ASTM International, West Conshohocken, PA, 2003.
- [15] ASTM G5-13 “Standard Reference Test Method for Making Potentiodynamic Anodic Polarization Measurements”, ASTM International, West Conshohocken, PA, 2013.
- [16] ASTM G1-03 “Standard Practice for Preparing, Cleaning, and Evaluating Corrosion Test Specimens”, ASTM International, West Conshohocken, PA, 2011.
- [17] P. Patimisco, G. Scamarco, F. Tittel, and V. Spagnolo, “Quartz-enhanced photoacoustic spectroscopy: a review, Sensors 14, p. 6165 2014.
- [18] T. Martin, “Tank Integrity Expert Panel Corrosion Subgroup March 2016 Meeting Outcomes”, RPP-ASMT-60833, Washington River Protection Solutions LLC, Richland, WA, May 2016.
- [19] ASTM G192-08, “Standard Test Method for Determining the Crevice Repassivation Potential of Corrosion-Resistant Alloys Using a Potentiodynamic-Galvanostatic-Potentiostatic Technique”, ASTM International, West Conshohocken, PA, 2014.
- [20] S. Tsujikawa and Y. Hisamatsu, “On the repassivation potential for crevice corrosion” Corrosion Engineering, Japan, 29, 37, 1980.
- [21] S. Matsuda and H. H. Uhlig, “Effect of pH, Sulfates and Chlorides on Behavior of Sodium Chromate and Nitrite as Passivators for Mild Steel”, Journal of the Electrochemical Society, Volume 3, No. 2, p. 156, February 1964.
- [22] A. D. Mercer, et. al., “Comparative Study of Factors Influencing the Action of Corrosion Inhibitors for Mild Steel in Neutral Solution, III. Sodium Nitrite”, Br. Corrosion Journal, Vol. 3, p. 136, 1968.
- [23] R. S. Ondrejcin, "Prediction of Stress Corrosion of Carbon Steel by Nuclear Process

- Liquid Wastes", DP-1478, August 1978.
- [24] J. W. Congdon, "Aggressive Anions in Washed Precipitate", DPST-86-803, November 24, 1986.
- [25] R. S. Ondrejcin, S. P. Rideout, and J. A. Donovan, "Control of Stress Corrosion Cracking in Storage Tanks Containing Radioactive Waste", Nuclear Technology, Vol. 44, No. 7, p. 297, 1979.
- [26] D. M. Brasher, et. al., "Comparative Study of Factors Influencing the Action of Corrosion Inhibitors for Mild Steel in Neutral Solution, IV. Mechanism of Action of Mixed Inhibitive and Aggressive Anions", Br. Corrosion Journal, Vol. 3, p. 144, 1968.
- [27] A. Macias and M. L. Escudero, "The Effect of Fluoride Ion on Corrosion of Reinforcing Steel in Alkaline Solutions", Corrosion Science, Vol. 36, No. 12, p. 2169.
- [28] Private Communication with Leon Stock. This was a summary of pitting data from 2005-2017.
- [29] P. E. Zapp and D. T. Hobbs, "Inhibiting Pitting Corrosion in Carbon Steel Exposed to Dilute Radioactive Waste Slurries", Corrosion 92, Paper No. 98, NACE International, Houston, TX, 1992.
- [30] R. B. Wyrwas et. al., "Development of a Corrosion Control Program for Hanford Waste Treatment Plant Recycle Strategy", Corrosion 2018, Paper No. 11455, NACE International, Houston, TX, 2018.
- [31] T. Aoki, S. Uemura and M. Munemori, "Continuous Flow Fluorometric Determination of Ammonia in Water", Analytical Chemistry, 55, p. 1620 (1983).
- [32] B. Peters and D. Hitchcock, memo to B. Wiersma, SRNL-L4410-2017-0016, October 11, 2017
- [33] R. P. Morco, J. M. Joseph, D. S. Hall, C. Medri, D. W. Shoesmith and J. C. Wren, "Modeling of Radiolytic Production of HNO_3 Relevant to Corrosion of a Used Fuel Container in Deep Geologic Repository Environments" University of Western Ontario, Canada
- [34] F. B. Longtin, "Air Radiolysis", DPSP-69-1403, September 19, 1969.
- [35] X-5 Monte Carlo Team, "MCNP – A General Monte Carlo N-Particle Transport Code", LA-UR-03-1987, Version 5, April 24, 2003 (Revised 10/03/05)
- [36] Monte Carlo Team, MCNP6 User's Manual, LA-CP-13-0643, May, 2013.
- [37] J. K. Engeman, C. L. Girardot, D. G. Harlow and C. L. Rosenkrance, "Tank 241-AY-102 Leak Assessment Report" RPP-ASMT-53793, October 2012
- [38] J. R. Bristol, "In-Tank Exposure Rate Estimates for the AY-102 Waste Retrieval", RPP-CALC-57237, May 12, 2014.

9.0 Appendices

Appendix A

**Chemical Composition of New Limits Task from an Augmented
Statistical Design with Electrochemical Results and Pictures after Test**

Appendix B

**Chemical Composition of New Limits Task using Interior Points from a Statistical Design
Analysis with Electrochemical Results and Pictures after Test**

Appendix C

**Chemical Composition of New Limits Task with ammonia from a Statistical Design
Analysis with Electrochemical Results and Pictures after Test**

Appendix D

**Chemical Composition of New Limits Task of effects of an organic specie and nitrous oxide
for AN-102 based simulant with Electrochemical Results and Pictures after Test**

Appendix E

Chemical Composition of Simulants used in Vapor Space Corrosion Testing

Appendix F

Pictures of Vapor Space Corrosion Samples after Test

Appendix G

Chemical Composition of Simulants used in Air Radiolysis Corrosion Testing

Appendix H

Pictures of Air Radiolysis Corrosion Samples after Test

Appendix I

**Open Circuit Potential, pH and Temperature vs. Time plots Air Radiolysis Corrosion
Testing**

Appendix J

**Direct Feed Low-Activity Waste Corrosion Testing performed at SRNL Memos (one from
May 16, 2017/ two from September 28, 2017)**

Appendix A

Chemical Composition of New Limits Task from an Augmented Statistical Design with Electrochemical Results and Pictures after Test

Table A1. Test conditions and results of testing performs using an augmented statistical approach to 1.2 M Hydroxide

Test	Temperature (°C)	Hydroxide (M)	Nitrite (M)	Nitrate (M)	Chloride (M)	Sulfate (M)	Carbonate (M)	Bicarbonate (M)	Target pH	Category		Pitting on sample		Logistic Approach
										run 1	run 2	run 1	run 2	
1	35	1.2	0	3.75	0	0.13	0.1	0	13.3	1	1	No	No	0
2	35	1.2	0	4.75	0	0.07	0.1	0	13.3	1	1	No	No	0
3	35	1.2	0	3.1	0.08	0.09	0.1	0	13.3	1	1	No	No	0
4	35	1.2	0	2.42	0.16	0.08	0.1	0	13.3	1	1	No	No	0
5	35	1.2	0	4.5	0.2	0.03	0.1	0	13.3	1	1	No	No	0
6	35	1.2	0	0.94	0.24	0.01	0.1	0	13.3	3	3	Yes	Yes	1
7	35	1.2	0	0.26	0.32	0.17	0.1	0	13.3	1	1	No	No	0
8	35	1.2	0	4.75	0.35	0.07	0.1	0	13.3	3	3	Yes	Yes	1
9	35	1.2	0	0	0.4	0.02	0.1	0	13.3	1	1	No	No	0
10	35	1.2	0.6	4.74	0.08	0.02	0.1	0	13.3	1	1	No	No	0
11	35	1.2	0.6	5.32	0.15	0	0.1	0	13.3	1	1	No	No	0
12	35	1.2	0.6	3.31	0.16	0.2	0.1	0	13.3	1	1	No	No	0
13	35	1.2	0.6	2.68	0.24	0.05	0.1	0	13.3	1	1	No	No	0
14	35	1.2	0.6	4.92	0.28	0.06	0.1	0	13.3	1	3	No	Yes	0
15	35	1.2	0.6	1.26	0.32	0.01	0.1	0	13.3	1	1	No	No	0
16	35	1.2	0.6	0.63	0.4	0.17	0.1	0	13.3	1	1	No	No	0
17	35	1.2	0.6	5.32	0.4	0.01	0.1	0	13.3	3	3	Yes	Yes	1
18	35	1.2	1.2	4.01	0.16	0.15	0.1	0	13.3	1	1	No	No	0
19	35	1.2	1.2	4.17	0.21	0.01	0.1	0	13.3	1	1	No	No	0
20	35	1.2	1.2	3.4	0.24	0.1	0.1	0	13.3	1	1	No	No	0
21	35	1.2	1.2	1.99	0.32	0.09	0.1	0	13.3	1	1	No	No	0
22	35	1.2	1.2	4.57	0.32	0.13	0.1	0	13.3	3	3	Yes	Yes	0
23	35	1.2	1.2	1.38	0.4	0.01	0.1	0	13.3	1	1	No	No	0
24	35	1.2	1.2	4.17	0.4	0.01	0.1	0	13.3	1	1	No	No	0

Table A2. Test conditions and results of testing performs using an augmented statistical approach to 1.2 M Hydroxide (continued)

Test	Temperature (°C)	Hydroxide (M)	Nitrite (M)	Nitrate (M)	Chloride (M)	Sulfate (M)	Carbonate (M)	Bicarbonate (M)	Target pH	Category		Pitting on sample		Logistic Approach
										run 1	run 2	run 1	run 2	
25	35	0.3	0.6	2.75	0.2	0.15	0.1	0	13.3	5	5	Yes	Yes	1
26	35	0.3	0.6	2.75	0.2	0.07	0.1	0	13.3	5	5	Yes	Yes	1
27	35	0.3	0.6	2.75	0.2	0.05	0.1	0	13.3	5	5	Yes	Yes	1

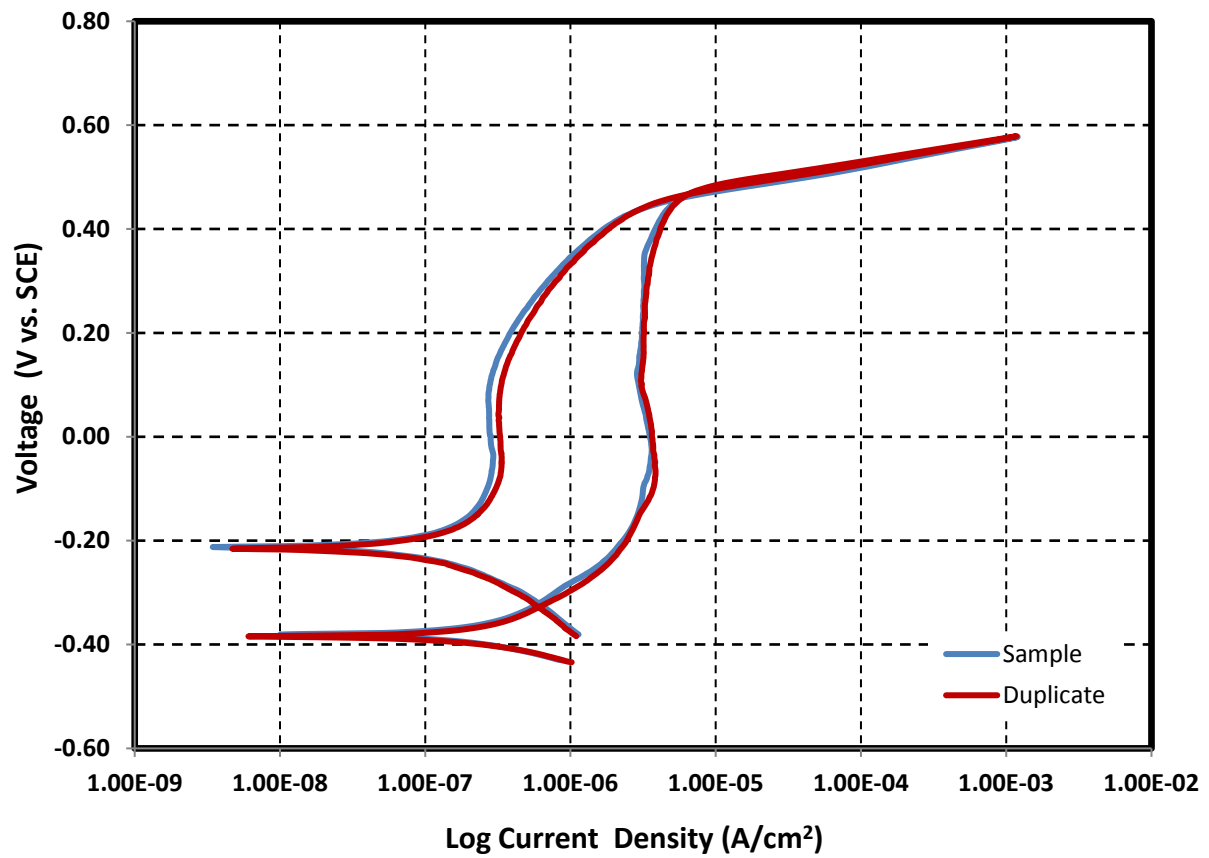
Composition of simulant for New Limits-Test 1

Test 1-NL

Temperature 35 °C
 pH at room temperature 13.53 Target 13.3
 pH before testing (at temp.) 13.38 pH after testing (at room temp.) 13.43
 Volume 1.4 L

Simulant Source	Formula	Molecular Weight (g/mol)	Concentration (M)	weight required (g)
Sodium hydroxide	NaOH	40.0000	1.2	67.2000
Sodium nitrite	NaNO ₂	69.0000	0	0.0000
Sodium nitrate	NaNO ₃	85.0000	3.75	446.2500
Sodium chloride	NaCl	58.4000	0	0.0000
Sodium sulfate	Na ₂ SO ₄	142.0000	0.13	25.8440
Sodium carbonate	Na ₂ CO ₃	106.0000	0.1	14.8400
Sodium bicarbonate	NaHCO ₃	84.0100	0	0.0000

Cyclic Potentiodynamic Polarization



Images of bullet samples after electrochemical tests

Test 1



Test 1D



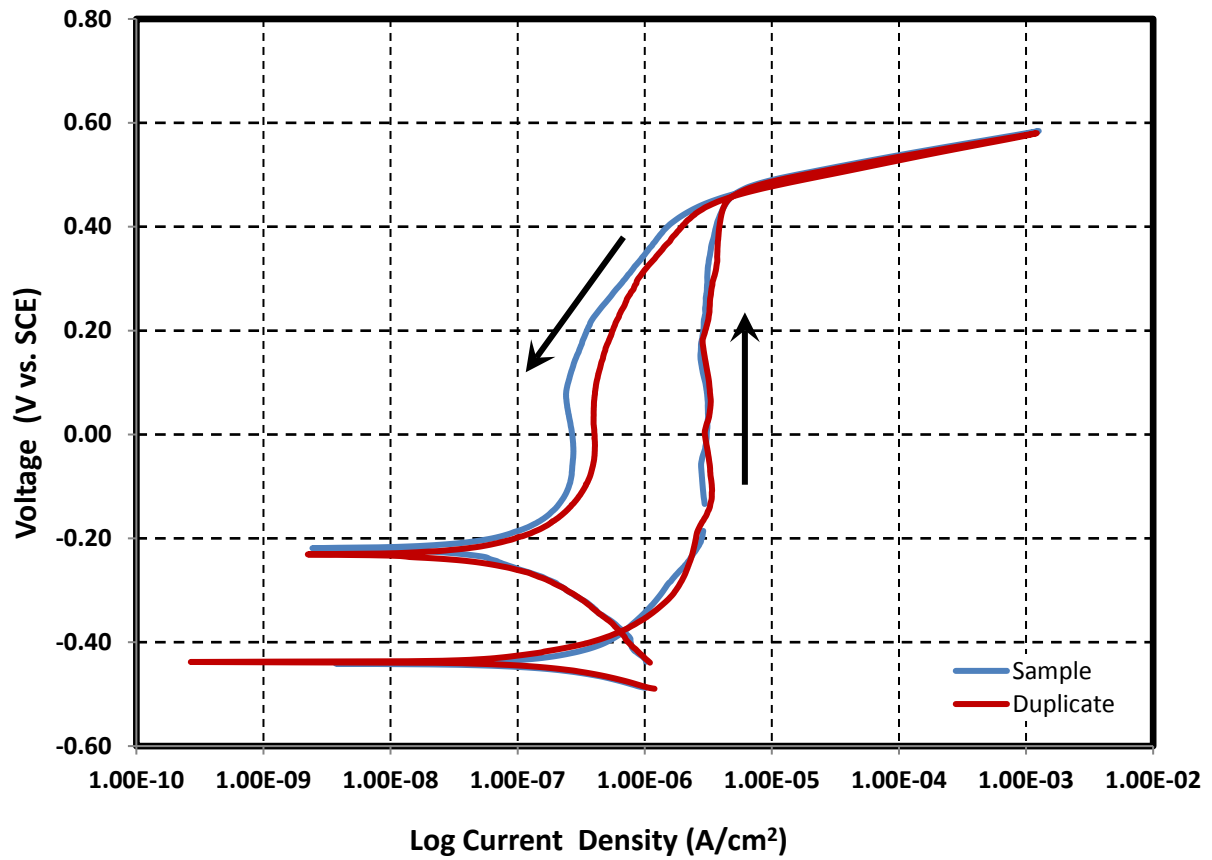
Composition of simulant for New Limits-Test 2

Test 2-NL

Temperature 35 °C
 pH at room temperature 13.54 Target 13.3
 pH before testing (at temp.) 13.46 pH after testing (at temp.) 13.48
 Volume 1.4 L

Simulant Source	Formula	Molecular Weight (g/mol)	Concentration (M)	weight required (g)
Sodium hydroxide	NaOH	40.0000	1.2	67.2000
Sodium nitrite	NaNO ₂	69.0000	0	0.0000
Sodium nitrate	NaNO ₃	85.0000	4.75	565.2500
Sodium chloride	NaCl	58.4000	0	0.0000
Sodium sulfate	Na ₂ SO ₄	142.0000	0.07	13.9160
Sodium carbonate	Na ₂ CO ₃	106.0000	0.1	14.8400
Sodium bicarbonate	NaHCO ₃	84.0100	0	0.0000

Cyclic Potentiodynamic Polarization



Images of bullet samples after electrochemical tests

Test 2



Test 2D



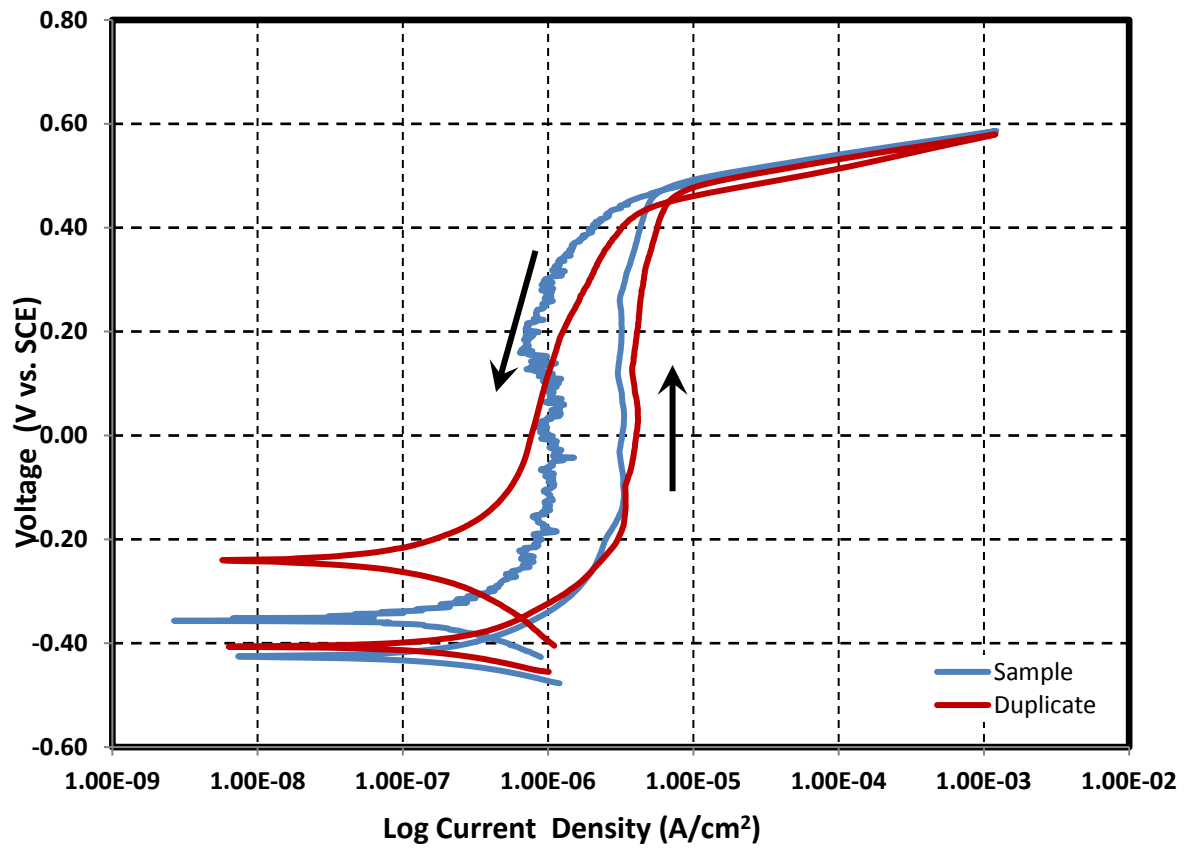
Composition of simulant for New Limits-Test 3

Test 3-NL

Temperature 35 °C
 pH at room temperature 13.62 Target 13.3
 pH before testing (at temp.) 13.38 pH after testing (at temp.) 13.44
 Volume 1.4 L

Simulant Source	Formula	Molecular Weight (g/mol)	Concentration (M)	weight required (g)
Sodium hydroxide	NaOH	40.0000	1.2	67.2000
Sodium nitrite	NaNO ₂	69.0000	0	0.0000
Sodium nitrate	NaNO ₃	85.0000	3.1	368.9000
Sodium chloride	NaCl	58.4000	0.08	6.5408
Sodium sulfate	Na ₂ SO ₄	142.0000	0.09	17.8920
Sodium carbonate	Na ₂ CO ₃	106.0000	0.1	14.8400
Sodium bicarbonate	NaHCO ₃	84.0100	0	0.0000

Cyclic Potentiodynamic Polarization



Images of bullet samples after electrochemical tests

Test 3



Test 3D



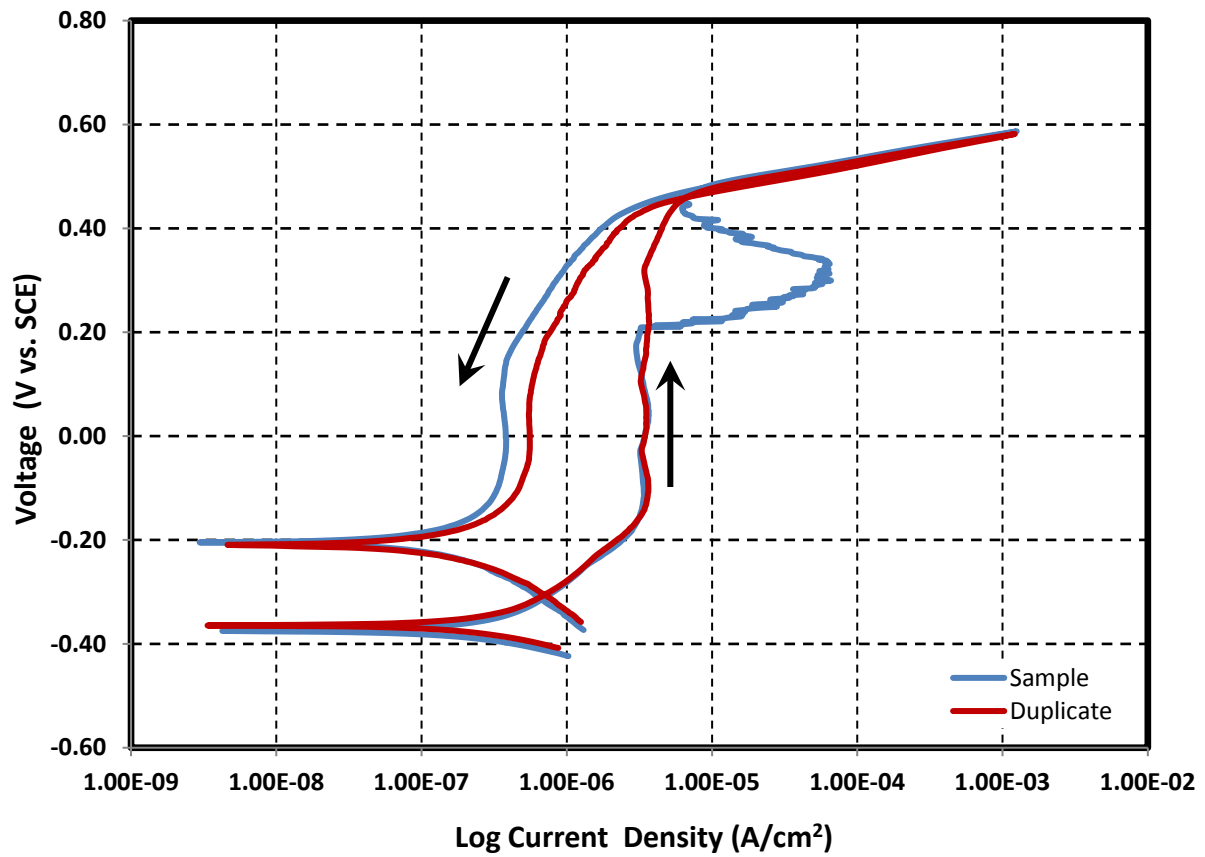
Composition of simulant for New Limits-Test 4

Test 4-NL

Temperature 35 °C
 pH at room temperature 13.52 Target 13.3
 pH before testing (at temp.) 13.45 pH after testing (at temp.) 13.28
 Volume 1.4 L

Simulant Source	Formula	Molecular Weight (g/mol)	Concentration (M)	weight required (g)
Sodium hydroxide	NaOH	40.0000	1.2	67.2000
Sodium nitrite	NaNO ₂	69.0000	0	0.0000
Sodium nitrate	NaNO ₃	85.0000	2.42	287.9800
Sodium chloride	NaCl	58.4000	0.16	13.0816
Sodium sulfate	Na ₂ SO ₄	142.0000	0.08	15.9040
Sodium carbonate	Na ₂ CO ₃	106.0000	0.1	14.8400
Sodium bicarbonate	NaHCO ₃	84.0100	0	0.0000

Cyclic Potentiodynamic Polarization



Images of bullet samples after electrochemical tests

Test 4



Test 4D



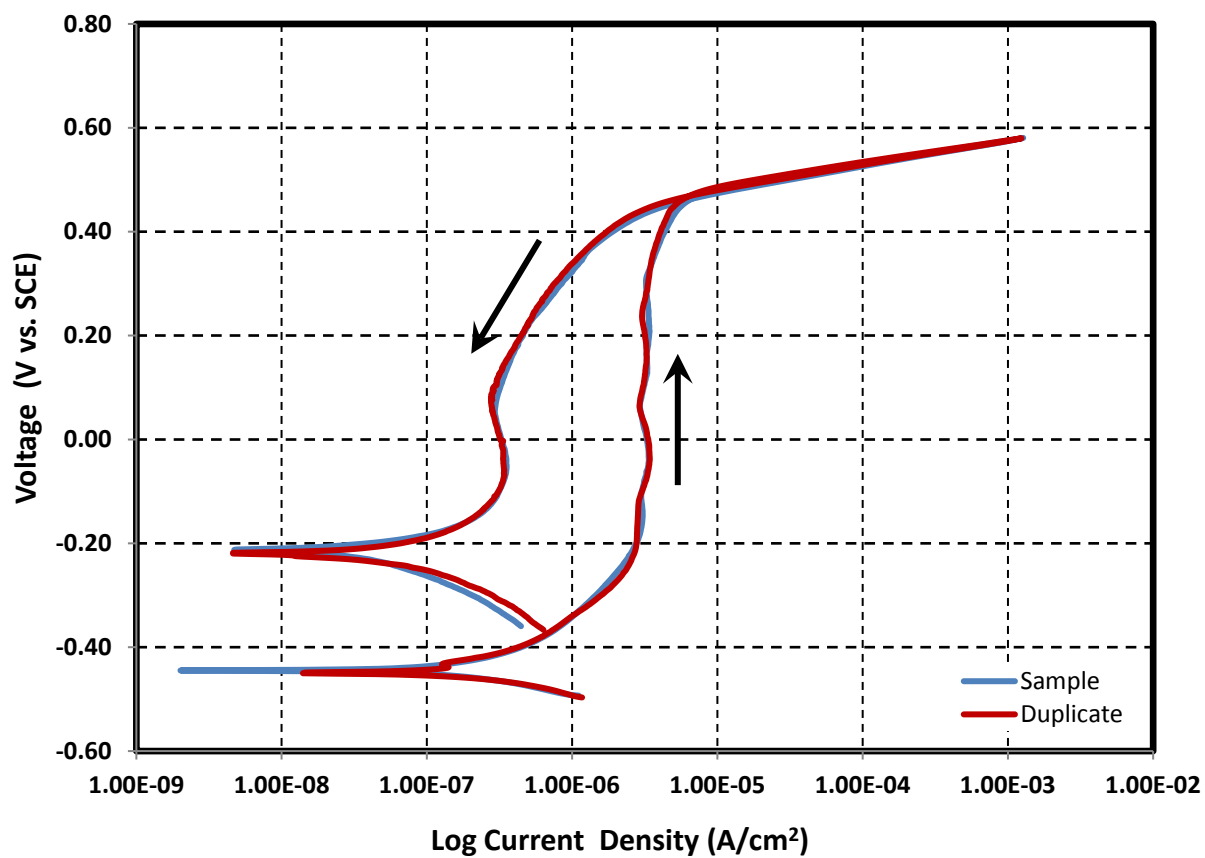
Composition of simulant for New Limits-Test 5

Test 5-NL

Temperature 35 °C
 pH at room temperature 13.53 Target 13.3
 pH before testing (at temp.) 13.38 pH after testing (at temp.) 13.68
 Volume 1.4 L

Simulant Source	Formula	Molecular Weight (g/mol)	Concentration (M)	weight required (g)
Sodium hydroxide	NaOH	40.0000	1.2	67.2000
Sodium nitrite	NaNO ₂	69.0000	0	0.0000
Sodium nitrate	NaNO ₃	85.0000	4.5	535.5000
Sodium chloride	NaCl	58.4000	0.2	16.3520
Sodium sulfate	Na ₂ SO ₄	142.0000	0.03	5.9640
Sodium carbonate	Na ₂ CO ₃	106.0000	0.1	14.8400
Sodium bicarbonate	NaHCO ₃	84.0100	0	0.0000

Cyclic Potentiodynamic Polarization



Images of bullet samples after electrochemical tests

Test 5



Test 5D



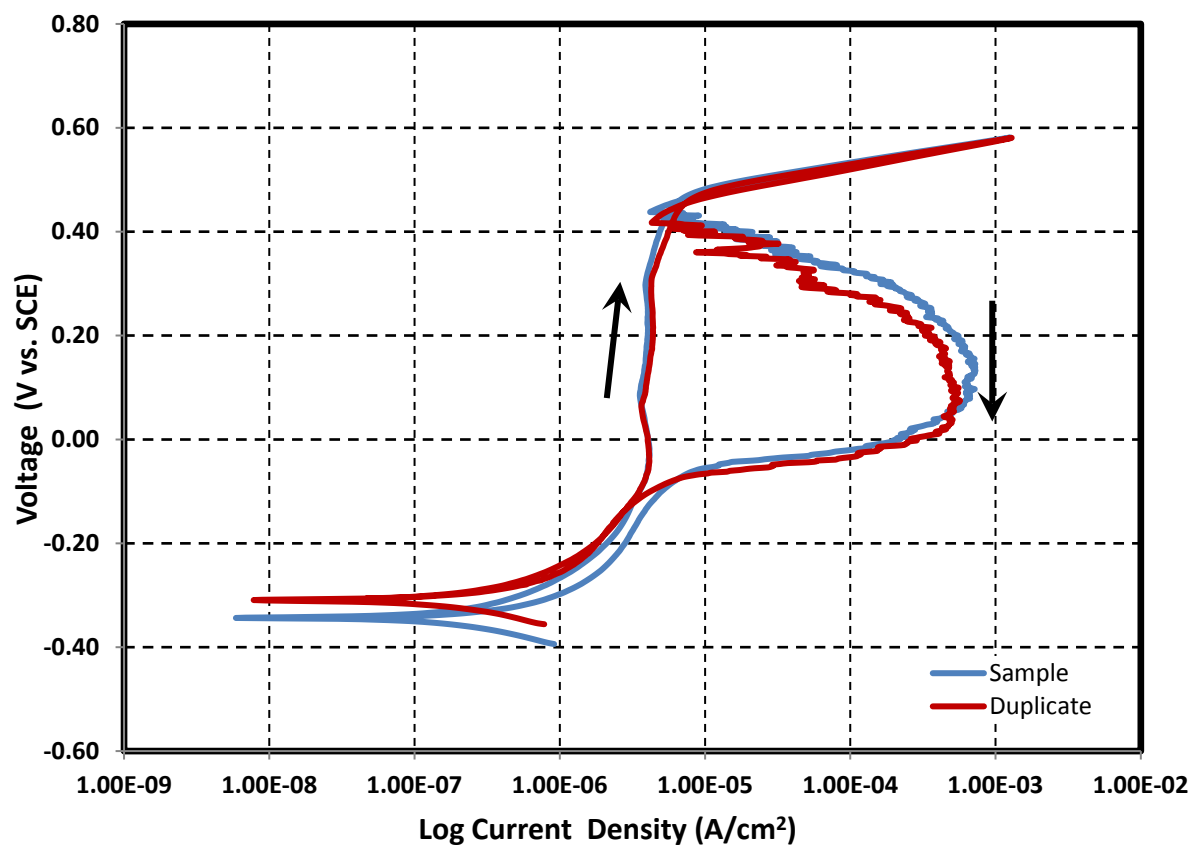
Composition of simulant for New Limits-Test 6

Test 6-NL

Temperature 35 °C
 pH at room temperature 13.41 Target 13.3
 pH before testing (at temp.) 13.45 pH after testing (at temp.) 13.52
 Volume 1.4 L

Simulant Source	Formula	Molecular Weight (g/mol)	Concentration (M)	weight required (g)
Sodium hydroxide	NaOH	40.0000	1.2	67.2000
Sodium nitrite	NaNO ₂	69.0000	0	0.0000
Sodium nitrate	NaNO ₃	85.0000	0.94	111.8600
Sodium chloride	NaCl	58.4000	0.24	19.6224
Sodium sulfate	Na ₂ SO ₄	142.0000	0.01	1.9880
Sodium carbonate	Na ₂ CO ₃	106.0000	0.1	14.8400
Sodium bicarbonate	NaHCO ₃	84.0100	0	0.0000

Cyclic Potentiodynamic Polarization



Images of bullet samples after electrochemical tests

Test 6



Test 6D



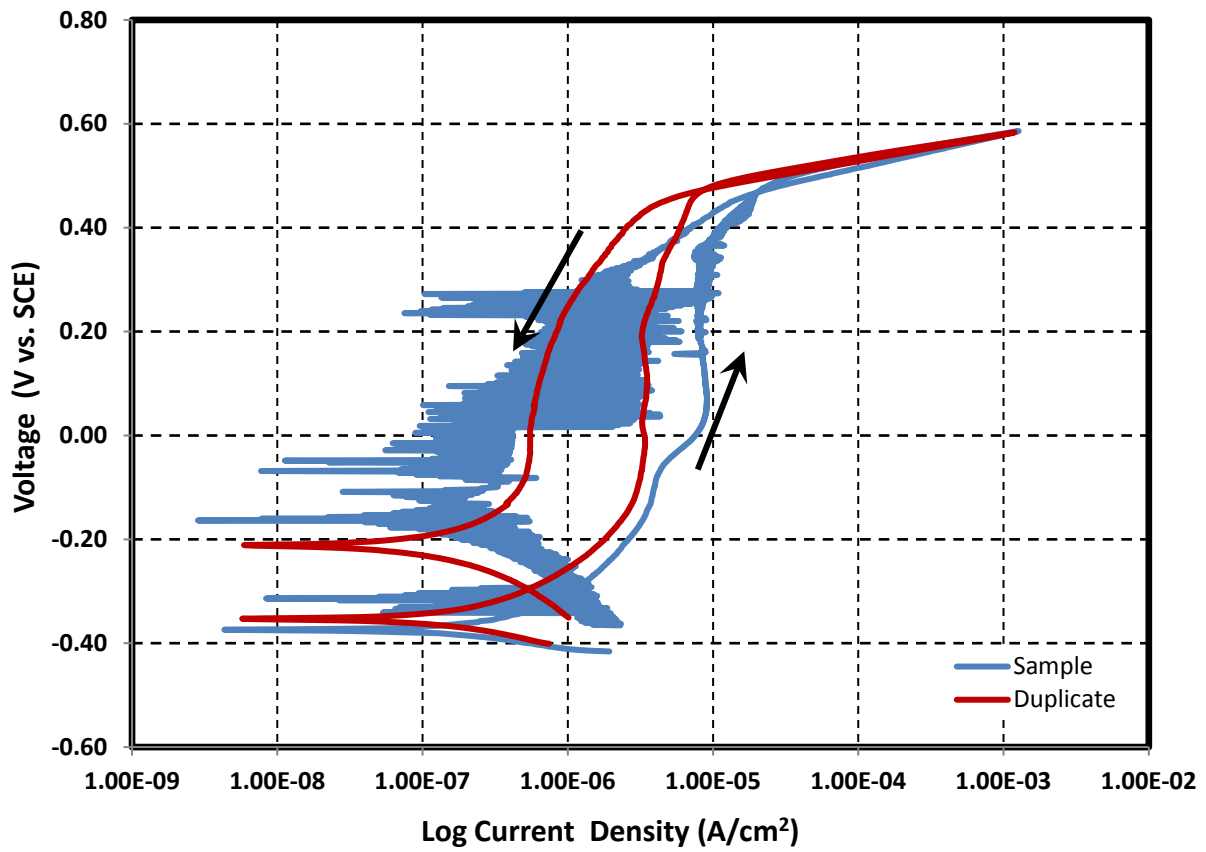
Composition of simulant for New Limits-Test 7

Test 7-NL

Temperature 35 °C
 pH at room temperature 13.38 Target 13.3
 pH before testing (at temp.) 13.29 pH after testing (at temp.) 13.35
 Volume 1.4 L

Simulant Source	Formula	Molecular Weight (g/mol)	Concentration (M)	weight required (g)
Sodium hydroxide	NaOH	40.0000	1.2	67.2000
Sodium nitrite	NaNO ₂	69.0000	0	0.0000
Sodium nitrate	NaNO ₃	85.0000	0.26	30.9400
Sodium chloride	NaCl	58.4000	0.32	26.1632
Sodium sulfate	Na ₂ SO ₄	142.0000	0.17	33.7960
Sodium carbonate	Na ₂ CO ₃	106.0000	0.1	14.8400
Sodium bicarbonate	NaHCO ₃	84.0100	0	0.0000

Cyclic Potentiodynamic Polarization



Images of bullet samples after electrochemical tests

Test 7



Test 7D



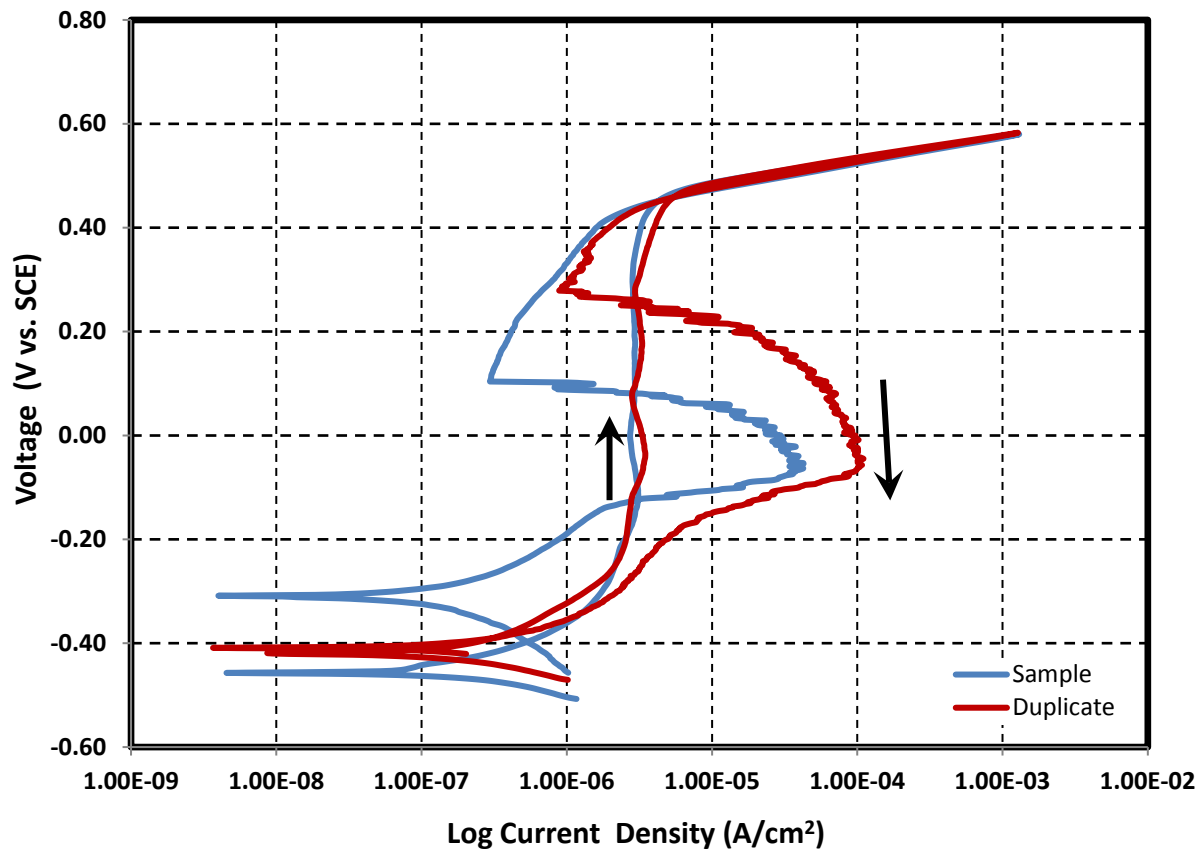
Composition of simulant for New Limits-Test 8

Test 8-NL

Temperature 35 °C
 pH at room temperature 13.64 Target 13.3
 pH before testing (at temp.) 13.47 pH after testing (at temp.) 13.56
 Volume 1.4 L

Simulant Source	Formula	Molecular Weight (g/mol)	Concentration (M)	weight required (g)
Sodium hydroxide	NaOH	40.0000	1.2	67.2000
Sodium nitrite	NaNO ₂	69.0000	0	0.0000
Sodium nitrate	NaNO ₃	85.0000	4.75	565.2500
Sodium chloride	NaCl	58.4000	0.35	28.6160
Sodium sulfate	Na ₂ SO ₄	142.0000	0.07	13.9160
Sodium carbonate	Na ₂ CO ₃	106.0000	0.1	14.8400
Sodium bicarbonate	NaHCO ₃	84.0100	0	0.0000

Cyclic Potentiodynamic Polarization



Images of bullet samples after electrochemical tests

Test 8

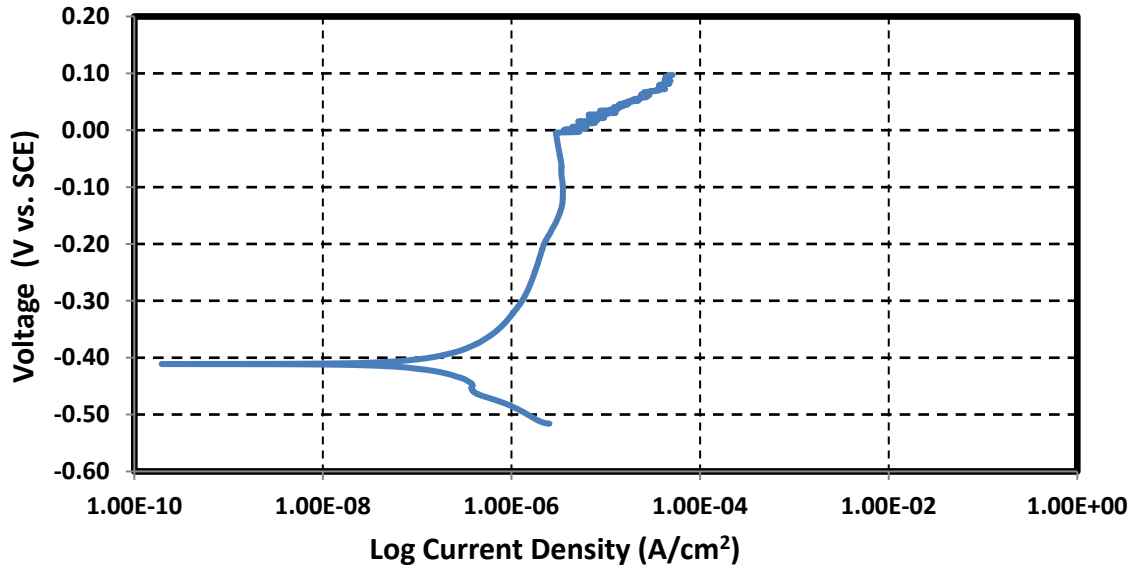


Test 8D

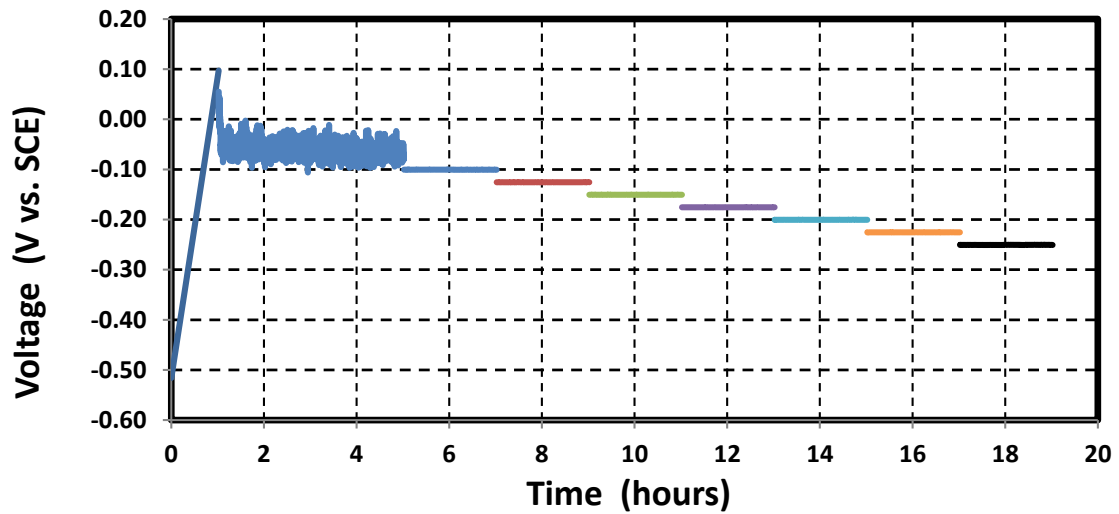
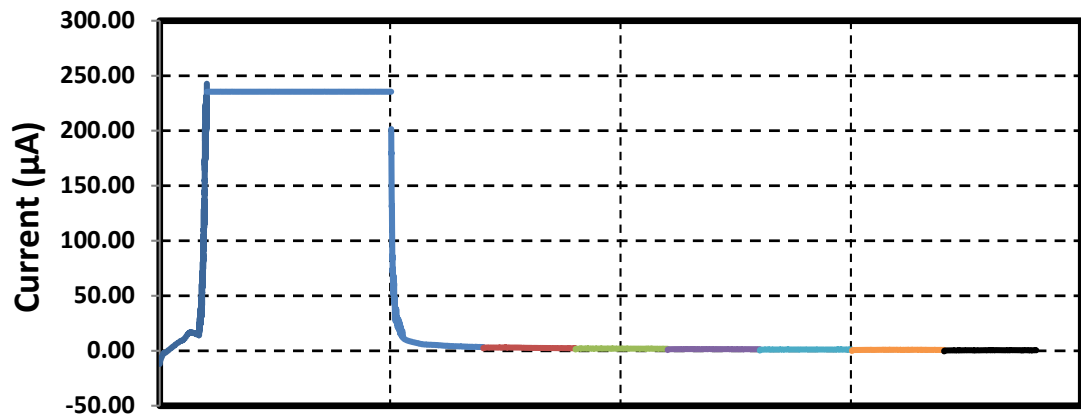


ASTM G192 test

Potentiodynamic



Galvanostatic period and potentiodynamic steps



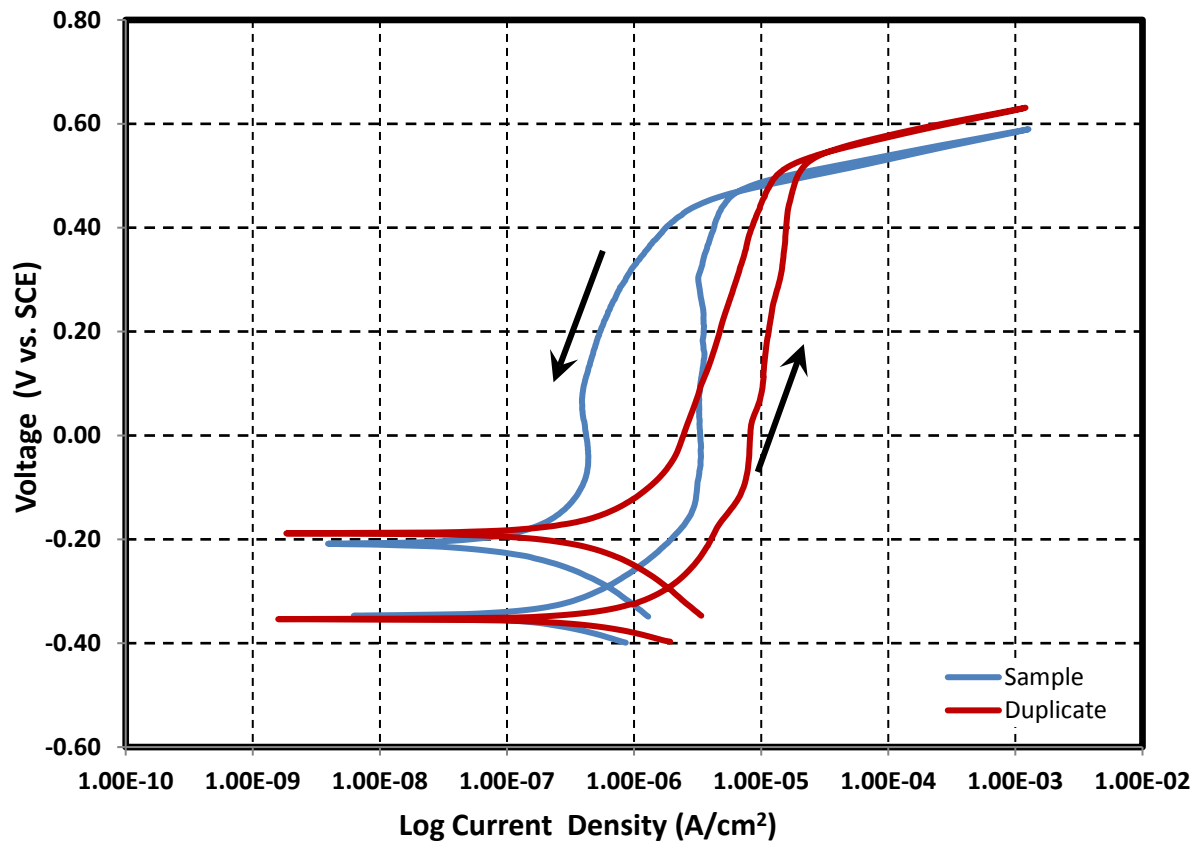
Composition of simulant for New Limits-Test 9

Test 9-NL

Temperature 35 °C
 pH at room temperature 13.35 Target 13.3
 pH before testing (at temp.) 13.42 pH after testing (at temp.) 13.48
 Volume 1.4 L

Simulant Source	Formula	Molecular Weight (g/mol)	Concentration (M)	weight required (g)
Sodium hydroxide	NaOH	40.0000	1.2	67.2000
Sodium nitrite	NaNO ₂	69.0000	0	0.0000
Sodium nitrate	NaNO ₃	85.0000	0	0.0000
Sodium chloride	NaCl	58.4000	0.4	32.7040
Sodium sulfate	Na ₂ SO ₄	142.0000	0.02	3.9760
Sodium carbonate	Na ₂ CO ₃	106.0000	0.1	14.8400
Sodium bicarbonate	NaHCO ₃	84.0100	0	0.0000

Cyclic Potentiodynamic Polarization



Images of bullet samples after electrochemical tests

Test 9



Test 9D



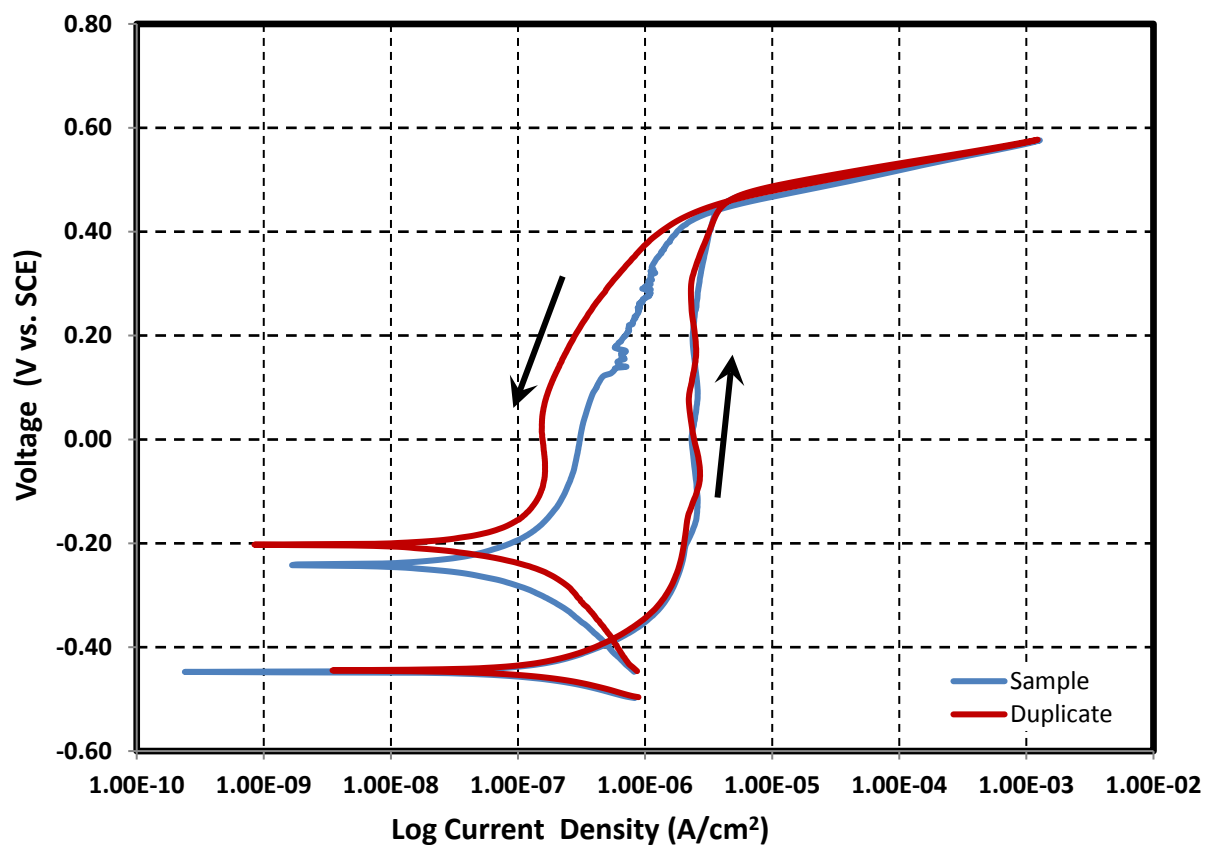
Composition of simulant for New Limits-Test 10

Test 10-NL

Temperature 35 °C
 pH at room temperature 13.52 Target 13.3
 pH before testing (at temp.) 13.42 pH after testing (at temp.) 13.56
 Volume 1.4 L

Simulant Source	Formula	Molecular Weight (g/mol)	Concentration (M)	weight required (g)
Sodium hydroxide	NaOH	40.0000	1.2	67.2000
Sodium nitrite	NaNO ₂	69.0000	0.6	57.9600
Sodium nitrate	NaNO ₃	85.0000	4.74	564.0600
Sodium chloride	NaCl	58.4000	0.08	6.5408
Sodium sulfate	Na ₂ SO ₄	142.0000	0.02	3.9760
Sodium carbonate	Na ₂ CO ₃	106.0000	0.1	14.8400
Sodium bicarbonate	NaHCO ₃	84.0100	0	0.0000

Cyclic Potentiodynamic Polarization



Images of bullet samples after electrochemical tests

Test 10



Test 10D



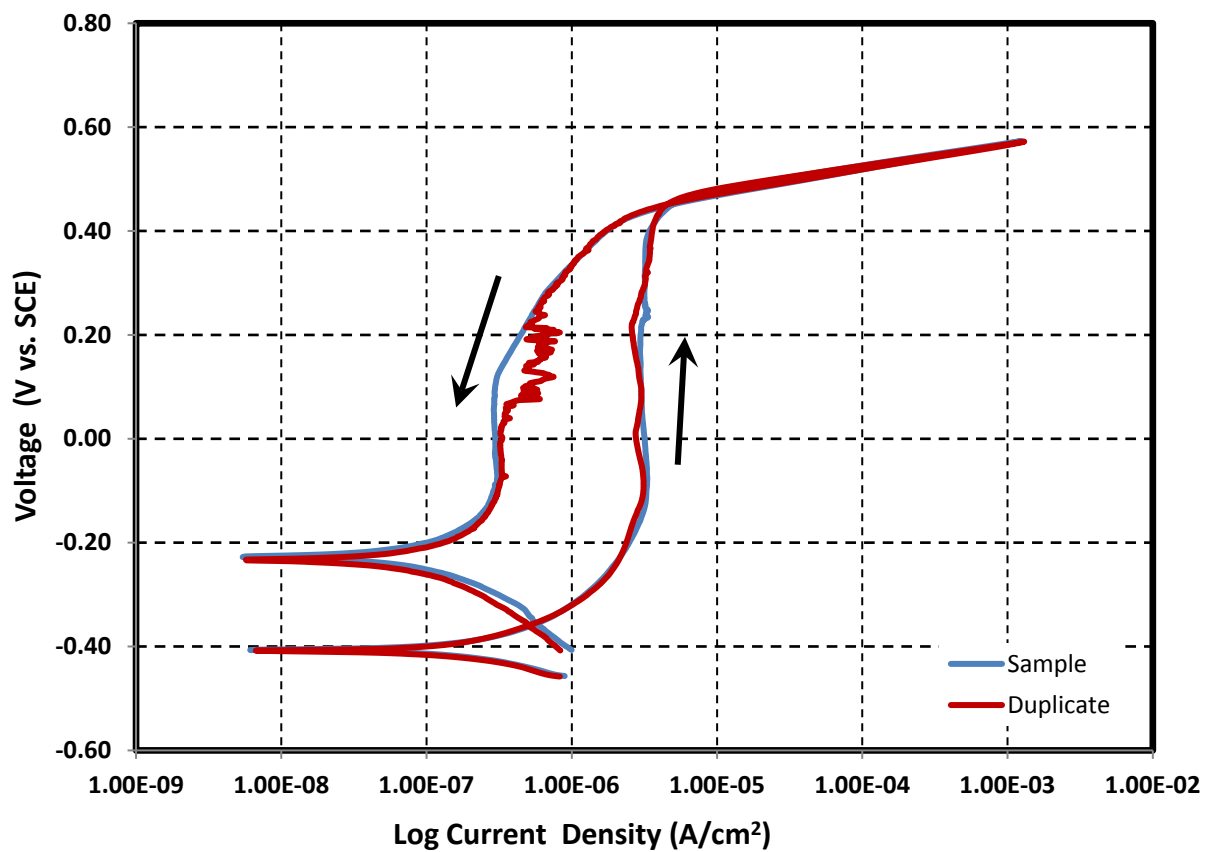
Composition of simulant for New Limits-Test 11

Test 11-NL

Temperature 35 °C
 pH at room temperature 13.62 Target 13.3
 pH before testing (at temp.) 13.48 pH after testing (at temp.) 13.52
 Volume 1.4 L

Simulant Source	Formula	Molecular Weight (g/mol)	Concentration (M)	weight required (g)
Sodium hydroxide	NaOH	40.0000	1.2	67.2000
Sodium nitrite	NaNO ₂	69.0000	0.6	57.9600
Sodium nitrate	NaNO ₃	85.0000	5.32	633.0800
Sodium chloride	NaCl	58.4000	0.15	12.2640
Sodium sulfate	Na ₂ SO ₄	142.0000	0	0.0000
Sodium carbonate	Na ₂ CO ₃	106.0000	0.1	14.8400
Sodium bicarbonate	NaHCO ₃	84.0100	0	0.0000

Cyclic Potentiodynamic Polarization



Images of bullet samples after electrochemical tests

Test 11



Test 11D



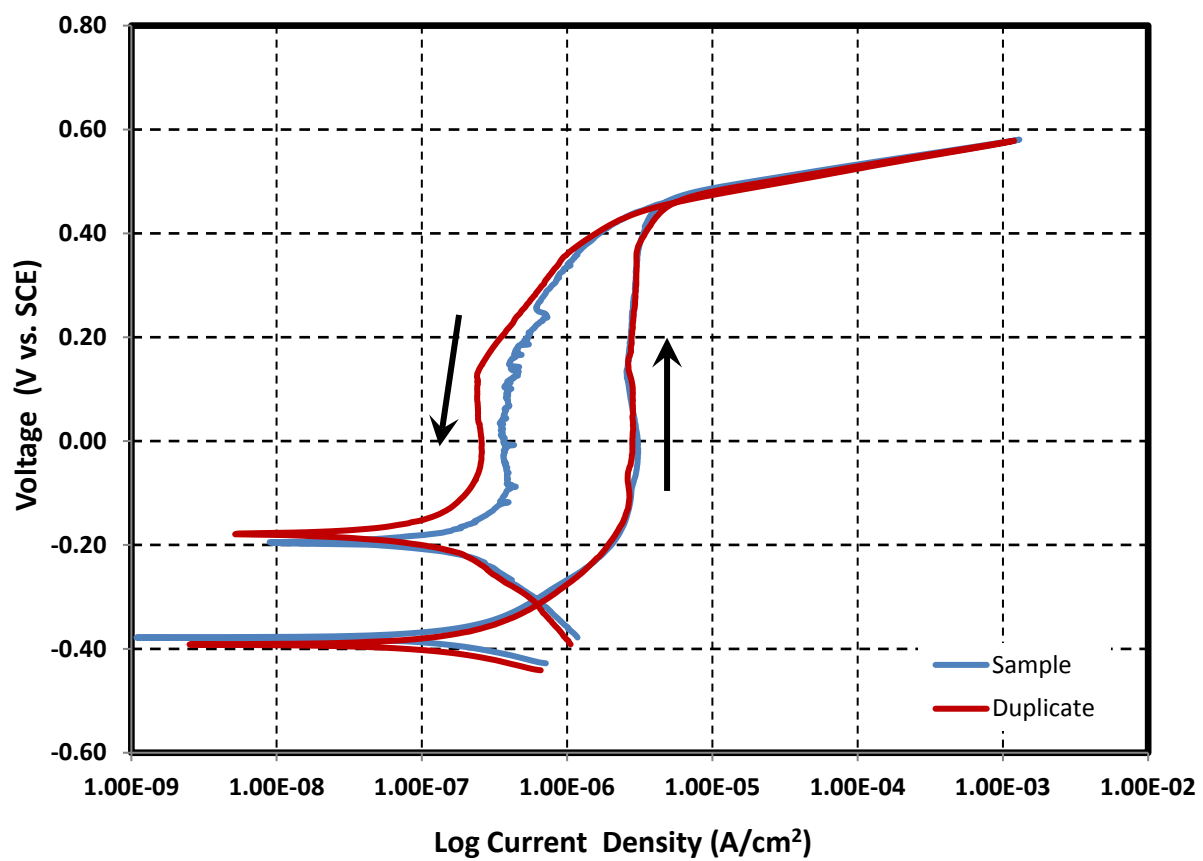
Composition of simulant for New Limits-Test 12

Test 12-NL

Temperature 35 °C
 pH at room temperature 13.57 Target 13.3
 pH before testing (at temp.) 13.48 pH after testing (at temp.) 13.42
 Volume 1.4 L

Simulant Source	Formula	Molecular Weight (g/mol)	Concentration (M)	weight required (g)
Sodium hydroxide	NaOH	40.0000	1.2	67.2000
Sodium nitrite	NaNO ₂	69.0000	0.6	57.9600
Sodium nitrate	NaNO ₃	85.0000	3.31	393.8900
Sodium chloride	NaCl	58.4000	0.16	13.0816
Sodium sulfate	Na ₂ SO ₄	142.0000	0.2	39.7600
Sodium carbonate	Na ₂ CO ₃	106.0000	0.1	14.8400
Sodium bicarbonate	NaHCO ₃	84.0100	0	0.0000

Cyclic Potentiodynamic Polarization



Images of bullet samples after electrochemical tests

Test 12



Test 12D

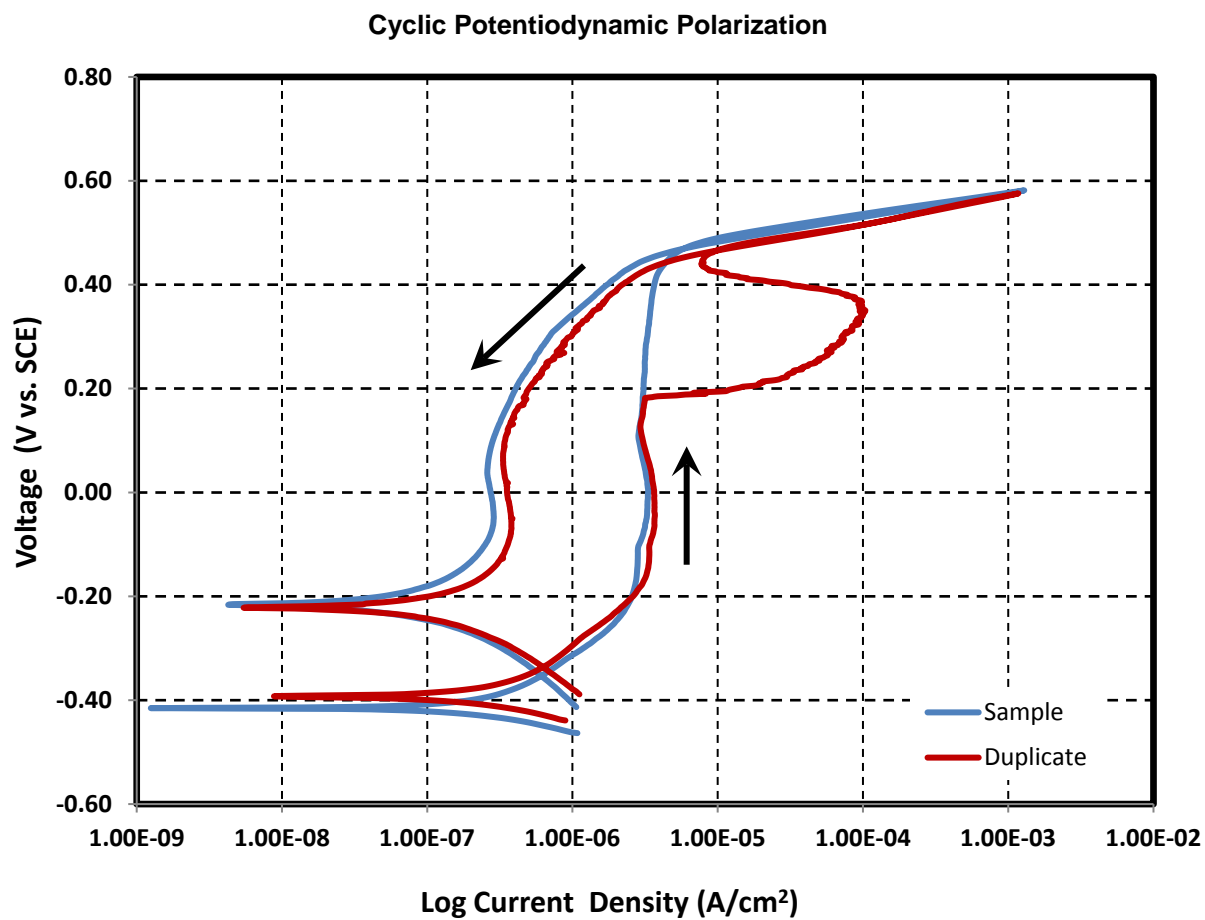


Composition of simulant for New Limits-Test 13

Test 13-NL

Temperature 35 °C
 pH at room temperature 13.33 Target 13.3
 pH before testing (at temp.) 13.18 pH after testing (at temp.) 13.10
 Volume 1.4 L

Simulant Source	Formula	Molecular Weight (g/mol)	Concentration (M)	weight required (g)
Sodium hydroxide	NaOH	40.0000	1.2	67.2000
Sodium nitrite	NaNO ₂	69.0000	0.6	57.9600
Sodium nitrate	NaNO ₃	85.0000	2.68	318.9200
Sodium chloride	NaCl	58.4000	0.24	19.6224
Sodium sulfate	Na ₂ SO ₄	142.0000	0.05	9.9400
Sodium carbonate	Na ₂ CO ₃	106.0000	0.1	14.8400
Sodium bicarbonate	NaHCO ₃	84.0100	0	0.0000



Images of bullet samples after electrochemical tests

Test 13



Test 13D



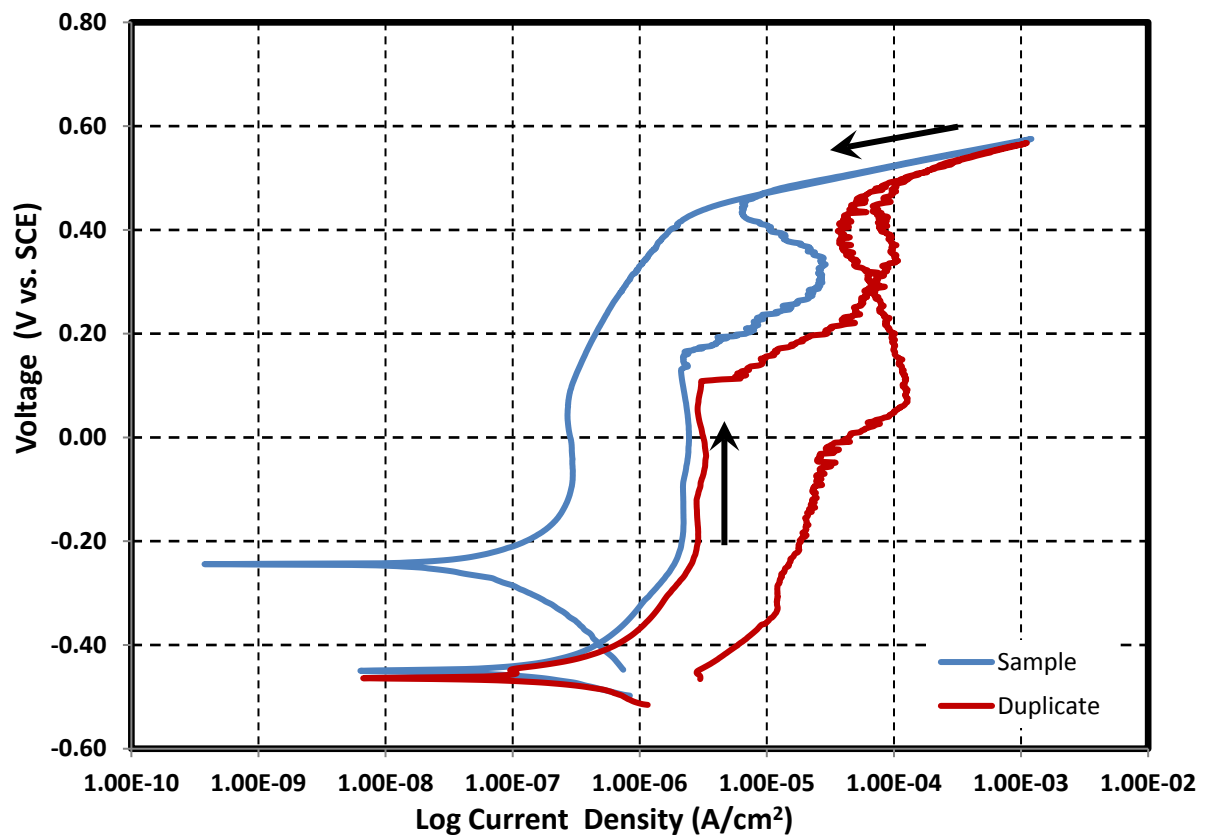
Composition of simulant for New Limits-Test 14

Test 14-NL

Temperature 35 °C
 pH at room temperature 13.15 Target 13.3
 pH before testing (at temp.) 12.98 pH after testing (at temp.) 13.35
 Volume 1.4 L

Simulant Source	Formula	Molecular Weight (g/mol)	Concentration (M)	weight required (g)
Sodium hydroxide	NaOH	40.0000	1.2	67.2000
Sodium nitrite	NaNO ₂	69.0000	0.6	57.9600
Sodium nitrate	NaNO ₃	85.0000	4.92	585.4800
Sodium chloride	NaCl	58.4000	0.28	22.8928
Sodium sulfate	Na ₂ SO ₄	142.0000	0.06	11.9280
Sodium carbonate	Na ₂ CO ₃	106.0000	0.1	14.8400
Sodium bicarbonate	NaHCO ₃	84.0100	0	0.0000

Cyclic Potentiodynamic Polarization



Images of bullet samples after electrochemical tests

Test 14



Test 14D



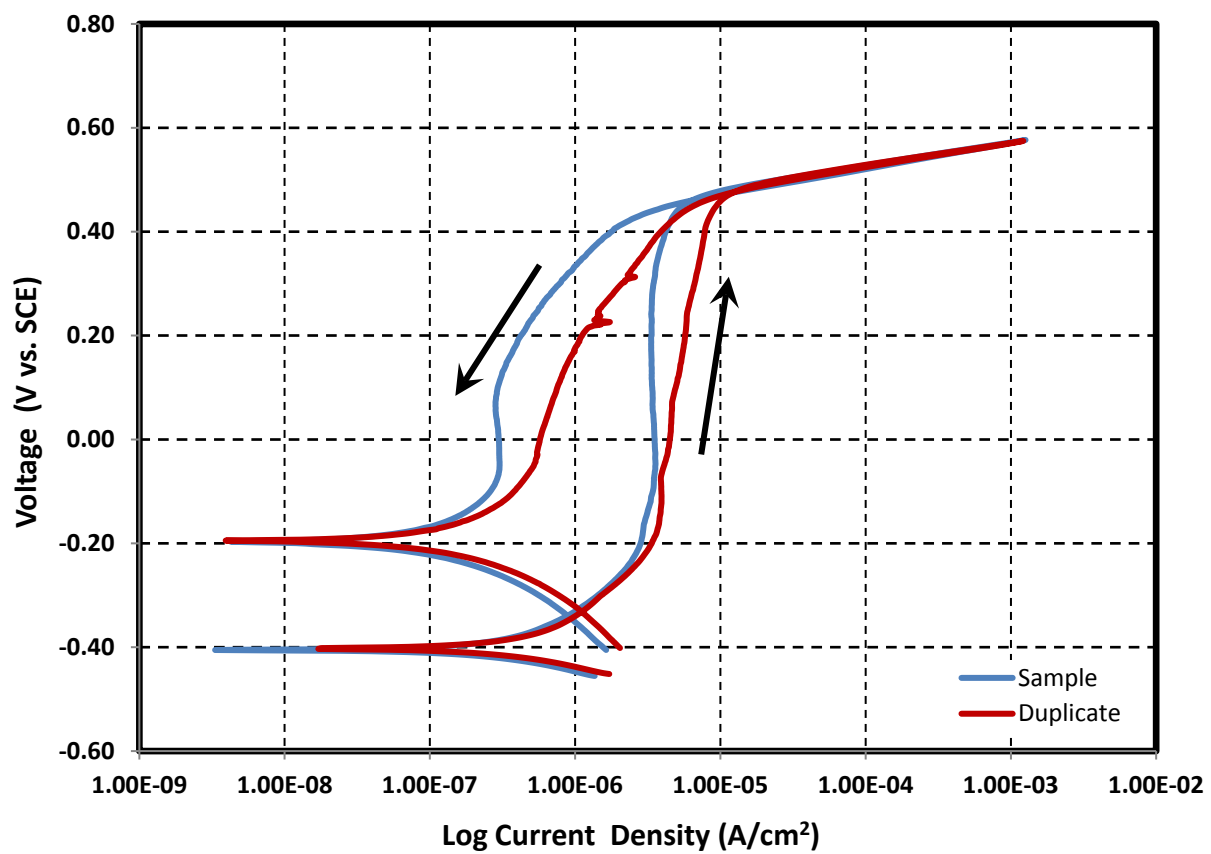
Composition of simulant for New Limits-Test 15

Test 15-NL

Temperature 35 °C
 pH at room temperature 13.38 Target 13.3
 pH before testing (at temp.) 13.28 pH after testing (at temp.) 13.31
 Volume 1.4 L

Simulant Source	Formula	Molecular Weight (g/mol)	Concentration (M)	weight required (g)
Sodium hydroxide	NaOH	40.0000	1.2	67.2000
Sodium nitrite	NaNO ₂	69.0000	0.6	57.9600
Sodium nitrate	NaNO ₃	85.0000	1.26	149.9400
Sodium chloride	NaCl	58.4000	0.32	26.1632
Sodium sulfate	Na ₂ SO ₄	142.0000	0.01	1.9880
Sodium carbonate	Na ₂ CO ₃	106.0000	0.1	14.8400
Sodium bicarbonate	NaHCO ₃	84.0100	0	0.0000

Cyclic Potentiodynamic Polarization



Images of bullet samples after electrochemical tests

Test 15



Test 15D



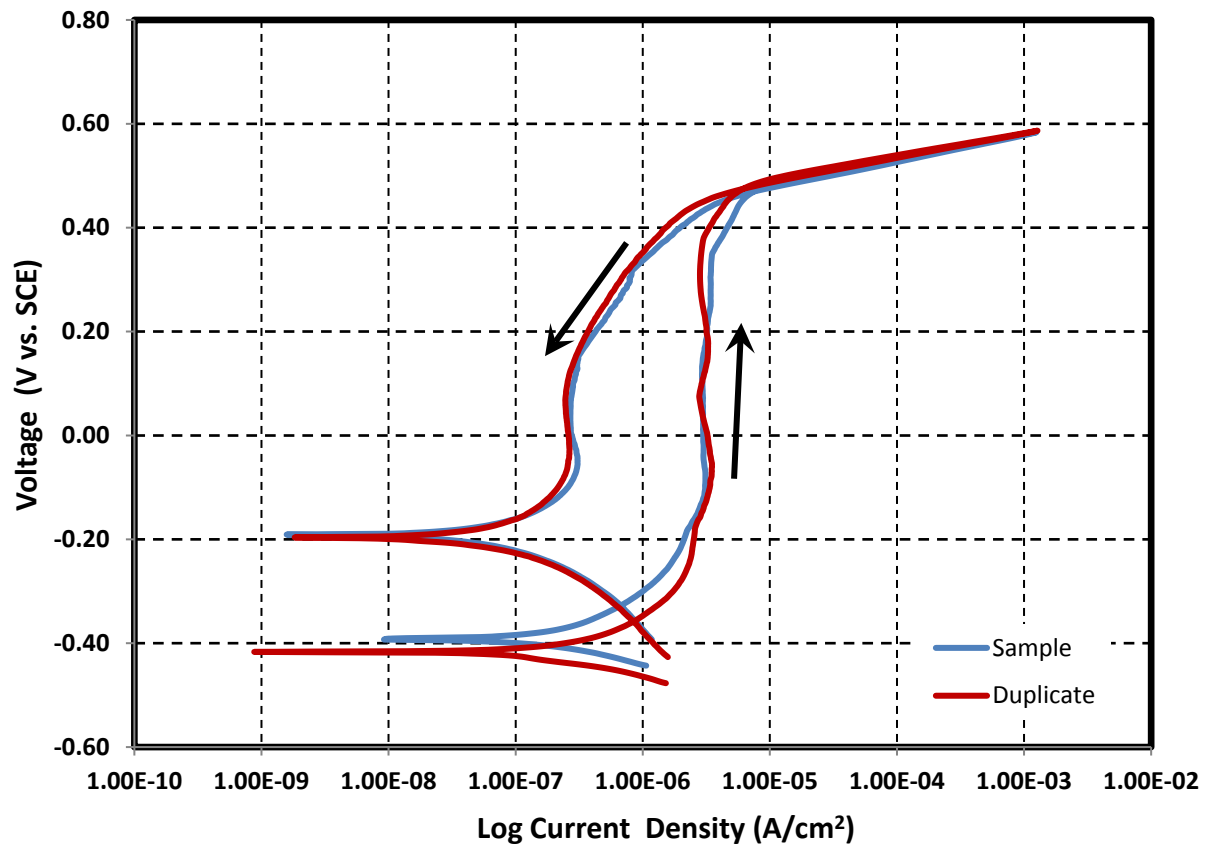
Composition of simulant for New Limits-Test 16

Test 16-NL

Temperature 35 °C
 pH at room temperature 13.41 Target 13.3
 pH before testing (at temp.) 13.47 pH after testing (at temp.) 13.51
 Volume 1.4 L

Simulant Source	Formula	Molecular Weight (g/mol)	Concentration (M)	weight required (g)
Sodium hydroxide	NaOH	40.0000	1.2	67.2000
Sodium nitrite	NaNO ₂	69.0000	0.6	57.9600
Sodium nitrate	NaNO ₃	85.0000	0.63	74.9700
Sodium chloride	NaCl	58.4000	0.4	32.7040
Sodium sulfate	Na ₂ SO ₄	142.0000	0.17	33.7960
Sodium carbonate	Na ₂ CO ₃	106.0000	0.1	14.8400
Sodium bicarbonate	NaHCO ₃	84.0100	0	0.0000

Cyclic Potentiodynamic Polarization



Images of bullet samples after electrochemical tests

Test 16



Test 16D



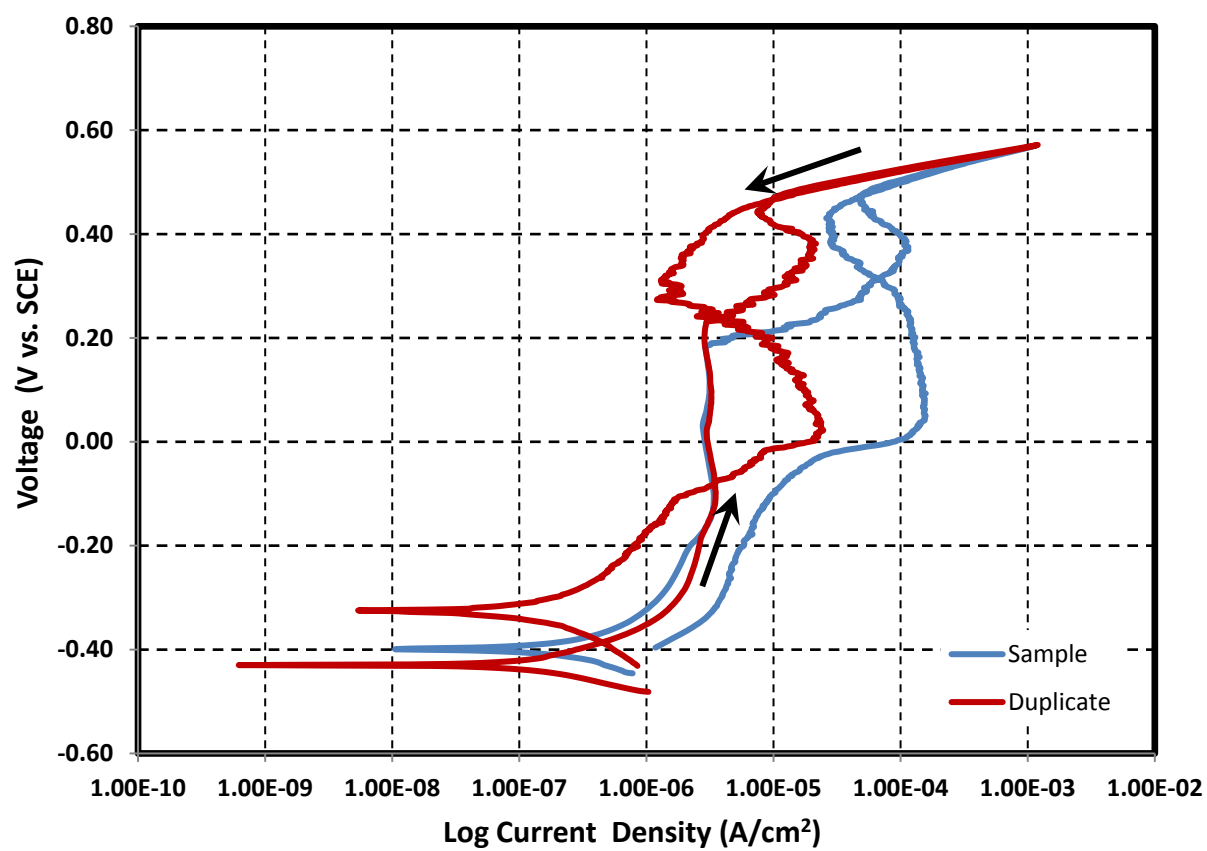
Composition of simulant for New Limits-Test 17

Test 17-NL

Temperature 35 °C
 pH at room temperature 13.72 Target 13.3
 pH before testing (at temp.) 13.47 pH after testing (at temp.) 13.41
 Volume 1.4 L

Simulant Source	Formula	Molecular Weight (g/mol)	Concentration (M)	weight required (g)
Sodium hydroxide	NaOH	40.0000	1.2	67.2000
Sodium nitrite	NaNO ₂	69.0000	0.6	57.9600
Sodium nitrate	NaNO ₃	85.0000	5.32	633.0800
Sodium chloride	NaCl	58.4000	0.4	32.7040
Sodium sulfate	Na ₂ SO ₄	142.0000	0.01	1.9880
Sodium carbonate	Na ₂ CO ₃	106.0000	0.1	14.8400
Sodium bicarbonate	NaHCO ₃	84.0100	0	0.0000

Cyclic Potentiodynamic Polarization



Images of bullet samples after electrochemical tests

Test 17

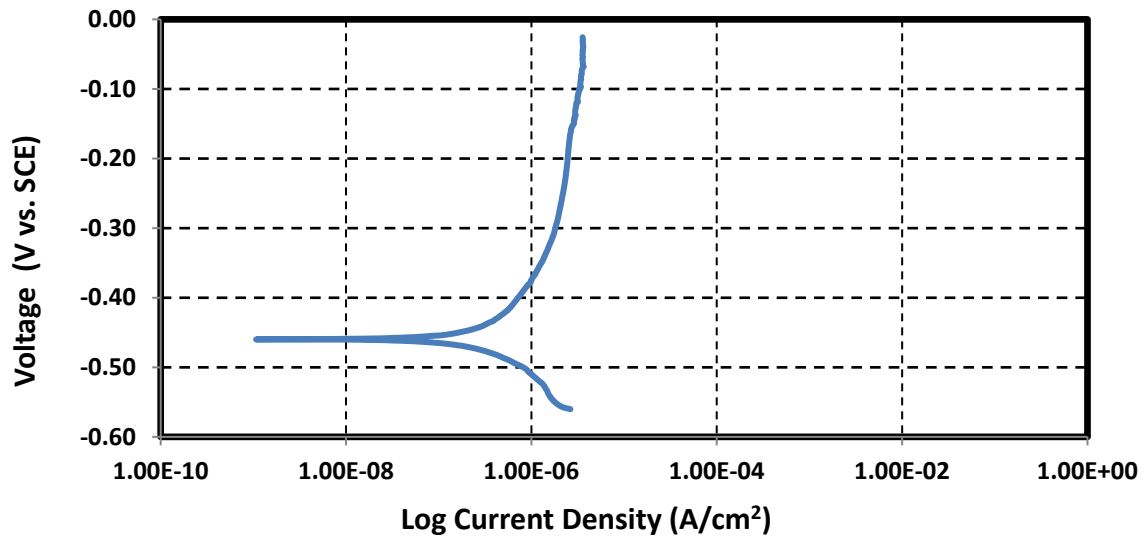


Test 17D

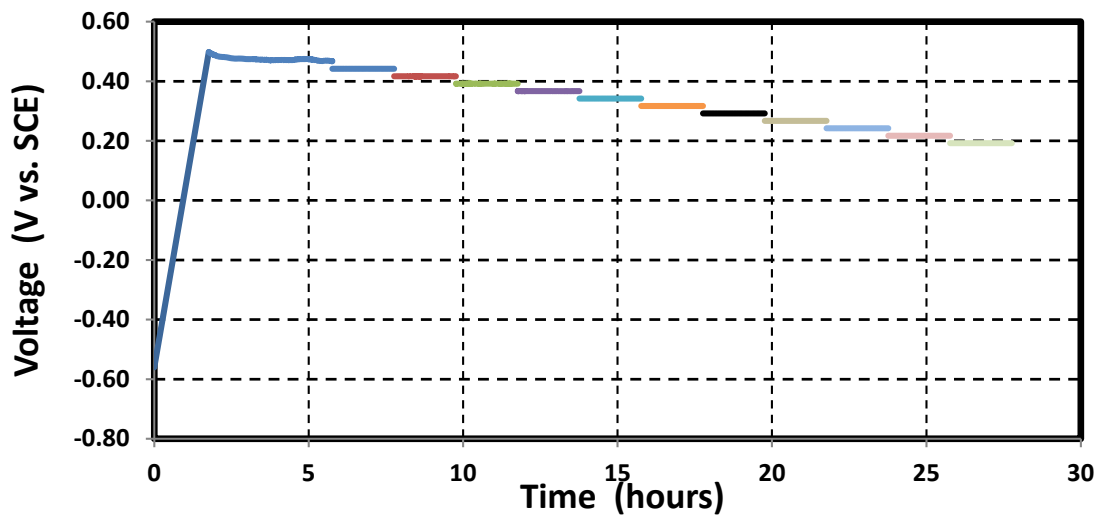
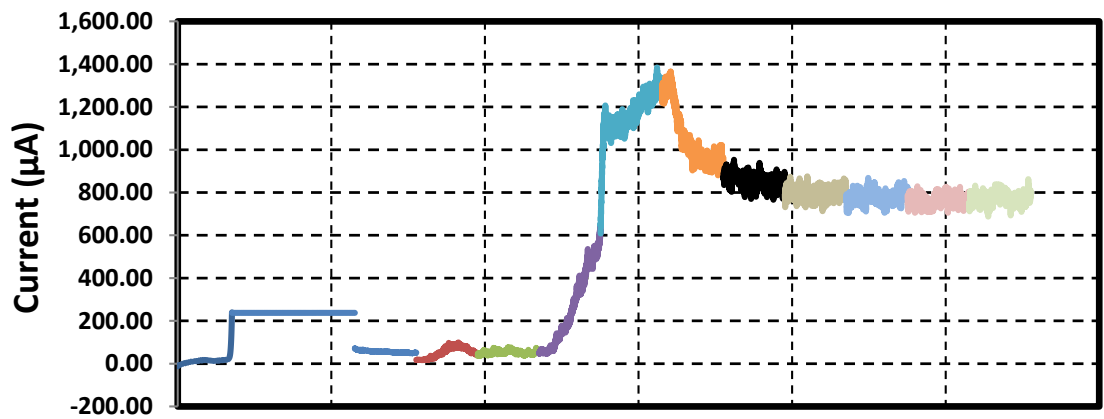


ASTM G192 test

Potentiodynamic



Galvanostatic period and potentiodynamic steps



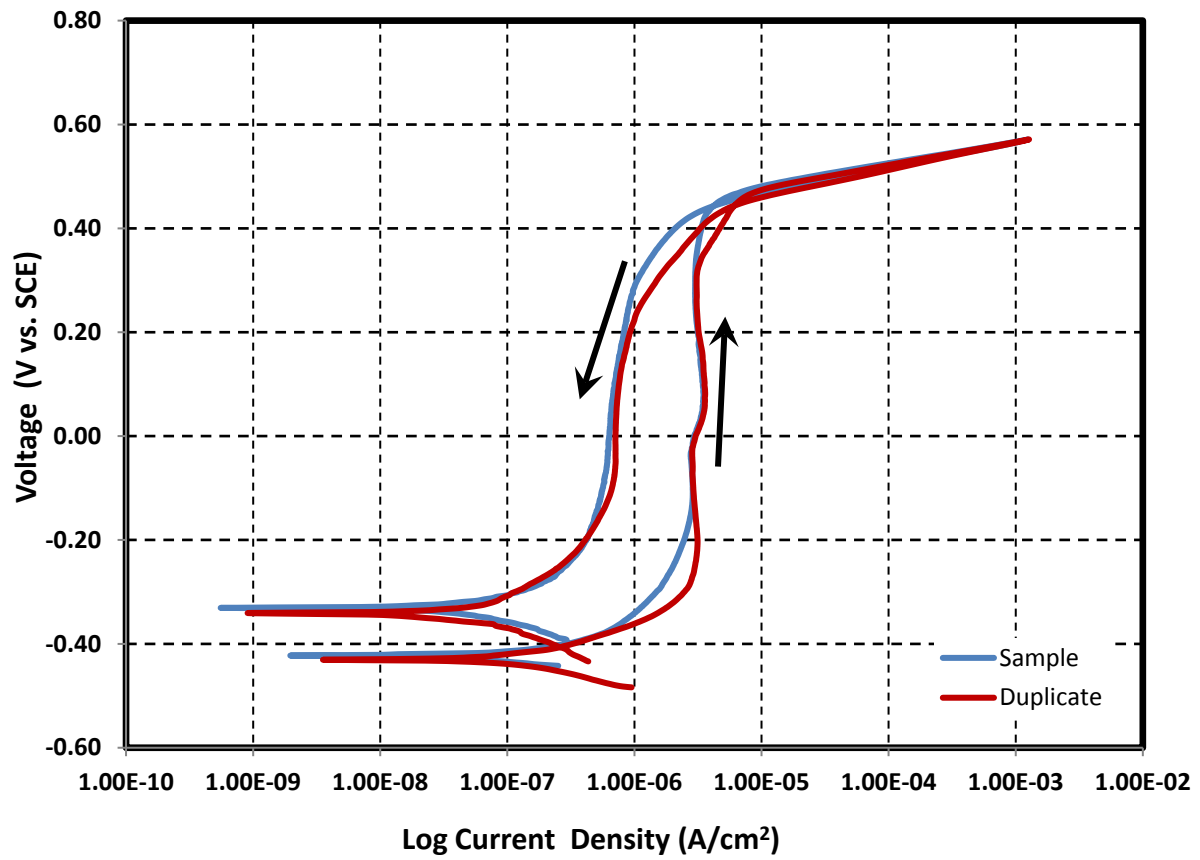
Composition of simulant for New Limits-Test 18

Test 18-NL

Temperature 35 °C
 pH at room temperature 13.70 Target 13.3
 pH before testing (at temp.) 13.54 pH after testing (at temp.) 13.59
 Volume 1.4 L

Simulant Source	Formula	Molecular Weight (g/mol)	Concentration (M)	weight required (g)
Sodium hydroxide	NaOH	40.0000	1.2	67.2000
Sodium nitrite	NaNO ₂	69.0000	1.2	115.9200
Sodium nitrate	NaNO ₃	85.0000	4.01	477.1900
Sodium chloride	NaCl	58.4000	0.16	13.0816
Sodium sulfate	Na ₂ SO ₄	142.0000	0.15	29.8200
Sodium carbonate	Na ₂ CO ₃	106.0000	0.1	14.8400
Sodium bicarbonate	NaHCO ₃	84.0100	0	0.0000

Cyclic Potentiodynamic Polarization



Images of bullet samples after electrochemical tests

Test 18



Test 18D



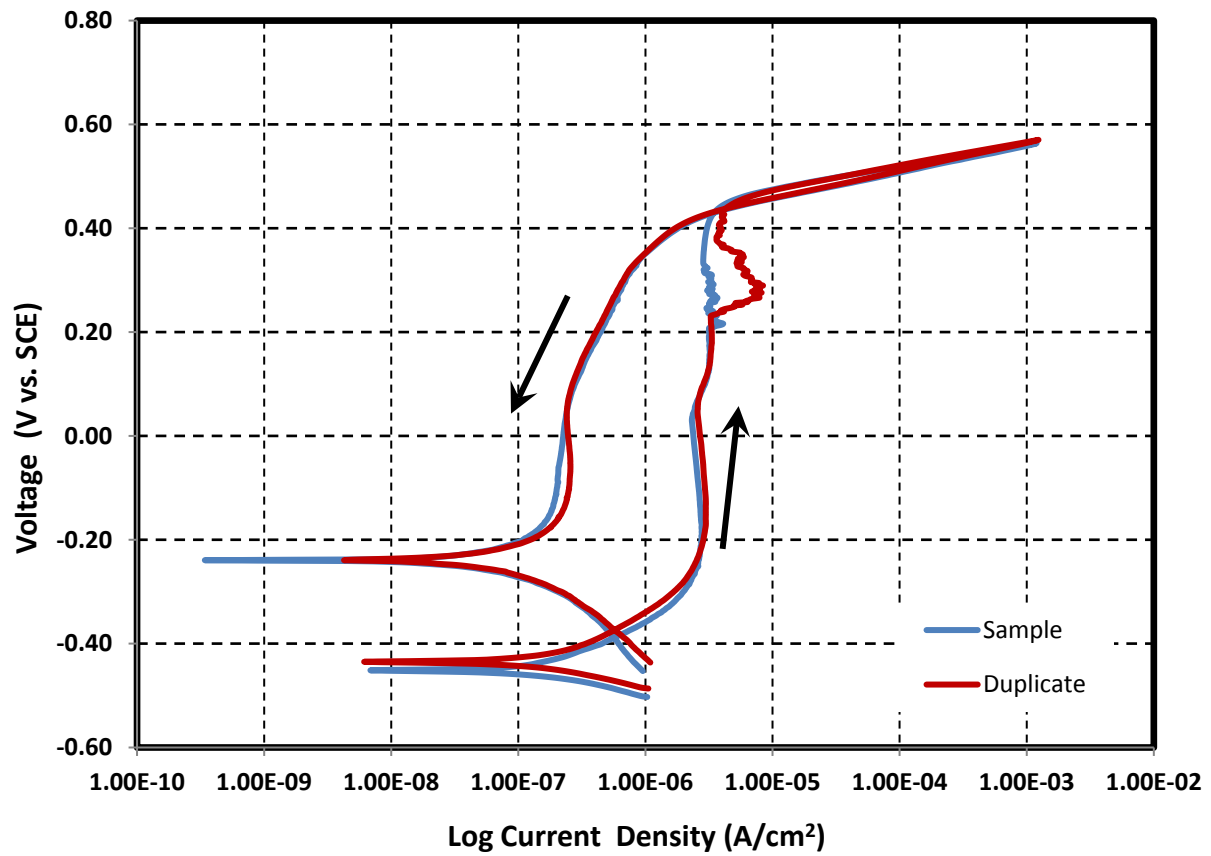
Composition of simulant for New Limits-Test 19

Test 19-NL

Temperature 35 °C
 pH at room temperature 13.59 Target 13.3
 pH before testing (at temp.) 13.41 pH after testing (at temp.) 13.64
 Volume 1.4 L

Simulant Source	Formula	Molecular Weight (g/mol)	Concentration (M)	weight required (g)
Sodium hydroxide	NaOH	40.0000	1.2	67.2000
Sodium nitrite	NaNO ₂	69.0000	1.2	115.9200
Sodium nitrate	NaNO ₃	85.0000	4.17	496.2300
Sodium chloride	NaCl	58.4000	0.21	17.1996
Sodium sulfate	Na ₂ SO ₄	142.0000	0.01	1.9880
Sodium carbonate	Na ₂ CO ₃	106.0000	0.1	14.8400
Sodium bicarbonate	NaHCO ₃	84.0100	0	0.0000

Cyclic Potentiodynamic Polarization



Images of bullet samples after electrochemical tests

Test 19



Test 19D



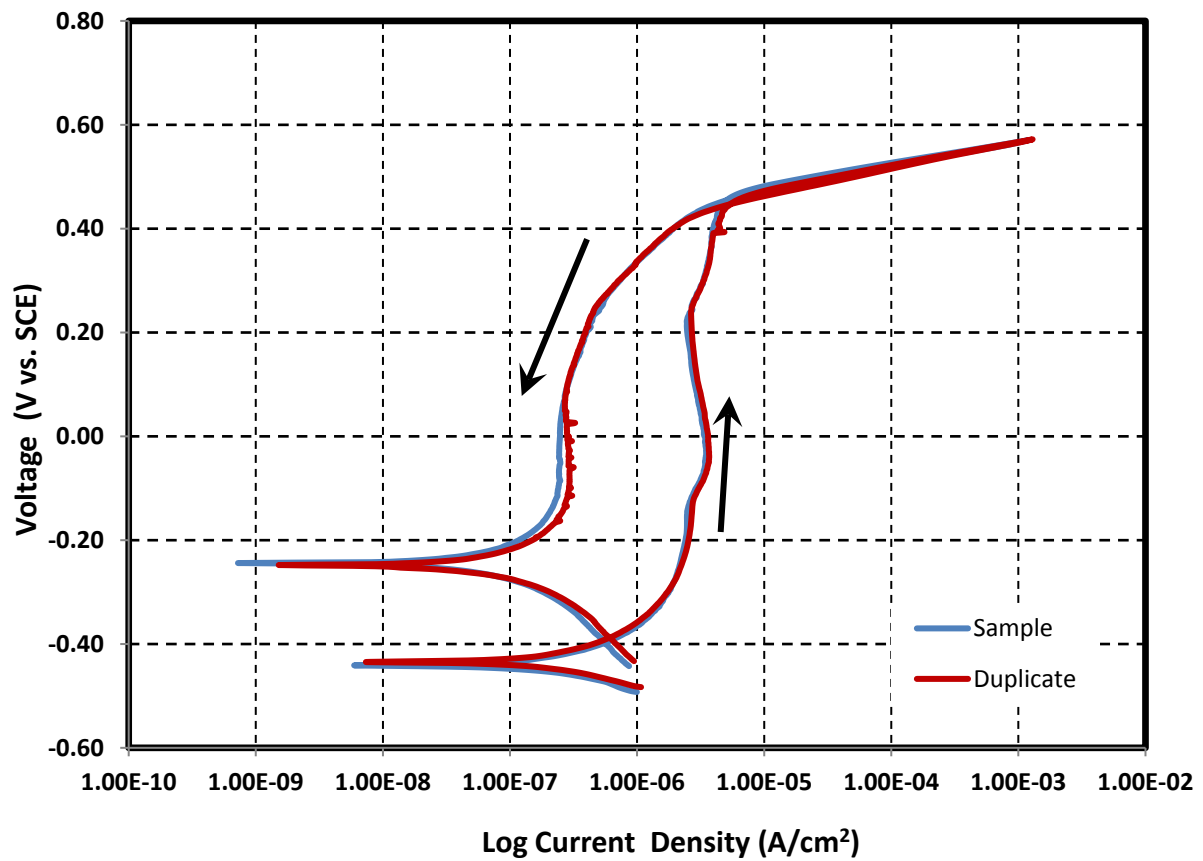
Composition of simulant for New Limits-Test 20

Test 20-NL

Temperature 35 °C
 pH at room temperature 13.74 Target 13.3
 pH before testing (at temp.) 13.57 pH after testing (at temp.) 13.61
 Volume 1.4 L

Simulant Source	Formula	Molecular Weight (g/mol)	Concentration (M)	weight required (g)
Sodium hydroxide	NaOH	40.0000	1.2	67.2000
Sodium nitrite	NaNO ₂	69.0000	1.2	115.9200
Sodium nitrate	NaNO ₃	85.0000	3.4	404.6000
Sodium chloride	NaCl	58.4000	0.24	19.6224
Sodium sulfate	Na ₂ SO ₄	142.0000	0.1	19.8800
Sodium carbonate	Na ₂ CO ₃	106.0000	0.1	14.8400
Sodium bicarbonate	NaHCO ₃	84.0100	0	0.0000

Cyclic Potentiodynamic Polarization

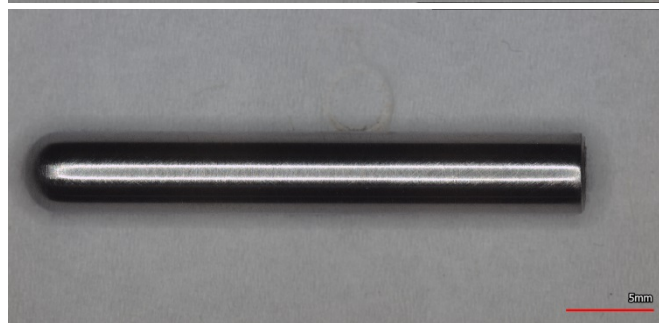


Images of bullet samples after electrochemical tests

Test 20



Test 20D



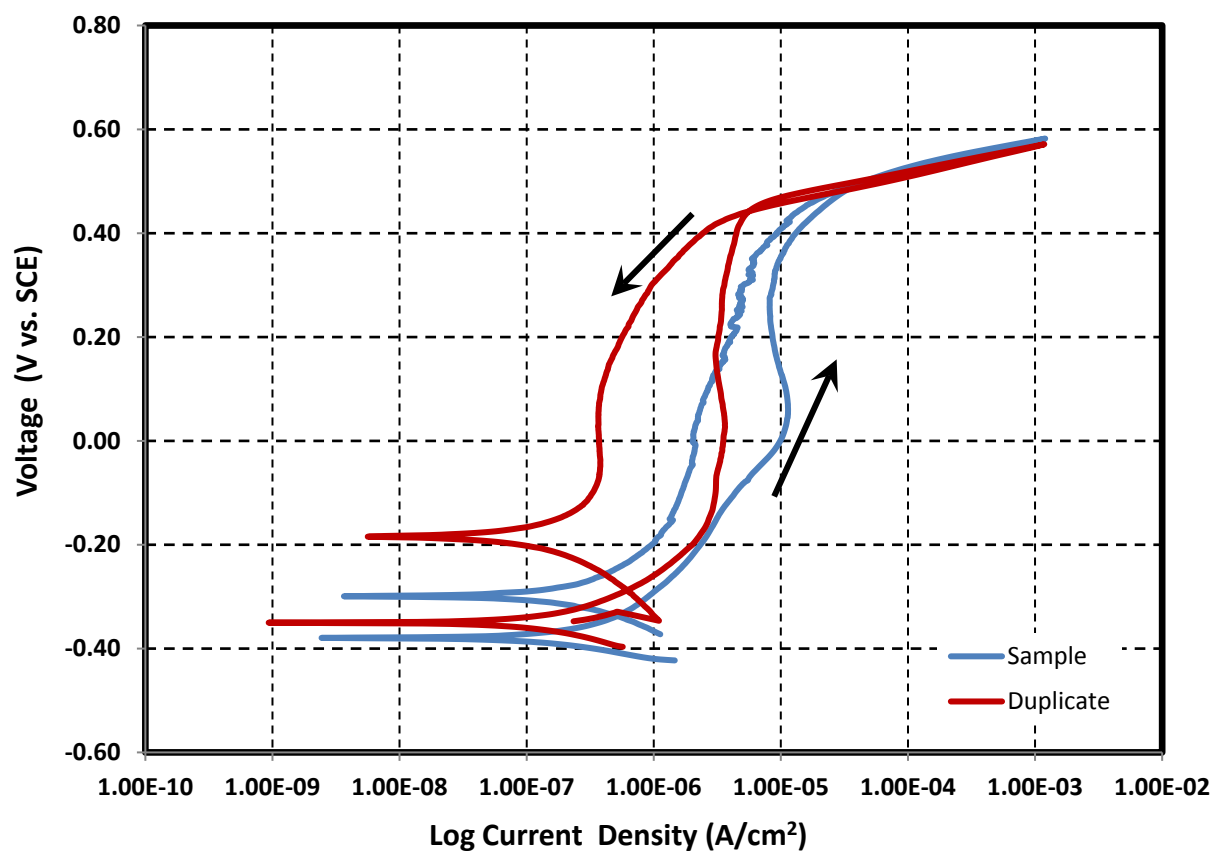
Composition of simulant for New Limits-Test 21

Test 21-NL

Temperature 35 °C
 pH at room temperature 13.46 Target 13.3
 pH before testing (at temp.) 13.36 pH after testing (at temp.) 13.52
 Volume 1.4 L

Simulant Source	Formula	Molecular Weight (g/mol)	Concentration (M)	weight required (g)
Sodium hydroxide	NaOH	40.0000	1.2	67.2000
Sodium nitrite	NaNO ₂	69.0000	1.2	115.9200
Sodium nitrate	NaNO ₃	85.0000	1.99	236.8100
Sodium chloride	NaCl	58.4000	0.32	26.1632
Sodium sulfate	Na ₂ SO ₄	142.0000	0.09	17.8920
Sodium carbonate	Na ₂ CO ₃	106.0000	0.1	14.8400
Sodium bicarbonate	NaHCO ₃	84.0100	0	0.0000

Cyclic Potentiodynamic Polarization



Images of bullet samples after electrochemical tests

Test 21



Test 21D



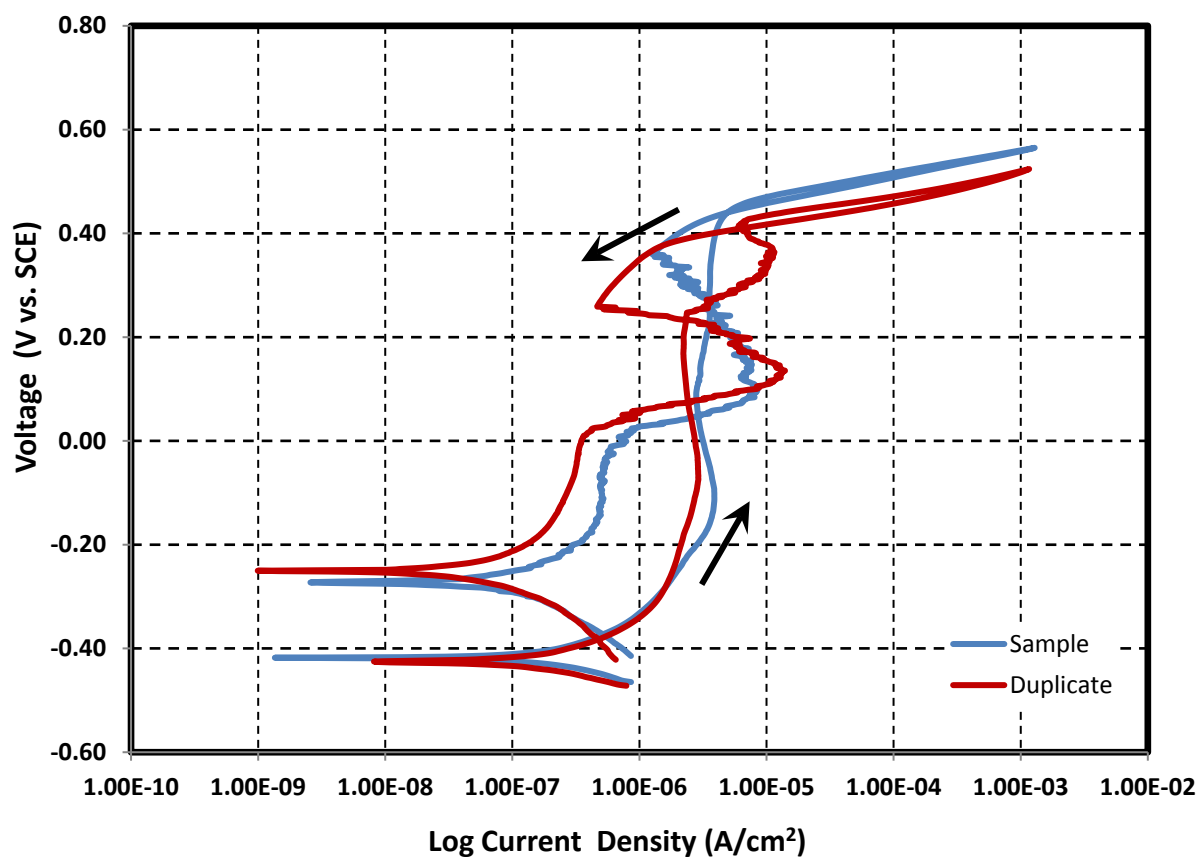
Composition of simulant for New Limits-Test 22

Test 22-NL

Temperature 35 °C
 pH at room temperature 13.89 Target 13.3
 pH before testing (at temp.) 13.63 pH after testing (at temp.) 13.52
 Volume 1.4 L

Simulant Source	Formula	Molecular Weight (g/mol)	Concentration (M)	weight required (g)
Sodium hydroxide	NaOH	40.0000	1.2	67.2000
Sodium nitrite	NaNO ₂	69.0000	1.2	115.9200
Sodium nitrate	NaNO ₃	85.0000	4.57	543.8308
Sodium chloride	NaCl	58.4000	0.32	26.1632
Sodium sulfate	Na ₂ SO ₄	142.0000	0.13	25.8440
Sodium carbonate	Na ₂ CO ₃	106.0000	0.1	14.8400
Sodium bicarbonate	NaHCO ₃	84.0100	0	0.0000

Cyclic Potentiodynamic Polarization



Images of bullet samples after electrochemical tests

Test 22

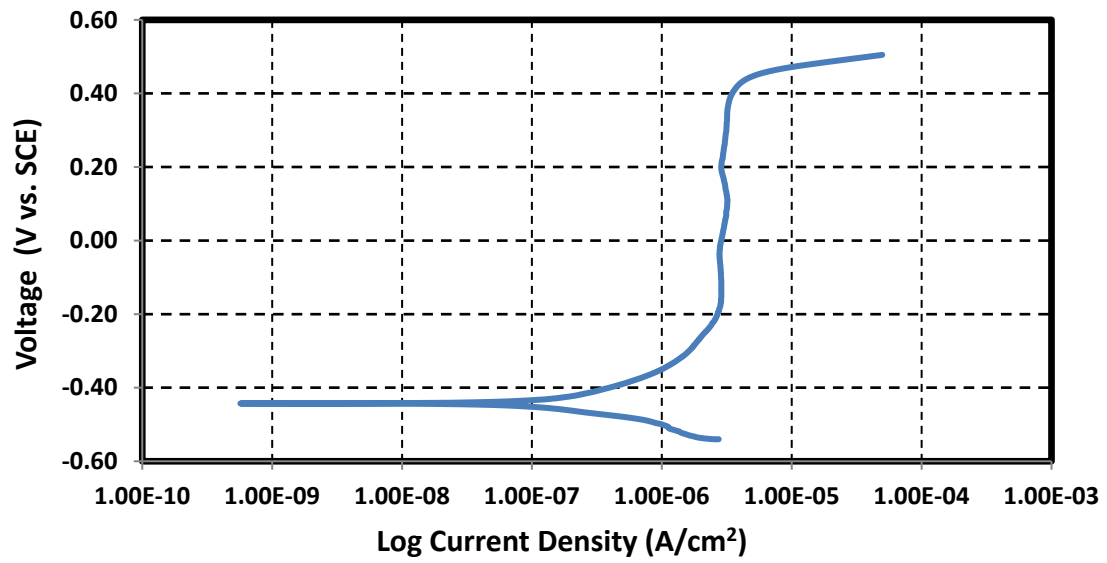


Test 22D

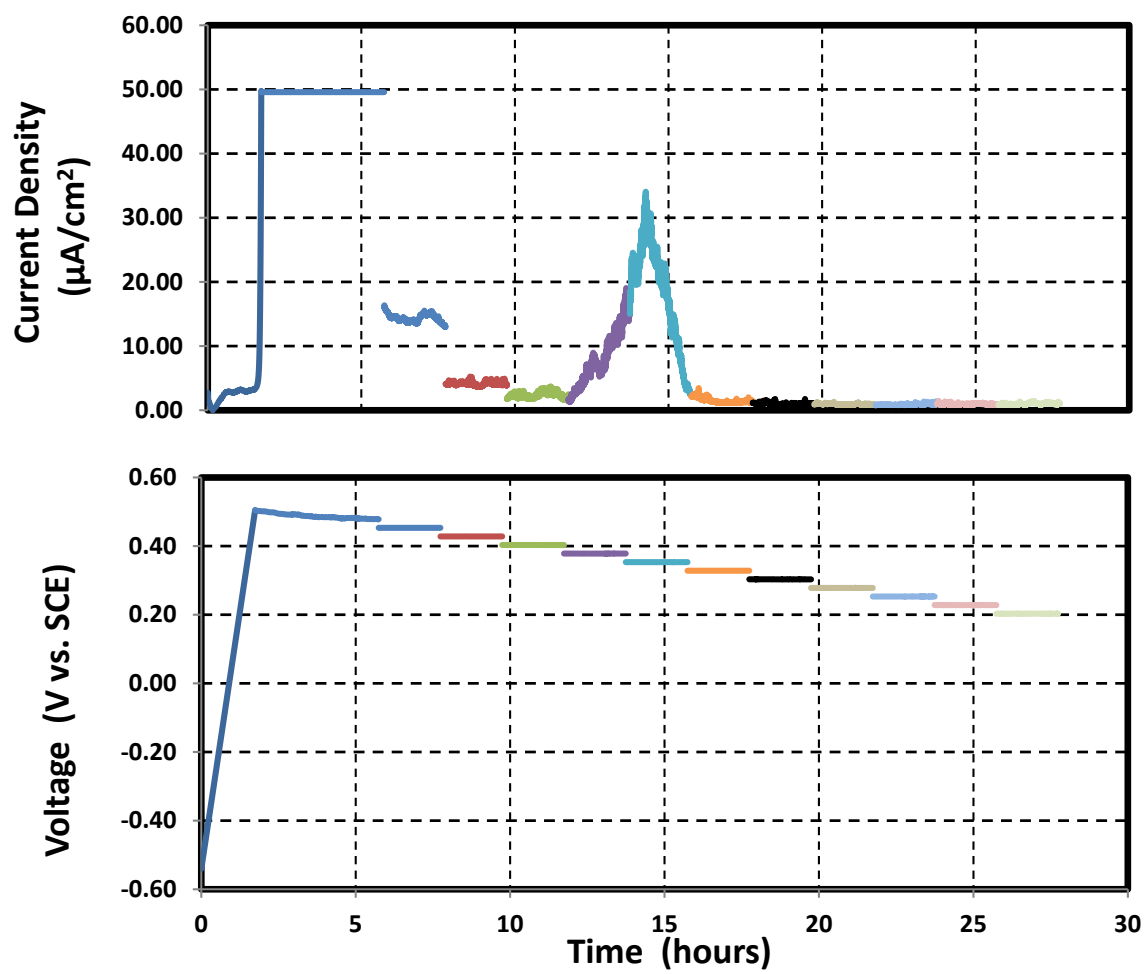


ASTM G192 test

Potentiodynamic



Galvanostatic period and potentiodynamic steps



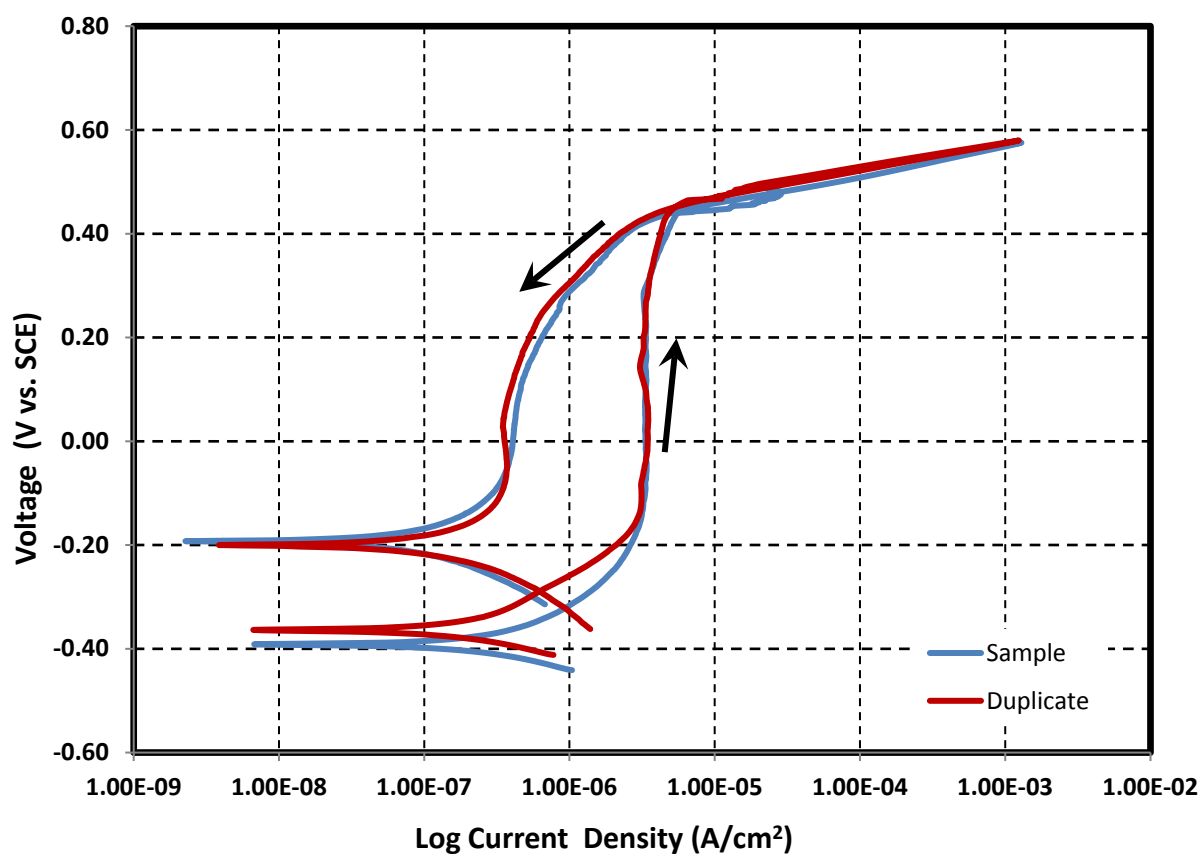
Composition of simulant for New Limits-Test 23

Test 23-NL

Temperature 35 °C
 pH at room temperature 13.47 Target 13.3
 pH before testing (at temp.) 13.50 pH after testing (at temp.) 13.54
 Volume 1.4 L

Simulant Source	Formula	Molecular Weight (g/mol)	Concentration (M)	weight required (g)
Sodium hydroxide	NaOH	40.0000	1.2	67.2000
Sodium nitrite	NaNO ₂	69.0000	1.2	115.9200
Sodium nitrate	NaNO ₃	85.0000	1.38	164.2200
Sodium chloride	NaCl	58.4000	0.4	32.7040
Sodium sulfate	Na ₂ SO ₄	142.0000	0.01	1.9880
Sodium carbonate	Na ₂ CO ₃	106.0000	0.1	14.8400
Sodium bicarbonate	NaHCO ₃	84.0100	0	0.0000

Cyclic Potentiodynamic Polarization



Images of bullet samples after electrochemical tests

Test 23



Test 23D



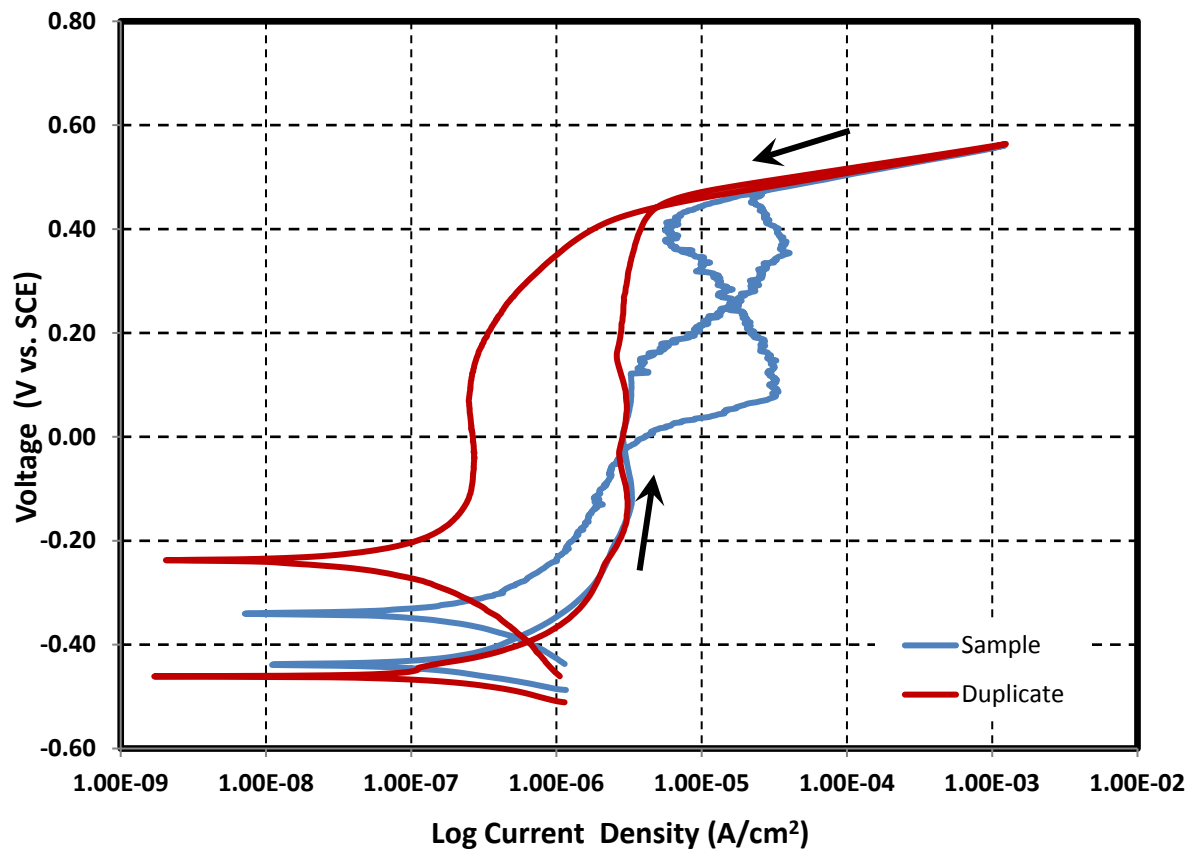
Composition of simulant for New Limits-Test 24

Test 24-NL

Temperature 35 °C
 pH at room temperature 13.47 Target 13.3
 pH before testing (at temp.) 13.39 pH after testing (at temp.) 13.31
 Volume 1.4 L

Simulant Source	Formula	Molecular Weight (g/mol)	Concentration (M)	weight required (g)
Sodium hydroxide	NaOH	40.0000	1.2	67.2000
Sodium nitrite	NaNO ₂	69.0000	1.2	115.9200
Sodium nitrate	NaNO ₃	85.0000	4.17	496.2300
Sodium chloride	NaCl	58.4000	0.4	32.7040
Sodium sulfate	Na ₂ SO ₄	142.0000	0.01	1.9880
Sodium carbonate	Na ₂ CO ₃	106.0000	0.1	14.8400
Sodium bicarbonate	NaHCO ₃	84.0100	0	0.0000

Cyclic Potentiodynamic Polarization



Images of bullet samples after electrochemical tests

Test 24



Test 24D



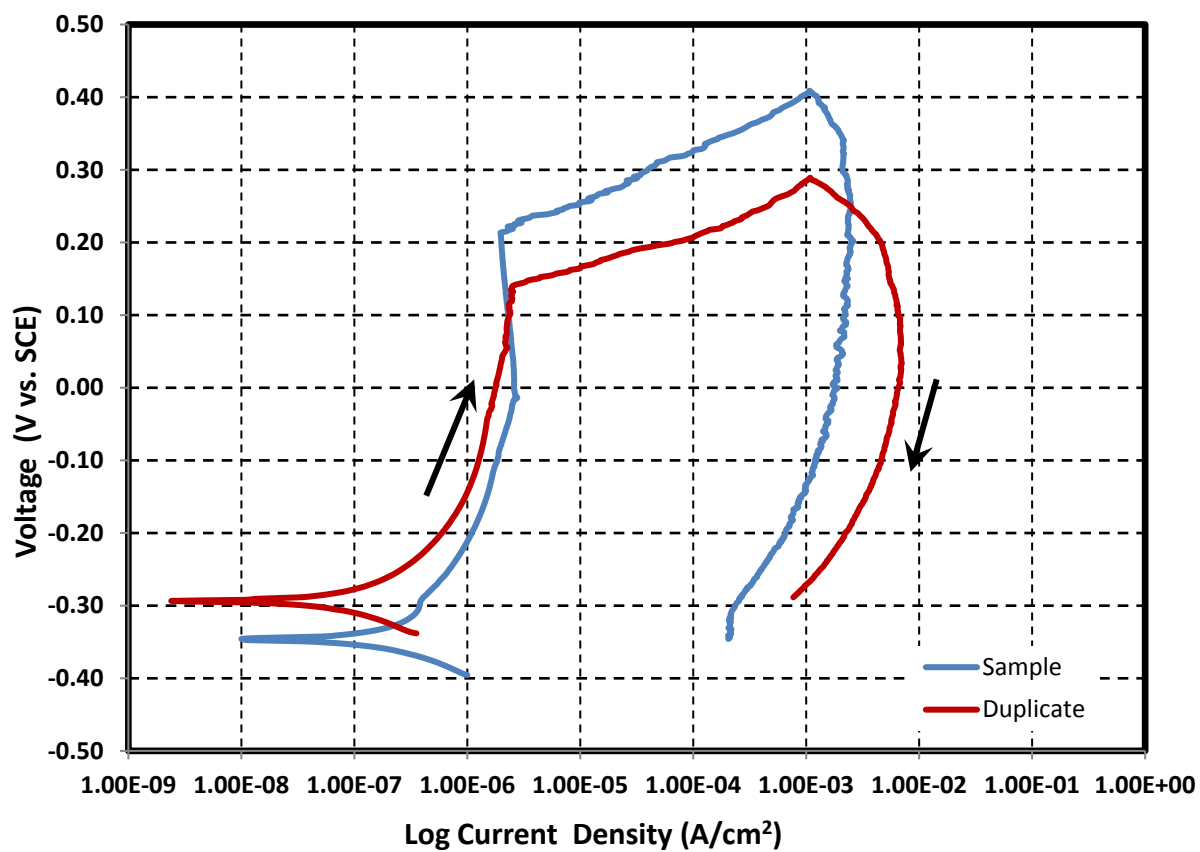
Composition of simulant for New Limits-Test 25

Test 25-NL

Temperature 35 °C
 pH at room temperature 13.31 Target 13.3
 pH before testing (at temp.) 13.21 pH after testing (at temp.) 12.86
 Volume 1.4 L

Simulant Source	Formula	Molecular Weight (g/mol)	Concentration (M)	weight required (g)
Sodium hydroxide	NaOH	40.0000	0.3	16.8000
Sodium nitrite	NaNO ₂	69.0000	0.6	57.9600
Sodium nitrate	NaNO ₃	85.0000	2.75	327.2500
Sodium chloride	NaCl	58.4000	0.2	16.3520
Sodium sulfate	Na ₂ SO ₄	142.0000	0.15	29.8200
Sodium carbonate	Na ₂ CO ₃	106.0000	0.1	14.8400
Sodium bicarbonate	NaHCO ₃	84.0100	0	0.0000

Cyclic Potentiodynamic Polarization



Images of bullet samples after electrochemical tests

Test 25



Test 25D



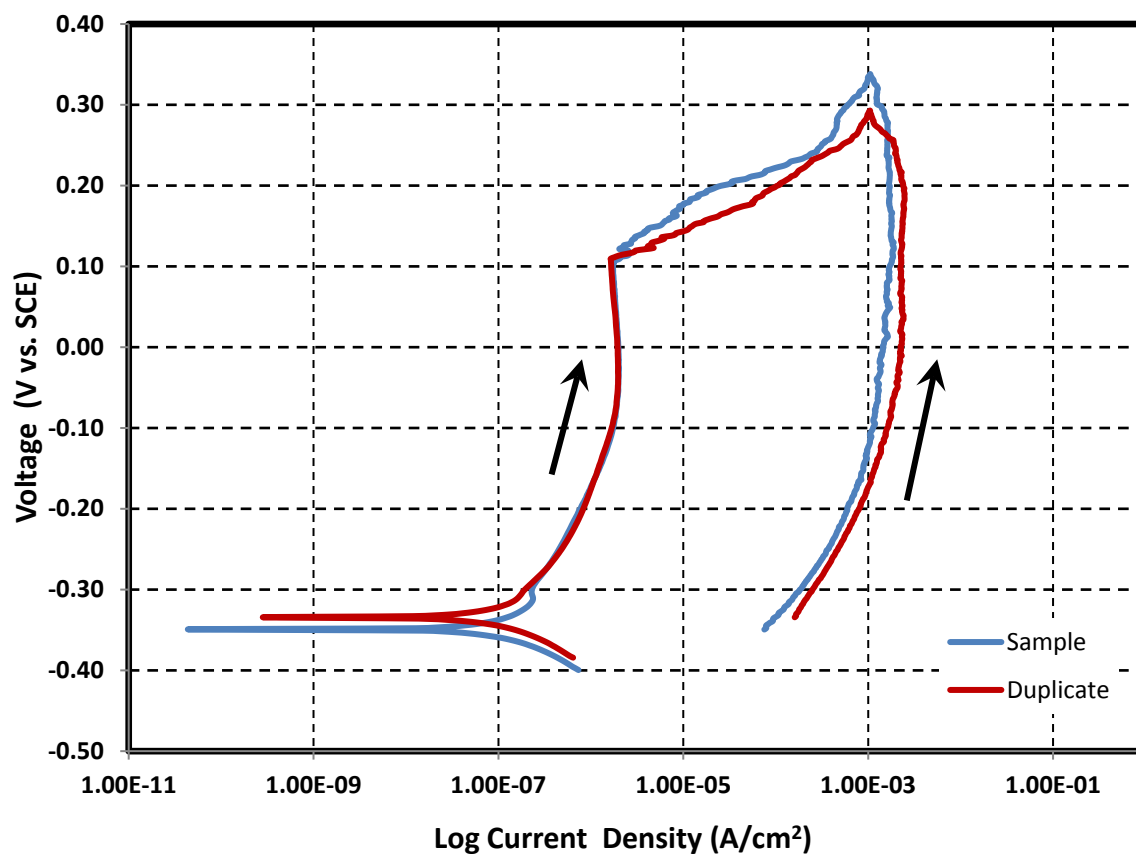
Composition of simulant for New Limits-Test 26

Test 26-NL

Temperature 35 °C
 pH at room temperature 13.24 Target 13.3
 pH before testing (at temp.) 13.17 pH after testing (at temp.) 13.18
 Volume 1.4 L

Simulant Source	Formula	Molecular Weight (g/mol)	Concentration (M)	weight required (g)
Sodium hydroxide	NaOH	40.0000	0.3	16.8000
Sodium nitrite	NaNO ₂	69.0000	0.6	57.9600
Sodium nitrate	NaNO ₃	85.0000	2.75	327.2500
Sodium chloride	NaCl	58.4000	0.2	16.3520
Sodium sulfate	Na ₂ SO ₄	142.0000	0.07	13.9160
Sodium carbonate	Na ₂ CO ₃	106.0000	0.1	14.8400
Sodium bicarbonate	NaHCO ₃	84.0100	0	0.0000

Cyclic Potentiodynamic Polarization



Images of bullet samples after electrochemical tests

Test 26



Test 26D



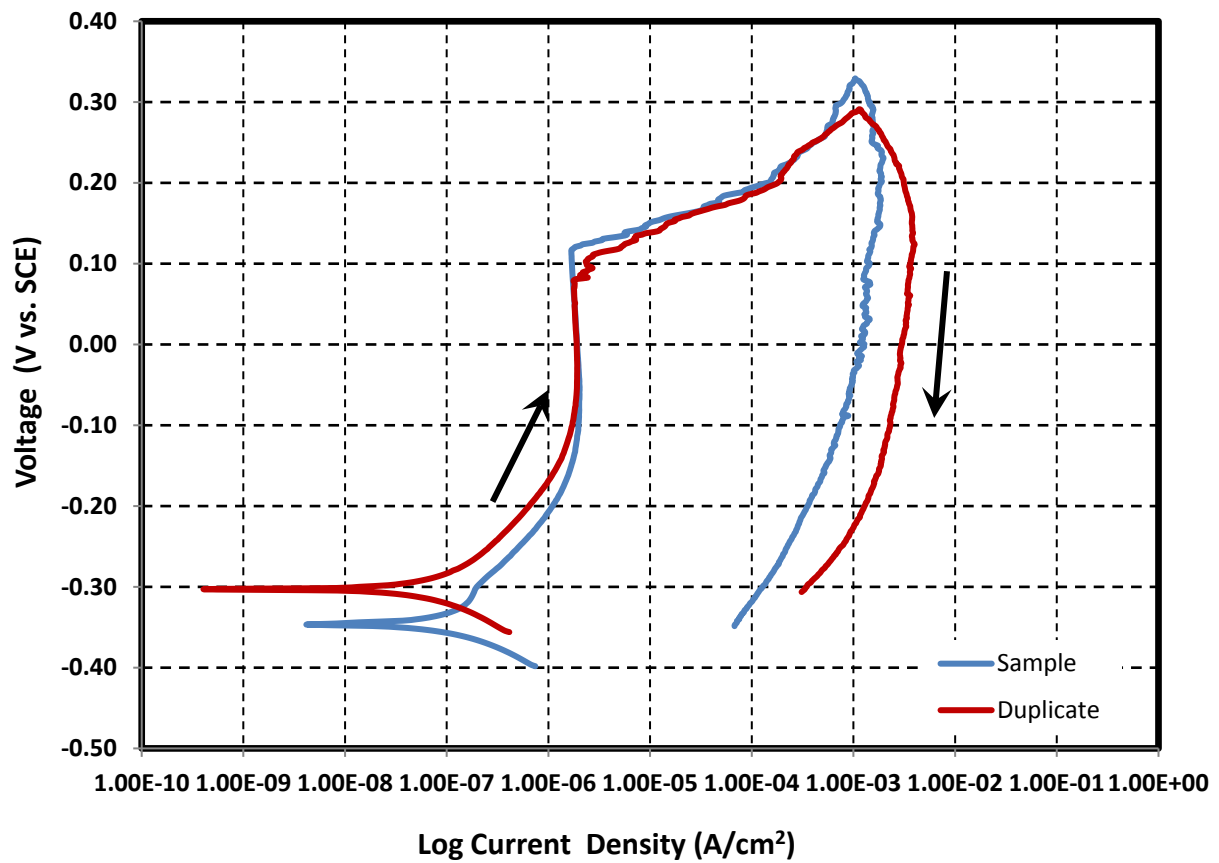
Composition of simulant for New Limits-Test 27

Test 27-NL

Temperature 35 °C
 pH at room temperature 13.10 Target 13.3
 pH before testing (at temp.) 13.02 pH after testing (at temp.) 13.03
 Volume 1.4 L

Simulant Source	Formula	Molecular Weight (g/mol)	Concentration (M)	weight required (g)
Sodium hydroxide	NaOH	40.0000	0.3	16.8000
Sodium nitrite	NaNO ₂	69.0000	0.6	57.9600
Sodium nitrate	NaNO ₃	85.0000	2.75	327.2500
Sodium chloride	NaCl	58.4000	0.2	16.3520
Sodium sulfate	Na ₂ SO ₄	142.0000	0.05	9.9400
Sodium carbonate	Na ₂ CO ₃	106.0000	0.1	14.8400
Sodium bicarbonate	NaHCO ₃	84.0100	0	0.0000

Cyclic Potentiodynamic Polarization



Images of bullet samples after electrochemical tests

Test 27



Test 27D



Appendix B

Chemical Composition of New Limits Task using Interior Points from a Statistical Design Analysis with Electrochemical Results and Pictures after Test

Table I1. Test conditions and results of testing using statistical approach from interior points

Test	Temperature (°C)	Hydroxide (M)	Nitrite (M)	Nitrate (M)	Chloride (M)	Sulfate (M)	Carbonate (M)	Bicarbonate (M)	Target pH	Category		Pitting on sample		Logistic Approach
										run 1	run 2	run 1	run 2	
1	35	0.3	1.2	0	0	0.2	0.1	0	13.3	1	1	No	No	0
2	35	0.3	0	0	0	0	0.1	0	13.3	1	1	No	No	0
3	35	0.3	1.2	0	0.4	0.2	0.1	0	13.3	5	5	Yes	Yes	1
4	35	0.3	1.2	0	0	0	0.1	0	13.3	1	1	No	No	0
5	35	0.3	1.2	5.5	0.4	0	0.1	0	13.3	5	5	Yes	Yes	1
6	35	1.2	1.2	0	0	0.2	0.1	0	13.3	1	1	No	No	0
7	35	0.3	0	5.5	0.4	0.2	0.1	0	13.3	5	5	Yes	Yes	1
8	35	0.3	0	5.5	0.4	0.2	0.1	0	13.3	5	5	Yes	Yes	1
9	35	0.3	0	5.5	0.4	0.2	0.1	0	13.3	5	5	Yes	Yes	1
10	35	0.3	0	0	0.4	0	0.1	0	13.3	5	3	Yes	Yes	1
11	35	0.0001	1.2	0.8	0	0.2	0.075	0.025	10	1	1	No	No	0
12	35	0.0001	0.9	0.6	0.025	0.16	0.075	0.025	10	1	1	No	No	0
13	35	0.0001	0.6	0.4	0.05	0.12	0.075	0.025	10	2	2	Yes	Yes	0
14	35	0.0001	0.3	0.2	0.075	0.08	0.075	0.025	10	5	5	Yes	Yes	1
15	35	0.0001	0	0	0.1	0.04	0.075	0.025	10	5	5	Yes	Yes	1

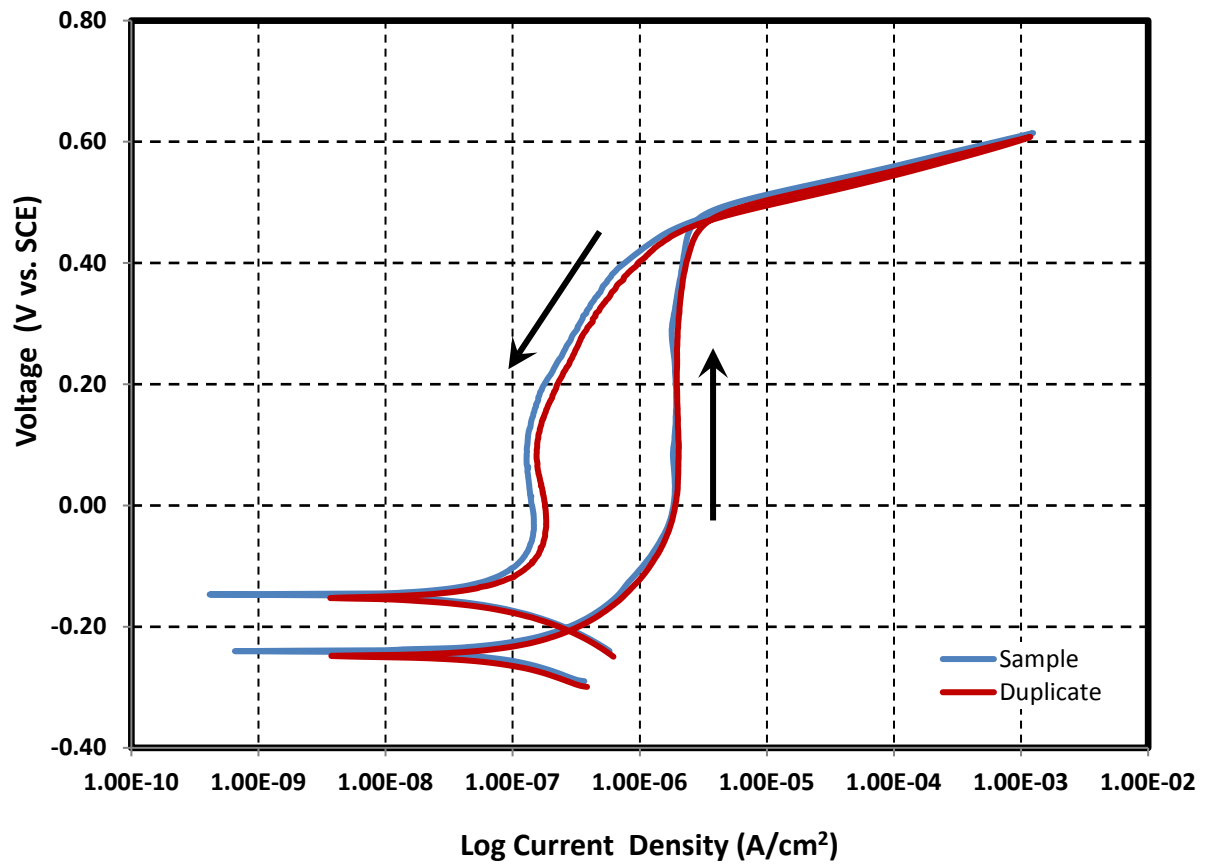
Composition of simulant for New Limits at Interior Points-Test 1

Test 1-NL-I

Temperature 35 °C
 pH at room temperature 13.57 Target 13.3
 pH before testing (at temp.) 12.92 pH after testing (at room temp.)
 Volume 1.4 L

Simulant Source	Formula	Molecular Weight (g/mol)	Concentration (M)	weight required (g)
Sodium hydroxide	NaOH	40.0000	0.3	16.8000
Sodium nitrite	NaNO ₂	69.0000	1.2	115.9200
Sodium nitrate	NaNO ₃	85.0000	0	0.0000
Sodium chloride	NaCl	58.4000	0	0.0000
Sodium sulfate	Na ₂ SO ₄	142.0000	0.2	39.7600
Sodium carbonate	Na ₂ CO ₃	106.0000	0.1	14.8400
Sodium bicarbonate	NaHCO ₃	84.0100	0.000	0.0000

Cyclic Potentiodynamic Polarization



Images of bullet samples after electrochemical tests



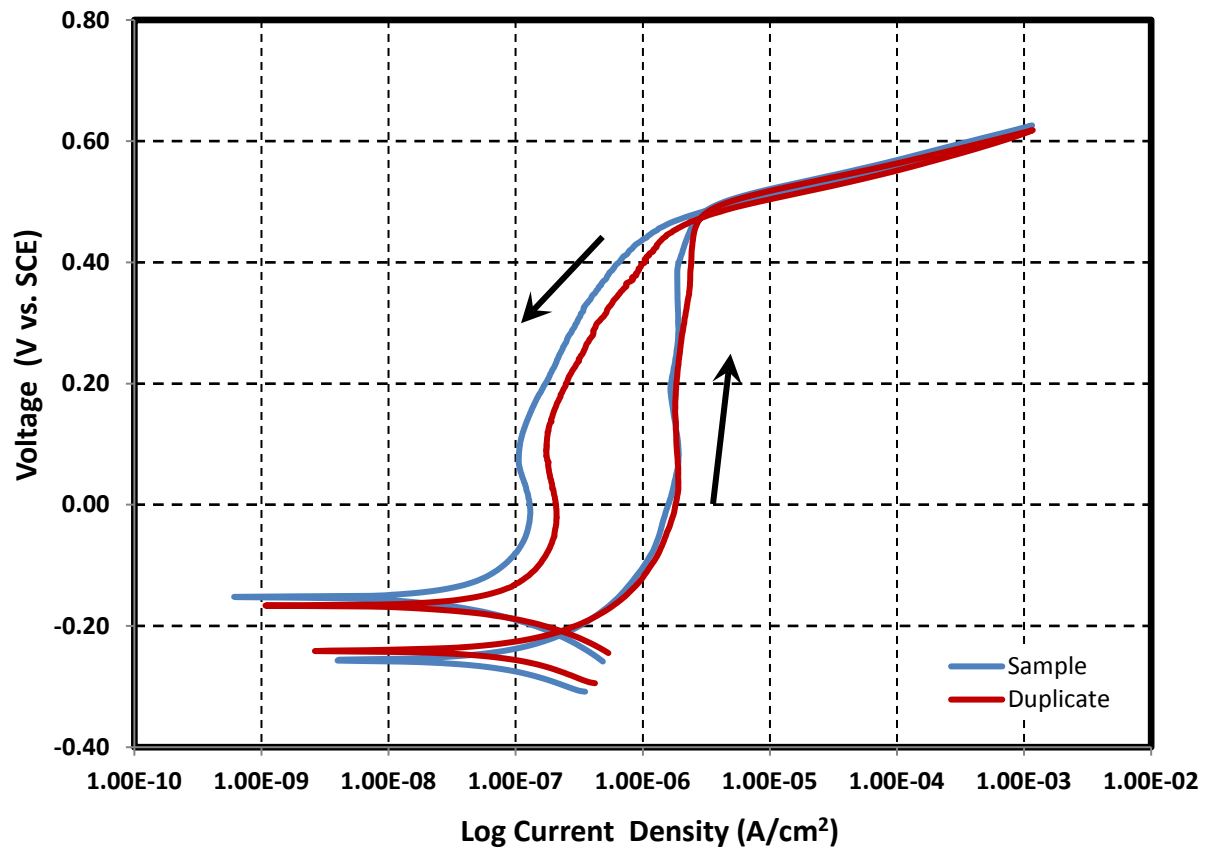
Composition of simulant for New Limits at Interior Points -Test 2

Test 2-NL-I

Temperature 35 °C
 pH at room temperature 13.71 Target 13.3
 pH before testing (at temp.) 13.18 pH after testing (at room temp.) 13.15
 Volume 1.4 L

Simulant Source	Formula	Molecular Weight (g/mol)	Concentration (M)	weight required (g)
Sodium hydroxide	NaOH	40.0000	0.3	16.8000
Sodium nitrite	NaNO ₂	69.0000	0	0.0000
Sodium nitrate	NaNO ₃	85.0000	0	0.0000
Sodium chloride	NaCl	58.4000	0	0.0000
Sodium sulfate	Na ₂ SO ₄	142.0000	0	0.0000
Sodium carbonate	Na ₂ CO ₃	106.0000	0.1	14.8400
Sodium bicarbonate	NaHCO ₃	84.0100	0.000	0.0000

Cyclic Potentiodynamic Polarization

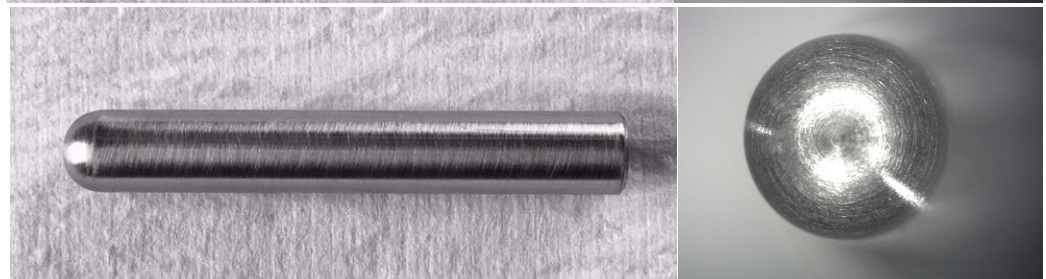


Images of bullet samples after electrochemical tests

Test 2



Test 2D



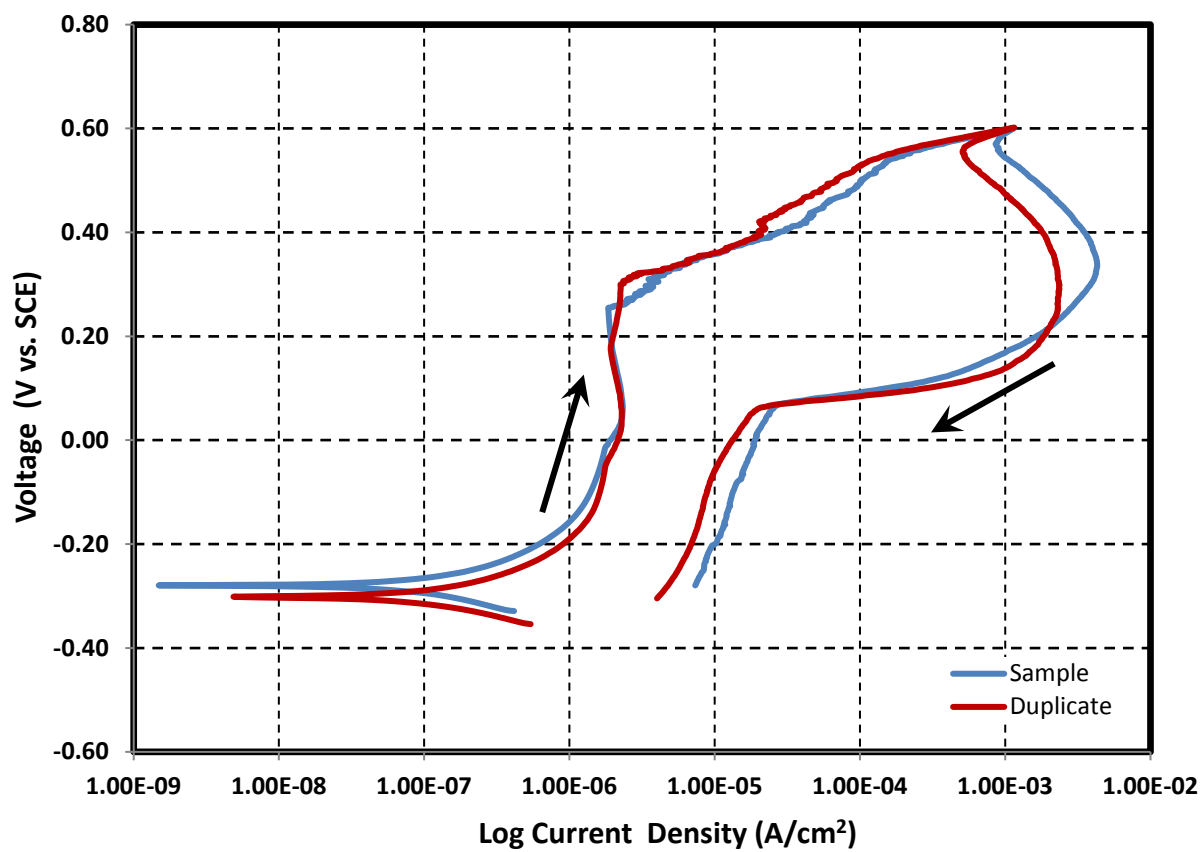
Composition of simulant for New Limits at Interior Points -Test 3

Test 3-NL-I

Temperature 35 °C
 pH at room temperature 13.42 Target 13.3
 pH before testing (at temp.) 12.93 pH after testing (at room temp.) 12.95
 Volume 1.4 L

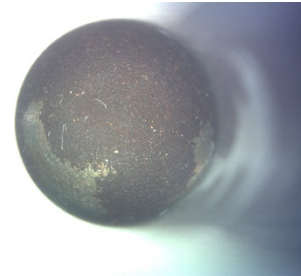
Simulant Source	Formula	Molecular Weight (g/mol)	Concentration (M)	weight required (g)
Sodium hydroxide	NaOH	40.0000	0.3	16.8000
Sodium nitrite	NaNO ₂	69.0000	1.2	115.9200
Sodium nitrate	NaNO ₃	85.0000	0	0.0000
Sodium chloride	NaCl	58.4000	0.4	32.7040
Sodium sulfate	Na ₂ SO ₄	142.0000	0.2	39.7600
Sodium carbonate	Na ₂ CO ₃	106.0000	0.1	14.8400
Sodium bicarbonate	NaHCO ₃	84.0100	0.000	0.0000

Cyclic Potentiodynamic Polarization

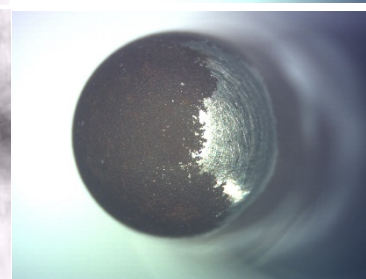


Images of bullet samples after electrochemical tests

Test 3



Test 3D



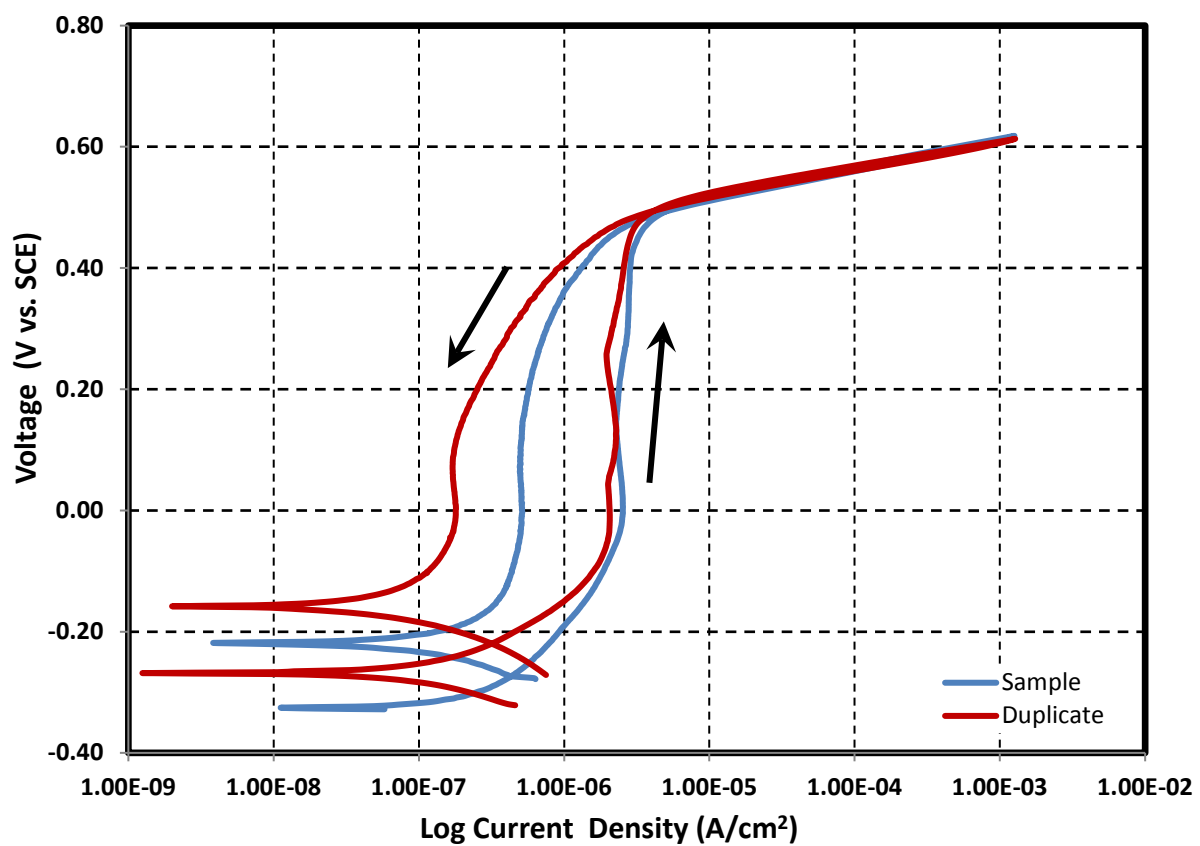
Composition of simulant for New Limits at Interior Points -Test 4

Test 4-NL-I

Temperature 35 °C
 pH at room temperature 13.37 Target 13.3
 pH before testing (at temp.) 12.90 pH after testing (at room temp.) 13.09
 Volume 1.4 L

Simulant Source	Formula	Molecular Weight (g/mol)	Concentration (M)	weight required (g)
Sodium hydroxide	NaOH	40.0000	0.3	16.8000
Sodium nitrite	NaNO ₂	69.0000	1.2	115.9200
Sodium nitrate	NaNO ₃	85.0000	0	0.0000
Sodium chloride	NaCl	58.4000	0	0.0000
Sodium sulfate	Na ₂ SO ₄	142.0000	0	0.0000
Sodium carbonate	Na ₂ CO ₃	106.0000	0.1	14.8400
Sodium bicarbonate	NaHCO ₃	84.0100	0.000	0.0000

Cyclic Potentiodynamic Polarization



Images of bullet samples after electrochemical tests

Test 4



Test 4D



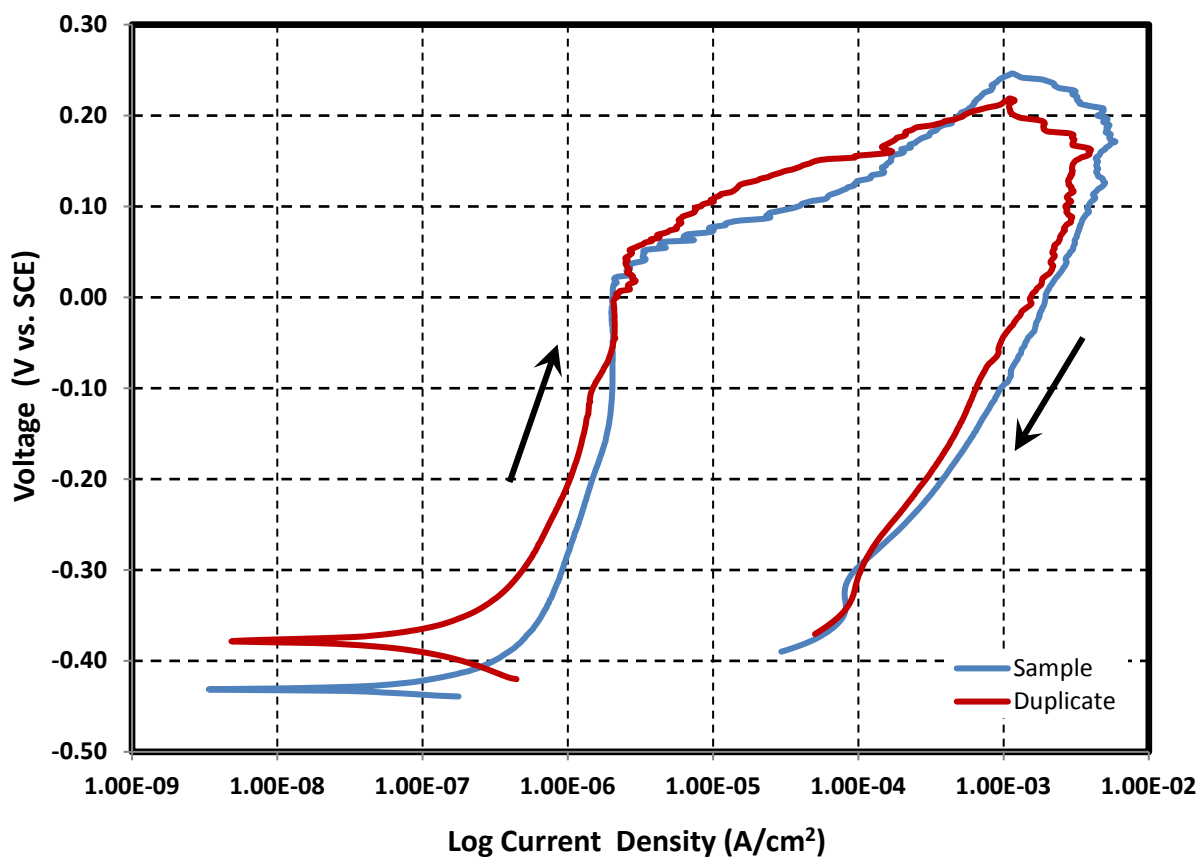
Composition of simulant for New Limits at Interior Points -Test 5

Test 5-NL-I

Temperature 35 °C
 pH at room temperature 13.42 Target 13.3
 pH before testing (at temp.) 12.87 pH after testing (at room temp.) 13.22
 Volume 1.4 L

Simulant Source	Formula	Molecular Weight (g/mol)	Concentration (M)	weight required (g)
Sodium hydroxide	NaOH	40.0000	0.3	16.8000
Sodium nitrite	NaNO ₂	69.0000	1.2	115.9204
Sodium nitrate	NaNO ₃	85.0000	5.5	654.5000
Sodium chloride	NaCl	58.4000	0.4	32.7040
Sodium sulfate	Na ₂ SO ₄	142.0000	0	0.0000
Sodium carbonate	Na ₂ CO ₃	106.0000	0.1	14.8400
Sodium bicarbonate	NaHCO ₃	84.0100	0.000	0.0000

Cyclic Potentiodynamic Polarization



Images of bullet samples after electrochemical tests



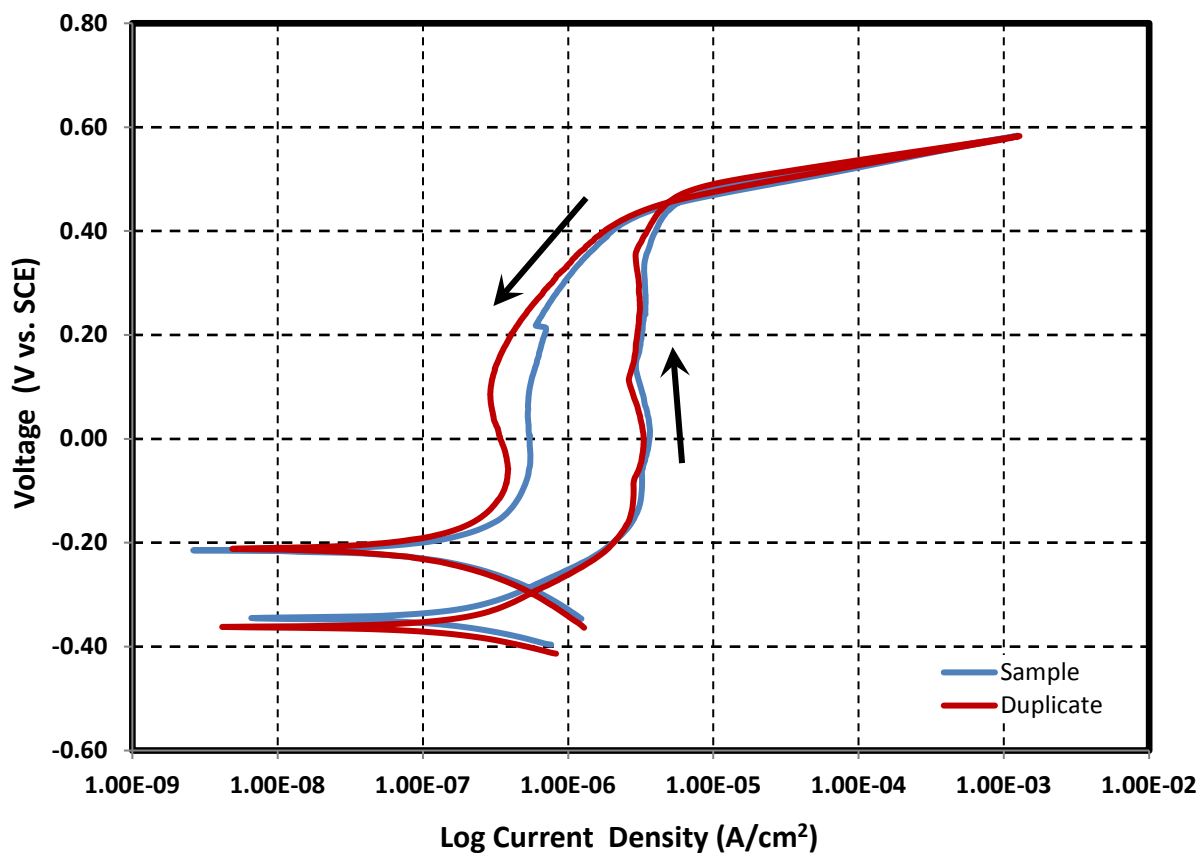
Composition of simulant for New Limits at Interior Points -Test 6

Test 6-NL-I

Temperature 35 °C
 pH at room temperature 13.83 Target 13.3
 pH before testing (at temp.) 13.28 pH after testing (at room temp.) 13.58
 Volume 1.4 L

Simulant Source	Formula	Molecular Weight (g/mol)	Concentration (M)	weight required (g)
Sodium hydroxide	NaOH	40.0000	1.2	67.2000
Sodium nitrite	NaNO ₂	69.0000	1.2	115.9200
Sodium nitrate	NaNO ₃	85.0000	0	0.0000
Sodium chloride	NaCl	58.4000	0	0.0000
Sodium sulfate	Na ₂ SO ₄	142.0000	0.2	39.7600
Sodium carbonate	Na ₂ CO ₃	106.0000	0.1	14.8400
Sodium bicarbonate	NaHCO ₃	84.0100	0.000	0.0000

Cyclic Potentiodynamic Polarization



Images of bullet samples after electrochemical tests



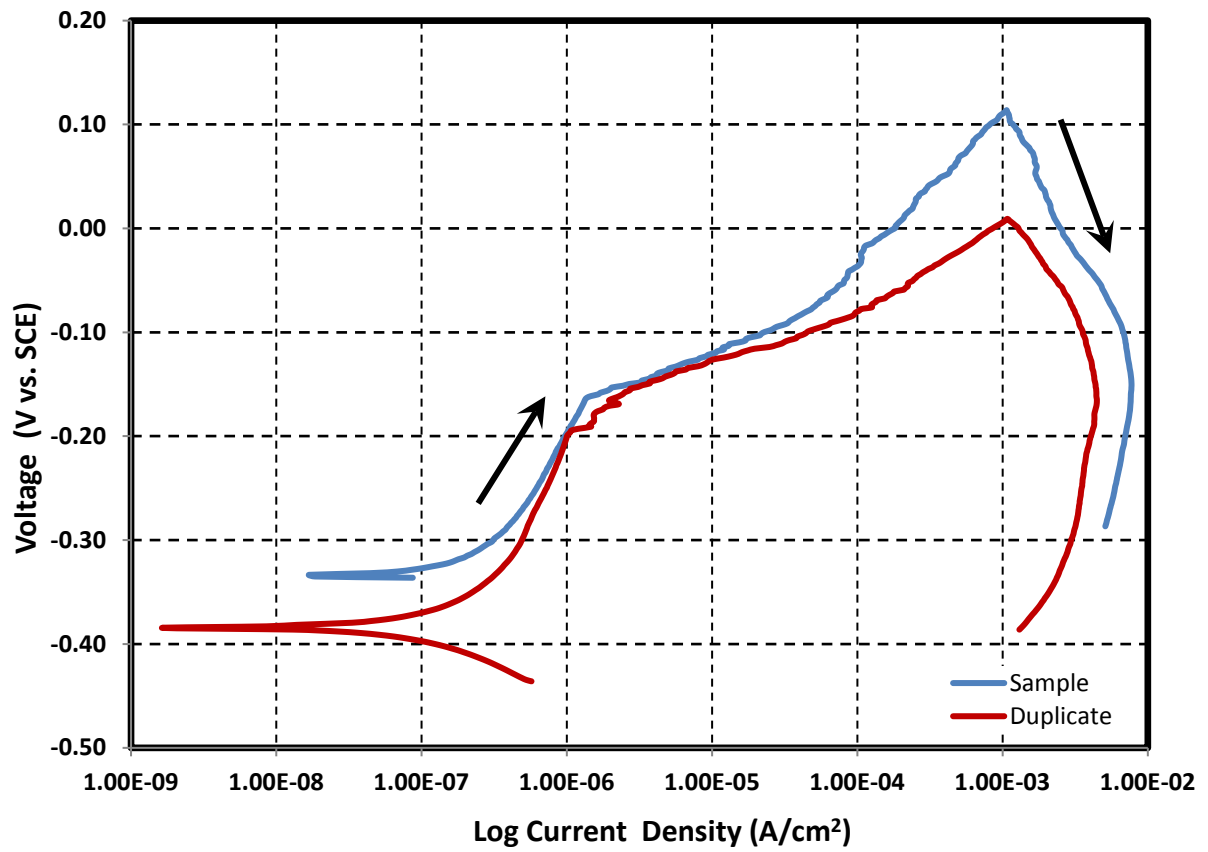
Composition of simulant for New Limits at Interior Points -Test 7

Test 7-NL-I

Temperature 35 °C
 pH at room temperature 13.45 Target 13.3
 pH before testing (at temp.) 12.86 pH after testing (at room temp.) 13.27
 Volume 1.4 L

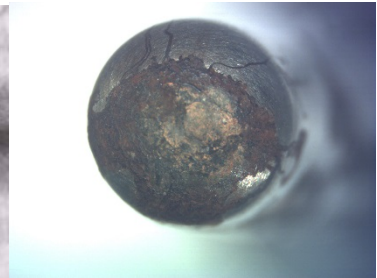
Simulant Source	Formula	Molecular Weight (g/mol)	Concentration (M)	weight required (g)
Sodium hydroxide	NaOH	40.0000	0.3	16.8000
Sodium nitrite	NaNO ₂	69.0000	0	0.0000
Sodium nitrate	NaNO ₃	85.0000	5.5	654.5000
Sodium chloride	NaCl	58.4000	0.4	32.7040
Sodium sulfate	Na ₂ SO ₄	142.0000	0.2	39.7600
Sodium carbonate	Na ₂ CO ₃	106.0000	0.1	14.8400
Sodium bicarbonate	NaHCO ₃	84.0100	0.000	0.0000

Cyclic Potentiodynamic Polarization



Images of bullet samples after electrochemical tests

Test 7



Test 7D



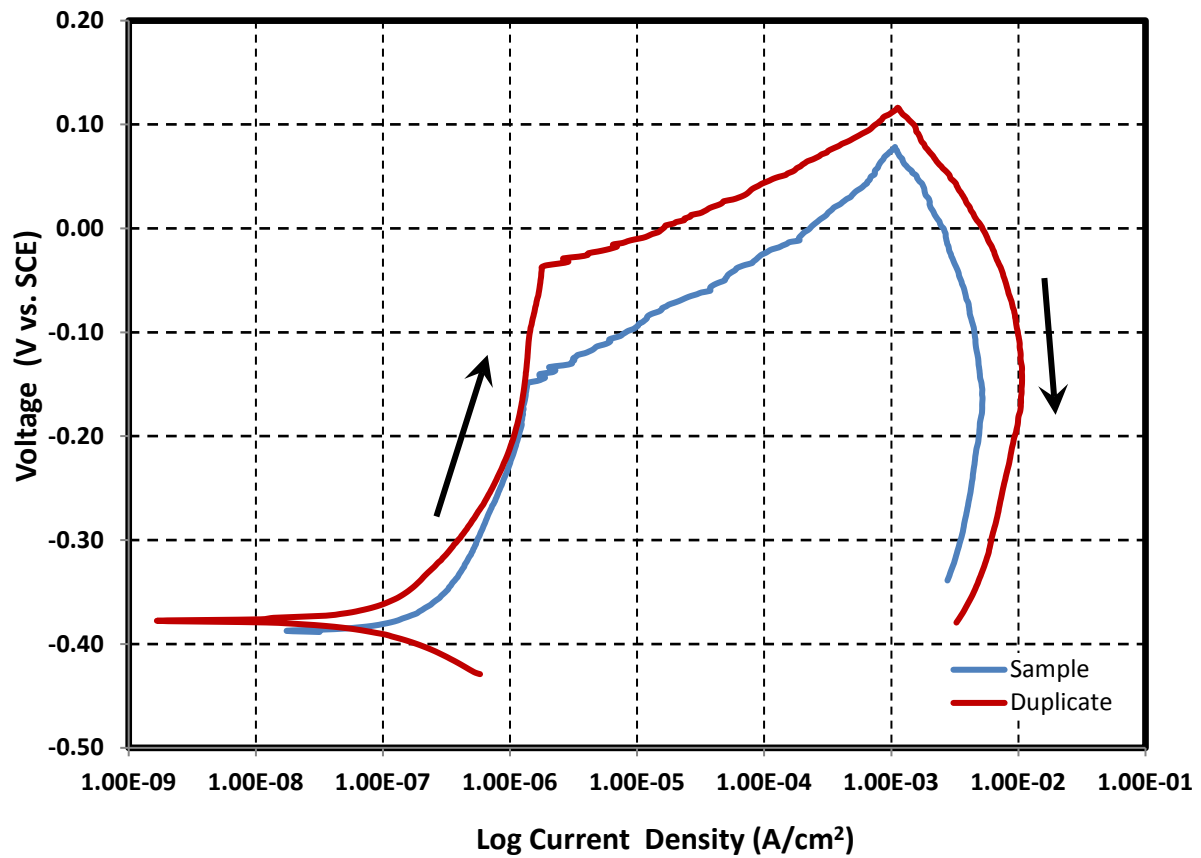
Composition of simulant for New Limits at Interior Points -Test 8

Test 8-NL-I

Temperature 35 °C
 pH at room temperature 13.47 Target 13.3
 pH before testing (at temp.) 12.85 pH after testing (at room temp.) 13.32
 Volume 1.4 L

Simulant Source	Formula	Molecular Weight (g/mol)	Concentration (M)	weight required (g)
Sodium hydroxide	NaOH	40.0000	0.3	16.8000
Sodium nitrite	NaNO ₂	69.0000	0	0.0000
Sodium nitrate	NaNO ₃	85.0000	5.5	654.5000
Sodium chloride	NaCl	58.4000	0.4	32.7040
Sodium sulfate	Na ₂ SO ₄	142.0000	0.2	39.7600
Sodium carbonate	Na ₂ CO ₃	106.0000	0.1	14.8400
Sodium bicarbonate	NaHCO ₃	84.0100	0.000	0.0000

Cyclic Potentiodynamic Polarization



Images of bullet samples after electrochemical tests

Test 8



Test 8D



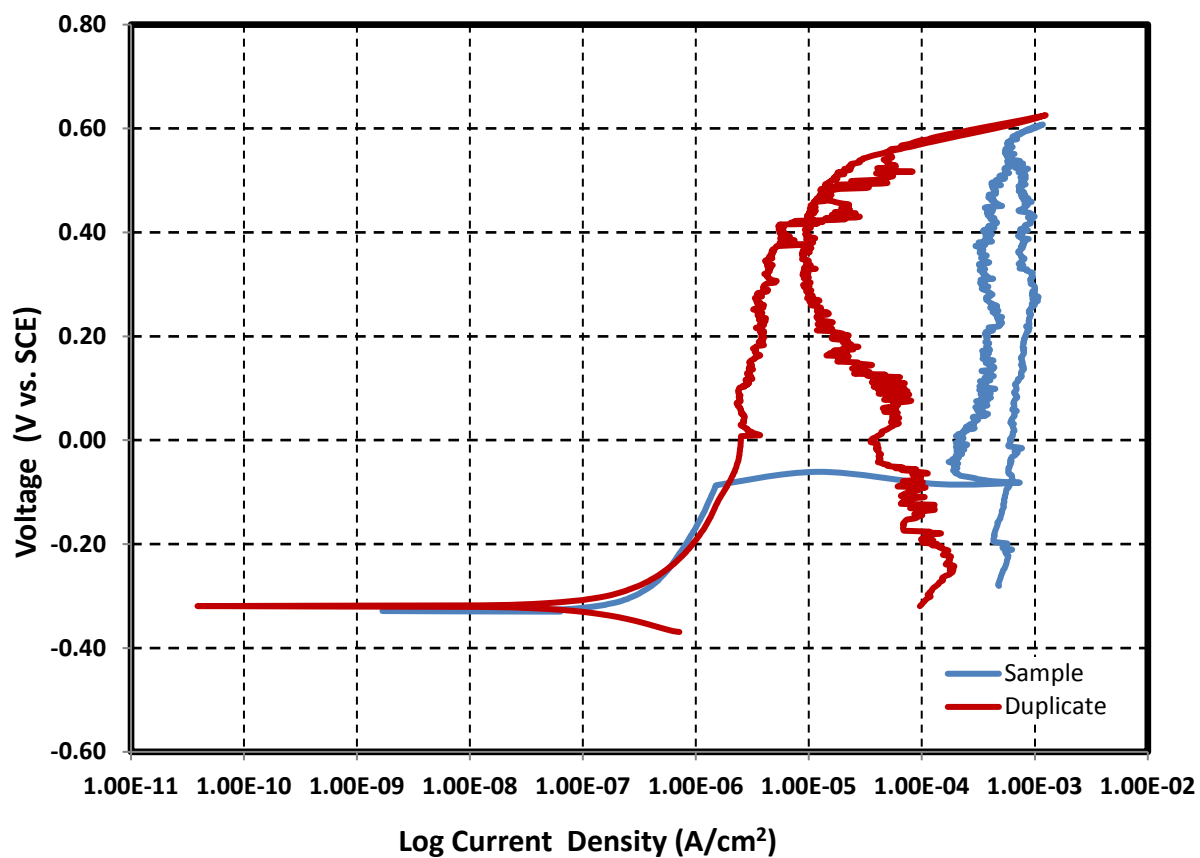
Composition of simulant for New Limits at Interior Points -Test 10

Test 10-NL-I

Temperature 35 °C
 pH at room temperature 13.54 Target 13.3
 pH before testing (at temp.) 13.02 pH after testing (at room temp.) 13.05
 Volume 1.4 L

Simulant Source	Formula	Molecular Weight (g/mol)	Concentration (M)	weight required (g)
Sodium hydroxide	NaOH	40.0000	0.3	16.8000
Sodium nitrite	NaNO ₂	69.0000	0	0.0000
Sodium nitrate	NaNO ₃	85.0000	0	0.0000
Sodium chloride	NaCl	58.4000	0.4	32.7040
Sodium sulfate	Na ₂ SO ₄	142.0000	0	0.0000
Sodium carbonate	Na ₂ CO ₃	106.0000	0.1	14.8400
Sodium bicarbonate	NaHCO ₃	84.0100	0.000	0.0000

Cyclic Potentiodynamic Polarization



Images of bullet samples after electrochemical tests



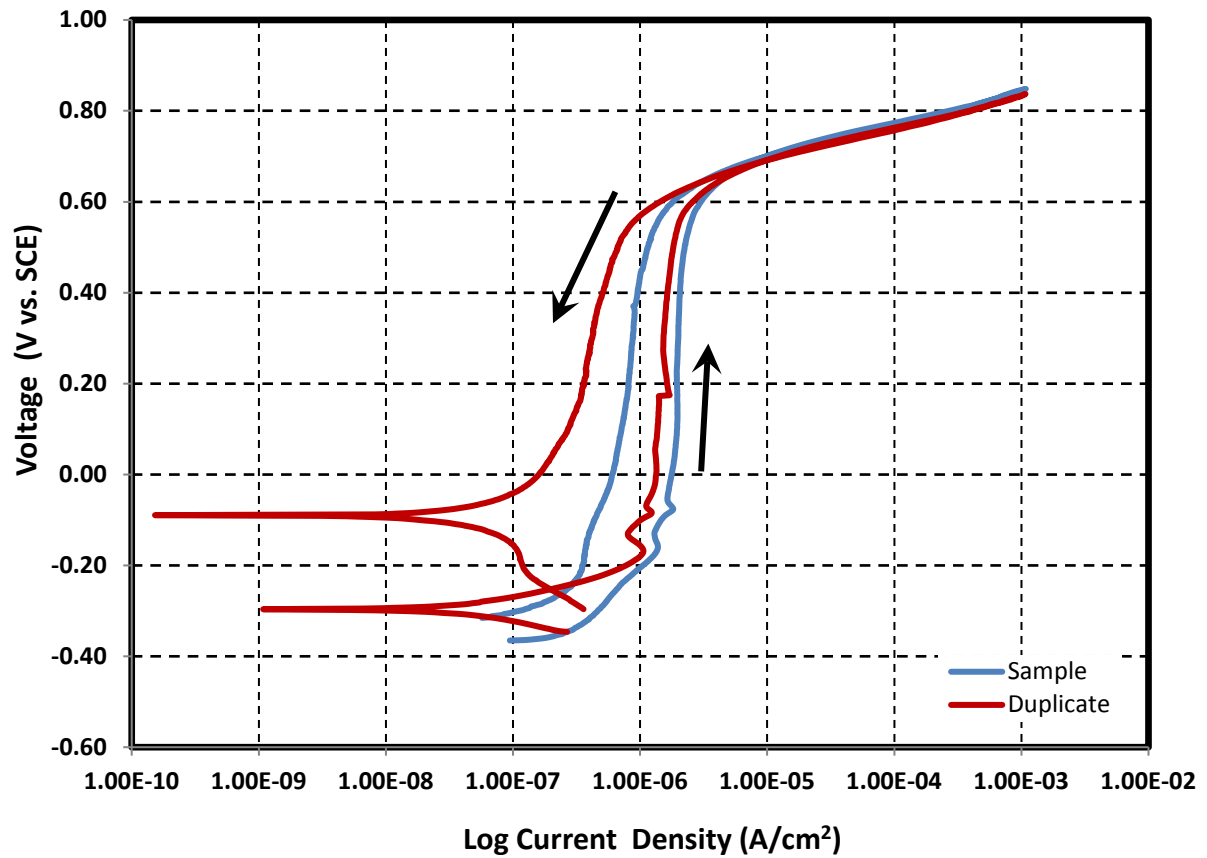
Composition of simulant for New Limits at Interior Points -Test 11

Test 11-NL-I

Temperature 35 °C
 pH at room temperature 10.02 Target 10
 pH before testing (at temp.) 10.03 pH after testing (at room temp.) 9.95
 Volume 1.4 L

Simulant Source	Formula	Molecular Weight (g/mol)	Concentration (M)	weight required (g)
Sodium hydroxide	NaOH	40.0000	0.0001	0.0056
Sodium nitrite	NaNO ₂	69.0000	1.2	115.9200
Sodium nitrate	NaNO ₃	85.0000	0.8	95.2000
Sodium chloride	NaCl	58.4000	0	0.0000
Sodium sulfate	Na ₂ SO ₄	142.0000	0.2	39.7600
Sodium carbonate	Na ₂ CO ₃	106.0000	0.075	11.1300
Sodium bicarbonate	NaHCO ₃	84.0100	0.025	2.9404

Cyclic Potentiodynamic Polarization



Images of bullet samples after electrochemical tests

Test 11



Test 11D



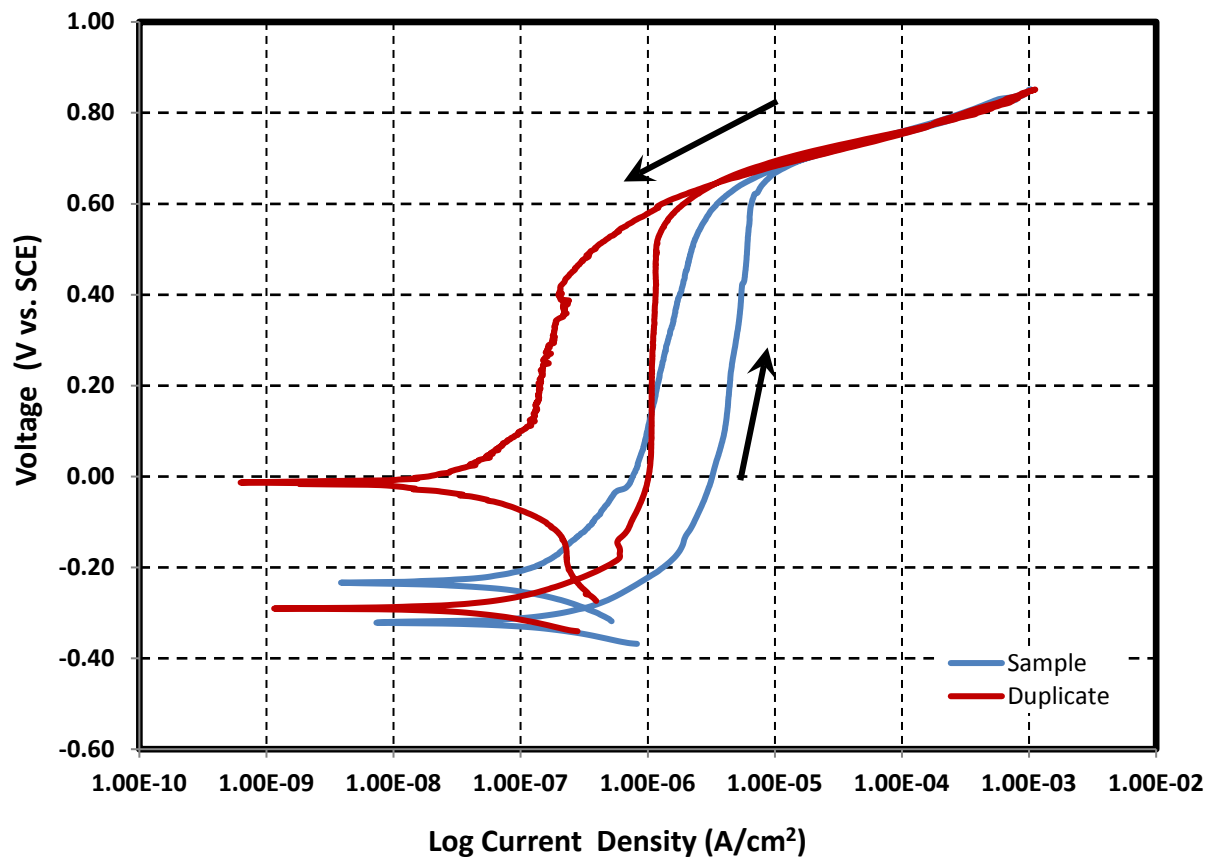
Composition of simulant for New Limits at Interior Points -Test 12

Test 12-NL-I

Temperature 35 °C
 pH at room temperature 10.85 Target 10
 pH before testing (at temp.) 10.03 pH after testing (at room temp.) 10.32
 Volume 1.4 L

Simulant Source	Formula	Molecular Weight (g/mol)	Concentration (M)	weight required (g)
Sodium hydroxide	NaOH	40.0000	0.0001	0.0056
Sodium nitrite	NaNO ₂	69.0000	0.9	86.9400
Sodium nitrate	NaNO ₃	85.0000	0.6	71.4000
Sodium chloride	NaCl	58.4000	0.025	2.0440
Sodium sulfate	Na ₂ SO ₄	142.0000	0.16	31.8080
Sodium carbonate	Na ₂ CO ₃	106.0000	0.075	11.1300
Sodium bicarbonate	NaHCO ₃	84.0100	0.025	2.9404

Cyclic Potentiodynamic Polarization



Images of bullet samples after electrochemical tests

Test 12



Test 12D



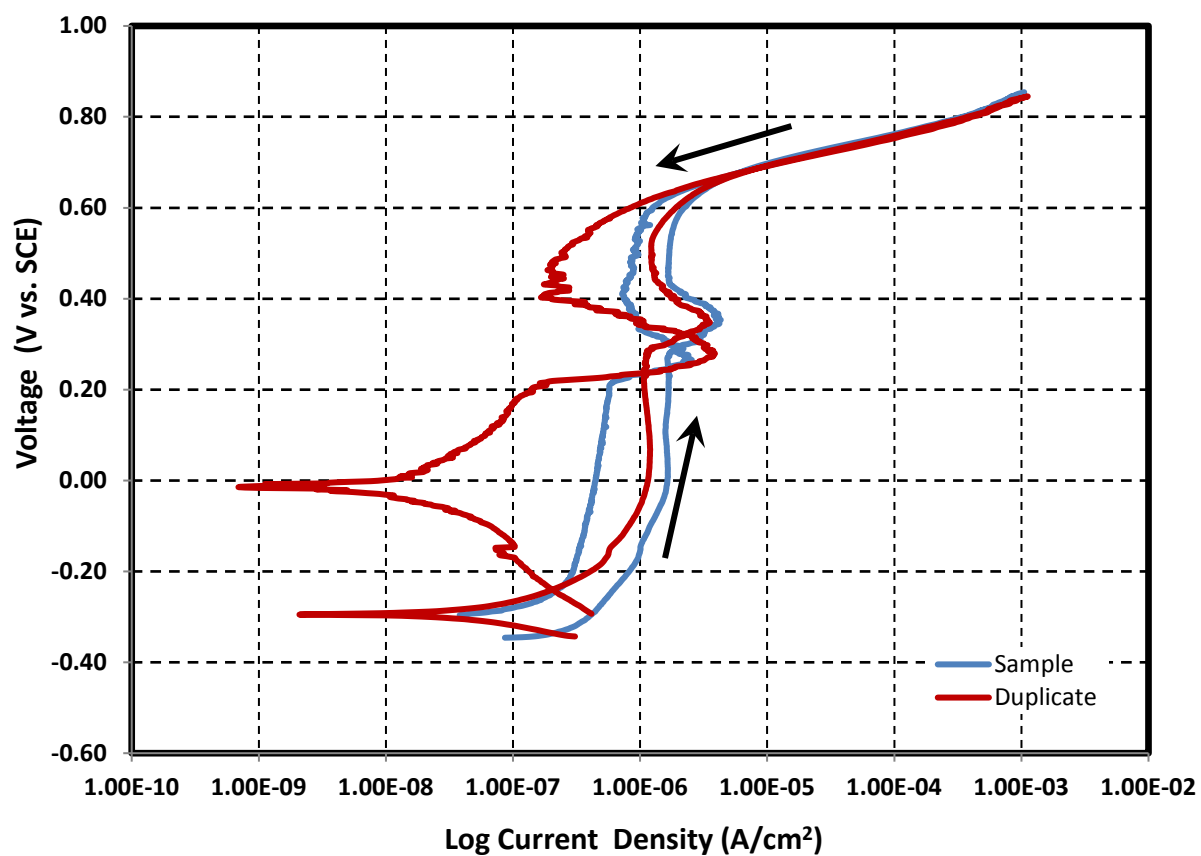
Composition of simulant for New Limits at Interior Points -Test 13

Test 13-NL-I

Temperature 35 °C
 pH at room temperature 10.98 Target 10
 pH before testing (at temp.) 10.06 pH after testing (at room temp.) 10.23
 Volume 1.4 L

Simulant Source	Formula	Molecular Weight (g/mol)	Concentration (M)	weight required (g)
Sodium hydroxide	NaOH	40.0000	0.0001	0.0056
Sodium nitrite	NaNO ₂	69.0000	0.6	57.9600
Sodium nitrate	NaNO ₃	85.0000	0.4	47.6000
Sodium chloride	NaCl	58.4000	0.05	4.0880
Sodium sulfate	Na ₂ SO ₄	142.0000	0.12	23.8560
Sodium carbonate	Na ₂ CO ₃	106.0000	0.075	11.1300
Sodium bicarbonate	NaHCO ₃	84.0100	0.025	2.9404

Cyclic Potentiodynamic Polarization



Images of bullet samples after electrochemical tests



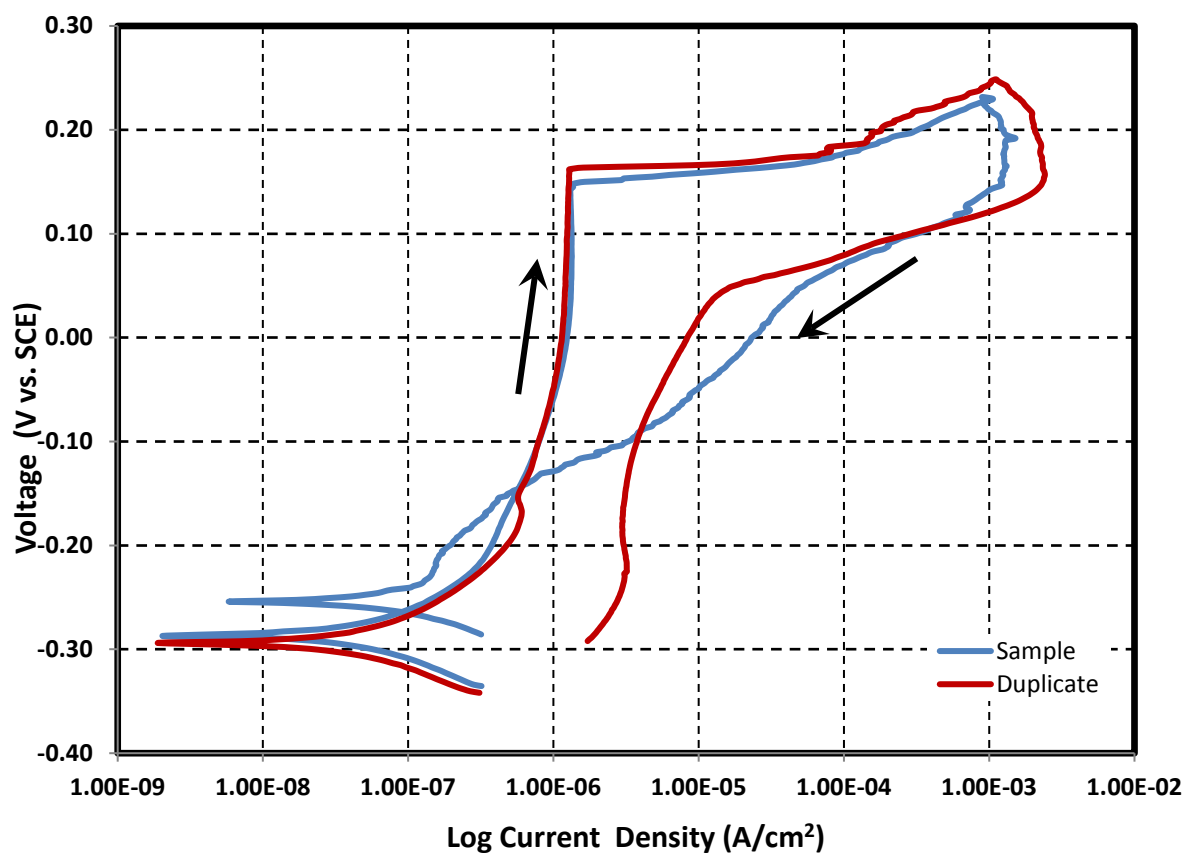
Composition of simulant for New Limits at Interior Points -Test 14

Test 14-NL-I

Temperature 35 °C
 pH at room temperature 11.28 Target 10
 pH before testing (at temp.) 10.02 pH after testing (at room temp.) 10.54
 Volume 1.4 L

Simulant Source	Formula	Molecular Weight (g/mol)	Concentration (M)	weight required (g)
Sodium hydroxide	NaOH	40.0000	0.0001	0.0056
Sodium nitrite	NaNO ₂	69.0000	0.3	29.9800
Sodium nitrate	NaNO ₃	85.0000	0.2	23.8000
Sodium chloride	NaCl	58.4000	0.075	6.1320
Sodium sulfate	Na ₂ SO ₄	142.0000	0.08	15.9040
Sodium carbonate	Na ₂ CO ₃	106.0000	0.075	11.1300
Sodium bicarbonate	NaHCO ₃	84.0100	0.025	2.9404

Cyclic Potentiodynamic Polarization



Images of bullet samples after electrochemical tests

Test 14



Test 14D



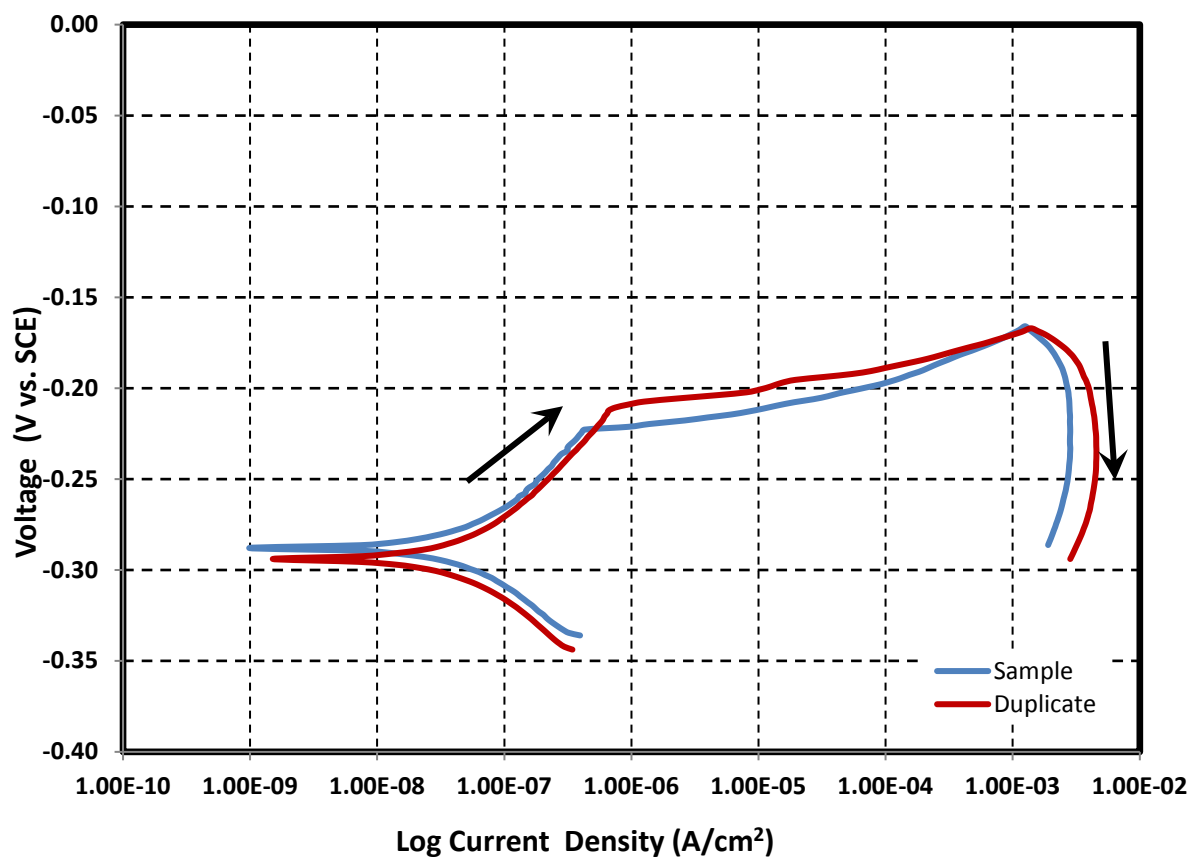
Composition of simulant for New Limits at Interior Points -Test 15

Test 15-NL-I

Temperature 35 °C
 pH at room temperature 11.43 Target 10
 pH before testing (at temp.) 10.07 pH after testing (at room temp.) 10.63
 Volume 1.4 L

Simulant Source	Formula	Molecular Weight (g/mol)	Concentration (M)	weight required (g)
Sodium hydroxide	NaOH	40.0000	0.0001	0.0056
Sodium nitrite	NaNO ₂	69.0000	0	0.0000
Sodium nitrate	NaNO ₃	85.0000	0	0.0000
Sodium chloride	NaCl	58.4000	0.1	8.1760
Sodium sulfate	Na ₂ SO ₄	142.0000	0.04	7.9520
Sodium carbonate	Na ₂ CO ₃	106.0000	0.075	11.1300
Sodium bicarbonate	NaHCO ₃	84.0100	0.025	2.9404

Cyclic Potentiodynamic Polarization



Images of bullet samples after electrochemical tests

Test 15



Test 15D



Appendix C

Chemical Composition of New Limits Task with ammonia from a Statistical Design Analysis with Electrochemical Results and Pictures after Test

Table C1. Test conditions and results of testing using an augmented statistical approach with ammonia

Test	Temperature (°C)	Hydroxide (M)	Nitrite (M)	Nitrate (M)	Chloride (M)	Sulfate (M)	Ammonium Nitrate (M)	Carbonate (M)	Target pH	Category		Pitting on sample		Logistic Approach
										run 1	run 2	run 1	run 2	
1	35	0.01	0	0	0.4	0.2	0.25	0.1	>12	5	5	Yes	Yes	1
2	35	0.3	0.6	2.75	0.2	0.1	0	0.1	>12	5	5	Yes	Yes	1
3	35	1.2	0	5.5	0.4	0	0.25	0.1	>12	3	3	Yes	Yes	1
4	35	0.01	0	5.5	0.4	0	0	0.1	>12	5	5	Yes	Yes	1
5	35	1.2	0	0	0.4	0.2	0	0.1	>12	1	1	No	No	0
6	35	0.605	0.6	2.75	0.2	0.1	0.125	0.1	>12	1	1	No	No	0
7	35	0.01	1.2	5.5	0.4	0.2	0	0.1	>12	5	5	Yes	Yes	1
8	35	1.2	1.2	5.5	0.4	0.2	0.25	0.1	>12	1	1	No	No	0
9	35	0.01	0	5.5	0	0.2	0.25	0.1	>12	3	3	Yes	Yes	1
10	35	0.01	1.2	0	0	0.2	0	0.1	>12	1	1	No	No	0
11	35	0.01	0	0	0	0	0	0.1	>12	1	1	No	No	0
12	35	0.3	0.6	2.75	0.2	0.1	0	0.1	>12	5	5	Yes	Yes	1
13	35	1.2	1.2	0	0.4	0	0	0.1	>12	1	1	No	No	0
14	35	0.01	1.2	0	0.4	0	0.25	0.1	>12	5	5	Yes	Yes	1
15	35	0.01	1.2	5.5	0	0	0.25	0.1	>12	1	1	No	No	0
16	35	1.2	1.2	5.5	0	0	0	0.1	>12	1	1	No	No	0
17	35	1.2	1.2	0	0	0.2	0.25	0.1	>12	1	1	No	No	0
18	35	1.2	0	0	0	0	0.25	0.1	>12	1	1	No	No	0
19	35	0.3	0.6	2.75	0.2	0.1	0	0.1	>12	3	3	Yes	Yes	1
20	35	1.2	0	5.5	0	0.2	0	0.1	>12	1	3	No	No	0

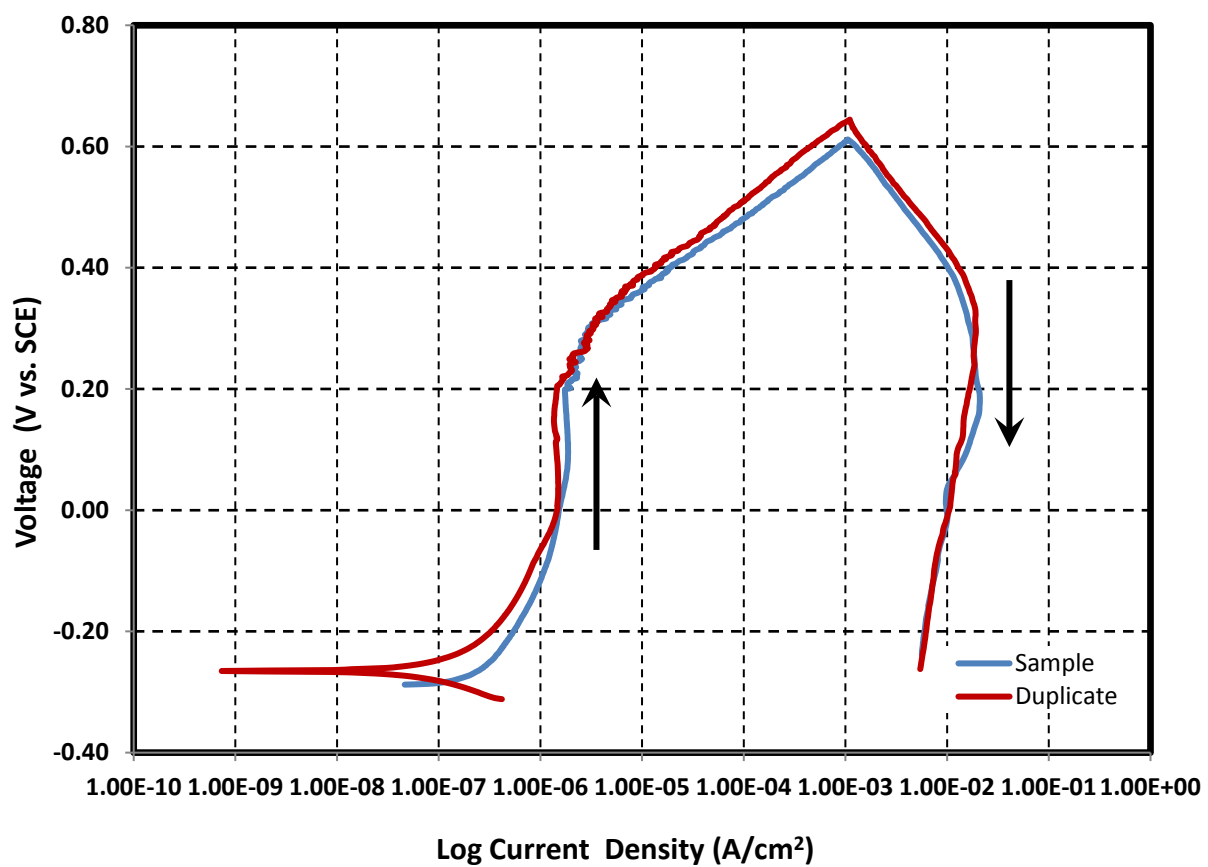
Composition of simulant for New Limits with ammonia-Test 1

Test 1-NL-NH3

Temperature 35 °C
 pH at room temperature 9.27 Target >12
 pH before testing (at temp.) 12.30 pH after testing (at room temp.) 12.38
 Volume 1.4 L

Simulant Source	Formula	Molecular Weight (g/mol)	Concentration (M)	weight required (g)
Sodium hydroxide	NaOH	40.0000	0.01	0.5600
Sodium nitrite	NaNO ₂	69.0000	0	0.0000
Sodium nitrate	NaNO ₃	85.0000	0	0.0000
Sodium chloride	NaCl	58.4000	0.4	32.7040
Sodium sulfate	Na ₂ SO ₄	142.0000	0.2	39.7600
Ammonium Nitrate	NH ₄ NO ₃	80.0520	0.25	28.0182
Sodium carbonate	Na ₂ CO ₃	106.0000	0.100	14.8400
Sodium bicarbonate	NaHCO ₃	84.0100	0.000	0.0000

Cyclic Potentiodynamic Polarization



Images of bullet samples after electrochemical tests



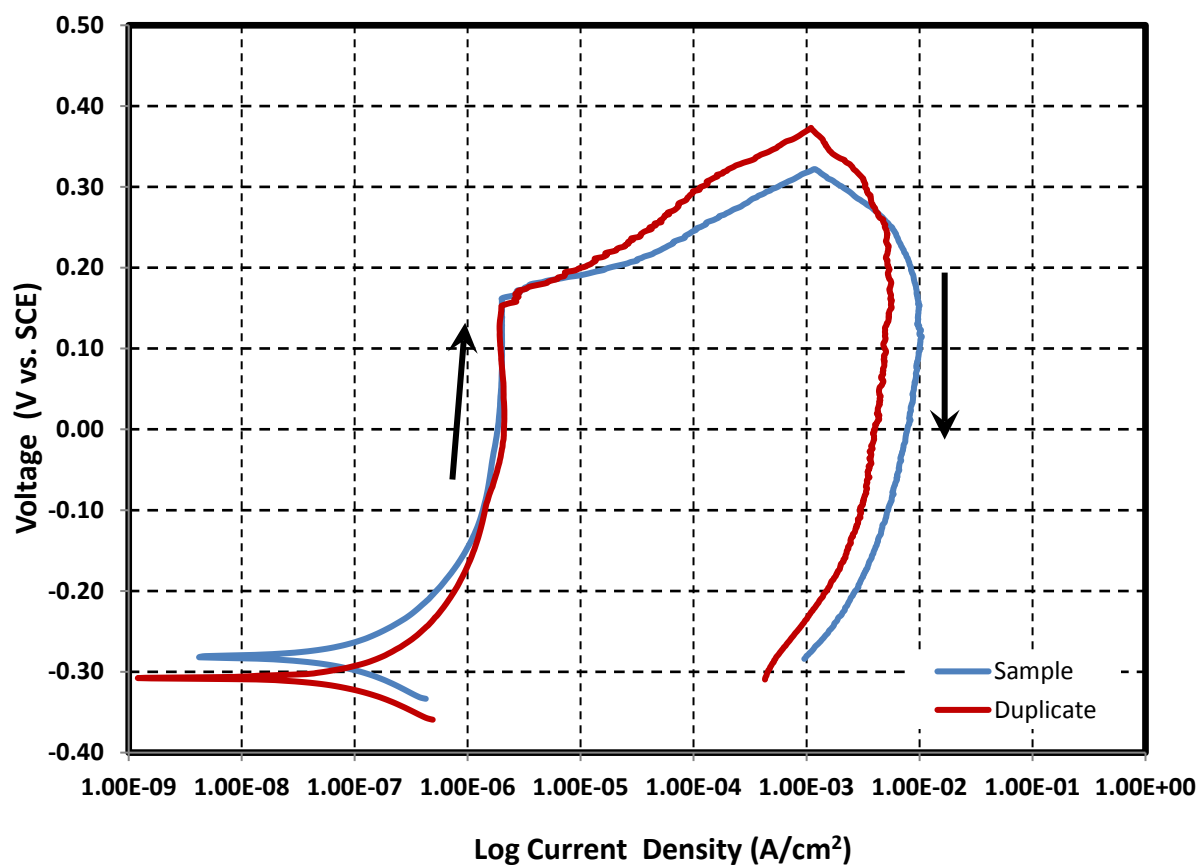
Composition of simulant for New Limits-Test 2

Test 2-NL-NH3

Temperature 35 °C
 pH at room temperature 13.16 Target >12
 pH before testing (at temp.) 12.93 pH after testing (at room temp.) 13.18
 Volume 1.4 L

Simulant Source	Formula	Molecular Weight (g/mol)	Concentration (M)	weight required (g)
Sodium hydroxide	NaOH	40.0000	0.3	16.8000
Sodium nitrite	NaNO ₂	69.0000	0.6	57.9600
Sodium nitrate	NaNO ₃	85.0000	2.75	327.2500
Sodium chloride	NaCl	58.4000	0.2	16.3632
Sodium sulfate	Na ₂ SO ₄	142.0000	0.1	19.8800
Ammonium Nitrate	NH ₄ NO ₃	80.0520	0	0.0000
Sodium carbonate	Na ₂ CO ₃	106.0000	0.1	14.8400
Sodium bicarbonate	NaHCO ₃	84.0100	0.000	0.0000

Cyclic Potentiodynamic Polarization



Images of bullet samples after electrochemical tests



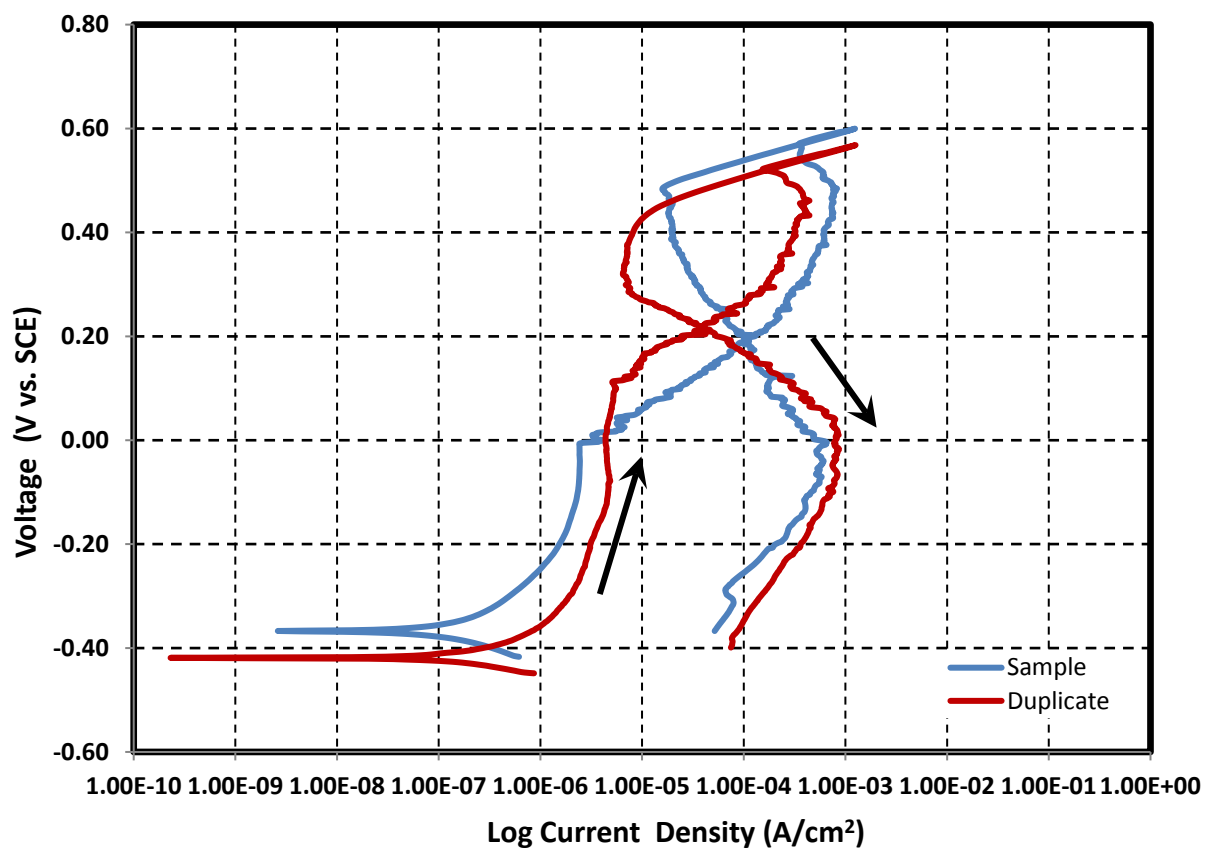
Composition of simulant for New Limits-Test 3

Test 3-NL-NH3

Temperature 35 °C
 pH at room temperature 13.73 Target >12
 pH before testing (at temp.) 13.81 pH after testing (at room temp.) 13.42
 Volume 1.4 L

Simulant Source	Formula	Molecular Weight (g/mol)	Concentration (M)	weight required (g)
Sodium hydroxide	NaOH	40.0000	1.45	81.2000
Sodium nitrite	NaNO ₂	69.0000	0	0.0000
Sodium nitrate	NaNO ₃	85.0000	5.25	624.7500
Sodium chloride	NaCl	58.4000	0.4	32.7264
Sodium sulfate	Na ₂ SO ₄	142.0000	0	0.0000
Ammonium Nitrate	NH ₄ NO ₃	80.0520	0.25	28.0182
Sodium carbonate	Na ₂ CO ₃	106.0000	0.100	14.8400
Sodium bicarbonate	NaHCO ₃	84.0100	0.000	0.0000

Cyclic Potentiodynamic Polarization



Images of bullet samples after electrochemical tests

Test 3



Test 3D



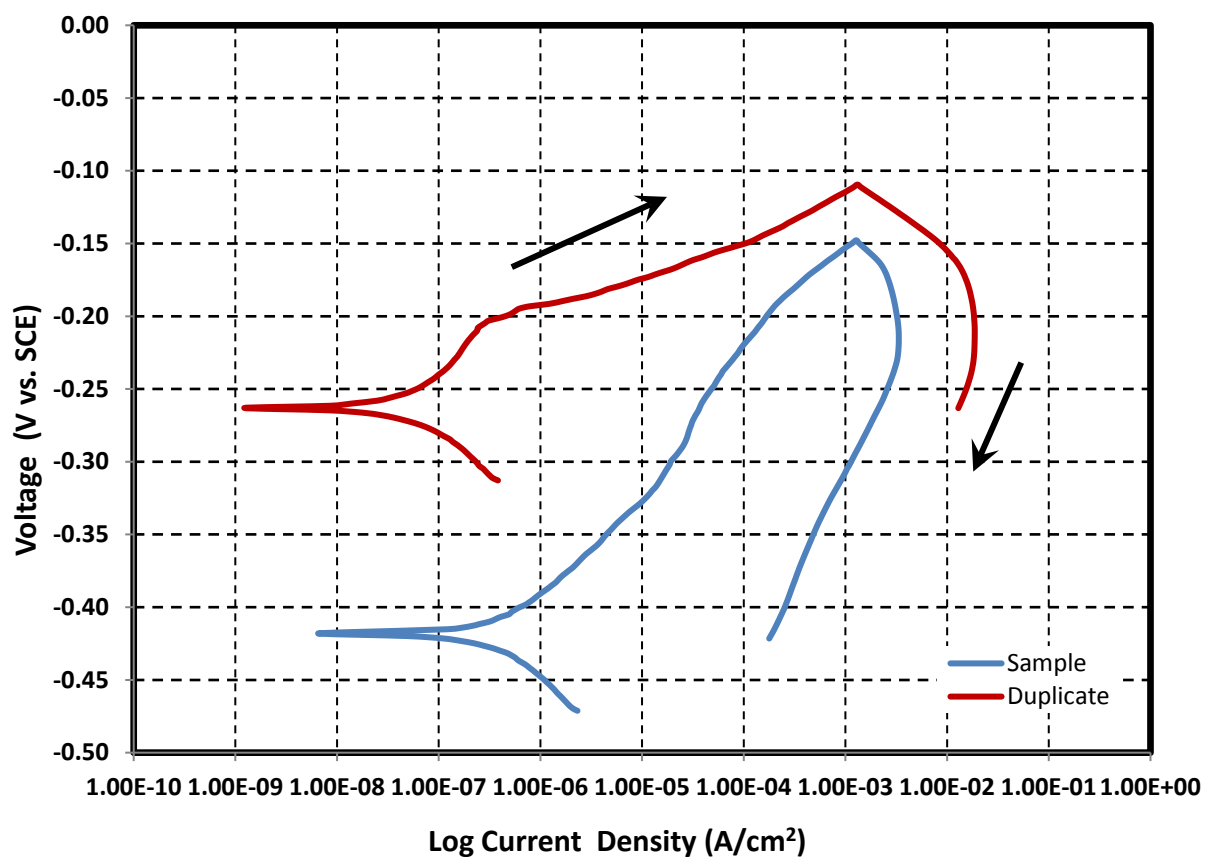
Composition of simulant for New Limits-Test 4

Test 4-NL-NH3

Temperature 35 °C
 pH at room temperature 11.78 Target >12
 pH before testing (at temp.) 12.04 pH after testing (at room temp.) 11.93
 Volume 1.4 L

Test 3D Simulant Source	Formula	Molecular Weight (g/mol)	Concentration (M)	weight required (g)
Sodium hydroxide	NaOH	40.0000	0.01	0.5596
Sodium nitrite	NaNO ₂	69.0000	0	0.0000
Sodium nitrate	NaNO ₃	85.0000	5.5	654.5000
Sodium chloride	NaCl	58.4000	0.4	32.7264
Sodium sulfate	Na ₂ SO ₄	142.0000	0	0.0000
Ammonium Nitrate	NH ₄ NO ₃	80.0520	0	0.0000
Sodium carbonate	Na ₂ CO ₃	106.0000	0.100	14.8400
Sodium bicarbonate	NaHCO ₃	84.0100	0.000	0.0000

Cyclic Potentiodynamic Polarization

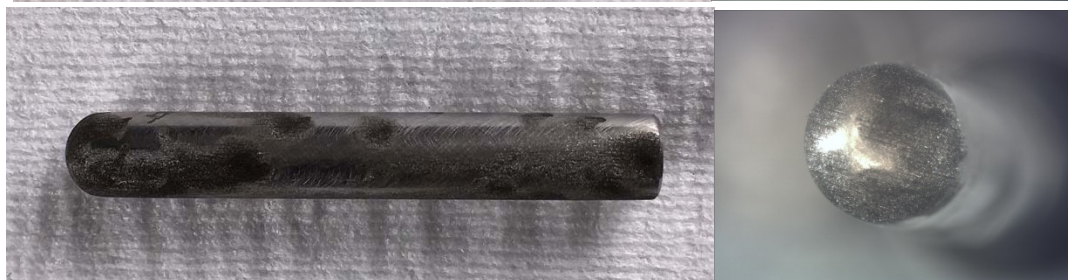


Images of bullet samples after electrochemical tests

Test 4



Test 4D



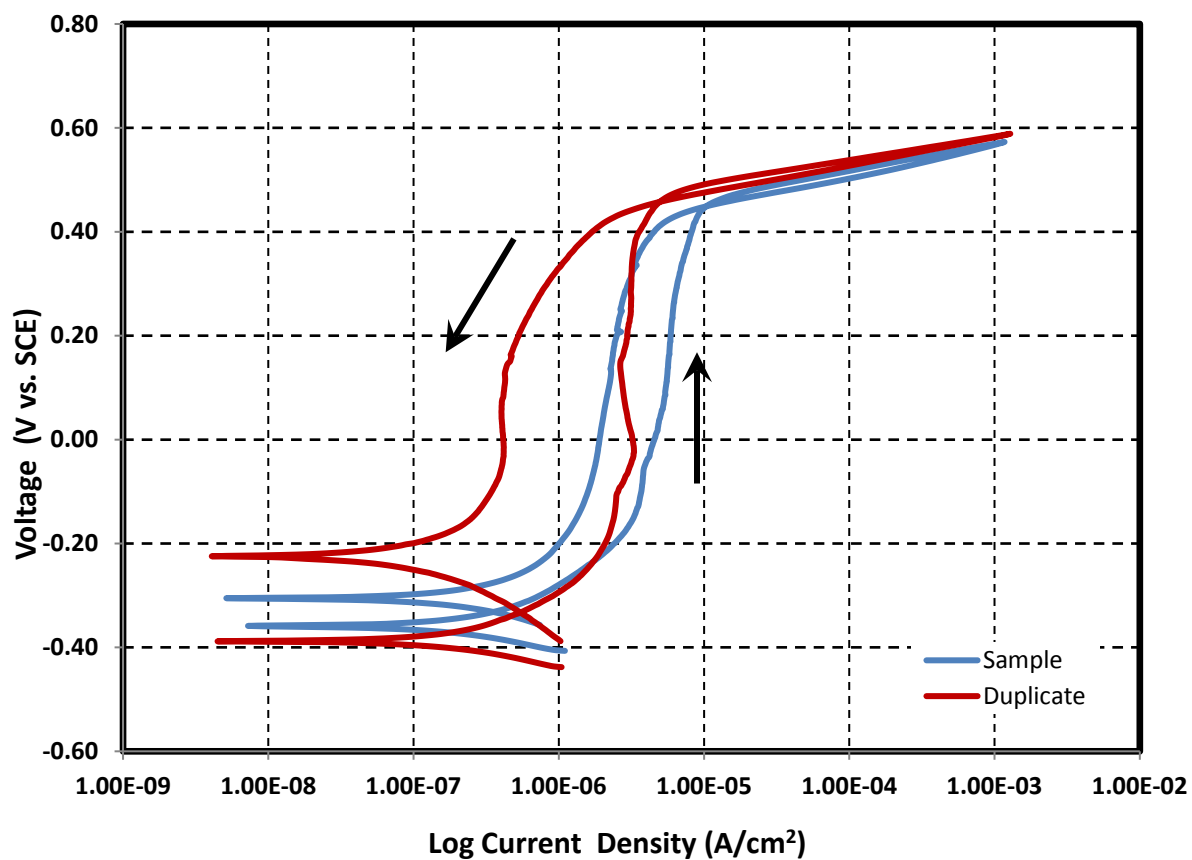
Composition of simulant for New Limits-Test 5

Test 5-NL-NH3

Temperature 35 °C
 pH at room temperature 13.30 Target >12
 pH before testing (at temp.) 13.01 pH after testing (at room temp.) 13.63
 Volume 1.4 L

Simulant Source	Formula	Molecular Weight (g/mol)	Concentration (M)	weight required (g)
Sodium hydroxide	NaOH	40.0000	1.2	67.2000
Sodium nitrite	NaNO ₂	69.0000	0	0.0000
Sodium nitrate	NaNO ₃	85.0000	0	0.0000
Sodium chloride	NaCl	58.4000	0.4	32.7040
Sodium sulfate	Na ₂ SO ₄	142.0000	0.2	39.7600
Ammonium Nitrate	NH ₄ NO ₃	80.0520	0	0.0000
Sodium carbonate	Na ₂ CO ₃	106.0000	0.100	14.8400
Sodium bicarbonate	NaHCO ₃	84.0100	0.000	0.0000

Cyclic Potentiodynamic Polarization



Images of bullet samples after electrochemical tests

Test 5



Test 5D



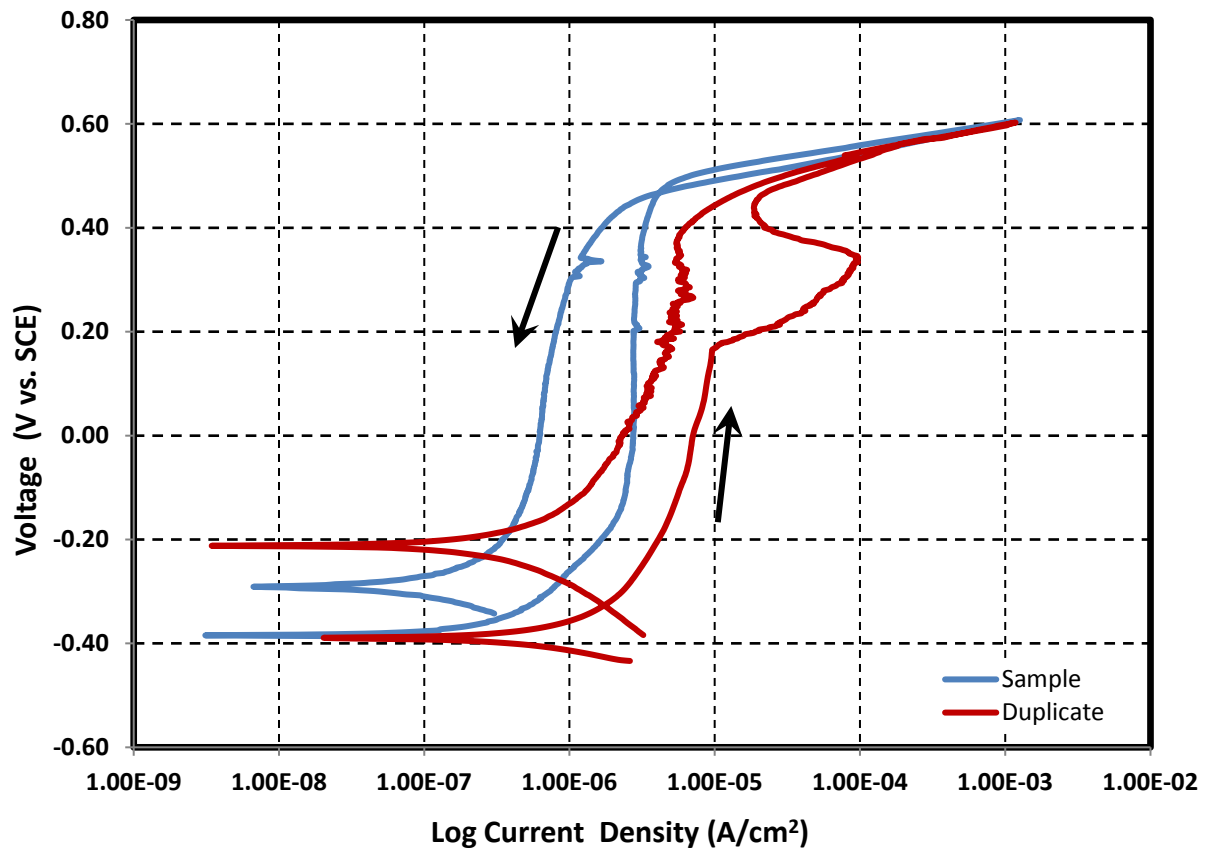
Composition of simulant for New Limits-Test 6

Test 6-NL-NH3

Temperature 35 °C
 pH at room temperature 13.45 Target >12
 pH before testing (at temp.) 13.53 pH after testing (at room temp.) 13.40
 Volume 1.4 L

Simulant Source	Formula	Molecular Weight (g/mol)	Concentration (M)	weight required (g)
Sodium hydroxide	NaOH	40.0000	0.73	40.8800
Sodium nitrite	NaNO ₂	69.0000	0.6	57.9600
Sodium nitrate	NaNO ₃	85.0000	2.625	312.3750
Sodium chloride	NaCl	58.4000	0.2	16.3632
Sodium sulfate	Na ₂ SO ₄	142.0000	0.1	19.8800
Ammonium Nitrate	NH ₄ NO ₃	80.0520	0.125	14.0091
Sodium carbonate	Na ₂ CO ₃	106.0000	0.100	14.8400
Sodium bicarbonate	NaHCO ₃	84.0100	0.000	0.0000

Cyclic Potentiodynamic Polarization



Images of bullet samples after electrochemical tests

Test 6



Test 6D



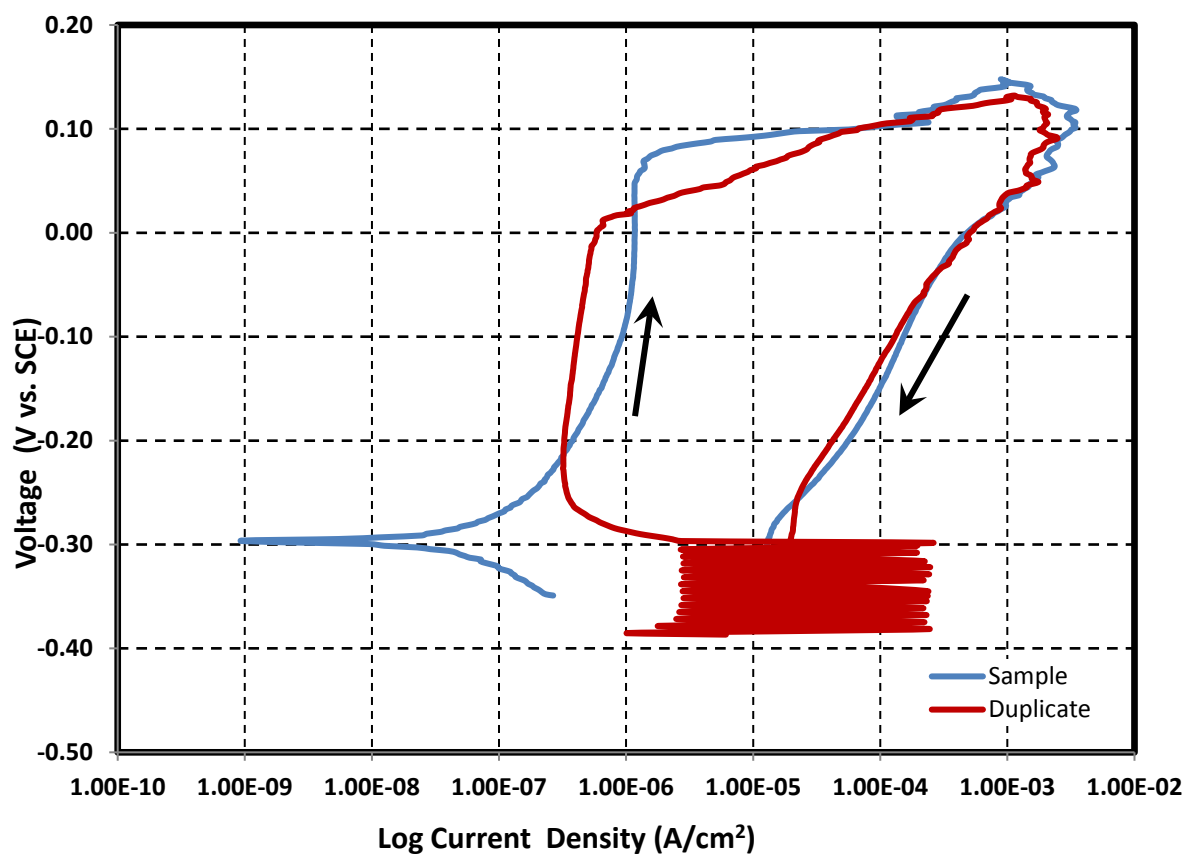
Composition of simulant for New Limits-Test 7

Test 7-NL-NH3

Temperature 35 °C
 pH at room temperature 12.04 Target >12
 pH before testing (at temp.) 12.09 pH after testing (at room temp.) 12.04
 Volume 1.4 L

Simulant Source	Formula	Molecular Weight (g/mol)	Concentration (M)	weight required (g)
Sodium hydroxide	NaOH	40.0000	0.01	0.5600
Sodium nitrite	NaNO ₂	69.0000	1.2	115.9200
Sodium nitrate	NaNO ₃	85.0000	5.5	654.5000
Sodium chloride	NaCl	58.4000	0.4	32.7040
Sodium sulfate	Na ₂ SO ₄	142.0000	0.2	39.7600
Ammonium Nitrate	NH ₄ NO ₃	80.0520	0	0.0000
Sodium carbonate	Na ₂ CO ₃	106.0000	0.100	14.8400
Sodium bicarbonate	NaHCO ₃	84.0100	0.000	0.0000

Cyclic Potentiodynamic Polarization



Images of bullet samples after electrochemical tests

Test 7



Test 7D



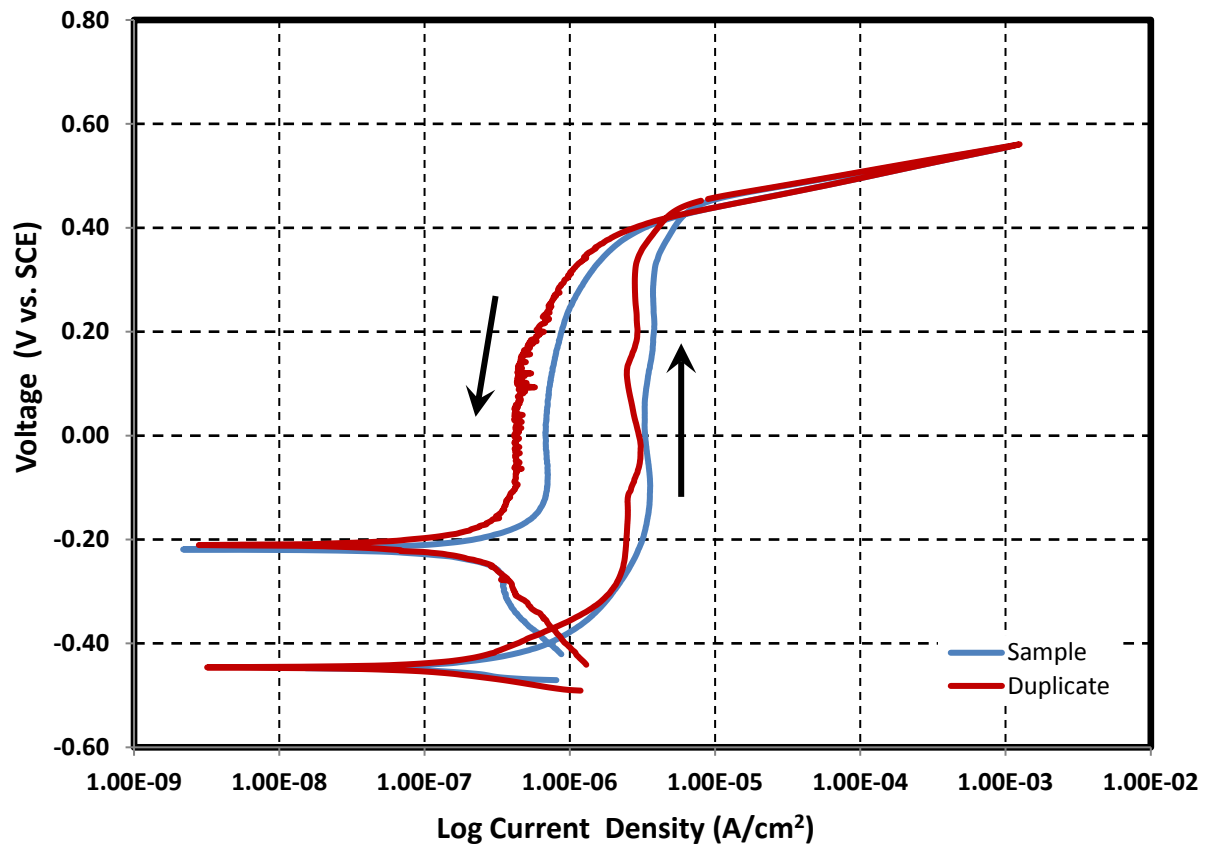
Composition of simulant for New Limits-Test 8

Test 8-NL-NH3

Temperature 35 °C
 pH at room temperature 13.88 Target >12
 pH before testing (at temp.) 13.93 pH after testing (at room temp.) 13.81
 Volume 1.4 L

Simulant Source	Formula	Molecular Weight (g/mol)	Concentration (M)	weight required (g)
Sodium hydroxide	NaOH	40.0000	1.45	81.2000
Sodium nitrite	NaNO ₂	69.0000	1.2	115.9200
Sodium nitrate	NaNO ₃	85.0000	5.25	624.7500
Sodium chloride	NaCl	58.4000	0.4	32.7264
Sodium sulfate	Na ₂ SO ₄	142.0000	0.2	39.7600
Ammonium Nitrate	NH ₄ NO ₃	80.0520	0.25	28.0182
Sodium carbonate	Na ₂ CO ₃	106.0000	0.100	14.8400
Sodium bicarbonate	NaHCO ₃	84.0100	0.000	0.0000

Cyclic Potentiodynamic Polarization



Images of bullet samples after electrochemical tests

Test 8



Test 8D



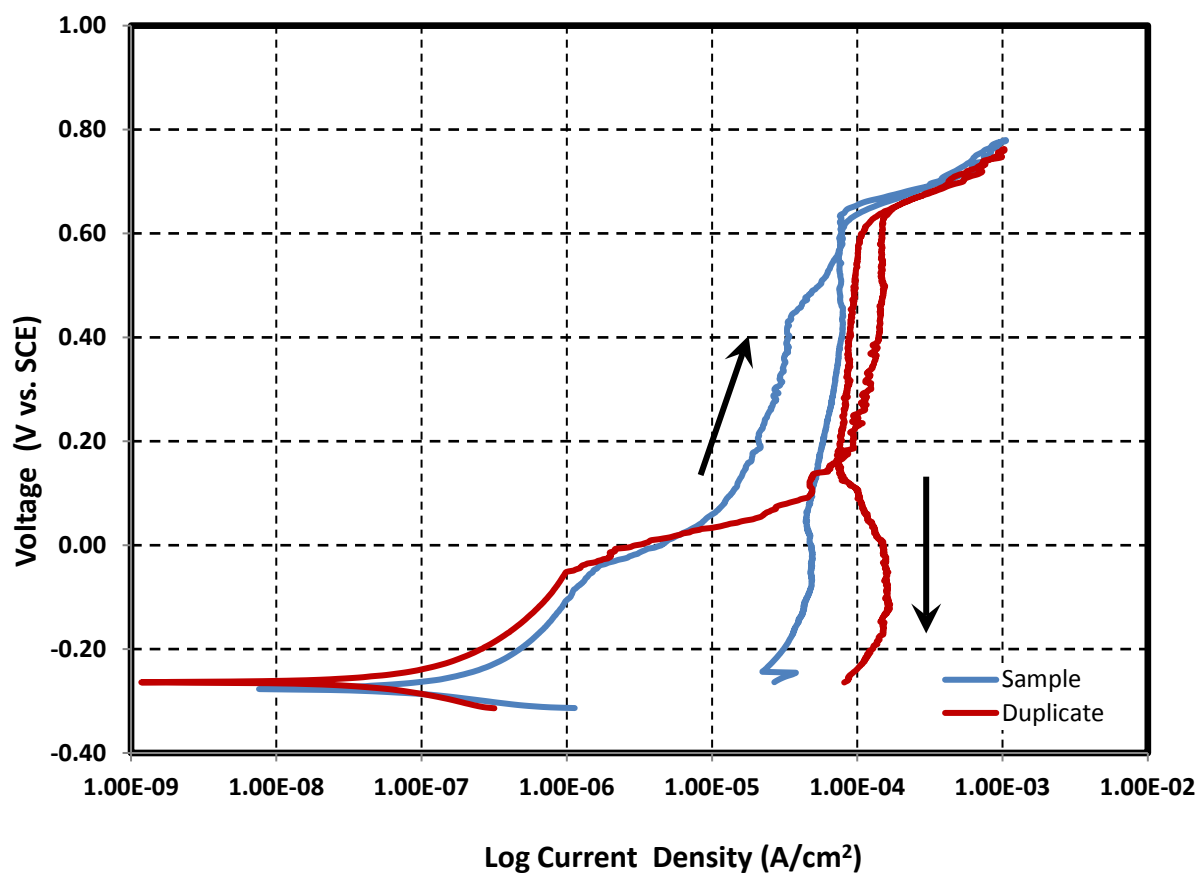
Composition of simulant for New Limits-Test 9

Test 9-NL-NH3

Temperature 35 °C
 pH at room temperature 12.10 Target >12
 pH before testing (at temp.) 12.24 pH after testing (at room temp.) 12.11
 Volume 1.4 L

Simulant Source	Formula	Molecular Weight (g/mol)	Concentration (M)	weight required (g)
Sodium hydroxide	NaOH	40.0000	0.01	0.5600
Sodium nitrite	NaNO ₂	69.0000	0	0.0000
Sodium nitrate	NaNO ₃	85.0000	5.5	654.5000
Sodium chloride	NaCl	58.4000	0	0.0000
Sodium sulfate	Na ₂ SO ₄	142.0000	0.2	39.7600
Ammonium Nitrate	NH ₄ NO ₃	80.0520	0.25	28.0182
Sodium carbonate	Na ₂ CO ₃	106.0000	0.100	14.8400
Sodium bicarbonate	NaHCO ₃	84.0100	0.000	0.0000

Cyclic Potentiodynamic Polarization



Images of bullet samples after electrochemical tests

Test 9



Test 9D



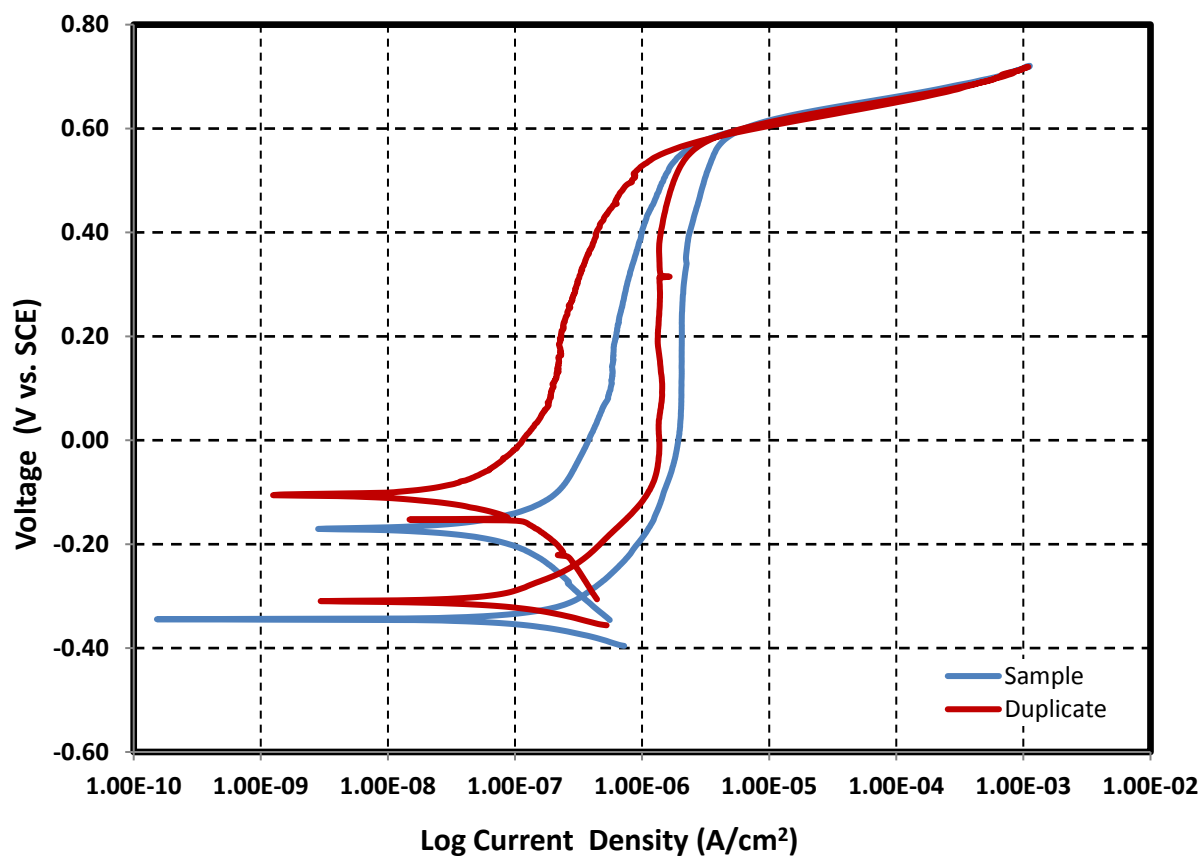
Composition of simulant for New Limits-Test 10

Test 10-NL-NH3

Temperature 35 °C
 pH at room temperature 12.14 Target >12
 pH before testing (at temp.) 12.18 pH after testing (at room temp.) 11.96
 Volume 1.4 L

Simulant Source	Formula	Molecular Weight (g/mol)	Concentration (M)	weight required (g)
Sodium hydroxide	NaOH	40.0000	0.01	0.5600
Sodium nitrite	NaNO ₂	69.0000	1.2	115.9200
Sodium nitrate	NaNO ₃	85.0000	0	0.0000
Sodium chloride	NaCl	58.4000	0	0.0000
Sodium sulfate	Na ₂ SO ₄	142.0000	0.2	39.7600
Ammonium Nitrate	NH ₄ NO ₃	80.0520	0	0.0000
Sodium carbonate	Na ₂ CO ₃	106.0000	0.100	14.8400
Sodium bicarbonate	NaHCO ₃	84.0100	0.000	0.0000

Cyclic Potentiodynamic Polarization



Images of bullet samples after electrochemical tests



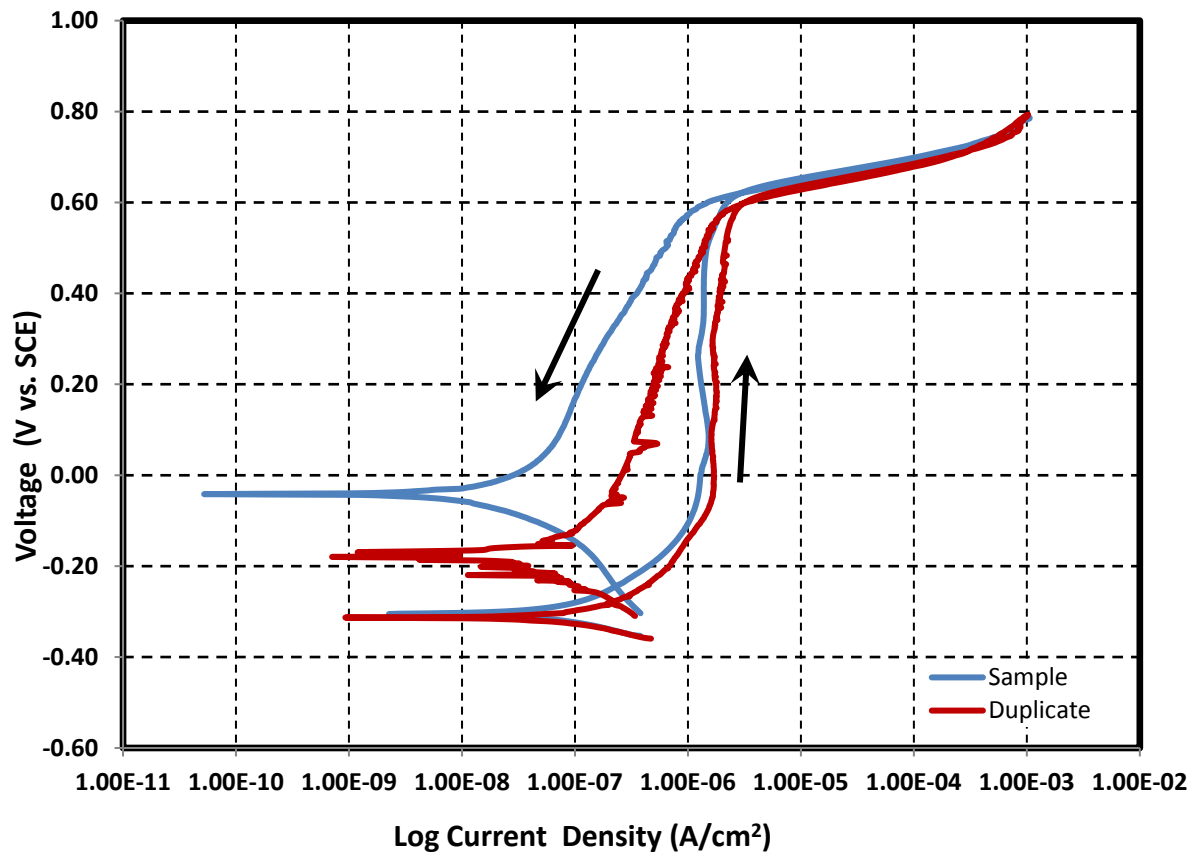
Composition of simulant for New Limits-Test 11

Test 11-NL-NH3

Temperature 35 °C
 pH at room temperature 12.21 Target >12
 pH before testing (at temp.) 12.18 pH after testing (at room temp.) 12.15
 Volume 1.4 L

Simulant Source	Formula	Molecular Weight (g/mol)	Concentration (M)	weight required (g)
Sodium hydroxide	NaOH	40.0000	0.01	0.5600
Sodium nitrite	NaNO ₂	69.0000	0	0.0000
Sodium nitrate	NaNO ₃	85.0000	0	0.0000
Sodium chloride	NaCl	58.4000	0	0.0000
Sodium sulfate	Na ₂ SO ₄	142.0000	0.2	39.7600
Ammonium Nitrate	NH ₄ NO ₃	80.0520	0.25	28.0182
Sodium carbonate	Na ₂ CO ₃	106.0000	0.100	14.8400
Sodium bicarbonate	NaHCO ₃	84.0100	0.000	0.0000

Cyclic Potentiodynamic Polarization



Images of bullet samples after electrochemical tests

Test 11



Test 11D



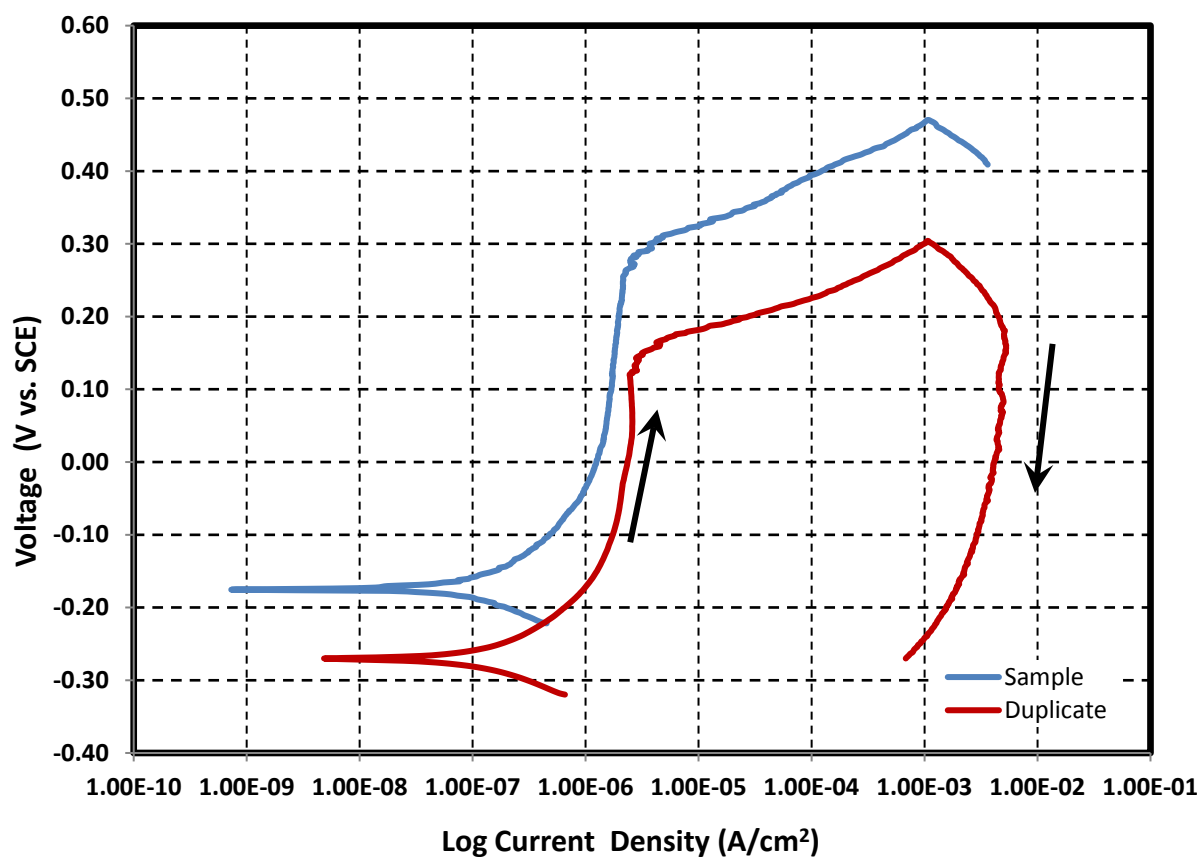
Composition of simulant for New Limits-Test 12

Test 12-NL-NH3

Temperature 35 °C
 pH at room temperature 13.22 Target >12
 pH before testing (at temp.) 13.15 pH after testing (at room temp.) 13.27
 Volume 1.4 L

Simulant Source	Formula	Molecular Weight (g/mol)	Concentration (M)	weight required (g)
Sodium hydroxide	NaOH	40.0000	0.3	16.8004
Sodium nitrite	NaNO ₂	69.0000	0.6	57.9600
Sodium nitrate	NaNO ₃	85.0000	2.75	327.2500
Sodium chloride	NaCl	58.4000	0.2	16.3520
Sodium sulfate	Na ₂ SO ₄	142.0000	0.1	19.8800
Ammonium Nitrate	NH ₄ NO ₃	80.0520	0	0.0000
Sodium carbonate	Na ₂ CO ₃	106.0000	0.100	14.8400
Sodium bicarbonate	NaHCO ₃	84.0100	0.000	0.0000

Cyclic Potentiodynamic Polarization



Images of bullet samples after electrochemical tests

Test 12



Test 12D



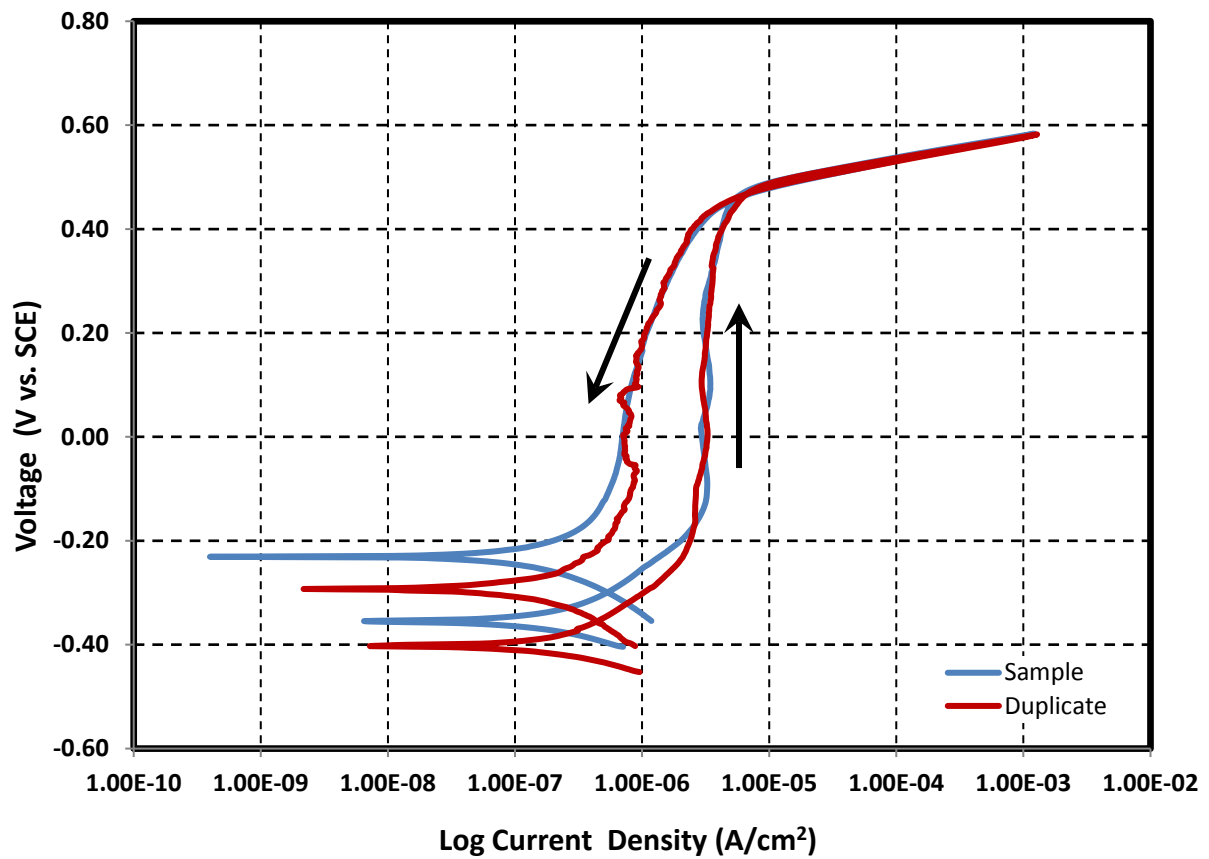
Composition of simulant for New Limits-Test 13

Test 13-NL-NH3

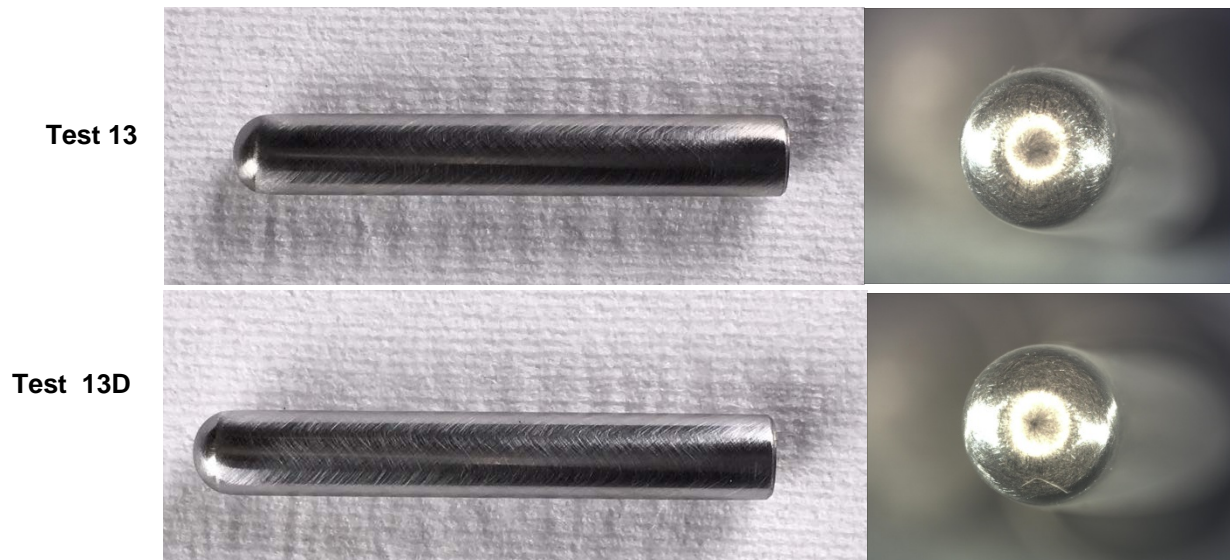
Temperature 35 °C
 pH at room temperature 13.62 Target >12
 pH before testing (at temp.) 13.55 pH after testing (at room temp.) 13.53
 Volume 1.4 L

Simulant Source	Formula	Molecular Weight (g/mol)	Concentration (M)	weight required (g)
Sodium hydroxide	NaOH	40.0000	1.2	67.2000
Sodium nitrite	NaNO ₂	69.0000	1.2	115.9200
Sodium nitrate	NaNO ₃	85.0000	0	0.0000
Sodium chloride	NaCl	58.4000	0.4	32.7040
Sodium sulfate	Na ₂ SO ₄	142.0000	0	0.0000
Ammonium Nitrate	NH ₄ NO ₃	80.0520	0	0.0000
Sodium carbonate	Na ₂ CO ₃	106.0000	0.100	14.8400
Sodium bicarbonate	NaHCO ₃	84.0100	0.000	0.0000

Cyclic Potentiodynamic Polarization



Images of bullet samples after electrochemical tests



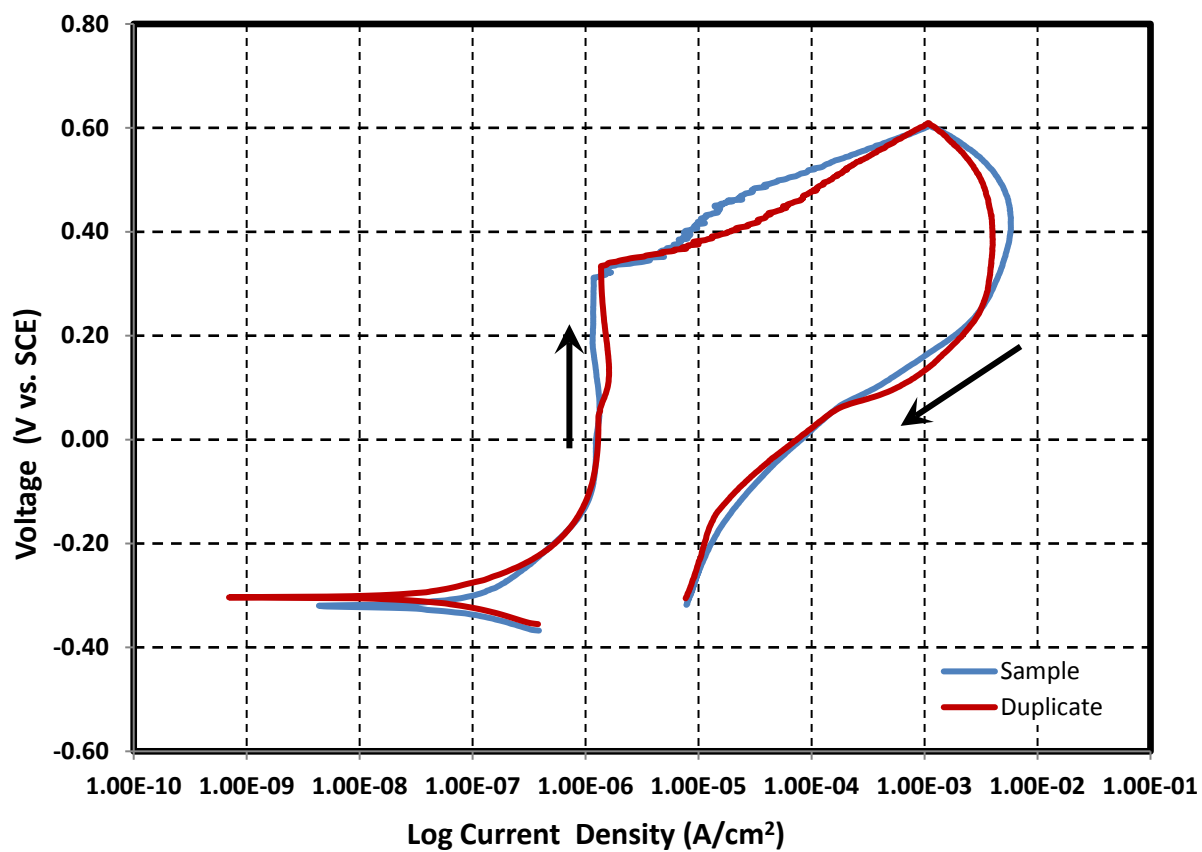
Composition of simulant for New Limits-Test 14

Test 14-NL-NH3

Temperature 35 °C
 pH at room temperature 9.34 Target >12
 pH before testing (at temp.) 12.16 pH after testing (at room temp.) 12.07
 Volume 1.4 L

Simulant Source	Formula	Molecular Weight (g/mol)	Concentration (M)	weight required (g)
Sodium hydroxide	NaOH	40.0000	0.01	0.5600
Sodium nitrite	NaNO ₂	69.0000	1.2	115.9200
Sodium nitrate	NaNO ₃	85.0000	0	0.0000
Sodium chloride	NaCl	58.4000	0.4	32.7040
Sodium sulfate	Na ₂ SO ₄	142.0000	0	0.000
Ammonium Nitrate	NH ₄ NO ₃	80.0520	0.25	28.0182
Sodium carbonate	Na ₂ CO ₃	106.0000	0.100	14.8400
Sodium bicarbonate	NaHCO ₃	84.0100	0.000	0.0000

Cyclic Potentiodynamic Polarization



Images of bullet samples after electrochemical tests



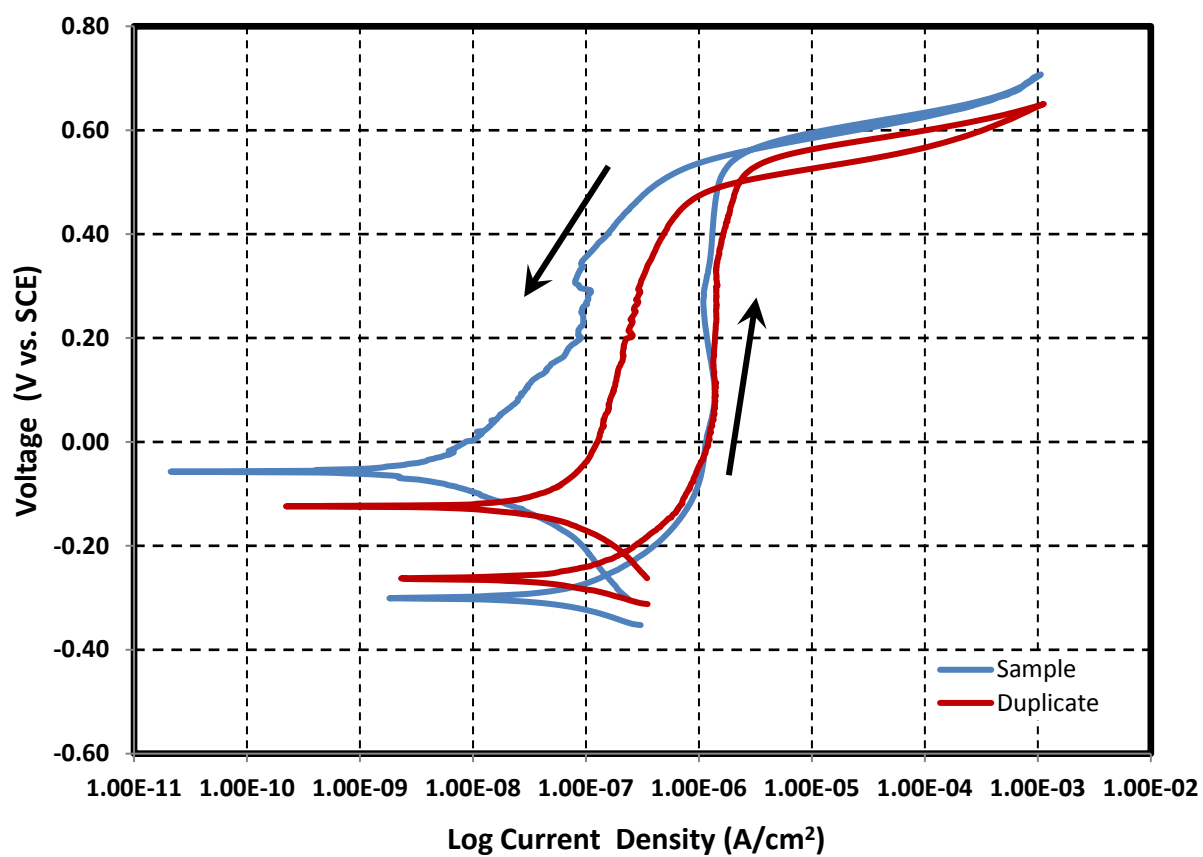
Composition of simulant for New Limits-Test 15

Test 15-NL-NH3

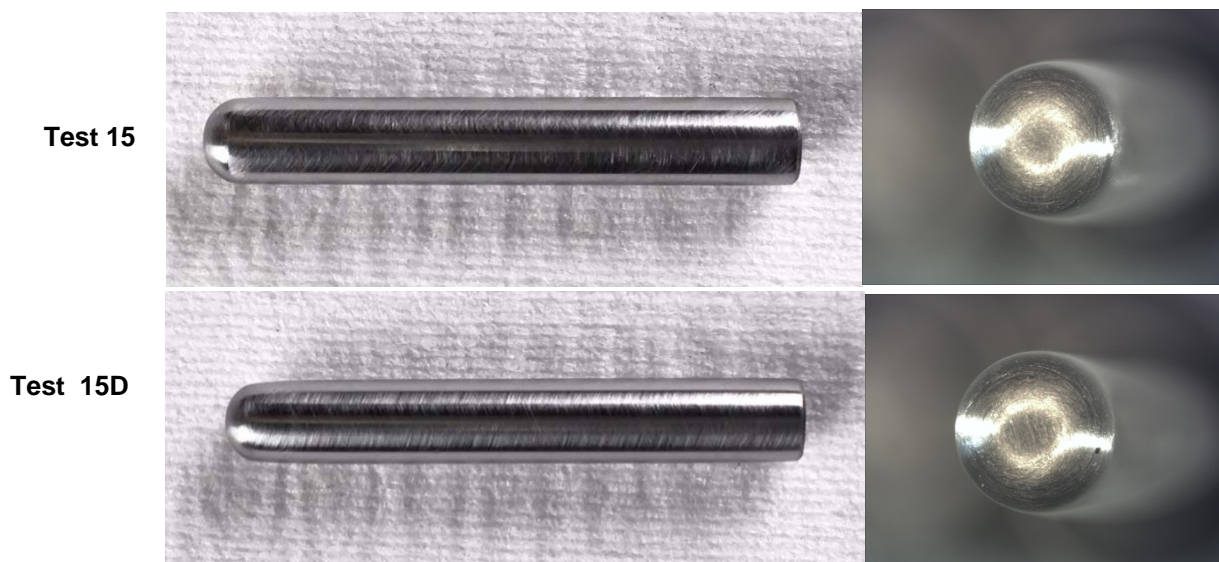
Temperature 35 °C
 pH at room temperature 12.03 Target >12
 pH before testing (at temp.) 12.05 pH after testing (at room temp.) 12.10
 Volume 1.4 L

Simulant Source	Formula	Molecular Weight (g/mol)	Concentration (M)	weight required (g)
Sodium hydroxide	NaOH	40.0000	0.26	14.5600
Sodium nitrite	NaNO ₂	69.0000	1.2	115.9200
Sodium nitrate	NaNO ₃	85.0000	5.25	624.7500
Sodium chloride	NaCl	58.4000	0	0.0000
Sodium sulfate	Na ₂ SO ₄	142.0000	0	0.0000
Ammonium Nitrate	NH ₄ NO ₃	80.0520	0.25	28.0182
Sodium carbonate	Na ₂ CO ₃	106.0000	0.100	14.8400
Sodium bicarbonate	NaHCO ₃	84.0100	0.000	0.0000

Cyclic Potentiodynamic Polarization



Images of bullet samples after electrochemical tests



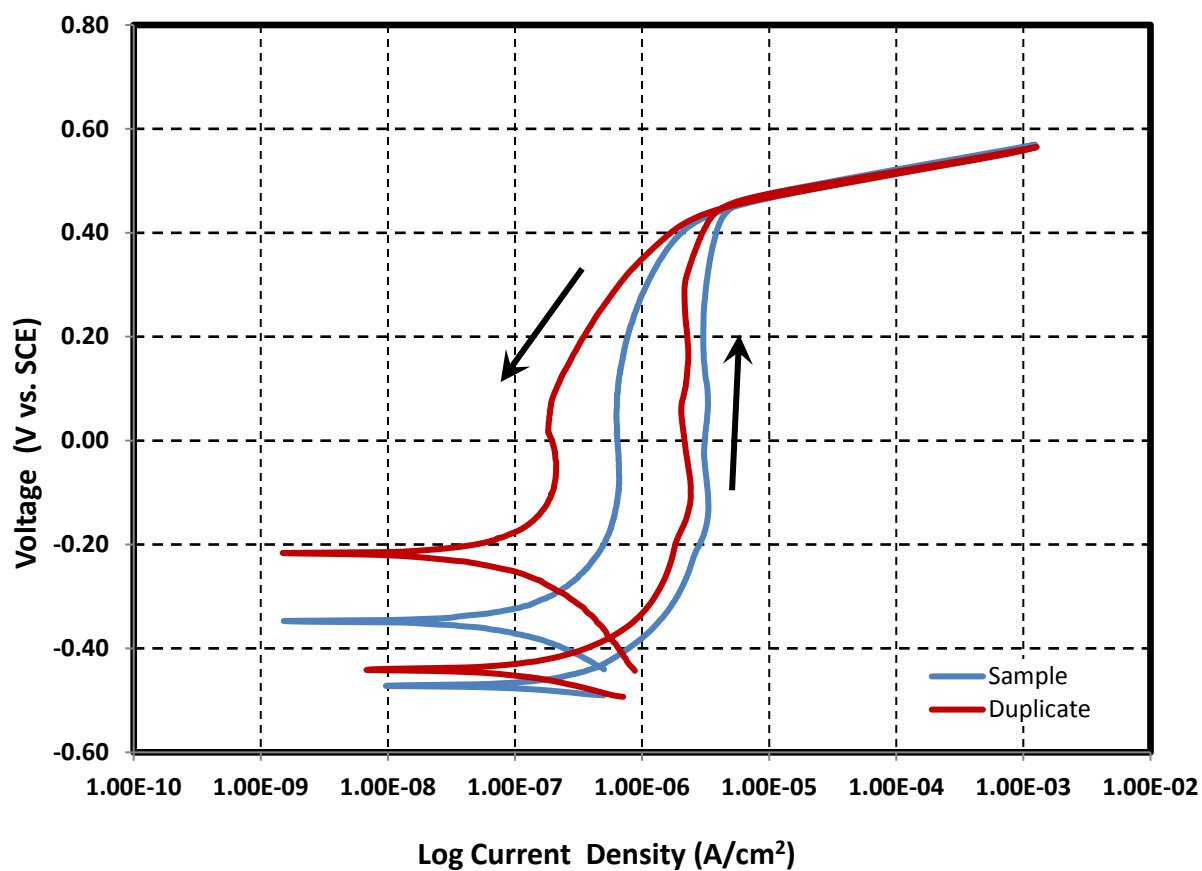
Composition of simulant for New Limits-Test 16

Test 16-NL-NH3

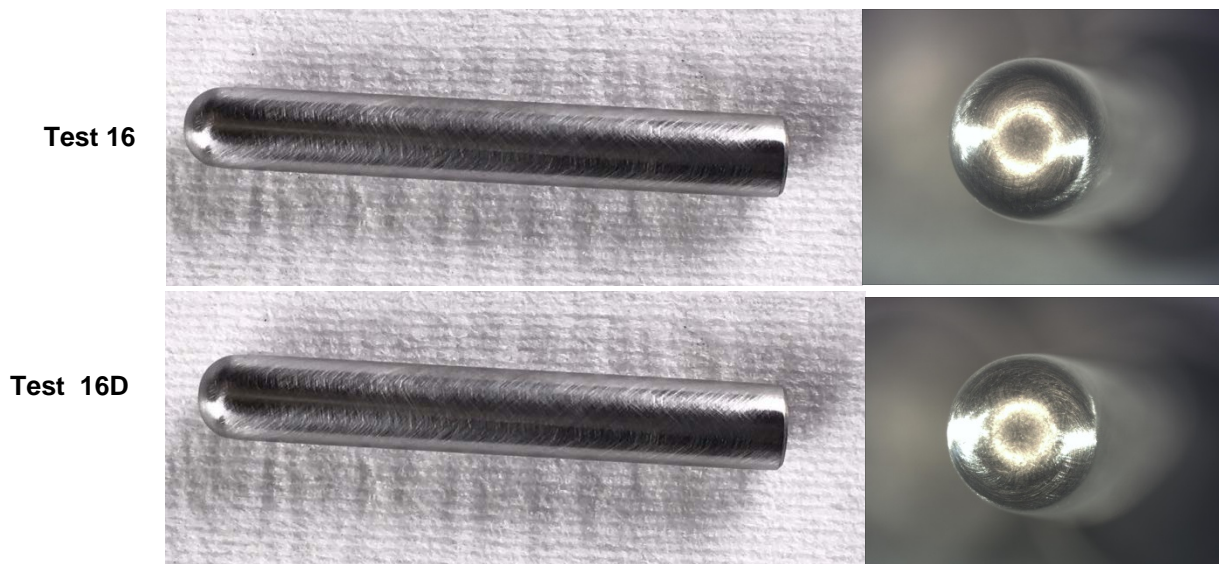
Temperature 35 °C
 pH at room temperature 13.52 Target >12
 pH before testing (at temp.) 13.56 pH after testing (at room temp.) 13.66
 Volume 1.4 L

Simulant Source	Formula	Molecular Weight (g/mol)	Concentration (M)	weight required (g)
Sodium hydroxide	NaOH	40.0000	1.2	67.2000
Sodium nitrite	NaNO ₂	69.0000	1.2	115.9200
Sodium nitrate	NaNO ₃	85.0000	5.5	654.5000
Sodium chloride	NaCl	58.4000	0	0.0000
Sodium sulfate	Na ₂ SO ₄	142.0000	0	0.0000
Ammonium Nitrate	NH ₄ NO ₃	80.0520	0	0.0000
Sodium carbonate	Na ₂ CO ₃	106.0000	0.100	14.8400
Sodium bicarbonate	NaHCO ₃	84.0100	0.000	0.0000

Cyclic Potentiodynamic Polarization



Images of bullet samples after electrochemical tests



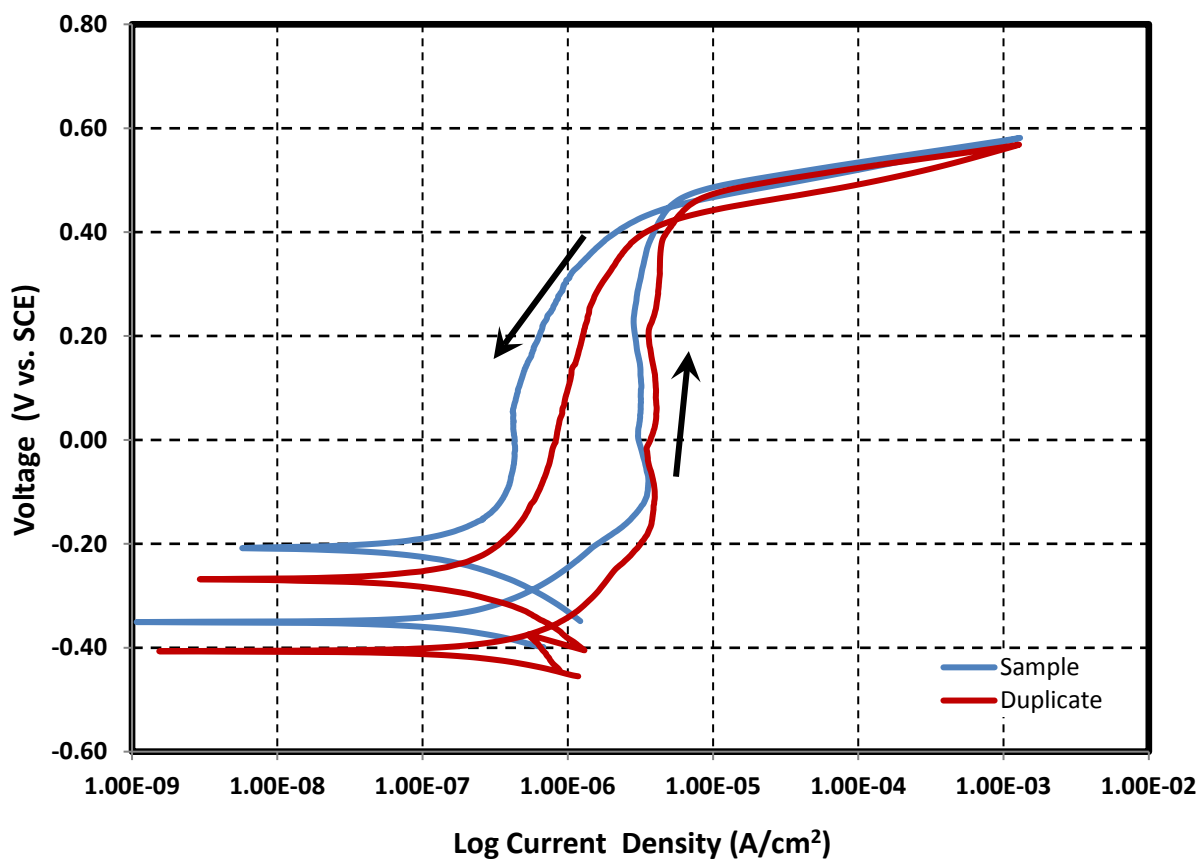
Composition of simulant for New Limits-Test 17

Test 17-NL-NH3

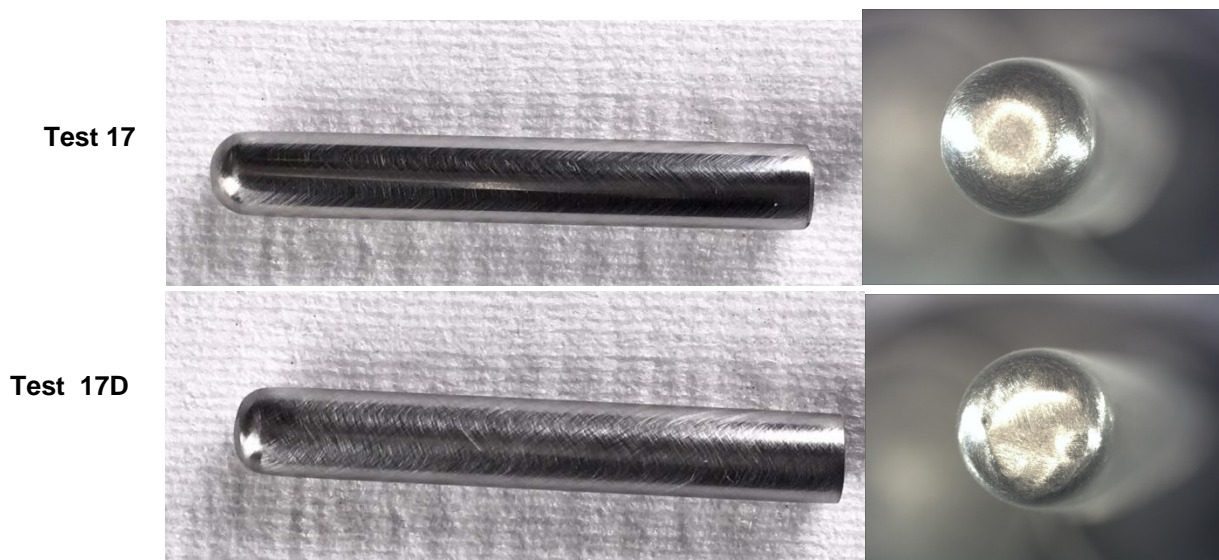
Temperature 35 °C
 pH at room temperature 13.56 Target >12
 pH before testing (at temp.) 13.61 pH after testing (at room temp.) 13.50
 Volume 1.4 L

Simulant Source	Formula	Molecular Weight (g/mol)	Concentration (M)	weight required (g)
Sodium hydroxide	NaOH	40.0000	1.45	81.2000
Sodium nitrite	NaNO ₂	69.0000	1.2	115.9200
Sodium nitrate	NaNO ₃	85.0000	0	0.0000
Sodium chloride	NaCl	58.4000	0	0.0000
Sodium sulfate	Na ₂ SO ₄	142.0000	0.2	39.7600
Ammonium Nitrate	NH ₄ NO ₃	80.0520	0.25	28.0182
Sodium carbonate	Na ₂ CO ₃	106.0000	0.100	14.8400
Sodium bicarbonate	NaHCO ₃	84.0100	0.000	0.0000

Cyclic Potentiodynamic Polarization



Images of bullet samples after electrochemical tests



Composition of simulant for New Limits-Test 18

Test 18-NL-NH3

Temperature 35 °C

pH at room

temperature

Target

>12

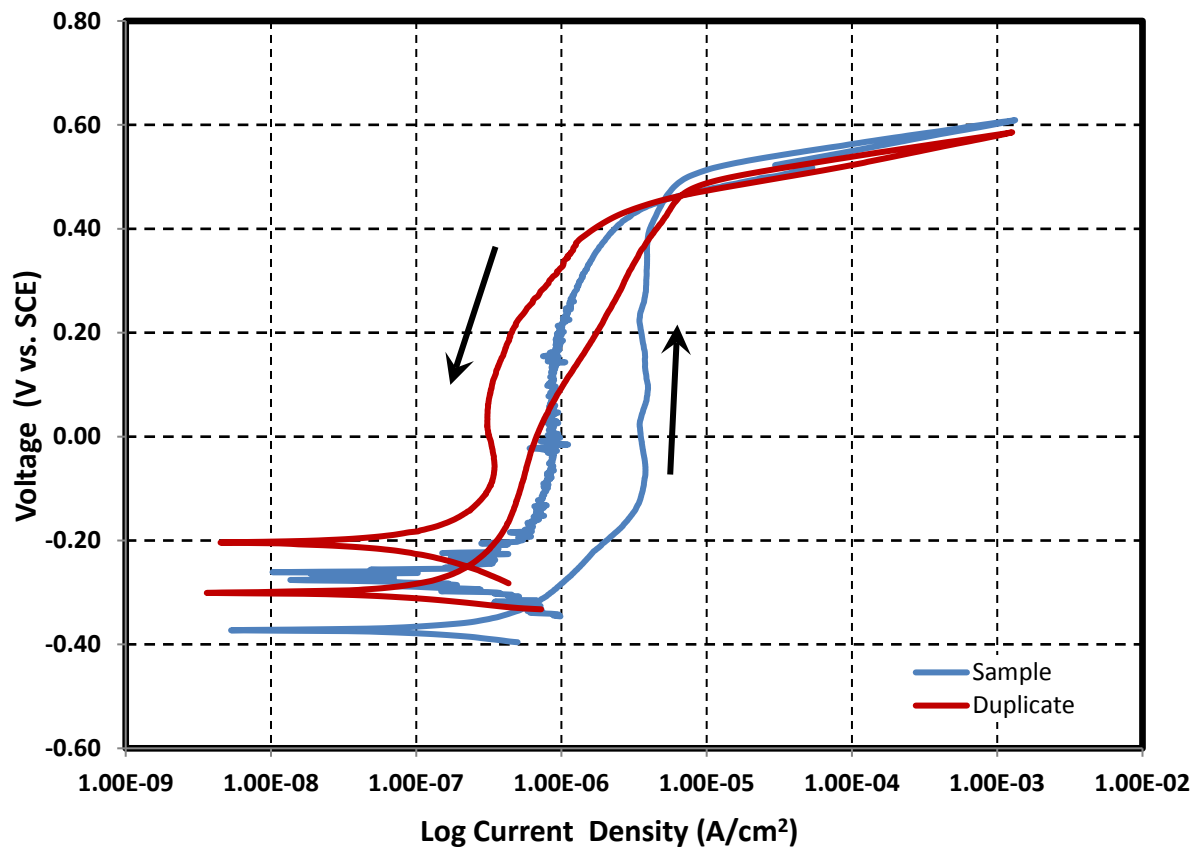
pH before testing (at
temp.)

pH after testing (at
room temp.)

Volume 1.4 L

Simulant Source	Formula	Molecular Weight (g/mol)	Concentration (M)	weight required (g)
Sodium hydroxide	NaOH	40.0000	0.26	14.5600
Sodium nitrite	NaNO ₂	69.0000	0	0.0000
Sodium nitrate	NaNO ₃	85.0000	0	0.0000
Sodium chloride	NaCl	58.4000	0.4	32.7040
Sodium sulfate	Na ₂ SO ₄	142.0000	0.2	39.7600
Ammonium Nitrate	NH ₄ NO ₃	80.0520	0.25	28.0182
Sodium carbonate	Na ₂ CO ₃	106.0000	0.100	14.8400
Sodium bicarbonate	NaHCO ₃	84.0100	0.000	0.0000

Cyclic Potentiodynamic Polarization



Images of bullet samples after electrochemical tests

Test 18



Test 18D



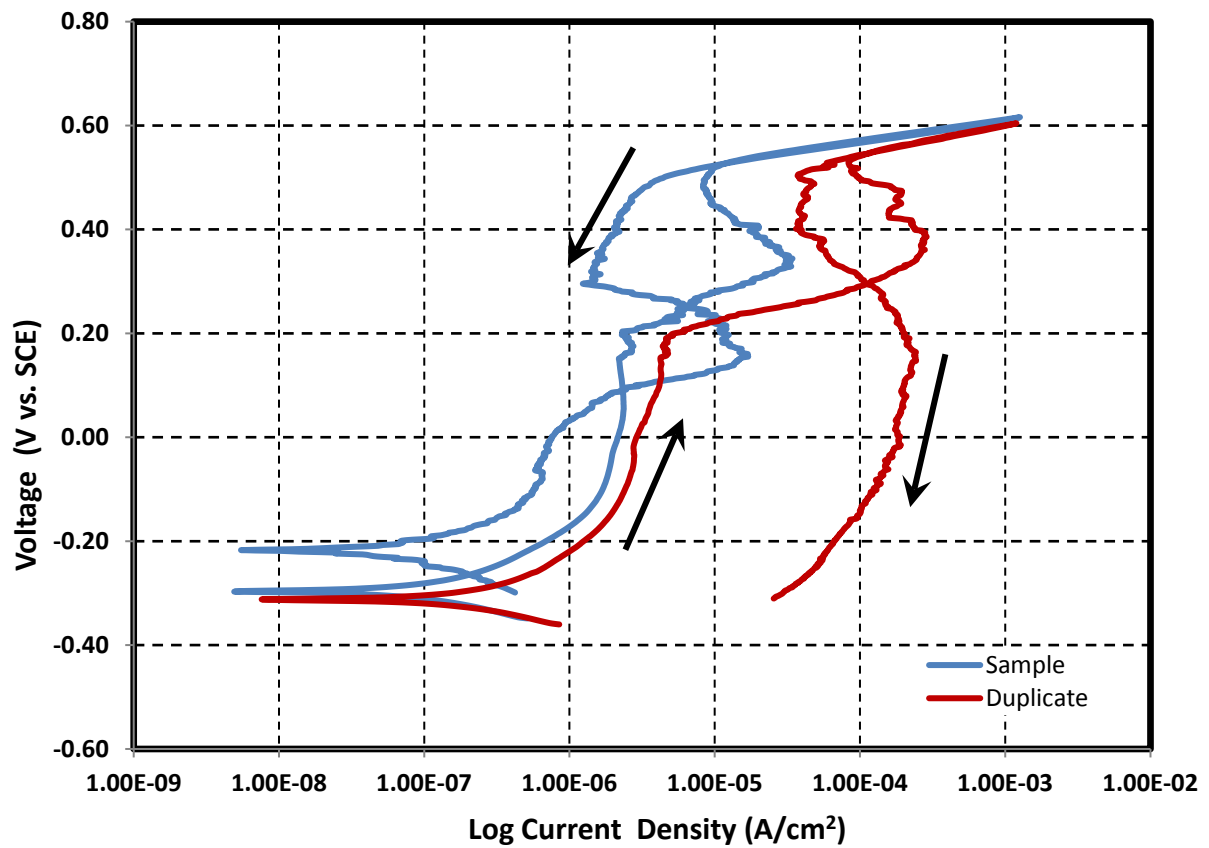
Composition of simulant for New Limits-Test 19

Test 19-NL-NH3

Temperature 35 °C
 pH at room temperature 13.37 Target >12
 pH before testing (at temp.) 13.43 pH after testing (at room temp.) 13.26
 Volume 1.4 L

Simulant Source	Formula	Molecular Weight (g/mol)	Concentration (M)	weight required (g)
Sodium hydroxide	NaOH	40.0000	0.3	16.8000
Sodium nitrite	NaNO ₂	69.0000	0.6	57.9600
Sodium nitrate	NaNO ₃	85.0000	2.75	327.2500
Sodium chloride	NaCl	58.4000	0.2	16.3520
Sodium sulfate	Na ₂ SO ₄	142.0000	0.1	19.8800
Ammonium Nitrate	NH ₄ NO ₃	80.0520	0	0.0000
Sodium carbonate	Na ₂ CO ₃	106.0000	0.1	14.8400
Sodium bicarbonate	NaHCO ₃	84.0100	0.0000	0.0000

Cyclic Potentiodynamic Polarization



Images of bullet samples after electrochemical tests

Test 19



Test 19D



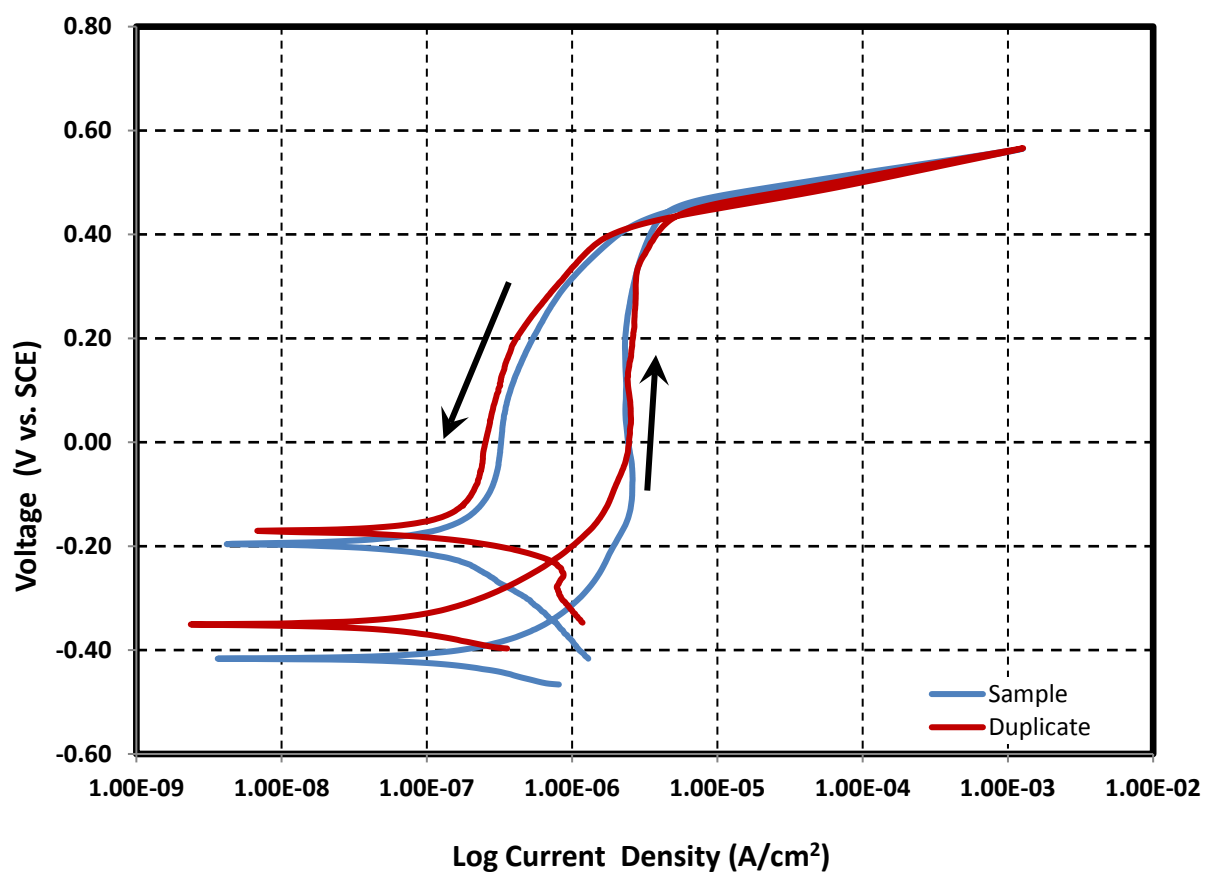
Composition of simulant for New Limits-Test 20

Test 1-NL-NH3

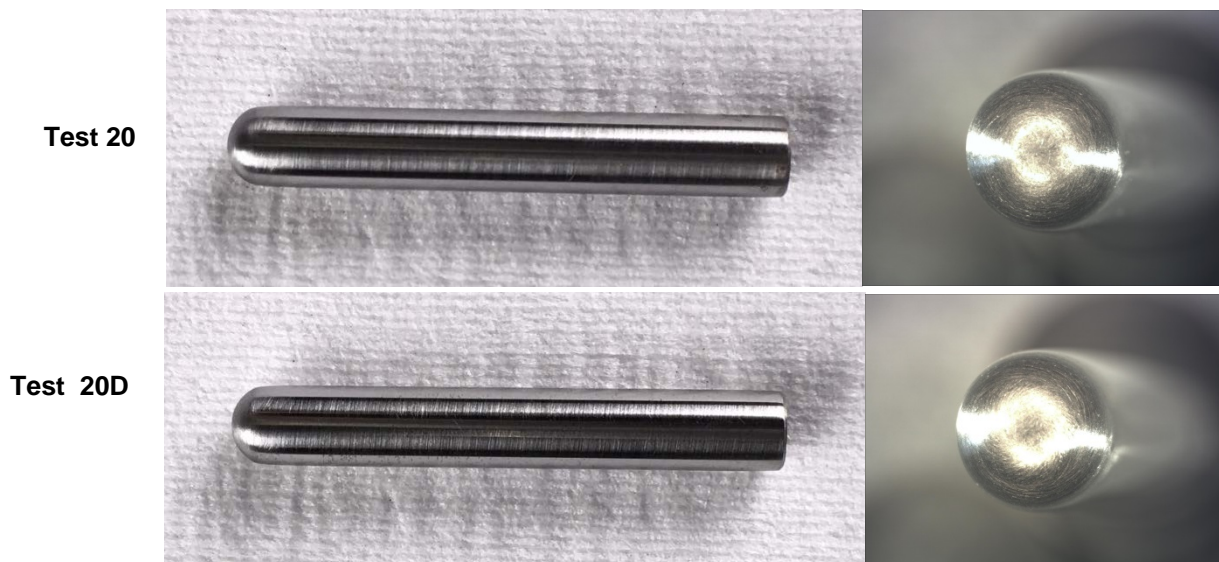
Temperature 35 °C
 pH at room temperature 14.10 Target >12
 pH before testing (at temp.) 14.17 pH after testing (at room temp.) 14.15
 Volume 1.4 L

Simulant Source	Formula	Molecular Weight (g/mol)	Concentration (M)	weight required (g)
Sodium hydroxide	NaOH	40.0000	1.2	67.2000
Sodium nitrite	NaNO ₂	69.0000	0	0.0000
Sodium nitrate	NaNO ₃	85.0000	5.5	654.5000
Sodium chloride	NaCl	58.4000	0	0.0000
Sodium sulfate	Na ₂ SO ₄	142.0000	0.2	39.7600
Ammonium Nitrate	NH ₄ NO ₃	80.0520	0	0.0000
Sodium carbonate	Na ₂ CO ₃	106.0000	0.100	14.8400
Sodium bicarbonate	NaHCO ₃	84.0100	0.000	0.0000

Cyclic Potentiodynamic Polarization



Images of bullet samples after electrochemical tests



Appendix D

Chemical Composition of New Limits Task of effects of an organic specie and nitrous oxide for AN-102 based simulant with Electrochemical Results and Pictures after Test

Table D1. Test conditions and results of testing for the addition of an organic species for AN-102 based simulant

Test	Temperature (°C)	Nitrate (M)	Nitrite (M)	Hydroxide (M)	Organic, Concentration (M)	measured pH	Category		Pitting on sample?	
							Run 1	Run2	Run 1	Run 2
1	40	1.1	0.5	0.01	Ammonia, 0.25	12.05	3	3	Yes	Yes
2	40	1.1	0.5	0.01	Iminodiacetic Acid, 0.25	12.31	3	3	Yes	Yes
3	40	1.1	0.5	0.01	N-Butylamine, 0.25	13.02	3	5	Yes	Yes
4	40	1.1	0.5	0.01	Dibutylphosphate, 0.25	12.16	3	3	Yes	Yes
5	40	1.1	0.5	0.01	Glycine. 0.25	12.48	1	3	No	No
6	40	1.1	0.5	0.01	Nitrous Oxide, sat.	12.34	5	5	Yes	Yes
7	40	1.1	1	0.05	Nitrous Oxide, sat.	12.97	1	1	Yes	Yes

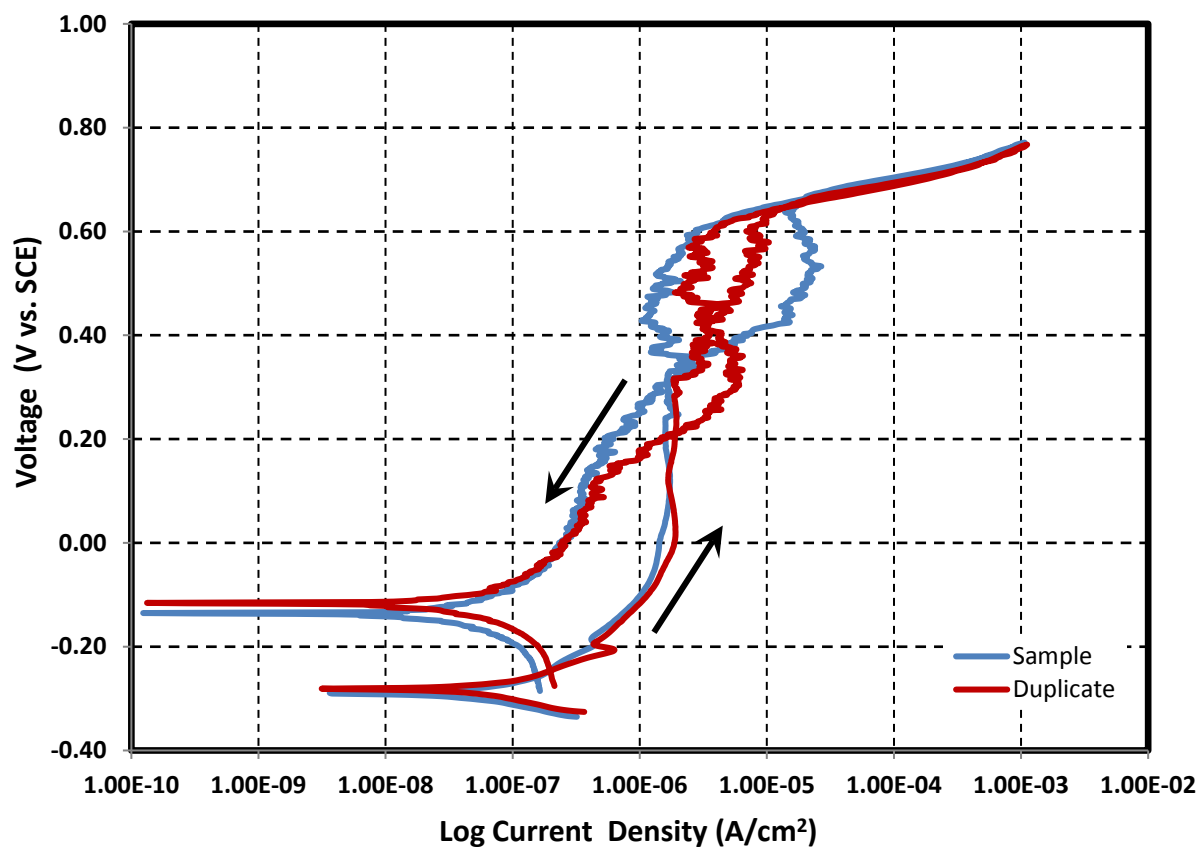
Composition of simulant for New Limits with organics inhibitors-Test 1

Test 1-NH3

Temperature 40 °C
 pH at room temperature 12.05 Target ~12
 pH before testing (at temp.) 11.87 pH after testing (at room temp.) 11.82
 Volume 1.4 L

Simulant Source	Formula	Molecular Weight (g/mol)	Concentration (M)	weight required (g)
Ammonium nitrate	NH ₄ NO ₃	80.0520	0.25	28.0182
Sodium chloride	NaCl	58.4000	0.106	8.6666
Sodium sulfate	Na ₂ SO ₄	142.0000	0.128	25.4464
Sodium hydroxide	NaOH	40.0000	0.01	0.5600
Sodium carbonate	Na ₂ CO ₃	106.0000	1.12	166.2080
Sodium nitrate	NaNO ₃	85.0000	0.85	101.1500
Sodium nitrite	NaNO ₂	69.0000	0.5	48.3000

Cyclic Potentiodynamic Polarization



Images of bullet samples after electrochemical tests



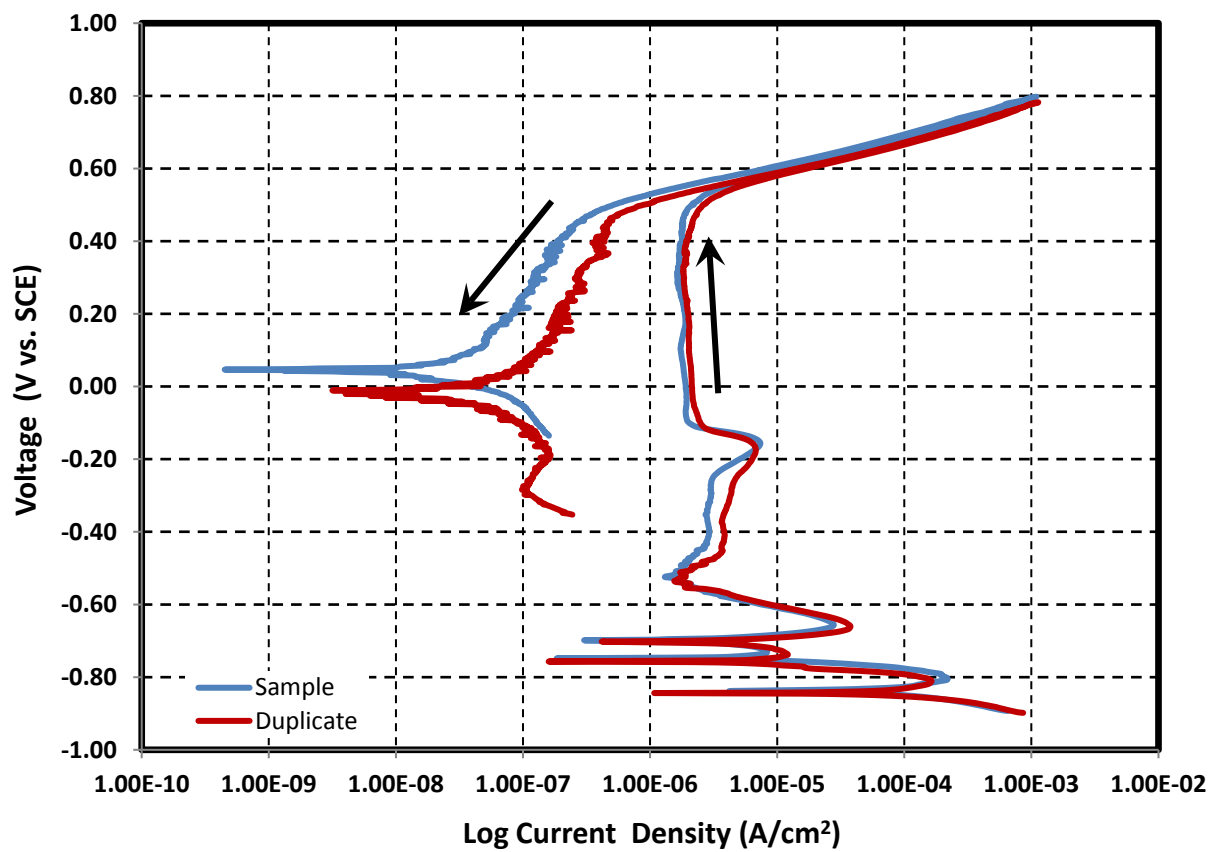
Composition of simulant for New Limits-Test 2

Test 2-IDA

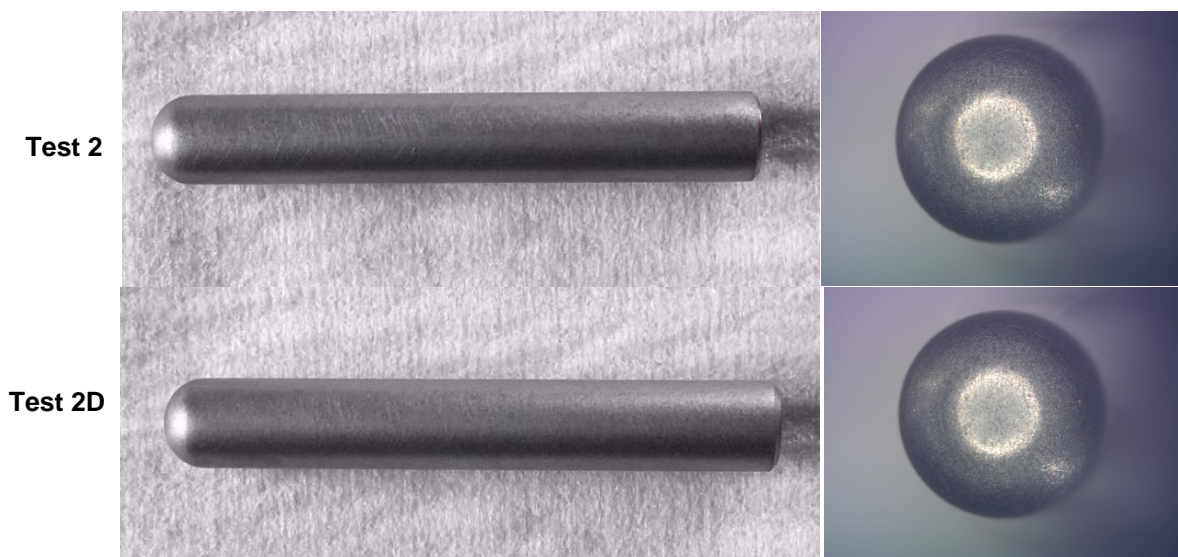
Temperature 40 °C
 pH at room temperature 10.63 Target >12
 pH before testing (at temp.) 12.04 pH after testing (at room temp.) 11.39
 Volume 1.4 L

Simulant Source	Formula	Molecular Weight (g/mol)	Concentration (M)	weight required (g)
Iminodiacetic Acid	C ₄ H ₇ NO ₄	133.0000	0.25	46.5504
Sodium chloride	NaCl	58.4000	0.106	8.6666
Sodium sulfate	Na ₂ SO ₄	142.0000	0.128	25.4464
Sodium hydroxide	NaOH	40.0000	0.26	14.5600
Sodium carbonate	Na ₂ CO ₃	106.0000	1.12	166.2080
Sodium nitrate	NaNO ₃	85.0000	1.1	130.9000
Sodium nitrite	NaNO ₂	69.0000	0.5	48.3000

Cyclic Potentiodynamic Polarization



Images of bullet samples after electrochemical tests



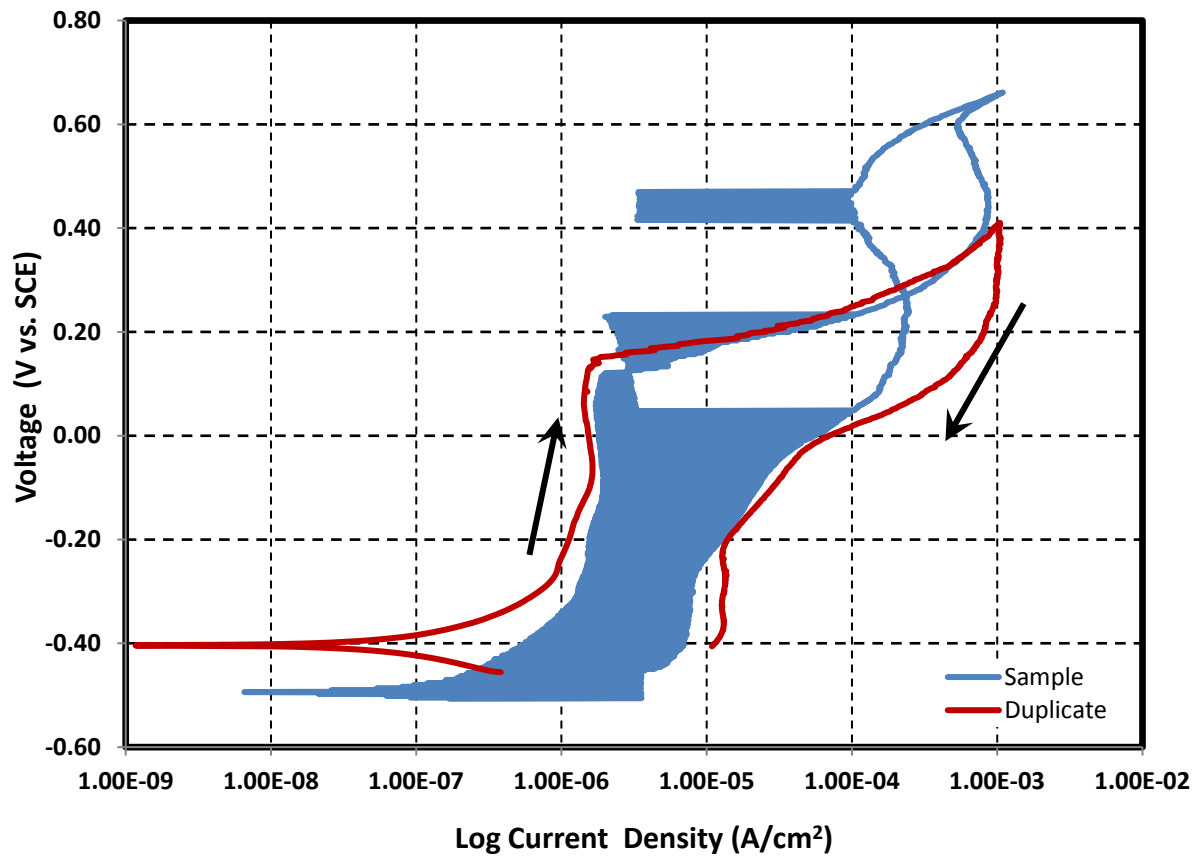
Composition of simulant for New Limits-Test 3

Test 3-N-BUT

Temperature 40 °C
 pH at room temperature 13.02 Target ~12
 pH before testing (at temp.) 12.85 pH after testing (at room temp.) 12.31
 Volume 1.4 L

Simulant Source	Formula	Molecular Weight (g/mol)	Concentration (M)	weight required (g)
N-butylamine	C ₄ H ₁₁ N	73.1500	0.25	25.6025
Sodium chloride	NaCl	58.4000	0.106	8.6666
Sodium sulfate	Na ₂ SO ₄	142.0000	0.128	25.4464
Sodium hydroxide	NaOH	40.0000	0.01	0.5600
Sodium carbonate	Na ₂ CO ₃	106.0000	1.12	166.2080
Sodium nitrate	NaNO ₃	85.0000	1.1	130.9000
Sodium nitrite	NaNO ₂	69.0000	0.5	48.3000

Cyclic Potentiodynamic Polarization



Images of bullet samples after electrochemical tests



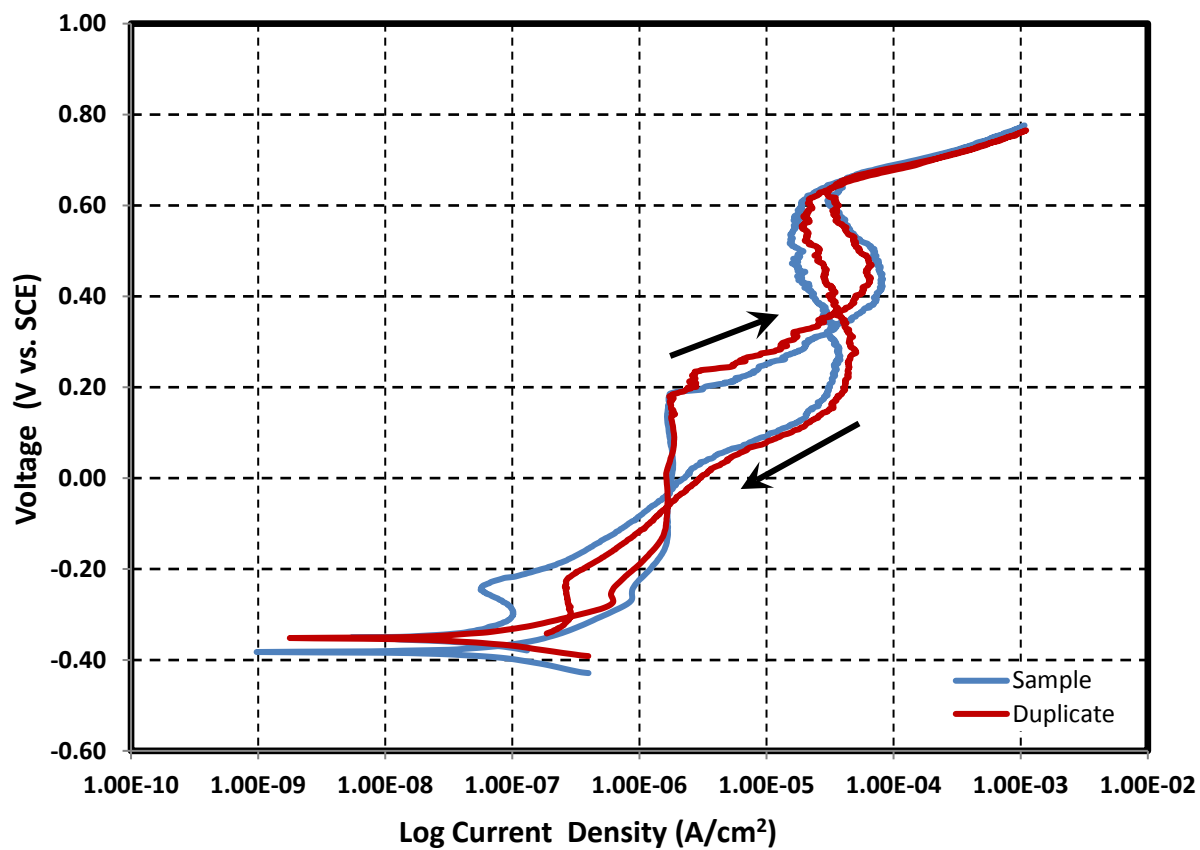
Composition of simulant for New Limits-Test 4

Test 4-DBP

Temperature 40 °C
 pH at room temperature 12.24 Target >12
 pH before testing (at temp.) 11.56 pH after testing (at room temp.) 11.96
 Volume 1.4 L

Simulant Source	Formula	Molecular Weight (g/mol)	Concentration (M)	weight required (g)
Dibutylphosphate	C ₈ H ₁₉ PO ₄	210.2100	0.25	73.5735
Sodium chloride	NaCl	58.4000	0.106	8.6666
Sodium sulfate	Na ₂ SO ₄	142.0000	0.128	25.4464
Sodium hydroxide	NaOH	40.0000	0.26	14.5600
Sodium carbonate	Na ₂ CO ₃	106.0000	1.12	166.2080
Sodium nitrate	NaNO ₃	85.0000	1.1	130.9000
Sodium nitrite	NaNO ₂	69.0000	0.5	48.3000

Cyclic Potentiodynamic Polarization



Images of bullet samples after electrochemical tests



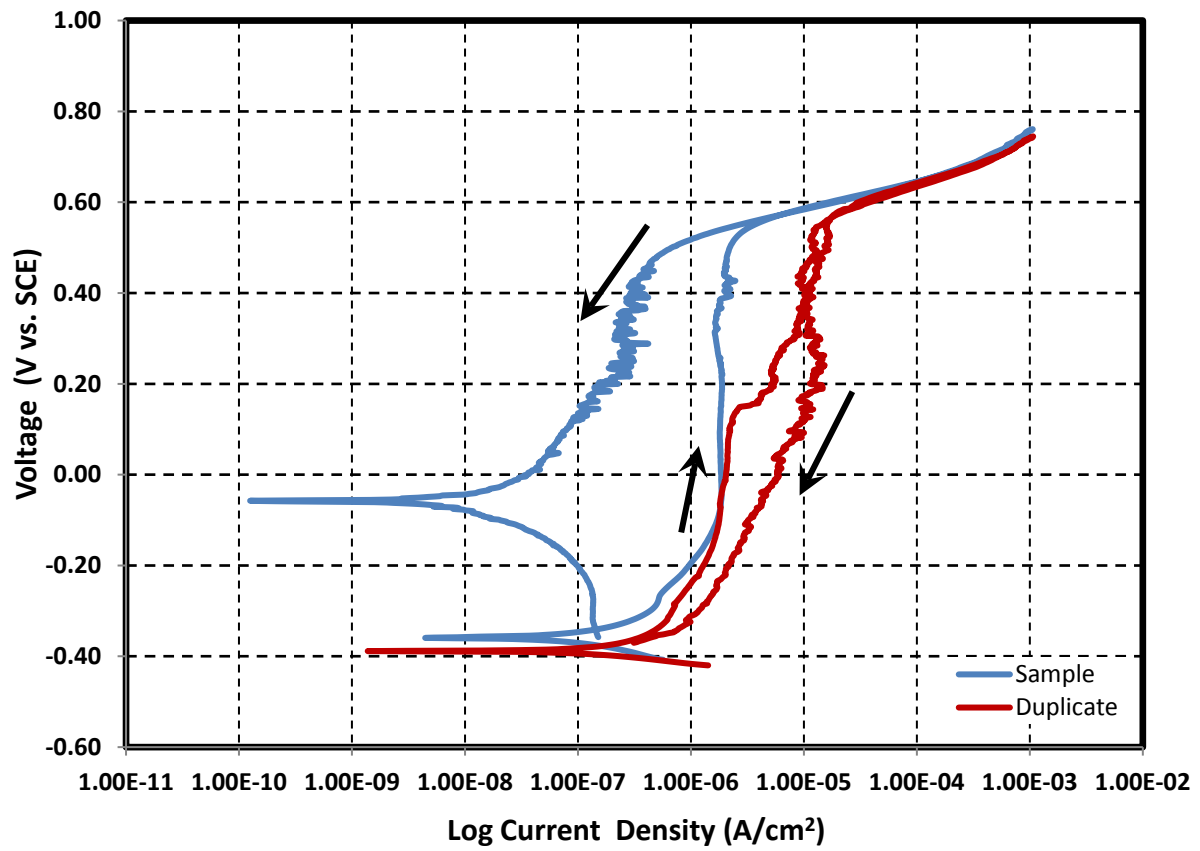
Composition of simulant for New Limits-Test 5

Test 5-G

Temperature 40 °C
 pH at room temperature 12.47 Target >12
 pH before testing (at temp.) 11.62 pH after testing (at room temp.) 12.18
 Volume 1.4 L

Simulant Source	Formula	Molecular Weight (g/mol)	Concentration (M)	weight required (g)
Glycine	NH ₅ C ₂ O ₂	75.0700	0.25	26.2745
Sodium chloride	NaCl	58.4000	0.106	8.6666
Sodium sulfate	Na ₂ SO ₄	142.0000	0.128	25.4464
Sodium hydroxide	NaOH	40.0000	0.26	14.5600
Sodium carbonate	Na ₂ CO ₃	106.0000	1.12	166.2080
Sodium nitrate	NaNO ₃	85.0000	1.1	130.9000
Sodium nitrite	NaNO ₂	69.0000	0.5	48.3000

Cyclic Potentiodynamic Polarization



Images of bullet samples after electrochemical tests



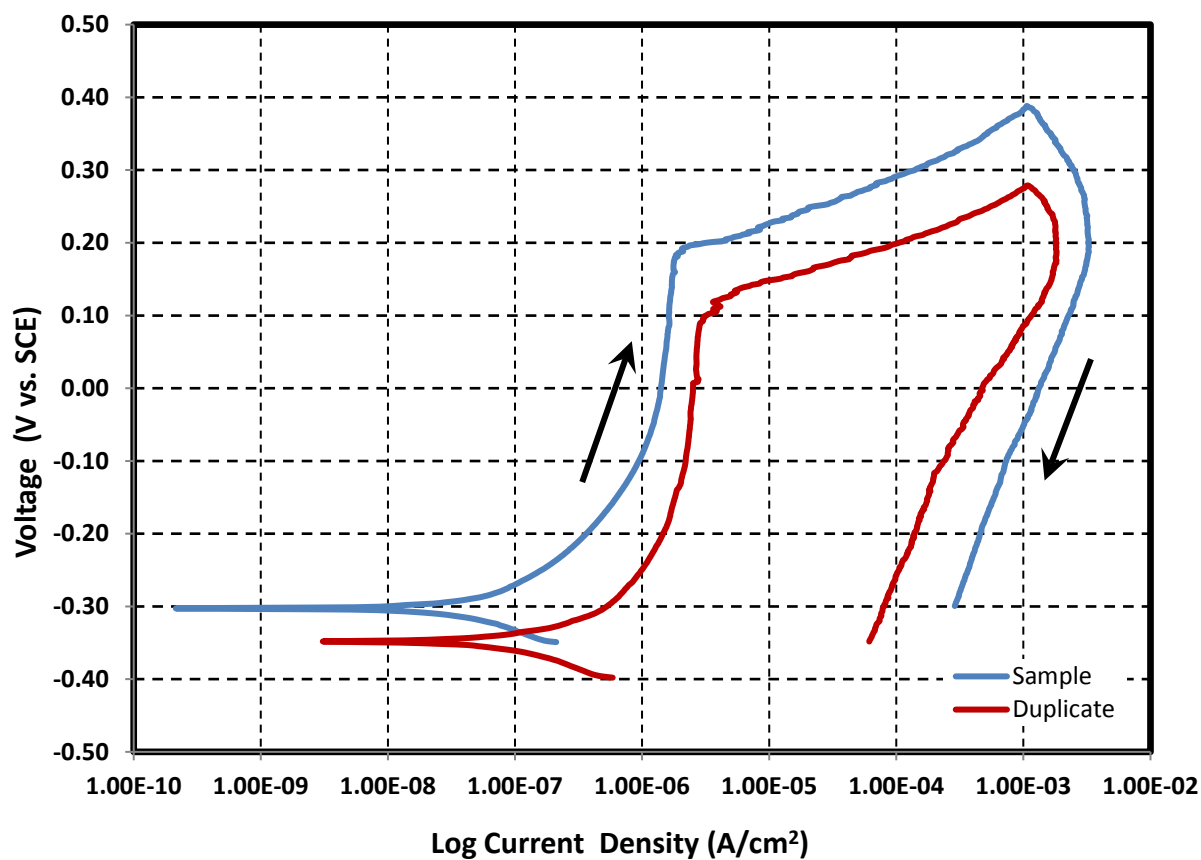
Composition of simulant for New Limits-Test 6

Test 6-NO-1

Temperature 40 °C
 pH at room temperature 12.34 Target >12
 pH before testing (at temp.) 11.55 pH after testing (at room temp.) 12.22
 Volume 1.4 L

Simulant Source	Formula	Molecular Weight (g/mol)	Concentration (M)	weight required (g)
Sodium chloride	NaCl	58.4000	0.106	8.6666
Sodium sulfate	Na ₂ SO ₄	142.0000	0.128	25.4464
Sodium hydroxide	NaOH	40.0000	0.01	0.5600
Sodium carbonate	Na ₂ CO ₃	106.0000	1.12	166.2080
Sodium nitrate	NaNO ₃	85.0000	1.1	130.9000
Sodium nitrite	NaNO ₂	69.0000	0.5	48.3000
Nitrous Oxide	N ₂ O	44.0130	Saturated (gas)	-

Cyclic Potentiodynamic Polarization



Images of bullet samples after electrochemical tests



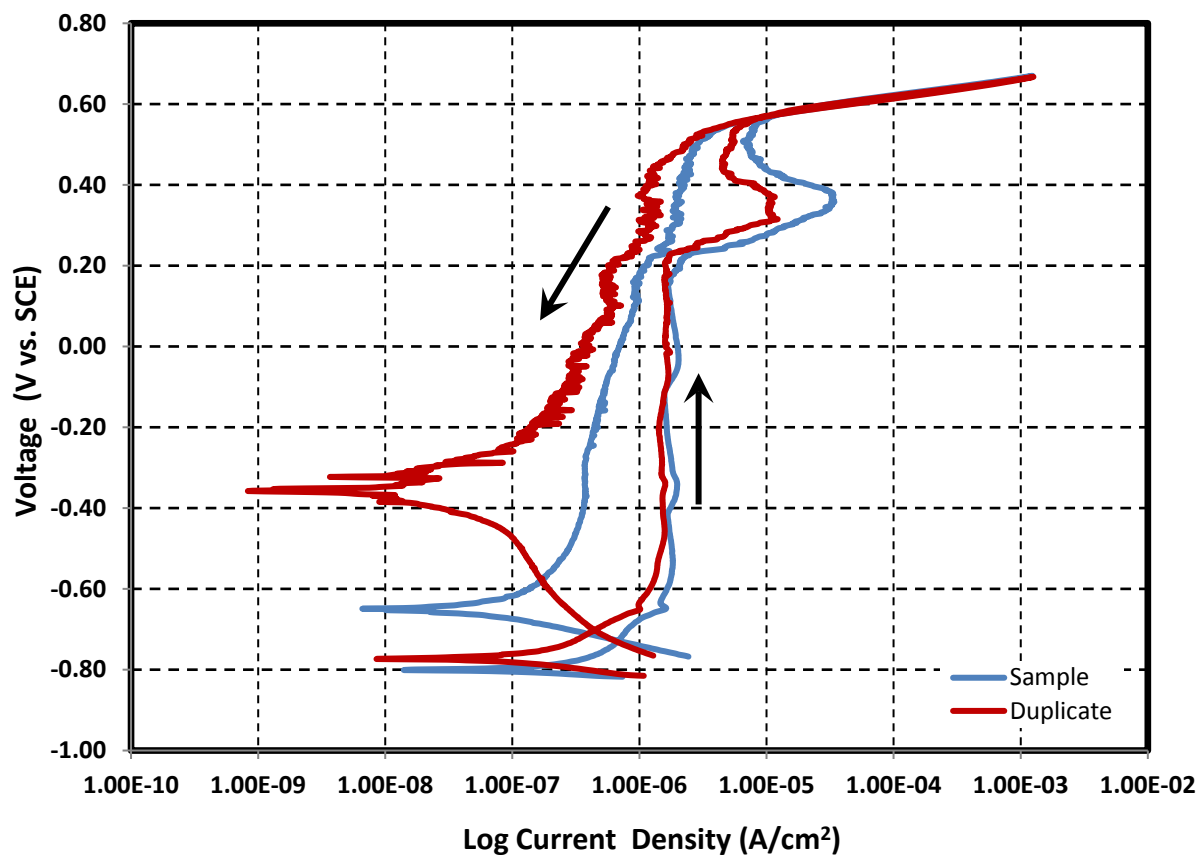
Composition of simulant for New Limits-Test 7

Test 7-NO-2

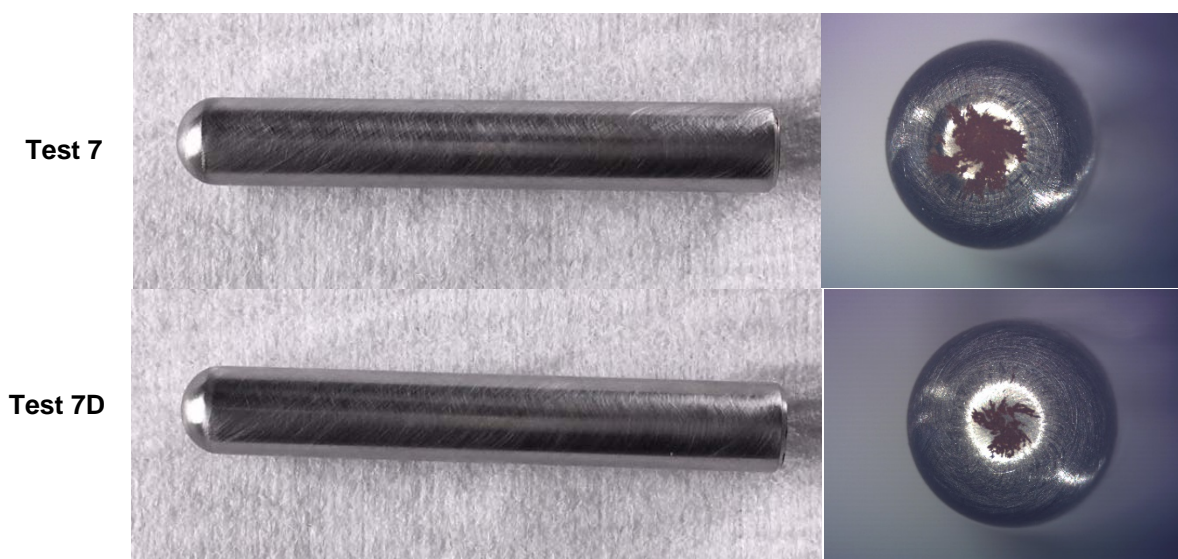
Temperature 40 °C
 pH at room temperature 12.97 Target >12
 pH before testing (at temp.) 12.38 pH after testing (at room temp.) 13.10
 Volume 1.4 L

Simulant Source	Formula	Molecular Weight (g/mol)	Concentration (M)	weight required (g)
Sodium chloride	NaCl	58.4000	0.106	8.6666
Sodium sulfate	Na ₂ SO ₄	142.0000	0.128	25.4464
Sodium hydroxide	NaOH	40.0000	0.05	2.8000
Sodium carbonate	Na ₂ CO ₃	106.0000	1.12	166.2080
Sodium nitrate	NaNO ₃	85.0000	1.1	130.9000
Sodium nitrite	NaNO ₂	69.0000	1	96.6000
Nitrous Oxide	N ₂ O	44.0130	Saturated (gas)	-

Cyclic Potentiodynamic Polarization



Images of bullet samples after electrochemical tests



Appendix E

Chemical Composition of Simulants used in Vapor Space Corrosion Testing

Composition of simulant for VS-Solution 2

Temperature 40 °C Ammonia
 pH Gas 550 ppm
 pH adjusted 10
 Volume 1.4 L

Simulant Source	Formula	Concentration (M)	Weight required (g)
Sodium Chloride	NaCl	0.02	1.6363
Sodium Nitrite	NaNO ₂	0.50	48.2967
Sodium Sulfate	Na ₂ SO ₄	0.4	79.5424
Sodium Phosphate	Na ₃ PO ₄ ·12H ₂ O	0.0065	3.4591
Sodium Carbonate	Na ₂ CO ₃	0.0230	2.7050
Sodium Bicarbonate	NaHCO ₃	0.0117	1.7361
Ammonium Nitrate	NH ₄ NO ₃	0.0128	1.4345
Potassium Nitrate	KNO ₃	0.01	1.4154
Sodium Nitrate	NaNO ₃	1.28	151.9773

Composition of simulant for VS-Solution 3

Temperature 40 °C Ammonia
 pH Gas 50 ppm
 pH adjusted 10
 Volume 2 L

Simulant Source	Formula	Concentration (M)	Weight required (g)
Sodium Chloride	NaCl	0.26	21.2722
Sodium Nitrite	NaNO ₂	2.67	257.9044
Sodium Sulfate	Na ₂ SO ₄	0.18	35.7941
Sodium Phosphate	Na ₃ PO ₄ ·12H ₂ O	0.0065	3.4591
Sodium Carbonate	Na ₂ CO ₃	0.0230	2.7050
Sodium Bicarbonate	NaHCO ₃	0.0124	1.8400
Ammonium Nitrate	NH ₄ NO ₃	0.0011	0.1233
Potassium Nitrate	KNO ₃	0.01	1.4154
Sodium Nitrate	NaNO ₃	2.39	284.2614

Composition of simulant for VS-Solution 4

Temperature 40 °C Ammonia
pH Gas 50 ppm
pH adjusted 10
Volume 1.4 L

Simulant Source	Formula	Concentration (M)	Weight required (g)
Sodium Chloride	NaCl	0.02	1.6363
Sodium Nitrite	NaNO ₂	0.50	48.2967
Sodium Sulfate	Na ₂ SO ₄	0.4	79.5424
Sodium Phosphate	Na ₃ PO ₄ ·12H ₂ O	0.0065	3.4591
Sodium Carbonate	Na ₂ CO ₃	0.0230	2.7050
Sodium Bicarbonate	NaHCO ₃	0.0117	1.7361
Ammonium Nitrate	NH ₄ NO ₃	0.0012	0.1345
Potassium Nitrate	KNO ₃	0.01	1.4154
Sodium Nitrate	NaNO ₃	1.29	153.3576

Composition of simulant for VS-Solution 5

Temperature 40 °C Air
pH pH adjusted 10
Volume 2 L

Simulant Source	Formula	Concentration (M)	Weight required (g)
Sodium Chloride	NaCl	0.26	21.2722
Sodium Nitrite	NaNO ₂	2.67	257.9044
Sodium Sulfate	Na ₂ SO ₄	0.18	35.7941
Sodium Phosphate	Na ₃ PO ₄ ·12H ₂ O	0.0065	3.4591
Sodium Carbonate	Na ₂ CO ₃	0.0230	2.7050
Sodium Bicarbonate	NaHCO ₃	0.0124	1.8400
Ammonium Nitrate	NH ₄ NO ₃	0.01	1.4154
Potassium Nitrate	KNO ₃	2.39	284.3923
Sodium Nitrate	NaNO ₃	0.26	21.2722

Composition of simulant for VS-Solution 6

Temperature 40 °C Air
pH pH adjusted 10
Volume 2 L

Simulant Source	Formula	Concentration (M)	Weight required (g)
Sodium Chloride	NaCl	0.02	1.6363
Sodium Nitrite	NaNO ₂	0.50	48.2967
Sodium Sulfate	Na ₂ SO ₄	0.400	79.5424
Sodium Phosphate	Na ₃ PO ₄ ·12H ₂ O	0.0065	3.4591
Sodium Carbonate	Na ₂ CO ₃	0.0230	2.7050
Sodium Bicarbonate	NaHCO ₃	0.0117	1.7361
Ammonium Nitrate	NH ₄ NO ₃	0.01	1.4154
Potassium Nitrate	KNO ₃	1.29	153.5004
Sodium Nitrate	NaNO ₃	0.02	1.6363

Composition of simulant for VS-Solution 7-LDP

Temperature 45 °C Air
pH pH adjusted 7.6
Volume 2 L

Simulant Source	Formula	Concentration (M)	Weight required (g)
Sodium bicarbonate	NaHCO ₃	1.120E-03	0.1882
Calcium hydroxide	Ca(OH) ₂	1.210E-04	0.0179
Potassium nitrate	KNO ₃	6.750E-05	0.0136
Magnesium Nitrate, 6-hydrate	Mg(NO ₃) ₂ ·6H ₂ O	1.520E-05	0.0078
Strontium Nitrate	Sr(NO ₃) ₂	4.040E-06	0.0017
Sodium sulfate	Na ₂ SO ₄	1.830E-06	0.0005
Sodium Metasilicate, 5-hydrate	Na ₂ SiO ₃ ·5H ₂ O	4.570E-05	0.0194
Ferric chloride	FeCl ₃	2.670E-06	0.0009
Manganese Nitrate	Mn(NO ₃) ₂	3.430E-07	0.0001
Acetic Acid	C ₂ H ₄ O ₂	3.000E-04	0.0360

Composition of simulant for VS-Solution 8-GW

Temperature 45 °C Air
pH pH adjusted 7.61
Volume 2 L

Simulant Source	Formula	Concentration (M)	Weight required (g)
Sodium bicarbonate	NaHCO ₃	1.750E-03	0.2940
Calcium hydroxide	Ca(OH) ₂	1.500E-03	0.2223
Potassium nitrate	KNO ₃	2.400E-04	0.0485
Ferric sulfate	Fe ₂ (SO ₄) ₃	6.250E-04	0.4999
Ferric chloride	FeCl ₃	7.667E-05	0.0249
Strontium Nitrate	Sr(NO ₃) ₂	2.874E-06	0.0012
Sodium Metasilicate, 5-hydrate	Na ₂ SiO ₃ .5H ₂ O	6.000E-04	0.2546
Magnesium Chloride	MgCl ₂	3.100E-04	0.0590
Acetic Acid	C ₂ H ₄ O ₂	3.000E-04	0.0360

Appendix G

Chemical Composition of Simulants used in Air Radiolysis Corrosion Testing

Composition of simulant for TI-Solution 2 (GW)

Temperature 45 °C

Volume 1 L

Simulant Source	Formula	Concentration (M)	Weight required (g)
Sodium bicarbonate	NaHCO ₃	1.75E-03	0.1470
Calcium hydroxide	Ca(OH) ₂	1.50E-03	0.1111
Potassium nitrate	KNO ₃	2.40E-04	0.0243
Ferric sulfate	Fe ₂ (SO ₄) ₃	6.25E-04	0.2499
Ferric chloride	FeCl ₃	7.67E-05	0.0124
Strontium Nitrate	Sr(NO ₃) ₂	2.87E-06	0.0006
Sodium Metasilicate, 5-hydrate	Na ₂ SiO ₃ .5H ₂ O	6.00E-04	0.1273
Magnesium Chloride	MgCl ₂	3.10E-04	0.0295
Acetic Acid	C ₂ H ₄ O ₂	3.00E-04	0.0180

pH after mixing:

Adjusted pH 5 and 6

Appendix F

Pictures of Vapor Space Corrosion Samples after Test

Samples cold mounted

Vessel 2: Level 3
4 months – 1



Vessel 2: Level 2
4 months – 2



2 months – 3



Vessel 2: Level 1

4 months – 4



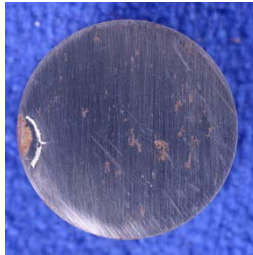
Vessel 2: Immersed
4 months – 5



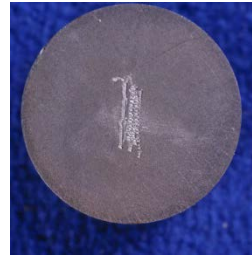
After removal of cold mount

Vessel 2: Level 3

4 months – 1



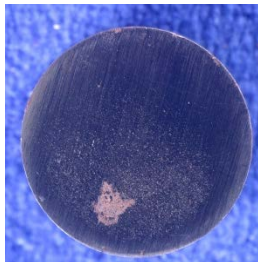
Front



Back

Vessel 2: Level 2

4 months – 2



Front



Back

Vessel 2: Level 1

2 months – 3

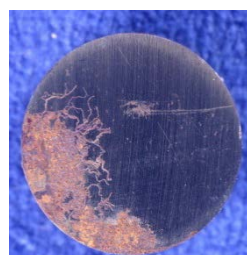


Front



Back

4 months – 4



Front



Back

Vessel 2: Immersed

4 months – 5



Front

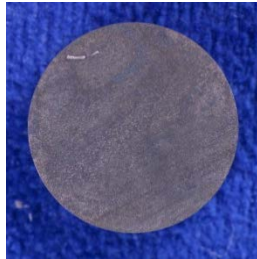


Back

Cleaned with Clarke solution

Vessel 2: Level 3

4 months – 1



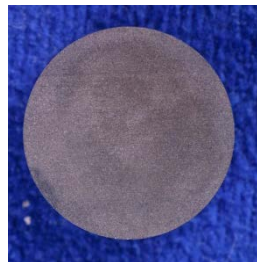
Front



Back

Vessel 2: Level 2

4 months – 2



Front



Back

Vessel 2: Level 1

4 months – 4



Front



Back

Vessel 2: Immersed

4 months – 5



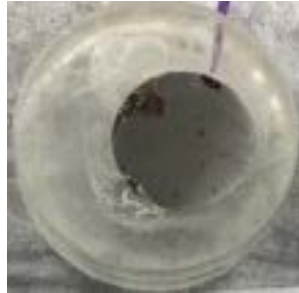
Front



Back

Samples cold mounted

Vessel 3: Level 3
4 months – 6



Vessel 3: Level 2
4 months – 7

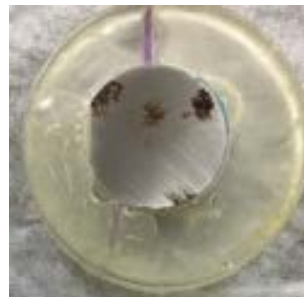


Vessel 3: Level 1

2 months – 8



4 months – 9



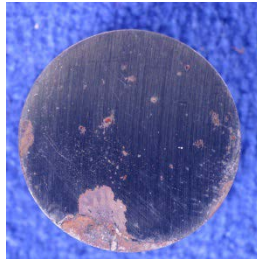
Vessel 3: Immersed
4 months – 10



After removal of cold mount

Vessel 3: Level 3

4 months – 6



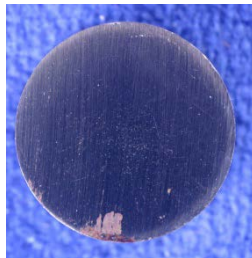
Front



Back

Vessel 3: Level 2

4 months – 7



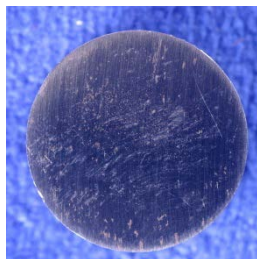
Front



Back

Vessel 3: Level 1

2 months – 8

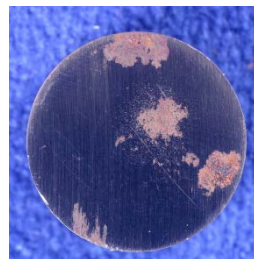


Front



Back

4 months – 9



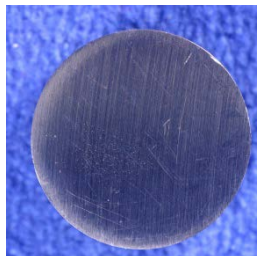
Front



Back

Vessel 3: Immersed

4 months – 10



Front



Back

Cleaned with Clark Solution

Vessel 3: Level 3

4 months – 6



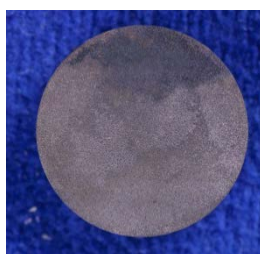
Front



Back

Vessel 3: Level 2

4 months – 7



Front



Back

Vessel 3: Level 1

4 months – 9



Front



Back

Samples cold mounted

Vessel 4: Level 3
4 months – 11



Vessel 4: Level 2
4 months – 12



2 months – 13



Vessel 4: Level 1

4 months – 14



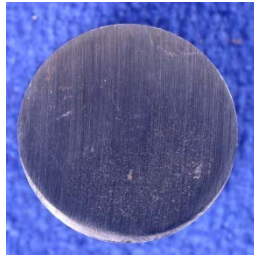
Vessel 4: Immersed
4 months – 15



After removal of cold mount

Vessel 4: Level 3

4 months – 11



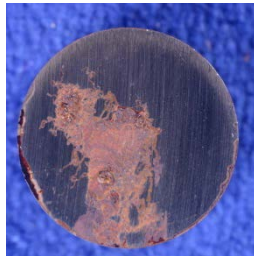
Front



Back

Vessel 4: Level 2

4 months – 12



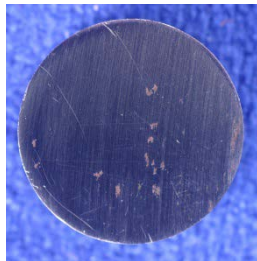
Front



Back

Vessel 4: Level 1

2 months – 13

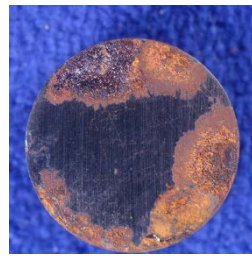


Front



Back

4 months – 14



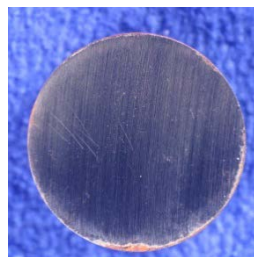
Front



Back

Vessel 4: Immersed Front

4 months – 15



Front



Back

Cleaned with Clarke Solution

Vessel 4: Level 2

4 months – 12



Front



Back

Vessel 4: Level 1

2 months – 13



Front



Back

4 months – 14



Front



Back

Samples cold mounted

Vessel 5: Level 3
4 months – 16



Vessel 5: Level 2
4 months – 17



2 months – 18



Vessel 5: Level 1

4 months – 19



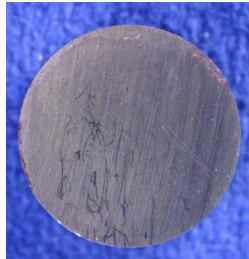
Vessel 5: Immersed
4 months – 20



After removal of cold mount

Vessel 5: Level 3

4 months – 16



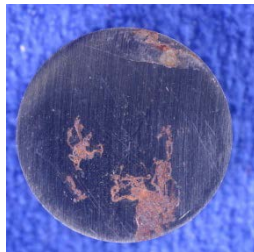
Front



Back

Vessel 5: Level 2

4 months – 17



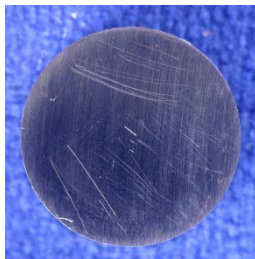
Front



Back

Vessel 5: Level 1

2 months – 18



Front



Back

4 months – 19



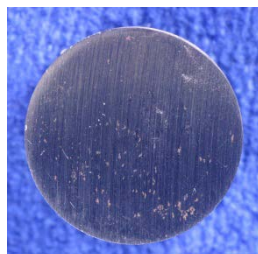
Front



Back

Vessel 5: Immersed Front

4 months – 20



Front



Back

Cleaned with Clarke Solution

Vessel 5: Level 2

4 months – 17



Front



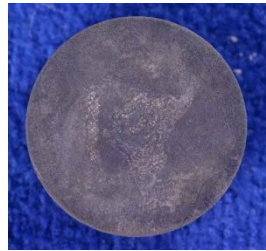
Back

Vessel 5: Level 1

4 months – 19



Front



Back

Samples cold mounted

Vessel 6: Level 3
4 months – 21



Vessel 6: Level 2
4 months – 22



2 months – 23

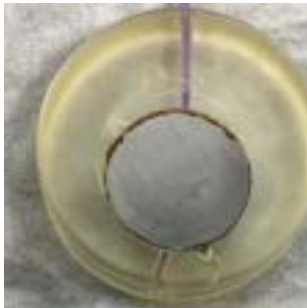


Vessel 6: Level 1

4 months – 24



Vessel 6: Immersed
4 months – 25



After removal of cold mount

Vessel 6: Level 3

4 months – 21



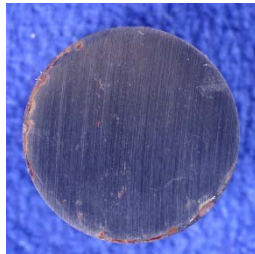
Front



Back

Vessel 6: Level 2

4 months – 22



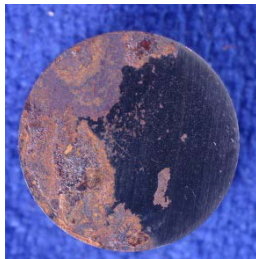
Front



Back

Vessel 6: Level 1

2 months – 23

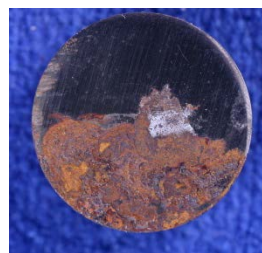


Front



Back

4 months – 24



Front



Back

Vessel 6: Immersed

4 months – 25



Front



Back

Cleaned with Clarke Solution

Vessel 6: Level 3

4 months – 21



Front



Back

Vessel 6: Level 2

4 months – 22



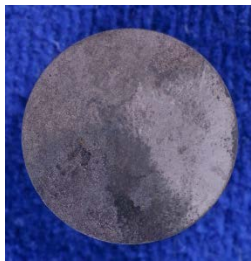
Front



Back

Vessel 6: Level 1

2 months – 23



Front



Back

4 months – 24



Front



Back

Vessel 6: Immersed Front

4 months – 25



Front



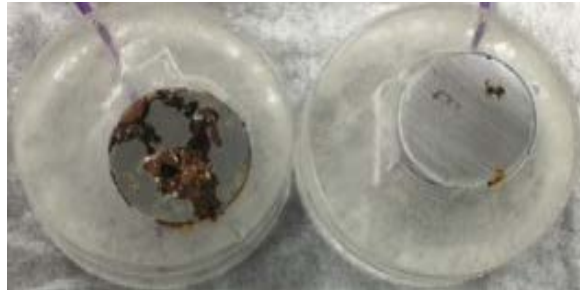
Back

Samples cold mounted

Vessel 7: Level 3
4 months – 26 and 27



Vessel 7: Level 2
4 months – 28 and 29

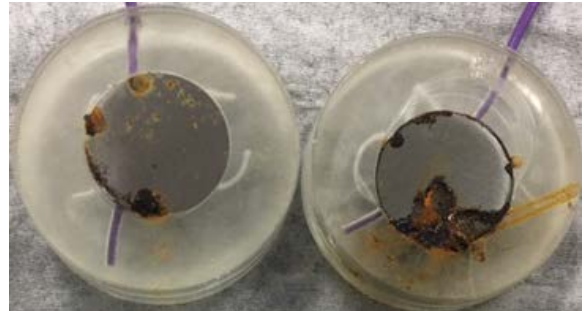


2 months – 30 and 31

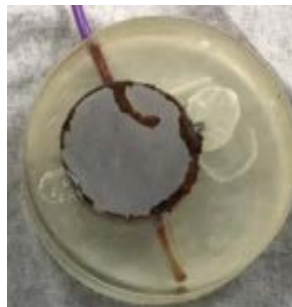


Vessel 7: Level 1

4 months – 32 and 33



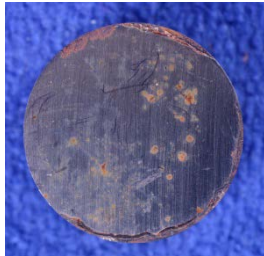
Vessel 7: Immersed
4 months – 34



After removal of cold mount

Vessel 7: Level 3

4 months – 26

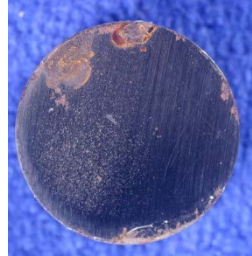


Front



Back

4 months – 27



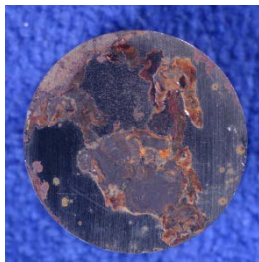
Front



Back

Vessel 7: Level 2

4 months – 28

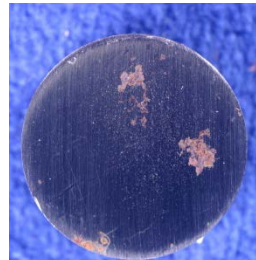


Front



Back

4 months – 29



Front



Back

Vessel 7: Level 1

2 months – 30



Front



Back

2 months – 31



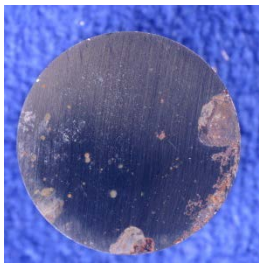
Front



Back

Vessel 7: Level 1

4 months – 32

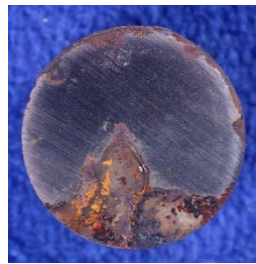


Front



Back

4 months – 33



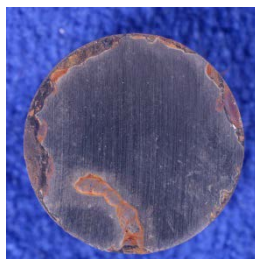
Front



Back

Vessel 7: Immersed

4 months – 34



Front



Back

Cleaned with Clarke solution

Vessel 7: Level 3

4 months – 26



Front



Back

4 months – 27



Front



Back

Vessel 7: Level 2

4 months – 28



Front



Back

4 months – 29



Front



Back

Vessel 7: Level 1

2 months – 30



Front



Back

2 months – 31



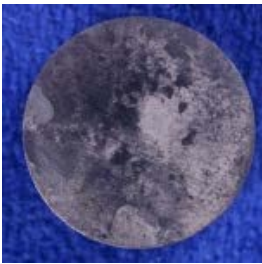
Front



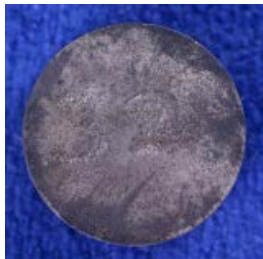
Back

Vessel 7: Level 1

4 months – 32



Front



Back

4 months – 33



Front



Back

Vessel 7: Immersed

4 months – 34



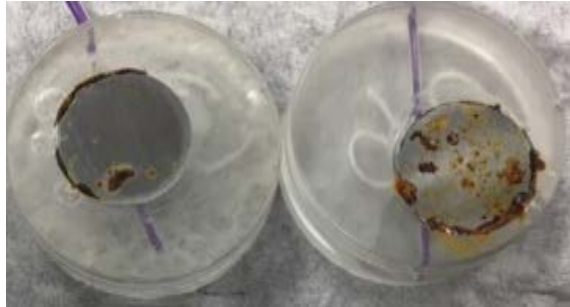
Front



Back

Samples cold mounted

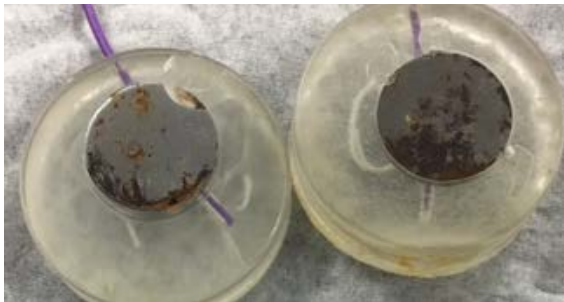
Vessel 8: Level 3
4 months – 35 and 36



Vessel 8: Level 2
4 months – 37 and 38

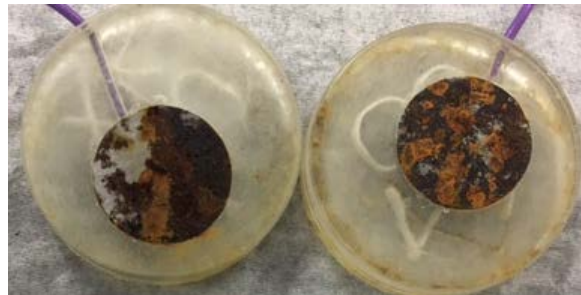


2 months – 39 and 40

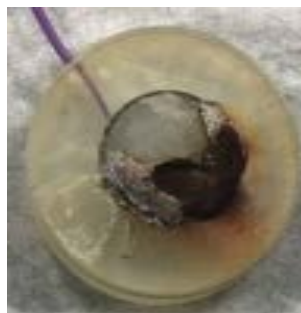


Vessel 8: Level 1

4 months – RC128 28 and RC128 27



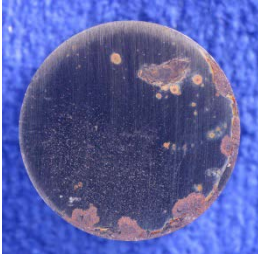
Vessel 8: Immersed
4 months – 41



After removal cold mount

Vessel 8: Level 3

4 months – 35

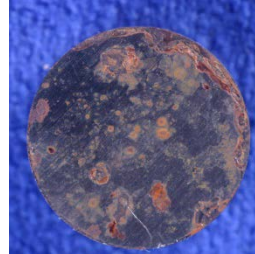


Front



Back

4 months – 36



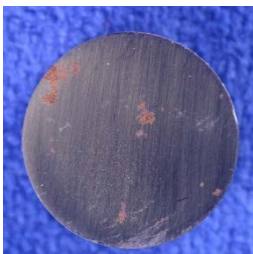
Front



Back

Vessel 8: Level 2

4 months – 37

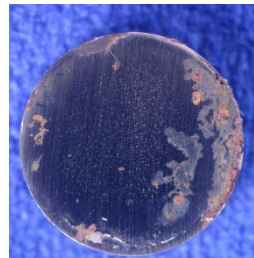


Front



Back

4 months – 38



Front



Back

Vessel 8: Level 1

2 months – 39

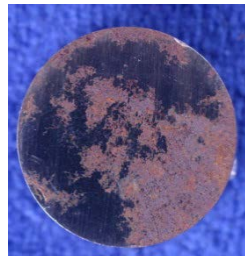


Front



Back

2 months – 40



Front



Back

Vessel 8: Level 1

4 months – RC128 27



Front

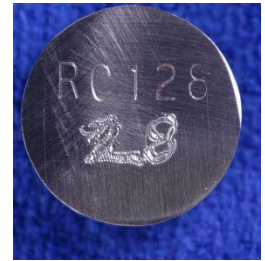


Back

4 months – RC128 28



Front



Back

Vessel 8: Immersed

4 months – 41



Front



Back

Cleaned with Clarke Solution

Vessel 8: Level 3

4 months – 35



Front



Back

4 months – 36



Front



Back

Vessel 8: Level 2

4 months – 37

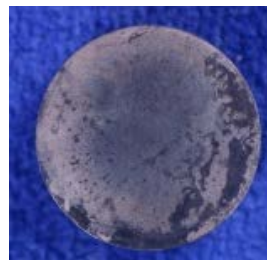


Front



Back

4 months – 38



Front



Back

Vessel 8: Level 1

2 months – 39



Front

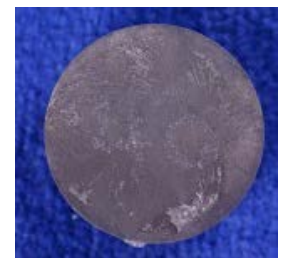


Back

2 months – 40



Front



Back

Vessel 8: Level 1

4 months – RC128 27

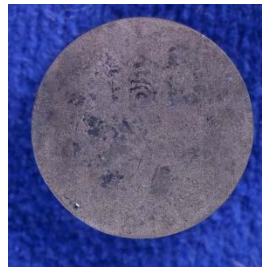


Front



Back

4 months – RC128 28



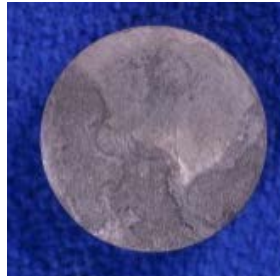
Front



Back

Vessel 8: Immersed

4 months – 41



Front



Back

Appendix H

Pictures of Air Radiolysis Corrosion Samples after Test

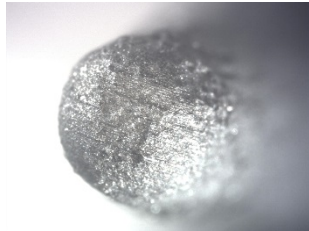
Solution 1-GW pH 6

4 months exposure-partial immersed sample

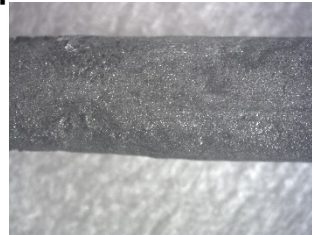
After cleaning



Microscope



Nose



Shank

4 months exposure-total immersed sample

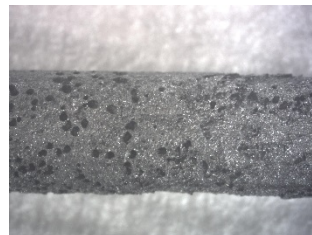
After cleaning



Microscope



Nose



Shank

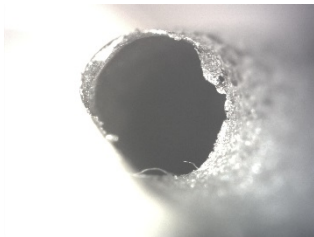
Solution 2-GW pH 5

4 months exposure-partial immersed sample

After cleaning



Microscope



Nose



Shank

4 months exposure-total immersed sample

After cleaning



Microscope



Nose

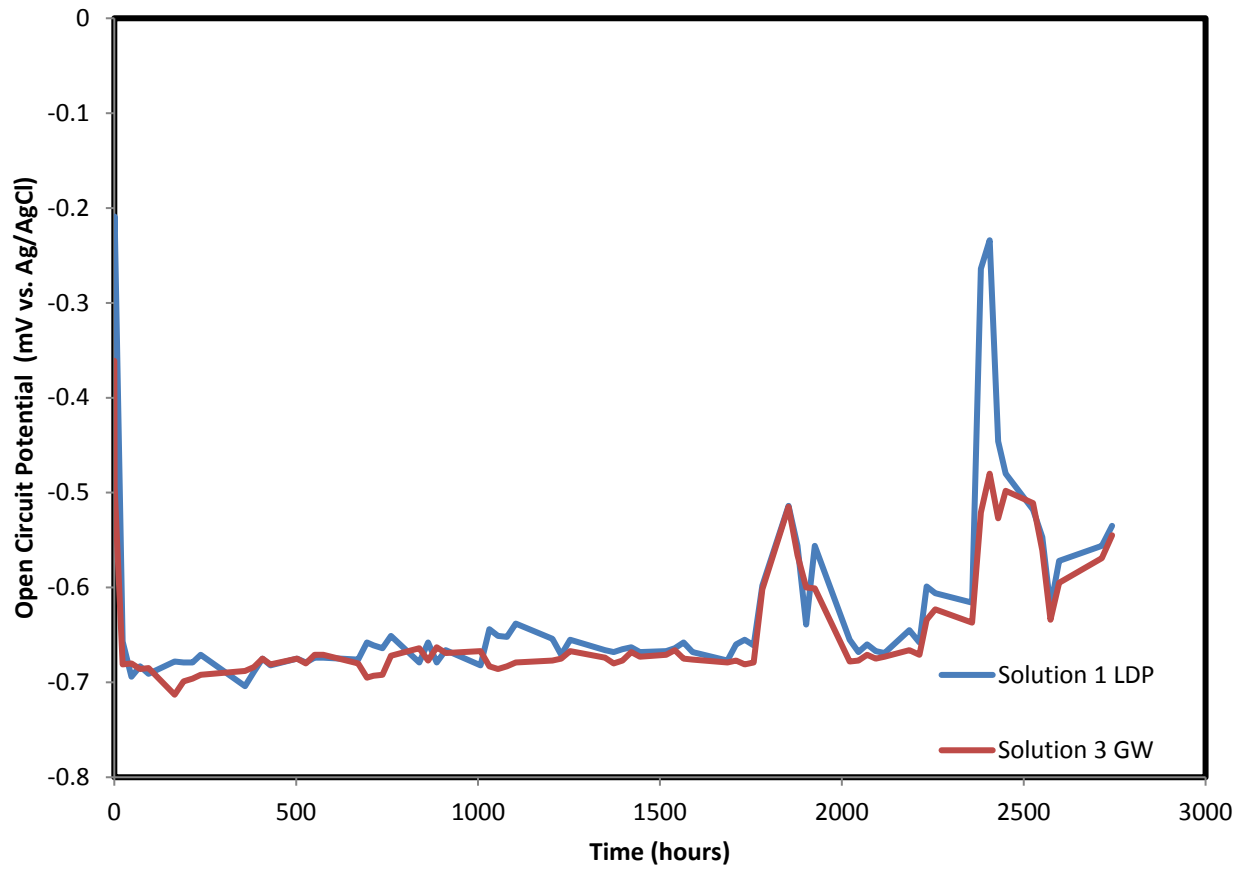


Shank

Appendix I

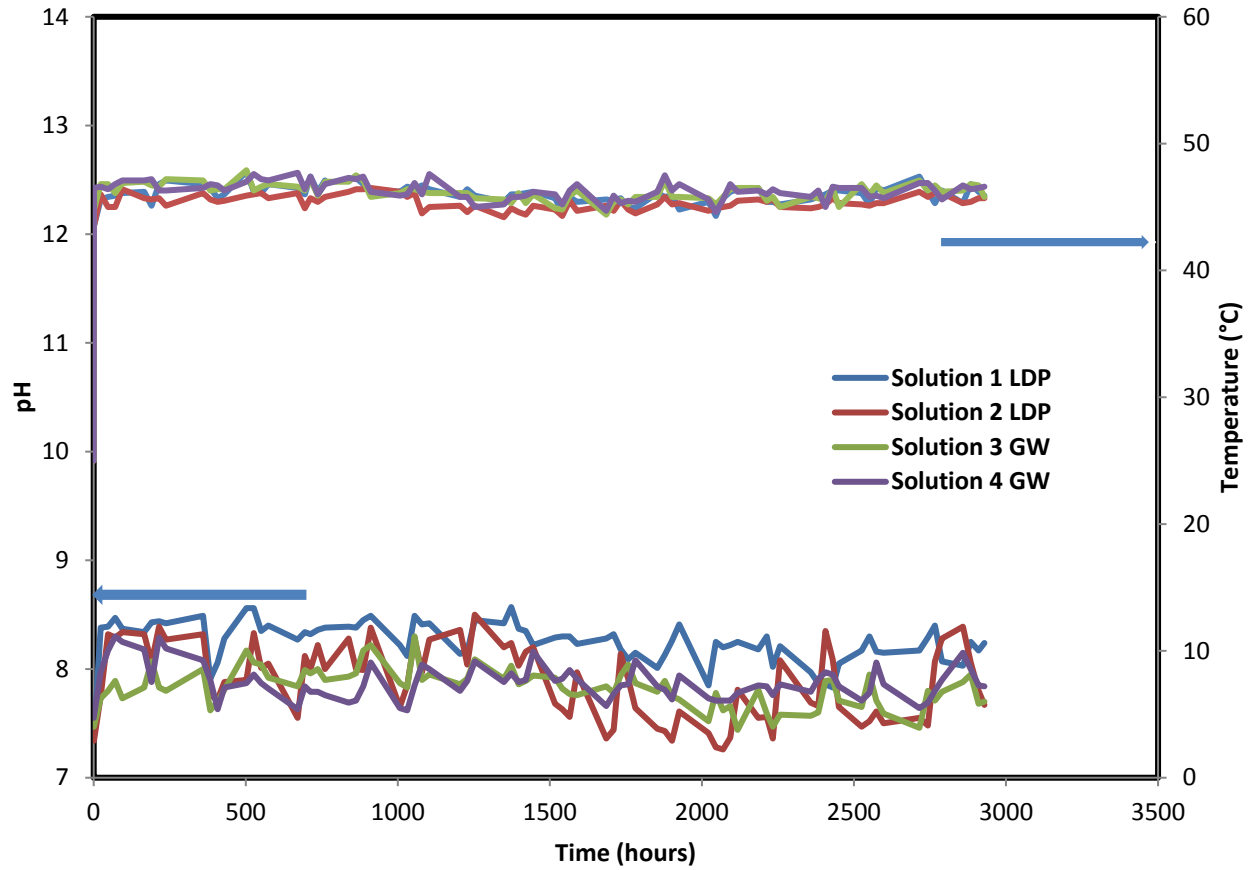
**Open Circuit Potential, pH and Temperature vs. Time plots Air Radiolysis
Corrosion Testing**

Solution 1 and 3
4 month exposure
Open circuit potential vs. Time



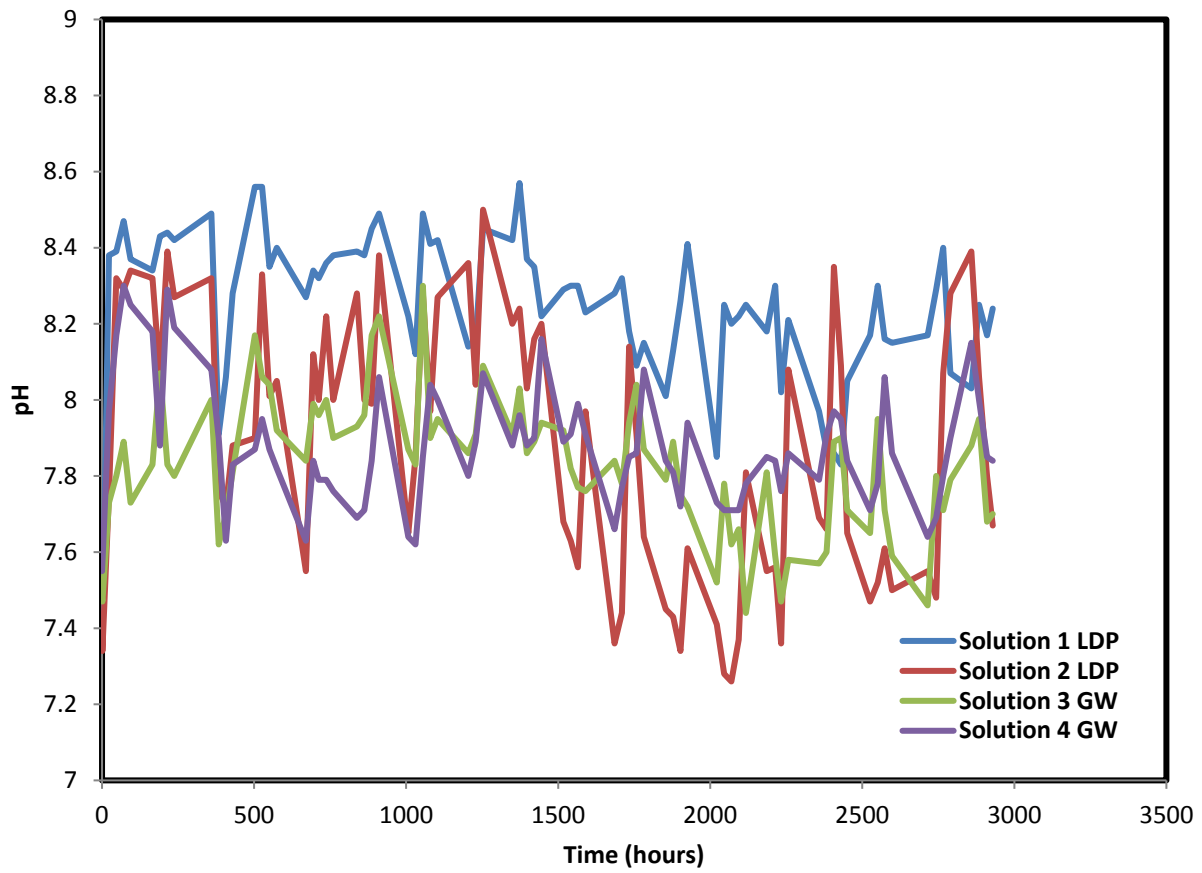
Solutions 1 to 4

pH and Temperature vs. Time



Solution 1 to 4

pH vs. Time



Appendix J

**Direct Feed Low-Activity Waste Corrosion Testing performed at SRNL
Memos (one from May 16, 2017/ two from September 28, 2017)**

May 16, 2017

To: S. T. Arm
One System Integrated Flowsheet Manager
Washington River Protection Solutions

From: R. B. Wyrwas

Approval: _____
B. J. Wiersma Date

Updated Corrosion Control Limits for Direct Feed Low-Activity Melter Off Gas Returns to Hanford Tank Farms

The Savannah River National Laboratory has been developing a corrosion model to facilitate implementation of Hanford's Direct Feed Low Activity Waste flowsheet. Laboratory testing and statistical analysis is being used to determine the necessary corrosion controls for returning effluent from the Hanford Waste Treatment and Immobilization Plant's Low Activity Waste Vitrification melter off-gas treatment system to the tank farms. These stream compositions are projected to contain components at relative concentrations that are significantly more corrosive toward carbon steel, specifically halide and sulfate anions, than the current waste compositions in the tank farms. The work performed in FY 16 has confirmed that the halide ions are the most aggressive species in the return stream compositions, and nitrite is the most effective inhibitor at pH 10 and 40°C.¹ This test program has employed statistically designed test matrices to determine the dependent variables and the interaction terms between the variables that are significant for the corrosion model and develops corrosion control specifications. The first phase of testing focused on identifying aggressive species in off-gas condensate return compositions that present a propensity for localized corrosion attack, namely pitting corrosion. The second phase of testing focused on developing a corrosion model from the interaction terms that will predict the susceptibility of pitting in the double shell tank system based on waste composition and the required amount of corrosion inhibitor. Further testing is still ongoing to validate the corrosion model and to optimize the chemistry adjustments needed for returns to tank farms. This memorandum documents the most recent results which have been used to refine the corrosion specifications presented in Ref. 1.

Using the most up to date results, the pitting corrosion control equation can be written as follows:

$$[NO_2^-] = 9.97 [Halide] + 0.65$$

The equation is valid for a minimum pH of 10 and a maximum temperature of 40 °C. This pitting corrosion control equation is based on 87 cyclic potentiodynamic polarization (CPP) tests. Figure 1 shows a plot of the pitting control equation along with the electrochemical test data. In addition to the 87 data points used to

We put science to work.™

define the model, data from testing performed in 2015 is also presented to further define the region of pitting susceptibility [2]. The probability of a pit occurring at nitrite concentrations above this line is less than 0.05. These tests further refined the model by reducing the error in the statistical model, particularly at the boundaries of the halide concentration (e.g., 0.01 M) [1]. Also included on the plot is the SRS chloride corrosion control model (i.e., blue line) [2]. This model was extrapolated from data that was obtained from testing at chloride concentrations less than 0.05 M. The new model is based on halide concentrations up to 1.6 M. The figure shows with the new model there is a considerable reduction in the minimum required nitrite as compared with the SRS equation.

At halide concentrations less than 0.2 M, there appears to be adequate margin between the pitting and no pitting regimes based on the test data. There does appear to be a region bounded by 0.25 to 0.4 M halide and 3 to 4 M nitrite where a few additional tests could be performed to strengthen the confidence that the margins on the model are adequate. This region became more evident with the addition of plotting the 2015 data. [Note: the 2015 data was not used in the model development].

Coupon immersion tests are underway to verify the results of the CPP tests. These tests will be completed by the end of June.

References

1. Wyrwas, R.B., "Tank Waste Disposition Integrated Flowsheet: Corrosion Specification Development FY 16 Interim Report," Savannah River National Laboratory, Aiken, South Carolina, SRNL-RP-2016-00633.
2. Wyrwas, R. B., "SRNL Report for the Tank Waste Disposition Integrated Flowsheet: Corrosion Testing," SRNL-STI-2015-00506, September 2015.

May 16, 2017

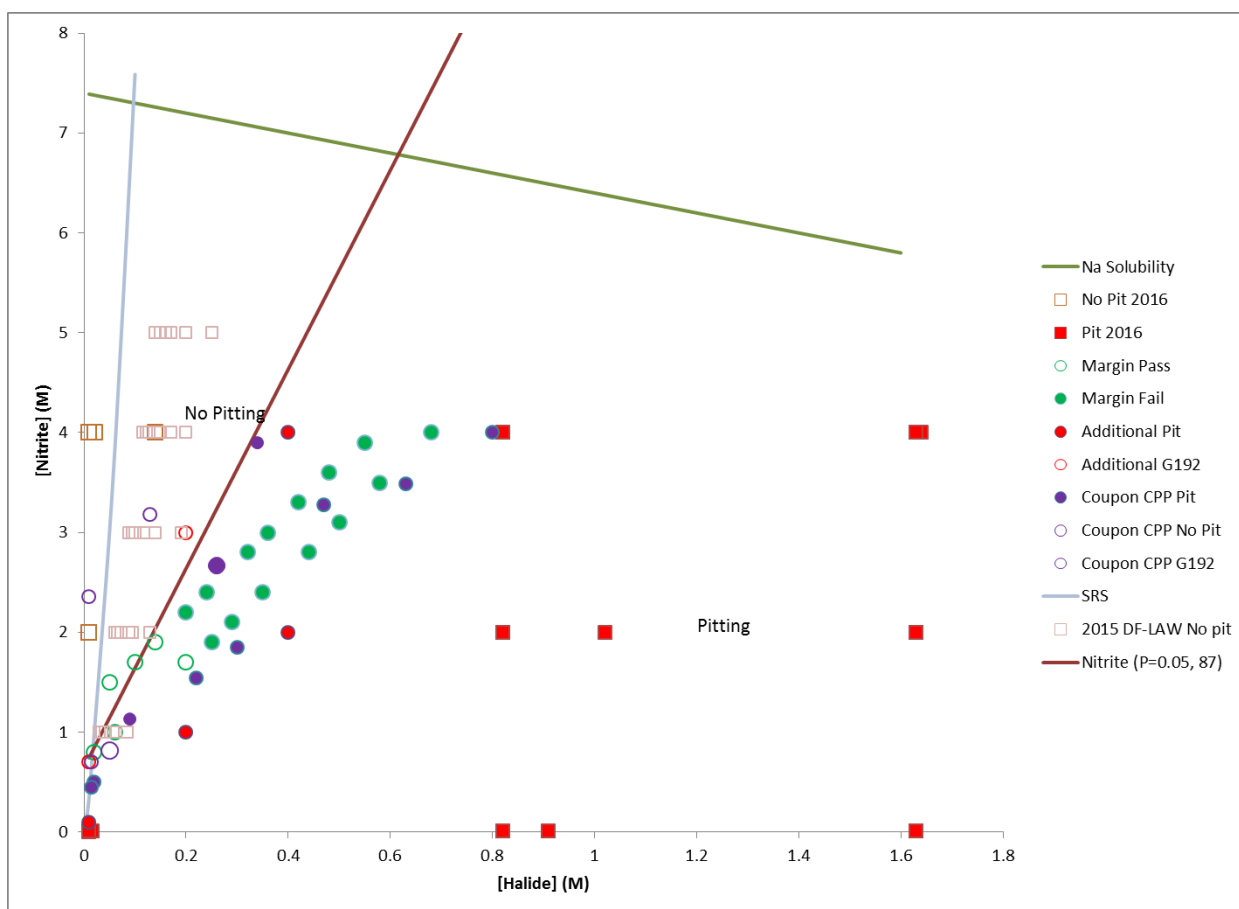


Figure 1. Pitting probability plot showing model equation for different probability level of 0.05 along with actual data from testing.

We put science to work.™

To: S. T. Arm
One System Integrated Flowsheet Manager
Washington River Protection Solutions

From: _____
R. B. Wyrwas Date

Approval: _____
B. J. Wiersma Date

Corrosion Control Requirements for Direct Feed Low-Activity Melter Off Gas Returns to Hanford Tank Farms

The Savannah River National Laboratory has been developing a corrosion model to facilitate implementation of Hanford's Direct Feed Low Activity Waste (DFLAW) flowsheet. Laboratory testing and statistical analysis is being used to determine the necessary corrosion controls for returning effluent from the Hanford Waste Treatment and Immobilization Plant's Low Activity Waste Vitrification melter off-gas treatment system to the tank farms. These stream compositions are projected to contain components at relative concentrations that are significantly more corrosive toward carbon steel, specifically halide and sulfate anions, than the current waste compositions in the tank farms. The work performed in FY 2016 has confirmed that the halide ions are the most aggressive species in the return stream compositions, and nitrite is the most effective inhibitor at pH 10 and 40°C.¹ Testing performed in FY 2017 evaluated chloride-induced pitting corrosion inhibited by nitrite.² Data collected from the DFLAW off-gas testing program in conjunction with the Hanford Tank Farms specifications testing program³, Savannah River Tank Farms Operations knowledge,⁴ and the Tank Integrity Expert Panel corrosion sub-group⁵ has determined the chemistry ranges and chemical species requirements for corrosion control in the Hanford double-shell tank system. These requirements are given in Table 1.

Limit L1 is a conservative limit that will bound most waste streams. This limit will be useful for operations. However, since the limit is conservative, it may require the addition of more inhibitors than are necessary. Limit L2 addresses a low hydroxide stream, that has nitrate as the controlling aggressive species (i.e., $[\text{Halide}]/[\text{NO}_3^-] < 0.03$), that must be inhibited with sufficient nitrite in order to prevent pitting. Limit L3 provides a minimum nitrite inhibitor requirement to prevent pitting for an extremely dilute solution. Finally, Limit L4 provides nitrite inhibitor requirements for the case where halide and/or sulfate is the controlling aggressive species (e.g., $[\text{Halide}]/[\text{NO}_3^-] > 0.03$), that must be inhibited with sufficient nitrite in order to prevent pitting.

We put science to work.TM

The limits and specifications in Table 1 are the incorporated results of the DFLAW corrosion testing program with the results of the other testing programs that will be used to construct a unified specification for the Hanford Tank Farms with the oversight of the Tank Integrity Expert Panel. The DFLAW corrosion testing program specifically addresses pitting corrosion of carbon steel, and the results will be integrated with the overall corrosion control program for Hanford Tank Farms, which provides control for stress-corrosion cracking as well as pitting of both carbon steel and stainless steel systems.

References

1. Wyrwas, R.B., "Tank Waste Disposition Integrated Flowsheet: Corrosion Specification Development FY 16 Interim Report," Savannah River National Laboratory, Aiken, South Carolina, SRNL-RP-2016-00633.
2. Wyrwas, R.B., "Updated Corrosion Control Limits for Direct Feed Low-Activity Melter Off Gas Returns to Hanford Tank Farms" Savannah River National Laboratory, Aiken, South Carolina, SRNL-L4440-2017-00007.
3. Fuentes, R. E., "Hanford Double Shell Waste Tank Corrosion Studies – Final Report FY2016," Savannah River National Laboratory, Aiken, South Carolina, SRNL-STI-2016-00721.
4. WSRC-TR-2002-00327, "CSTF Corrosion Control Program", Savannah River Site, Aiken, SC.
5. Feero, A.J., Follet, J.R., Stock, L.M., "Specifications for the Minimization of Stress Corrosion Cracking Threat in Double-Shell Tank Wastes," Washington River Protection Solutions LLC, Richland, WA.

Table 1. Applicable limits and specifications for return stream chemistry.

Limits	Applicability, for $T \leq 35^{\circ}\text{C}$		Inhibitor Requirement
	Variable	Range	
L1	$[\text{NO}_3^-]$	$\leq 1.5 \text{ M}$	$[\text{OH}^-] > 1 \text{ M}$ $[\text{NO}_2^-] > 0.5 \text{ M}$
	$[\text{SO}_4^{2-}]$	$\leq 0.2 \text{ M}$	
	$[\text{Halide}]^a$	$\leq 0.25 \text{ M}$	
L2	$[\text{OH}^-]$	$< 1 \text{ M}$	$[\text{NO}_2^-]/[\text{NO}_3^-] > 1.7$
	pH	≥ 12	
	$[\text{NO}_3^-]$	$0.02 \text{ M} \leq [\text{NO}_3^-] \leq 1.5 \text{ M}$	
	$[\text{SO}_4^{2-}]/[\text{NO}_3^-]$	≤ 0.3	
	$[\text{Halide}]/[\text{NO}_3^-]$	≤ 0.03	
L3	$[\text{OH}^-]$	$< 1 \text{ M}$	$[\text{NO}_2^-] > 0.033 \text{ M}$
	pH	≥ 12	
	$[\text{NO}_3^-]$	$\leq 0.02 \text{ M}$	
	$[\text{SO}_4^{2-}]/[\text{NO}_3^-]$	≤ 0.3	
	$[\text{Halide}]/[\text{NO}_3^-]$	< 0.03	
L4	$[\text{OH}^-]$	$< 1 \text{ M}$	Maximum of
	pH	≥ 12	
	$[\text{Halide}]/[\text{NO}_3^-]$	> 0.03	$[\text{NO}_2^-] > 0.3 \text{ M}$ or
	$[\text{NO}_3^-]$	$\leq 1.5 \text{ M}$	
	$[\text{SO}_4^{2-}]$	$\leq 0.2 \text{ M}$	$[\text{NO}_2^-]/[\text{Halide}] > 10$
	$[\text{Halide}]^a$	$\leq 0.25 \text{ M}$	

a-Chloride +Fluoride

L1: A conservative bounding limit that covers the expected range of EMF return compositions

L2: A limit for high nitrate streams

L3: A limit for streams that are extremely dilute (i.e., practically water)

L4: A limit for streams that are high in sulfate and/or halide.

We put science to work.™